MECHANISMS OF ACTION OF DRUGS WITH DUAL OR MULTIPLE ANTIVIRAL ACTIVITIES

Egor Petrovitch Tchesnokov

Department of Microbiology & Immunology
McGill University, Montreal

June, 2009

A thesis submitted to McGill University in partial fulfillment of the requirements
of the
degree of Doctor of Philosophy

ABSTRACT

Viral enzymes that catalyze replication of the viral genome remain the main subject of currently available antiviral therapies. This work focuses on three anti-viral agents that target viral DNA polymerases: foscarnet, acyclovir and entecavir. Though the broad spectrum of antiviral activities of foscarnet has been recognized for decades, only recently has it been shown that the anti-herpesvirus drug acyclovir and the anti-hepatitis B virus drug entecavir are also active against the human immunodeficiency virus (HIV) 1. The clinical benefits of the multiple antiviral activities of foscarnet have been demonstrated in treating HIV/herpesvirus co-infections. Foscarnet is currently approved for treating human cytomegalovirus infections. But the precise molecular mechanism of foscarnet action and resistance remains poorly understood. The study of foscarnet's mode of action against the HCMV DNA polymerase (UL54) is complicated in part by the difficulty in expressing and purifying the viral enzyme. To address the first issue, I conducted biochemical studies of foscarnet/UL54 interactions using an unpurified viral enzyme. I then proposed a model based on these studies for the presumptive foscarnet binding site within UL54. To address the second issue I generated the RB69 bacteriophage/HCMV polymerase chimera, which is easily purifiable and displays the UL54 phenotype with respect to foscarnet and acyclovir. The recent discovery of the anti-HIV activity of acyclovir has been followed by a report showing the selection of the V75I mutation within HIV-1 reverse transcriptase (RT) under the selective pressure of acyclovir. My own biochemical studies have revealed that the major effect of V75I substitution involves reducing the catalytic rate of acyclovir incorporation. The recent report of entecavir anti-HIV-1 activity has demonstrated the selection of M184V-containing HIV-1. Subsequent biochemical studies have revealed that M184V-containing RT discriminates against entecavir at the level of incorporation. My own studies show that the major effect of entecavir incorporation has been the delayed chain termination (DCT) of the DNA synthesis. DCT protects the incorporated drug from excision. The research project described in this thesis

provides novel tools and reveals new concepts for future drug design and development.

RÉSUMÉ

Les enzymes virales qui sont responsables pour la réplication du génome viral constituent l'objet principal des thérapies antivirales actuelles. Ce travail se concentre sur trois agents anti-viraux qui inhibitent les polymérases d' ADN virales. Malgré le fait que plusieurs activités antivirales du foscarnet sont connues depuis des décennies, il a éte démontré seulement récemment que l'acyclovir, un agent contre le virus de l`herpes, et entecavir, un agent contre le virus de l`hepatite B, ont une activité anti-VIH-1. Les avantages cliniques des multiples activités antivirales du foscarnet dans le traitement des co-infections VIH/herpes ont été démontrés. Le foscarnet est présentement approuvé pour traiter les infections du cytomégalovirus humain. Le mécanisme précis de l'action antivirale du foscarnet, ainsi que le mécanisme de résistance au foscarnet demeurent mal compris. L'étude du mécanisme d'action de foscarnet contre l'ADN polymérase du VCMH (UL54) est compliquée en partie par deux problématiques : l'expression de l'enzyme virale et la purification de cette protéine. Pour adresser le premier problème, j'ai poursuivis des études biochimiques sur les interactions foscarnet-UL54 en utilisant une enzyme virale non-purifiée. En se basant sur ces études, j'ai ensuite proposé un model du site de liaison du foscarnet. Pour addresser le deuxième problème, j'ai généré une protéine chimère bactériophage/HCMV polymérase. Cette protéine est facilement purifiable et possède le profile de la UL54 polymérase envers foscarnet et acyclovir. La découverte récente de l'activité anti-VIH de l'acyclovir a été suivie d`une étude démontrant la sélection de la mutation V75I dans la transcriptase inverse (TI) du VIH-1 sous la pression sélective de l'acyclovir. Mes propres études biochimiques ont révélées que l'effet majeur de la substitution V75I implique la réduction du rythme catalytique de l'incorporation de l'acyclovir. L`étude récente portant sur l'activité anti-VIH-1 d'entecavir a démontré la sélection de TI contenant la mutation M184V. Des études biochimiques subséquentes ont révélées que la TI contenant la M184V démontre une préférence sélective envers l'entecavir au niveau de l'incorporation. Mes propres études démontrent que l'effet majeur se situe au niveau de

l'abrogation de la synthèse d'ADN ultérieure (ASAU). L'ASAU protège l'entecavir incorporé de l'excision. Le projet de recherche décrit dans cette thèse apporte de nouveaux outils et révèle de nouvelles approches pour la conception et le développement de médicaments.

PREFACE

This thesis was written in accordance with McGill University's "Guideline for Thesis Preparation". The format of this thesis conforms to the "Manuscript-based thesis" option which states:

"Candidates have the option of including, as part of the thesis, the text of one or more papers submitted, or to be submitted, for publication, or the clearly-duplicated text (not the reprints) of one or more published papers. These texts must conform to the "Guidelines for Thesis Preparation" with respect to font size, line spacing and margin sizes and must be bound together as an integral part of the thesis."

Manuscripts included in this thesis:

Tchesnokov EP, Gilbert C, Boivin G, Götte M.
Role of helix P of the human cytomegalovirus DNA polymerase in resistance and hypersusceptibility to the antiviral drug foscarnet.
J Virol. 2006 Feb;80(3):1440-50.

Tchesnokov E.P., Obikhod A., Schinazi I. R. F. and Götte M.
Engineering of a chimeric RB69 DNA polymerase sensitive to drugs targeting the cytomegalovirus enzyme.
Journal of Biological Chemistry. Submitted

Tchesnokov E.P., Obikhod A., Massud I., Lisco A., Vanpouille C., Brichacek B., Balzarini J., McGuigan C., Derudas M., Margolis L., Schinazi R. F. and Götte M.
Mechanisms associated with HIV-1 resistance to acyclovir by the V75I mutation in reverse transcriptase.
Journal of Biological Chemistry. Submitted

Tchesnokov EP, Obikhod A, Schinazi RF, and Götte M.
Delayed chain-termination protects the anti-HBV drug entecavir from excision by HIV-1 reverse transcriptase.
J Biol Chem. 2008 Dec 5;283(49):34218-28

The contribution of co-authors to published or submitted articles appears in the section "CONTRIBUTIONS OF AUTHORS". The journal of submission and information from published articles can be found on the title page of the concerned chapters.

Other manuscripts not included in this thesis, but to which a significant contribution was made by the candidate, are listed as follows:

Marchand B, **Tchesnokov EP**, Götte M.
The pyrophosphate analogue foscarnet traps the pre-translocational state of HIV-1 reverse transcriptase in a Brownian ratchet model of polymerase translocation.
J Biol Chem. 2007 Feb 2;282(5):3337-46.

Lisco A, Vanpouille C, **Tchesnokov EP**, Grivel JC, Biancotto A, Brichacek B, Elliott J, Fromentin E, Shattock R, Anton P, Gorelick R, Balzarini J, McGuigan C, Derudas M, Götte M, Schinazi RF, Margolis L.
Acyclovir is activated into a HIV-1 reverse transcriptase inhibitor in herpesvirus-infected human tissues.
Cell Host Microbe. 2008 Sep 11;4(3):260-70.

Ehteshami M, Scarth BJ, **Tchesnokov EP**, Dash C, Le Grice SF, Hallenberger S, Jochmans D, Götte M.
Mutations M184V and Y115F in HIV-1 reverse transcriptase discriminate against nucleotide-competing reverse transcriptase inhibitors**.**
J Biol Chem. 2008 Oct 31;283(44):29904-11.

Ehteshami M, Beilhartz GL, Scarth BJ, **Tchesnokov EP**, McCormick S, Wynhoven B, Harrigan PR, Götte M.
Connection domain mutations N348I and A360V in HIV-1 reverse transcriptase enhance resistance to 3'-azido-3'-deoxythymidine through both RNase H-dependent and -independent mechanisms.
J Biol Chem. 2008 Aug 8;283(32):22222-32.

ACKNOWLEDGEMENTS

I would first like to thank my supervisor, Matthias Götte, for his unconditional support throughout my studies, especially when good data was scarce.

I am grateful to my parents, Petr Petrovitch Chesnokov and Maria Lvovna Chesnokova.

I would like to thank my wife, Yesim Sökmen, without whom this thesis would have never happened.

I would like to thank Paula Lavery for teaching me the discipline of a lab life.

I would like to thank Dr. Jérome Deval for teaching me the pre-steady state kinetics as well as his involvement in my other projects.

I would also especially like to thank Dr. Bruno Marchand and Dr. Claudia D'Abramo for the assistance that they have given me in my earlier days in Matthias' lab.

I would like to thank Suzanne McCormick for her kind assistance throughout the years.

I would like to thank the current and former members of Matthias' lab for their friendship and their support: Stephen Barry, Aneeta Mistry, Rose Chen, , Meoin Hagege, Maryam Ehteshami, Dimitry Coutsinos, Brian Scarth, Greg Beilhartz, Dr. Konstantin Ivanov, Megan Powdrill, Jordan Gagnon, Colin Vasquez, Mia Biondi and Jean Bernatchez.

I would also like to thank Colin Vasquez, Greg Beilhartz, Brian Scarth for proofreading this manuscript and Jean Bernatchez for translating the abstract in French.

I would like to thank Dr. Jan Ryder for final proofreading and editing the manuscript.

CONTRIBUTIONS OF AUTHORS

The manuscript entitled “Role of helix P of the human cytomegalovirus DNA polymerase in resistance and hypersusceptibility to the antiviral drug foscarnet” was written in collaboration with Dr. C. Gilbert and Dr. G. Boivin, who provided the nucleic acid sequences of the HCMV DNA polymerase.

The manuscripts entitled “Engineering of a chimeric RB69 DNA polymerase sensitive to drugs targeting the cytomegalovirus enzyme” and “Delayed chain-termination protects the anti-HBV drug entecavir from excision by HIV-1 reverse transcriptase” were written in collaboration with Dr. A. Obikhod and Dr. R.F. Schinazi who synthesized acyclovir.

The manuscript entitled “Mechanisms associated with HIV-1 resistance to acyclovir by the V75I mutation in reverse transcriptase” was written in collaboration with Dr. A.Obikhod, Dr. I. Massud, Dr. A. Lisco, Dr. C. Vanpouille, Dr. B. Brichacek, Dr. J. Balzarini, Dr. C. McGuigan, Dr. M. Derudas, Dr. L. Margolis and Dr. R.F. Schinazi. Dr. A. Obikhod and Dr. R.F. Schinazi synthesized acyclovir. Dr. C. McGuigan and Dr. M. Derudas synthesized CF2648. Dr. I. Massud, Dr. A. Lisco, Dr. C. Vanpouille, Dr. B. Brichacek, Dr. J. Balzarini and Dr. L. Margolis were responsible for the selection of resistance with CF2648 and genotyping of the drug-exposed HIV -1 strains (Table 1). Tchesnokov E.P. conducted the rest of the experimental work (Tables 2 and 3, Figures 2, 3, 4, 5, 6, 7 and S1).

FREQUENTLY USED ABBREVIATIONS

ACV, acyclovir

ACV-MP, acyclovir-monophosphate

ACV-TP, acyclovir-triphosphate

DEC, dead-end complex

dNTP, deoxyribonucleotide

EEM, excision enhancing mutations, also known as thymidine analogue-associated mutation, TAM

gp43, catalytic subunit of the RB69 DNA polymerase

NRTI, nucleoside-analogue RT inhibitor

NNRTI, non-nucleoside-analogue RT inhibitor

PFA, foscarnet

PPi, pyrophosphate

RT, reverse transcriptase

TK, thymidine kinase

UL30, catalytic subunit of the HSV DNA polymerase

UL54, catalytic subunit of the HCMV DNA polymerase

TABLE OF CONTENTS

CHAPTER 1

INTRODUCTION

1.1 History of antivirals

A virus is an obligate intracellular parasite. The course of a viral infection is thus a complex interplay between viral and host cell processes, defined as a viral life cycle. Potentially, any of these processes—viral or cellular—can be exploited by antiviral agents to disrupt an infection. With only few exceptions such as interferon alpha and maraviroc [1, 2], the majority of current antiviral regimens target viral processes. In particular, although recent antiviral developments have targeted a variety of steps in the viral life cycle, viral enzymes that catalyze replication of the viral genome remain the main subject of currently available antiviral therapies (Table 1.1).

In the context of a multicellular organism such as a human being, certain viral characteristics are of particular interest: (1) the ubiquitous penetration of host cells by some viruses, while infections with others lead to host cell tropism, and (2) the capacity of ubiquitous and tropic viruses to establish latent infections. Therefore, regardless of the possibility of several heterogeneous viruses infecting the same cell, which is nonetheless observable (discussed in detail in the section *Co-infection*), viral infection as a concept implies a co-infection: at the level of a multicellular organism involving different cells, and/or at the level of a single cell.

The objective of this chapter is to give the reader some historical perspective on the development of antiviral drugs that inhibit viral genome replication, stressing drugs with dual or multiple antiviral activities. The examples of four viruses, namely, herpes simplex virus (HSV-1, HSV-2), human cytomegalovirus (HCMV), hepatitis B virus (HBV) and human immunodeficiency virus 1 (HIV-1), will be used to place viral enzymes and the antiviral drugs implicated in viral genome replication within the context of the viral life cycle.

In 1959, the idea that viral replication could be inhibited by a synthetic chemical substance was first supported by the discovery of idoxurine [3], which became the

first antiviral drug to treat herpes keratitis [4-6]. Evidence that adenine arabinoside inhibited DNA and RNA viruses [7], and that acyclic side chains could be recognized as a pentose by adenosine deaminase [8], prompted Gertrude B. Elion to investigate the antiviral activity of acyclic purine nucleosides [9]. This led to the discovery of a purine nucleoside analogue, acyclovir (ACV) (Figure 1.1). This antiviral drug exhibits low toxicity towards the host, but is highly potent and selective for treating both HSV-1 and HSV-2 as well as varicella zoster virus (VZV) infections [10-14]. Elion and George H. Hitchings together shared the Nobel Prize in Medicine in 1988 in part for their discovery of acyclovir.

Acyclovir is a synthetic analogue of a natural nucleoside 2´-deoxyguanosine. Nucleosides consist of a cyclic 5-carbon sugar moiety, ribose and a nucleobase (Figure 1.2). To become substrates for the nucleic acid synthesis during genome replication, nucleosides have to be phosphorylated by cellular kinases. The phosphorylation occurs at the 5`-hydroxyl of the ribose in three successive steps. This generates a nucleoside triphosphate with α-, β- and γ-phosphates. Nucleic acid synthesis is catalyzed by nucleotidyl transferases commonly referred to as DNA or RNA polymerases. In this reaction, the 3`-hydroxyl of the preceding nucleotide conducts a nucleophilic attack on the α-phosphate of the incoming nucleotide substrate. The result of this attack is the formation of the phosphodiester bond between the 3`-oxygen of the preceding nucleotide and the α-phosphate of the incorporated nucleotide. As a byproduct of the reaction, the β- and γ-phosphate moiety, or pyrophosphate, is released. The double-stranded nature of the nucleic acid is generated by the hydrogen bonding between the nucleobases of the incoming and templating nucleotides.

Acyclovir is uniquely phosphorylated compared with natural nucleosides. In herpes-infected cells, the prodrug form of acyclovir is phosphorylated by both cellular and viral kinases. The addition of the α-phosphate to form ACV-monophosphate (ACV-MP) is specifically catalyzed by the herpes virus

thymidine kinase [13]. Subsequent di- and tri-phophorylation by cellular kinases yields the activated ACV-triphosphate (ACV-TP) [15, 16].

The addition of the α-phosphate by a cellular enzyme is also possible, but this reaction is inefficient [17]. As a result, very little of ACV-MP is formed in uninfected cells [18], thereby explaining the high specificity and low toxicity of acyclovir. Furthermore, ACV-TP as a substrate is preferred more by the herpes DNA polymerase as compared with cellular DNA polymerases [19, 20].

The potency of ACV-TP against herpes-virus DNA polymerases is explained by its molecular mechanism of action. ACV-TP competes with its natural substrate counterpart, 2´-deoxyguanosine-triphosphate (dGTP), for nucleotide incorporation. Once incorporated, ACV-MP acts as an obligate chain terminator owing to a lack of the 3`-hydroxyl group. Consequently, herpes DNA polymerase forms a stable dead-end complex (ACV-MP-terminated primer-template and the next incoming nucleotide) such that the enzyme-associated 3`-5` exonuclease activity cannot remove the incorporated ACV-MP [10, 21].

In 1981, acyclovir was approved for the clinical treatment of herpes infections (Table 1.2). But despite its excellent characteristics, treatment with acyclovir eventually generates viral resistance to the drug at the level of the virally encoded thymidine kinase and/or DNA polymerase [22]. At the time, the only option for treating an ACV-resistant herpes infection was a pyrophosphate analogue, foscarnet.

Foscarnet is a broad-spectrum antiviral drug (Figure 1.3). It is active against DNA viruses such as HCMV and HSV-1 of the *Herpesviridae* family, as well as retroviruses, namely HIV [23, 24]. The similarity between foscarnet and naturally occurring pyrophosphate confers high cellular toxicity. Thus, foscarnet usage is limited to anti-herpetic and anti-HIV salvage therapy—when the first-line antivirals have failed because of drug resistance [25, 26].

Similar to acyclovir, treatment with foscarnet also results in resistant viruses [22]. In the context of HIV infection, foscarnet has an advantageous resistance profile. Mutations that reduce the effectiveness of the treatment with anti-HIV nucleoside and non-nucleoside analogue inhibitors do not affect the susceptibility of the virus to foscarnet in most cases [27-29]. On the other hand, mutations that generate resistance to foscarnet have been reported to increase susceptibility to zidovudine, an anti-HIV nucleoside analogue [30, 31].

The precise molecular mechanisms of drug action and drug resistance associated with foscarnet remain largely unknown. It has been concluded on the basis of scarce biochemical data that foscarnet acts noncompetitively with respect to the deoxynucleotide triphosphate substrate [32, 33]. It has also been suggested that the pyrophosphate analogue binds to a site close to the active center, which may overlap, at least in part, with the pyrophosphate binding site [34]. But in the context of the HIV-1 reverse transcriptase (RT), it has been recently shown that foscarnet traps the HIV-1 RT/nucleic acid complex in a conformation that precludes binding of the next incoming nucleotide [35]. The mechanism of foscarnet action against other viruses, especially against HCMV, remains to be determined.

Acyclovir and foscarnet are of particular interest in the context of co-infection. As acyclovir was being approved as an effective anti-herpes treatment, a new disease was rapidly spreading in humans. Interestingly, the most prevalent manifestations of this disease included both HCMV and HSV infections [36, 37]. At the time, persistent HSV infections for more than a month combined with infections by other pathogens were used to define what would later be termed acquired immune deficiency syndrome, or AIDS [38]. Therefore, the nature of AIDS represents an example of co-infection with multiple pathogens, including multiple viruses. The virus responsible for the onset of AIDS was identified in 1983, and was later on named HIV-1 [39, 40]. The first anti-HIV specific drug became available only in

1987 [41]. Thus, for almost 6 years, acyclovir and foscarnet were commonly used to treat HCMV and HSV infections in HIV-infected individuals [36-38, 42, 43].

In principle, drugs with dual or multiple antiviral activities may seem beneficial in the context of co-infection. For example, the synergy between HIV-1 and HSV-2 infections has been recognized [44], and benefits of treating HSV-2 infection on the status of HIV-1 infection have been also documented [45, 46]. It has recently been shown that acyclovir expresses dual antiviral activity, inhibiting both human herpesvirus 6 (HHV-6) and HIV-1 [47]. A subsequent study illustrated *in vitro* that acyclovir can select for a mutation in HIV-1 RT that confers resistance to the anti-HIV drug, lamivudine. The occurrence of the V75I mutation within HIV-1 RT further illustrated the selection of anti-HIV drug-resistant mutations by acyclovir [48]. These findings suggest that selective pressure by acyclovir treatment may be sufficient to generate resistance prior to initiating HIV-specific antiviral therapy. Thus, using drugs with dual or multiple antiviral activities can be foreseen only after the precise mechanism of their antiviral action and/or resistance is known. The precise molecular mechanism of resistance to acyclovir by HIV-1 remains to be explained.

The discovery of zidovudine [49], a nucleoside analogue of thymidine, and its approval for clinical use in HIV-infected patients in 1987, was followed by the discovery of more than 20 anti-HIV drugs (Table 1.3) [41, 50]. In the context of co-infection, one of these anti-HIV drugs, lamivudine, is of particular interest: in addition to being active against HIV, it is also used for treating HBV infections [51]. The US Food and Drug Administration (FDA) approved its use in anti-HIV therapy in 1995 [52]. Subsequently it became the first nucleoside analogue to be approved for treatment of chronic HBV infection in 1998 (Table 1.4) [53].

Lamivudine is a cytidine analogue that targets the DNA polymerases of HIV-1 and HBV through a chain termination mechanism [54, 55]. Treatment with lamivudine generates drug resistance that maps to a single amino acid substitution

(M184V and M204V in HIV-1 RT and HBV-RT, respectively) within a highly conserved region among DNA polymerases, that is, the YMDD motif. In addition, the lamivudine target sites of both the HIV and HBV polymerases are structurally similar. This exemplifies the possibility that dual anti-viral activity may be extended to other drugs.

Entecavir is a potent anti-HBV polymerase drug (Table 1.4) [56-58]. It was approved by the FDA in 2005 for treating patients with HBV and HIV/HBV infections. But although entecavir treatment has been shown to have an excellent resistance profile in HBV patients [59], the drug has recently been reported to also possess an anti-HIV activity [59-61]. Importantly, entecavir therapy in HIV/HBV co-infected patients selects for the M184V mutation within HIV-1 RT [60], which imposes limitations on entecavir use in the context of HIV/HBV co-infection [60, 62].

Entecavir is a 2`-deoxyguanosine analogue. It differs from other nucleoside analogues in that it contains a 3`-hydroxyl group on the ribose moiety (Figure 1.4). This feature disqualifies it as an obligate chain terminator. Although non-obligate chain terminators with anti-herpes [63] or anti-HIV activity have been reported [64], entecavir is the first drug of this type to combine both anti-HIV activity and low toxicity [65, 66]. This suggests a potential use of entecavir as a model for the future development of anti-HIV drugs. Entecavir also has an interesting aspect in the context of HBV/HCV co-infection. *In vitro* studies have reported that ribavirin, an anti-HCV drug, showed a synergistic potency with entecavir against HBV wild-type as well as lamivudine-resistant mutants [67].

The examples of ACV and ETV as antiviral drugs with dual or multiple activity illustrate a dichotomy of their therapeutic application. On one hand, these drugs can be deleterious in that they can generate drug resistance in one of the viruses prior to initiation of the respective antiviral therapy; in HBV/HIV and HSV/HIV co-infected individuals, the anti-HIV treatment is not started at the diagnosis but

rather when the number of CD4+ cells reaches a critical minimum. On the other hand, these antivirals may be beneficial by preventing the synergy between the co-infecting viruses. They can also be used as models for the next generation of antiviral drugs. Knowing the precise mechanism of action and resistance to drugs with dual or multiple antiviral activities is a prerequisite for their efficient use in current therapy and future drug development.

In this thesis I focus on the mechanisms of action in terms of how compounds with dual or multiple antiviral activities interact with DNA polymerases as their targets.

1.2 Viruses

Viruses can be classified as DNA or RNA viruses based on the genome of their infectious particles. Human herpes viruses and HBV are DNA viruses, whereas HIV is an RNA virus. HBV and HIV are similar in that their replication cycle involves a step where viral RNA is retrotranscribed into a DNA intermediate. But reverse transcription is an error-prone process. In addition, the genome replication machinery of HBV and HIV does not have a proofreading function to correct for replication errors. Thus, HBV and HIV exist as a population of variant quasispecies [68] whose relative distribution is a function of their respective fitness [69]. The concept of genomic quasispecies has had a profound effect on the study of resistance to antiviral drugs [70]. Finally, common to the aforementioned viruses is the persistence of the viral DNA in the host cell, which is the source of the latent phase in the viral life cycle. None of the currently available antiviral treatments is capable of targeting viral latency specifically and efficiently. Resistance to antiviral regimens and reactivation of viral infection owing to the latent phase remain the two main problems associated with antiviral therapy. But as the history of acyclovir shows, significant progress has been made in dealing with the toxicity of the antiviral regimens.

The human *Herpesviridae* family consists of eight viruses that are partitioned into three subgroups based on the sequence alignment of the conserved structural protein gH: *Alpha*-, *Beta*- and *Gammaherpesvirinae*. HSV-1 and HCMV, discussed in detail in this thesis, are members of the *Alphaherpesvirinae* and *Gammaherpesvirinae* subgroups, respectively. All human *Herpesviridae* viruses share a number of features. The infectious particle consists of a nucleocapsid containing genomic DNA, an envelope embedding viral glycoproteins and a tegument located in the space between the nucleocapsid and the envelope. These viruses also go through a latent viral life cycle and will subsequently reactivate if the host immune system is suppressed. Hence, these viruses are important in immunocompromized individuals. Lastly, they have a relatively high prevalence in the human population, reaching almost 100% for VZV, HHV-6 and HHV-7 [71].

The HBV belongs to the *Hepadnaviridae* family. This viral family includes two genera based on the nature of the host: the *Orthohepadnavirus*, members of which infect mammals, and the *Avihepadnavirus*, members of which infect birds [72]. HBV belongs to the *Orthohepadnavirus* genus. The woodchuck hepatitis virus and the duck hepatitis B virus of the *Orthohepadnavirus* genus were extensively used to study the mechanisms of viral replication. Moreover, the respective woodchuck and duck models provided a means to assess potential anti-HBV drugs [73]. The particularity of HBV is a partially double-stranded DNA genome as compared with fully double-stranded herpes DNA viruses.

Retroviruses are characterized by a diploid positive sense ((+)) RNA genome and a retrotranscription step in their life cycle. On the basis of the sequence conservation of the reverse transcriptase, the *Retroviridae* family is organized into seven genera, which can be further subgrouped into simple and complex retroviruses. The genome of complex retroviruses encodes for a set of regulatory and accessory proteins in addition to prototypic structural proteins and the reverse

transcriptase. HIV-1 and HIV-2 belong to the complex retroviruses of the *Lentivirus* genus [74].

1.2.1.1 HSV virology

The incidence of HSV-1 and HSV-2 in industrialized countries is approximately 50% and 20%, respectively [75]. HSV-1, HSV-2 and the varicella-zoster virus belong to the *Alphaherpesvirinae* subfamily, and are neurotropic viruses. Productive HSV infection of a cell proceeds through the following main steps: entry, viral gene expression, viral genome replication, virion assembly, viral DNA encapsidation and exit of the infectious viral particle [76]. In addition to this lytic life cycle, HSV can establish a latent infection, where the viral genome is located in the nucleus of the cell as a circular, extra-chromosomal DNA [77]. The mechanism of silencing viral gene expression in latently infected cells is poorly understood [78].

The HSV-1 viral genome is 152 kbp, and its complete DNA sequence was established in 1988 [79]. It consists of 74 identified genes that encode viral proteins [80]. The viral genes have been classified, based on their temporal expression, as immediate early, early and late [81]. Immediate early genes are responsible for regulating viral gene expression and modulating the cellular immune response [82, 83]. Early-gene products are involved in viral DNA replication or nucleic acid metabolism. Lastly, late genes encode proteins responsible for virion formation and composition [84].

Seven viral early-gene products were found to be essential for viral genome replication [85]. These products include an origin binding protein (UL9), a single-stranded (ss) DNA binding protein (UL29), a helicase/primase complex and a DNA polymerase holoenzyme [86-88]. The UL9 contains ATP-binding and DNA helicase motifs. UL9 binds to one of three possible origins of replication within the HSV genome. This binding bends and distorts the DNA such that a single-

stranded stem loop structure is formed [89]. UL29 binds ssDNA regions and promotes the helicase function of UL9 as well as the activity of the helicase/primase and DNA polymerase complexes [90-92]. The helicase/primase complex consists of three viral proteins, UL5, UL8 and UL52. The enzymatic activity is generated by ATP-binding and helicase motifs within UL5, and by the divalent metal-binding motif in UL52. UL8 stimulates the enzymatic activity of the UL5/UL52 subcomplex [93].

The HSV DNA polymerase holoenzyme is a heterodimer consisting of UL30 (catalytic subunit) and UL42 (accessory protein) [94, 95]. UL30 contains 5`-3` polymerase and 3`-5` exonuclease activities [96], which serves as a proofreading tool in maintaining the fidelity of genome replication [97]. UL42 increases the processivity of the catalytic subunit [98]. UL30/UL42 interaction is required for viral DNA replication [99]. The HSV polymerase catalytic subunit belongs to the family B, or α-like, polymerases [100], based on the sequence conservation between DNA polymerases. Members of this family are defined by the presence of several conserved domains constituting polymerase and exonuclease functions (Table 1.5). Several crystal structures of the family B bacteriophage Rb69 DNA polymerase have been reported [101-103]. These data provided direct evidence for the overall orientation of and conformational changes within the polymerase/nucleic acid complex during polymerase or exonuclease (editing) mode. Recently, a crystal structure of the catalytic subunit of the HSV polymerase in the absence of nucleic acid or a nucleotide substrate was resolved [104]. These data translated the sequence similarity of the conserved regions into an overall structural conservation of the polymerase and exonuclease domains of the catalytic subunit of the HSV polymerase as a member of the family B polymerases. In addition, the authors revived the controversial issue of the ribonuclease H (RNase H) function within the HSV polymerase [94] by assigning a possible RNase H activity to the N-terminal portion of the polymerase.

Other viral proteins participate in DNA replication, including the thymidine kinase, ribonucleotide reductase, uracil glycosylase and deoxyuridine triphosphatase [82]. These proteins are involved in nucleotide metabolism. This finding supports the notion that viral DNA replication can occur in resting cells, such as neurons, where the nucleotide pools are limited [78].

1.2.1.2 HSV therapy and drug resistance

Currently approved anti-HSV drugs include the acyclic guanosine-nucleoside analogs acyclovir and penciclovir (PCV) and their respective oral prodrugs valacyclovir (L-valyl ester of acyclovir) and famciclovir (Figure 1.1 and Table 1.2) [105-107]. Penciclovir's mode of action against HSV is very similar to acyclovir's: both compounds require selective monophosphorylation by the virally encoded thymidine kinase (vTK) [105], and they both have higher affinity for viral than for cellular DNA polymerases [108, 109]. But some differences do exist [110]. In the context of an infected cell, penciclovir has a higher affinity for vTK than acyclovir does at the level of monophosphorylation [111], which leads to higher intracellular levels of penciclovir [109]. In addition, PCV-TP is more stable intracellularly [105]. In the context of drug/HSV DNA polymerase interaction, PCV-TP has a lower affinity for the polymerase than ACV-TP does [112]. Nonetheless, taking into account a better phosphorylation by vTK makes penciclovir similar in its overall antiviral effect [110].

The most important difference between the two compounds is structural. Acyclovir is an obligate chain terminator. On the other hand, the acyclic side chain of penciclovir does have the functional analogue of a 3`-hydroxyl group, which disqualifies it as an obligate chain terminator. While an ACV-MP-mediated chain termination of DNA synthesis occurs at the site of drug incorporation, PCV-MP generates a chain terminating effect several nucleotides downstream. Interestingly, the efficiency of the abruption of DNA synthesis is higher with penciclovir [112]. Although the incorporated ACV-MP cannot be excised by the

3`-5` exonuclease activity of the HSV-1 DNA polymerase [10], little is known about the mechanism of incorporated PCV-MP/exonuclease interaction.

Treatment with acyclovir leads to resistance in immunocompetent patients in 0.3% of cases [113]. In immunocompromized individuals, the resistance is significantly higher, reaching as high as 6% [114-116]. In the context of ACV-resistant infections, treatment with foscarnet generated foscarnet resistance in 61% of immunocompromized patients. Acyclovir action requires both vTK and a DNA polymerase, but most clinical drug-resistant HSV isolates are generated by mutations in vTK [117, 118]. vTK contains three catalytic sites: ATP- and nucleoside-binding and amino-acid residue 336 [119]. Mutations within these regions can alter vTK function, resulting in drug resistance at the level of monophosphorylation of the nucleoside analogues [22]. Mutant vTKs are grouped according to their function: vTK-negative (vTKn), vTK-partial and vTK-altered (vTKa) [110]. vTKa mutants maintain the ability to phosphorylate thymidine, but not acyclovir or penciclovir. The majority of mutants are vTKn and vTKp [117]. vTKn HSV isolates tend to be resistant to both acyclovir and penciclovir [120].

Clinical drug-resistant HSV isolates that bear mutations in their DNA polymerase have been identified [121-123], but their contribution to drug-resistant HSV is relatively small [22, 110]. In principle, resistance to acyclovir or penciclovir at the level of the HSV DNA polymerase can be explained either by reduced affinity of the mutant polymerases for the drugs, or increased excision of incorporated ACV- and PCV-MP by the 3`-5` exonuclease activity of the HSV polymerase. Mapping of the majority of drug resistant mutations to conserved regions coding for polymerase or exonuclease activity within the HSV polymerase supports this notion [22], although the precise mechanism of resistance at the level of the HSV polymerase has yet to be reported.

The future in drug development for HSV infection follows two directions: exploring other proteins essential to the viral life cycle as drug targets, and

attempting to control viral latency and reactivation. For example, inhibitors of HSV helicase/primase, an enzyme that is essential for replicating viral DNA [124-126], have been shown to inhibit HSV-1 and -2 replication *in vivo* better than ACV [124, 127]. Furthermore, the new drug resiquimod, a modulator of innate immunity, was shown to be effective in preventing reactivation of genital HSV in a Phase II clinical trial [128].

1.2.2.1 HCMV virology

The incidence of HCMV is lower in industrialized countries (40-60%) than in the developing world, where it approaches 100% [71, 129]. HCMV infection is a major cause of birth defects [130] and morbidity/mortality in transplant patients [131]. Since the clinical benefits of introducing highly active antiretroviral therapy (HAART) may take months to observe, and because of possible unresponsiveness to and unavailability of treatment, HCMV continues to be an important pathogen in patients with HIV/AIDS [132].

HCMV, HHV-6 and HHV-7 belong to the *Betaherpesvirinae* subfamily. The cell tropism of this subfamily is not well defined [133]. Productive HCMV infection was shown to occur in a wide range of epithelial tissues [134] as well as in endothelial, smooth muscle and mesenchymal cells, and hepatocytes, granulocytes and monocyte-derived macrophages [135]. This correlates with HCMV multiorgan involvement.

HCMV infections proceed through the viral life cycle and temporal gene expression similarly to HSV, as discussed above. The structure and composition of the infectious viral particle is similar to HSV, but different in that it also contains five viral mRNAs whose functions remain to be determined [136]. The HCMV viral genome is 230 kbp double-stranded linear DNA, which is the largest of the *Herpesviridae* family [137]. HCMV differs from other members of the *Herpesviridae* in that its genome does not encode a viral thymidine kinase as well

as other viral enzymes involved in DNA biosynthesis [138]. Therefore, instead of downregulating host transcription and translation, HCMV infection stimulates cellular gene expression. For example, an increase in cellular thymidine kinase expression was shown upon HCMV infection [139, 140]. HCMV prevents possible competition with cellular DNA replication by blocking the host cell-cycle progression [141]. Thus, even though both HSV and HCMV infect non-dividing cells, they take very different approaches to dealing with limited DNA precursor synthesis: HSV1 encodes its own deoxyribonucleotide biosynthetic enzymes, while HCMV has to upregulate the host cell expression of those enzymes.

The HCMV viral replication machinery is similar to that of HSV in that it is based on the functional and physical cooperation between proteins specialized in genome replication: origin-binding/activating and ssDNA-binding proteins, helicase/primase heterotrimer and the DNA polymerase holoenzyme [137]. The HCMV DNA polymerase holoenzyme, as well as the HCMV protein kinase, is of particular interest in the context of anti-HCMV therapy.

The HCMV DNA polymerase holoenzyme consists of two subunits: (1) a catalytic subunit (UL54), which is responsible for the nucleotide incorporation reaction [142, 143], and (2) an accessory protein (UL44), which acts as a processivity factor [144] and is essential for HCMV genome replication [145]. UL54 is similar to its HSV counterpart in that it also possesses a 3`-5` proofreading exonuclease activity [146].

The catalytic subunits of the HSV and HCMV polymerases show a high degree of sequence, and possibly structural homology [104, 147]. Herpesvirus DNA polymerases belong to the α-family (or family B) of viral and cellular DNA polymerases [100], based on the sequence conservation among polymerases. A member of this family, the DNA polymerase of bacteriophage RB69 (gp43), is frequently used as a structural model to study the structure/function relationship

of herpesvirus DNA polymerases. Structurally, DNA polymerases resemble a partially open right hand consisting of structurally conserved regions: the palm, fingers and thumb subdomains [101, 148]. The conserved residues of the palm are responsible for catalysis, the fingers subdomain is involved in coordinating the binding of the next incoming nucleotide and the single-stranded DNA template, while the thumb domain interacts with the minor groove of duplex DNA [149]. Recently, a crystal structure of the catalytic subunit of the herpes simplex virus polymerase has been reported, supporting the open right hand analogy, as have molecular modeling studies on UL54 [104, 147].

Several sequence-conserved regions of the family B polymerases have been identified within the herpesvirus DNA polymerases (Table 1.5) [100]. Regions I – VII are involved in the DNA polymerization reaction [150], motifs ExoI - III contain conserved amino acids that constitute the 3`-5` exonuclease function of family B DNA polymerases and δ-region C represents an overlap between the two functions [151, 152]. Within the context of the HCMV DNA polymerase, it has been reported that regions I – III are involved in coordinating the binding of the primer/template, the incoming nucleotide and magnesium ions [153].

HCMV encodes a serine/threonine phosphotransferase that shares several conserved regions with the protein kinase family [154]. This protein kinase (UL97) is a multifunctional protein that is important in the HCMV replication cycle [155]. It may be involved in the pre-elongation step during DNA synthesis [156], and it is required for viral DNA encapsidation and/or assembly [157] and viral nuclear egress [158]. Most importantly, it was reported that UL44 is a natural substrate for UL97 [159]. Finally, UL97 is the only herpesvirus kinase that selectively monophosphorylates the anti-HCMV drug ganciclovir and not the natural nucleosides [160, 161]. Amino-acid substitutions that confer resistance to the anti-HCMV regimen tend to cluster within the conserved regions of the UL54 and UL97 gene products [132].

1.2.2.2 HCMV therapy and drug resistance

Currently approved drugs for anti-HCMV therapy can be grouped into three classes according to their targets: (1) drugs that target the HCMV DNA polymerase: ganciclovir [162], its oral prodrug valganciclovir [163], cidofovir [164] and foscarnet; (2) maribavir, a drug that targets the viral protein kinase [165]; and (3) fomivirsen, a drug that targets viral mRNA (Table 1.6) [166].

Ganciclovir (GCV) is an acyclic nucleoside analogue of 2´-deoxyguanosine (Figure 1.1). Its mechanism of action is similar to acyclovir's but with some differences. Ganciclovir was shown to be better phosphorylated than acyclovir in HCMV-infected cells, which translated into improved anti-HCMV activity [140]. Ganciclovir is specifically monophosphorylated by the HCMV-encoded protein kinase UL97 [160, 167], followed by di- and triphosphorylation by cellular enzymes [160, 167]. GCV-TP competes with its natural counterpart, dGTP, for binding to the HCMV polymerase, while having a higher affinity for HCMV than for cellular polymerases [168]. In contrast to acyclovir but similar to penciclovir, the incorporated GCV-MP is not an obligate chain terminator because it does have the functional equivalent of a 3´-hydroxyl group. Thus, it was shown that DNA synthesis stalls at a site one nucleotide after GCV-MP incorporation [168]. The exact nature of interaction between the chain-stalled primers containing GCM-MP and the 3`-5` exonuclease activity of UL54 remains to be determined. Valganciclovir is the L-ester of ganciclovir and is rapidly converted to ganciclovir by cellular enzymes. Its principal advantage over ganciclovir is a 10-fold higher oral bioavailability [169].

Cidofovir (CDV or HPMPC) is an acyclic nucleoside phosphonate analogue of the 2´-deoxycytidine monophosphate (dCMP) (Figure 1.1). Cidofovir's mechanism of action differs from that of nucleoside analogues in that it does not require monophosphorylation by a virally encoded protein kinase since it already has a monophosphate group [170]. Cidofovir is a phosphonate because the

phosphate group is attached to the nucleoside through a phosphonomethyl ether linkage, rather than through a phosphate ester as in monophosphorylated nucleosides, acyclovir or ganciclovir, for example (Figure 1.4). This makes cidofovir and other phosphonates resistant to an attack by cellular esterases, thereby improving the intracellular stability of the compound [164]. Cidofovir is converted to its putative antiviral metabolite HPMPC-diphosphate (HPMPCpp) by cellular enzymes [171]. Similar to acyclic nucleosides, HPMPCpp is a competitive inhibitor of dCTP and is an alternate substrate for the viral polymerase [172]. In the same study it was shown that incorporation of cidofovir did not result in an immediate chain termination, since incorporation of the next nucleotide was possible. The same group subsequently showed that the incorporated cidofovir could not be excised by the 3'-5' exonuclease activity of the viral polymerase and that chain termination occurred after sequential incorporation of two cidofovir molecules [173]. Treatment with cidofovir causes significant renal toxicity; hence, it is used primarily as a second-line therapy [155].

Foscarnet (PFA) is a trisodium salt of phosphonoformic acid, which is a pyrophosphate analogue (Figure 1.3). It has been suggested that the mechanism of foscarnet action involves reversible binding to, or in close proximity to, the pyrophosphate binding site, thereby inhibiting the release of pyrophosphate [23, 174]. Thus, foscarnet is an inhibitor of the product release of the reaction of nucleotide incorporation. Foscarnet does not require any activation by cellular or viral enzymes. Because of its toxicity, foscarnet is considered a second-line antiviral drug and is reserved for patients who have failed ganciclovir therapy [175].

Maribavir (MBV) (1-(β-L-ribofuranosyl)-2isopropylamino5,6-dichlorobenzimidaszole) is a riboside analogue. The antiviral activity of maribavir against clinical ganciclovir and foscarnet-resistant HCMV isolates was first reported in 2002 [156]. The same report showed that even though it is a riboside

analogue, maribavir was not inhibiting viral DNA polymerase, but instead was specifically inhibiting the viral protein kinase (UL97). In addition, maribavir resistance mapped to the gene coding for UL97. Since the UL97 protein kinase is a multifunctional enzyme (as discussed above), it has been suggested that maribavir may inhibit HCMV replication through at least two different mechanisms: (1) by preventing the phosphorylation of the polymerase accessory subunit by UL97 [159, 176], and (2) by interfering with the role of UL97 in the HCMV nucleocapsid egress [158]. Subsequently, maribavir activity against cidofovir-resistant HCMV has been reported [177]. But maribavir has been also reported to be counterproductive with respect to ganciclovir [178]. The exact mechanism of maribavir anti-HCMV activity remains to be determined, since a maribavir-resistant mutant that did not have alterations in the UL97 gene has been reported [179].

Fomivirsen is a 21-nucleotide RNA that is complementary to the immediate early IE2 mRNA [180] encoded by the UL123 gene [137]. It specifically targets the immediate/early stage of viral replication. Fomivirsen possibly acts by trapping IE2 mRNA, thereby preventing its translation into the IE2 protein [155], which in turn inhibits HCMV genome replication. But the exact mechanism of fomivirsen anti-HCMV activity remains to be determined, since a fomivirsen-resistant mutant that did not have alterations in the UL123 gene has been reported [166].

Resistance to HCMV treatments is of particular concern in immunocompromized individuals. In HIV/HCMV co-infected patients, treatment with ganciclovir for more than 6 months results in resistance in 7-12% of HCMV isolates [181, 182]. Ganciclovir resistance is frequently associated with amino acid substitutions in conserved regions of UL54 and UL97 [132].Ganciclovir resistance-conferring mutations in UL97 involve the ATP- and substrate-binding regions [132]. Ganciclovir-resistant UL54 mutants are frequently also resistant to cidofovir [137], whereas UL97 mutants are not [155]. Ganciclovir-resistant UL54 mutants can also be resistant to foscarnet, but this cross-resistant phenotype is less

common [132]. Most ganciclovir/cidofovir resistance-conferring mutations map to the conserved regions coding for the exonuclease function of UL54 [132, 155].

Cidofovir resistance is relatively rare owing to its limited use as a second-line antiviral agent [183]. But clinical ganciclovir/cidofovir cross-resistant HCMV isolates have been reported [132]. Since cidofovir activation by phosphorylation is independent of the viral protein kinase, the ganciclovir resistant UL97 mutants remain sensitive to cidofovir therapy.

Resistance to foscarnet involves point mutations within the conserved regions of UL54 (Table 1.5). The most frequently observed foscarnet resistance-conferring mutations are located within conserved regions II, III and VI of UL54 [132]. Region III contains a cluster of ganciclovir, cidofovir and foscarnet resistance-conferring mutations. A point mutation in region III, A809V, also confers cross-resistance to ganciclovir [184]. Finally, a V812L substitution in region III of UL54 was shown to confer cross-resistance to ganciclovir, cidofovir and foscarnet [185, 186]. These observations suggest an important role for region III in the context of resistance to anti-HCMV therapy. Two observations can be made upon reviewing the drug resistance literature: (1) mapping of the nucleoside analogue resistance to the conserved regions involved in the 3'-5' exonuclease activity of UL54 has not been reconciled with reports showing that this function cannot remove the incorporated drugs, and (2) the relative importance of the conserved region III in drug resistance has not been assessed with respect to the role of this region in the catalysis of nucleotide incorporation by UL54. Part of this thesis deals with the second observation.

Mutations conferring resistance to maribavir have been identified *in vitro* [187, 188]. Another *in vitro* study reported no cross-resistance between maribavir and ganciclovir, nor between cidofovir and foscarnet [177]. But no maribavir-resistant clinical HCMV isolates have yet been reported [165, 189].

1.2.3.1 HBV virology

The total number of persons in the world with chronic HBV infection has been estimated at more than 350 million [190]. About 10% of chronic liver disease and cirrhosis in the USA is due to chronic HBV infection [191]. Vaccines to prevent HBV infections have been available since 1981 [192]. The vaccines are 95% effective, and their use from 1990 to 2005 produced a 78% decline in acute hepatitis B [193]. Nevertheless, the World Health Organization estimates that HBV is responsible for the deaths of 1 million people every year [194].

The HBV-infectious viral particle [195] consists of a lipid bilayer envelope embedding the hepatitis B surface antigen (HBsAg) and a nucleocapsid containing the viral genome [196]. The persistent presence of anti-HBsAg antibodies in the serum of a patient is used to diagnose a chronic HBV infection [197, 198]. The HBV genome is a 3.2-kilobase, circular, partially double-stranded DNA molecule. There are four overlapping open reading frames: P, S, C and X. The pre-S and S ORF are responsible for the expression of surface glycoproteins HBsAgs [199]. The pre-C and C ORF encode the polypeptide precursor of the soluble HBV e antigen and the nucleocapsid protein. ORF X encodes the regulatory protein X, which is required for HBV infectivity and pathogenesis [200]. Finally, ORF P generates the viral DNA polymerase with reverse transcriptase and RNase H activities [201, 202].

HBV genome replication involves three curious particularities: covalently closed circular DNA (cccDNA), pregenomic RNA (pgRNA) and the covalently linked polymerase/primer complex. cccDNA is generated in the nucleus of infected hepatocytes by repairing the partially double-stranded HBV genome. Host enzymes are responsible for completion of the shorter (+) strand and repair of the nick in the (-) DNA strand [203, 204]. cccDNA persists in the nucleus of infected hepatocytes [205], possibly through a recycling pathway from the cytosol [203]. It is thought to be the major cause of viral rebound associated with the cessation of

anti-HBV therapy [206]. As a matter of fact, the currently available anti-HBV regimen is not effective against cccDNA persistence in the host cell nucleus [207, 208] even after long-term therapy [209]. Though integration of HBV DNA into the host genome has been reported [210], it is not required for viral replication [194]. Thus, HBV is capable of maintaining an antiviral drug-induced latent state from the persistent cccDNA. cccDNA serves as a template for mRNA synthesis by host cell RNA polymerase II [72, 196]. In addition to mRNAs for the expression of viral proteins, a pgRNA of 3.5 kilobases is also synthesized and transported to the cytosol [211]. When the viral polymerase is produced, it interacts with the 5` end of the pgRNA, which triggers the encapsidation of the polymerase/pgRNA complex by the nucleocapsid protein [212]. pgRNA serves as a template for (-) DNA strand synthesis by the HBV polymerase.

The HBV DNA polymerase gene is subdivided into four coding regions: terminal protein (TP), spacer domain, reverse transcriptase (RT) and ribonuclease H (RH) [213]. Each is responsible for the corresponding function of the polymerase: DNA priming, reverse transcription and degradation of pgRNA. The RT domain contains a highly conserved YMDD motif [214]. The spacer domain has not yet been assigned a function. The tyrosine residue of the terminal protein provides a functional equivalent of the 3`-hydroxyl group of a terminating nucleotide for the synthesis of a short, 3-4 nucleotide primer by the RT [215] using a particular secondary structure at the 5` end of the pgRNA as a template [216]. Further steps in DNA synthesis involve translocation and annealing of the RT/primer complex to the 3` end of the pgRNA, followed by the 5`-3` DNA polymerization of the (-) DNA strand and degradation of the pgRNA by the RH. But approximately 18 bases of pgRNA are not degraded and serve as a primer for (+) DNA strand synthesis upon translocation and annealing to the homologous region within the 5` end of the newly synthesized (-) DNA strand. RT translocates to the 3` end of the (-) DNA strand and initiates the synthesis of the (+) DNA strand. Since RT is covalently attached to the 5` end of the (-) DNA strand, the overall product of DNA polymerization will effectively be circular with a nick in the (-) DNA

strand. HBV genome replication occurs within the nucleocapsid, where the pool of nucleotides is replenished through the nucleocapsid pores. But after the nucleocapsid is enveloped, the (+) DNA strand synthesis cannot be finished because the nucleotide pool cannot be replenished, thus resulting in an incomplete (+) DNA strand annealed to an effectively circular nicked (-) DNA stand [217].

1.2.3.2 HBV therapy and drug resistance

Members of currently approved anti-HBV regimens are either immunomodulatory agents like interferon and peginterferon alpha, or nucleoside analogues inhibiting HBV RT, such as lamivudine, adefovir dipivoxil, entecavir, telbivudine and tenofovir (Table 1.4). Two subgroups can be identified within the anti-HBV RT agents: nucleoside (lamivudine, telbivudine and entecavir) and nucleoside phosphonate (adefovir and tenofovir) analogues (Figure 1.1).

Interferon alpha (INF-α) was the first available drug to treat HBV infection. But only a third of patients receiving the drug show positive response, and various side effects are common [194]. INF-α is a cytokine, and as such binds to the cell surface receptor. This interaction triggers a cell-signaling cascade that activates the expression of genes that are responsible for an antiviral or immunomodulatory response. In particular, INF-α induces a 2`,5`-oligoadenylate synthetase/RNase L system, which is responsible for the degradation of single-stranded RNA, thus inhibiting viral replication requiring an RNA intermediate. In addition, INF-α enhances destruction of virally infected cells by CD8+ cytotoxic T cells (CTL) through upregulating the expression of MHC class I. MHC class I are cell surface molecules responsible for presenting viral antigens to CTL [218]. Two types of interferon are available for anti-HBV therapy: IFN-α-2b, and a pegylated form of interferon (peginterferon alpha-2a), which has a longer half-life. Peginterferon alpha-2a was shown to be more efficient than lamivudine [219]. More importantly, peginterferon alpha-2a in combination with adefovir has recently been shown to have a strong effect on reducing cccDNA [220].

Lamivudine (3TC) is an L-nucleoside analogue of 2`-deoxycytidine (Figure 1.1). The particularity of lamivudine is an inversion of its ribose configuration from D- to L-ribose (Figure 1.4). It is also an obligate chain terminator and is licensed for treatment of HIV and HBV infections. Lamivudine must be activated to its triphosphate form 3TC-TP through phosphorylation by cellular enzymes [221]. 3TC-TP specifically targets HBV RT, rather than cellular polymerases, by competing with dCTP for incorporation into the growing chain of viral DNA, which causes an immediate chain termination [222, 223].

Adefovir (PMEA) is an acyclic nucleoside phosphonate analogue of 2`-deoxyadenine monophosphate (Figure 1.1). It also exists in an esterified version, adefovir dipivoxil, which has higher oral bioavailability. Adefovir does not require monophosphorylation since it already contains a phosphate group. It is further phosphorylated to its active form PMEApp by cellular kinases [224]. PMEApp acts as an immediate chain terminator. Competition of PMEApp with its natural counterpart as a substrate for nucleotide incorporation inhibits HBV RT primer synthesis/priming and viral (-) DNA strand synthesis [225]. It has also been reported to have an effect on the persistence of cccDNA [226].

Entecavir (ETV) is a potent and selective inhibitor of HBV replication [56, 57] with no *in vitro* mitochondrial toxicity reported [66]. *In vitro* studies have shown a more efficient phosphorylation than other nucleosides by cellular enzymes [227]. On the basis of *in vitro* studies, entecavir was predicted to have potent antiviral activity against lamivudine-resistant HBV [228]. Recently, it was reported to be >100-fold more effective at inhibiting HBV replication in culture than either lamivudine or adefovir [58]. The same study clearly showed that entecavir incorporation results in a chain termination several nucleotides downstream from the incorporated ETV-MP, which is consistent with the presence of the 3`-hydroxyl on the ribose. The researchers conducted three-dimensional homology modeling based on the structure of HIV RT and predicted

a hydrophobic pocket in the rear of the dNTP binding site that may accommodate the exocyclic alkene moiety of entecavir. This finding provided a potential structural basis for the superior potency of entecavir as compared with lamivudine and adefovir. Finally, modeling of lamivudine or adefovir resistance-conferring substitutions either reduced or did not affect, respectively, the hydrophobic pocket. These predictions correlated with the *in vitro* data. Langley et al. 2007 [58] also reported the absence of significant activity against HIV, which has been challenged by clinical observation, selection in cell culture and biochemical characterization of the entecavir resistance-conferring mutation M184V within HIV RT [60, 61]. Chapter 5 of this thesis explores the precise molecular mechanism of entecavir anti-HIV activity and generated resistance.

Recent *in vitro* studies reported that ribavirin, an anti-HCV drug, showed a synergistic effect on entecavir potency against wild-type HBV as well as a lamivudine-resistant mutant [67]. The potential mechanism for this interaction is a ribavirin-dependent reduction of intracellular dGTP concentration, which in turn increases the effective relative concentration of ETV-TP, allowing it to better target the HBV RT.

Telbivudine (LdT) is an L-nucleoside analogue of 2`-deoxythymidine (Figure 1.1). As such, it undergoes activation to its triphosphate form by cellular enzymes [229]. It is a specific anti-HBV compound [230]. Telbivudine preferentially inhibits HBV RT at the level of (+) DNA synthesis through a mechanism of chain termination [231, 232].

Tenofovir (PMPA) is an acyclic nucleoside phosphonate analogue that is structurally and functionally related to adefovir [233, 234] and has low cytotoxicity (Figure 1.1) [235]. Tenofovir disoproxil fumarate, a bis-alkoxyester prodrug of tenofovir, is a potent drug against HIV and HIV/HBV co-infections [236]. It remains active against viruses containing mutations that confer resistance to lamivudine and adefovir [237, 238].

All mutations conferring resistance to nucleoside analogues map to the polymerase domain of HBV RT [69]. Since lamivudine resistance can reach high levels (65-70%) after 5 years of therapy, it is currently used only as a second-line agent [239]. Mutations within the highly conserved YMDD motif (M204V/I) confer high-level resistance to lamivudine [240]. Those mutations do not affect binding of the natural substrate as much as of lamivudine. On the basis of three-dimensional homology modeling studies, it has been suggested that the sulfur atom of the oxathiolane ring is in steric conflict with the side chain of M204V/I substitutions [241]. These mutations are associated with the compensatory mutations V173L and L180M, which restore the capacity of the lamivudine-resistant mutants to replicate [242, 243]. Lamivudine resistance resulting from a mutation in theYMDD motif can be treated with adefovir, which in turn prevents generation of subsequent adefovir resistance [244].

Development of resistance to adefovir is a function of treatment duration, but overall it is much less frequent than lamivudine resistance [245]. The mutations that confer resistance to adefovir are A181V and N236T within HBV-RT [246, 247], although mutant viruses remain susceptible to lamivudine or entecavir [222, 248]. Adefovir resistance is more common in patients with lamivudine-resistant HBV infections [249], especially if lamivudine treatment is discontinued [250].

Entecavir has a very good resistance profile in treating naïve patients [59, 251], while in lamivudine-resistant patients, high levels of resistance were reported with time [252]. Entecavir resistance-associated mutations within HBV-RT (S184G, I169T, S202I and M250V) are tightly linked with mutations conferring resistance to lamivudine [252]. It has been proposed that such mutations reduce the entecavir-specific hydrophobic pocket within the nucleotide binding site of HBV-RT [58].

Telbivudine is reserved for patients with undetectable serum HBV DNA by week 24 of therapy, since if this is achieved, the rate of resistance remains low even by week 96 [253]. Otherwise, the rate of resistance can reach significant levels with time [254]. Telbivudine is subject to cross-resistance towards lamivudine-resistant HBV [255]. The M204I mutation within the YMDD motif of HBV RT has been observed in patients on telbivudine therapy [256].

An HBV RT mutation, A194T, distal from the catalytic YMDD motif has been reported in patients on tenofovir therapy for more than 12 months [257]. The mutation was associated with substitutions conferring resistance to lamivudine. But those findings have been challenged based on the absence of an increase in viral load [258], and they were not confirmed in subsequent *in vitro* studies [233]. Thus, at the moment resistance to tenofovir has yet to be reported [259].

Several patterns can be observed in the way resistance to anti-HBV regimens is generated. First, there is a wide range in the observed rates of resistance within the anti-HBV regimen, with lamivudine generating the highest [260] and adefovir, entecavir and tenofovir the lowest rates [259, 261, 262]. Second, even a drug with a low resistance rate such as adefovir will eventually generate significant resistance with time on continued therapy [245]. Third, resistance to all nucleoside analogues is associated with and accelerated by a background of lamivudine mutations in the YMDD motif of HBV RT [59, 250]. Fourth, nucleoside phosphonate analogues remain active against mutations conferring resistance to nucleosides [244]. Fifth, mutations conferring resistance to nucleoside phosphonate analogues are located outside the YMDD motif. These observations suggest that, similar to HAART for HIV infection, an anti-HBV combination therapy may be beneficial in the context of resistance and cross-resistance [263].

Several conceptually new agents and targets for anti-HBV therapy have been explored. Inhibition of nucleocapsid formation by a non-nucleoside HBV

inhibitor BAY41-4109 [264] and by a peptide aptamer has been reported [265]. This approach targets virion production and, most importantly, cccDNA persistence, which is a prerequisite for chronic HBV infection. Inhibition of viral RNA has also been explored as a potential target: helioxanthin and its analogues [266, 267] as well as small interfering RNAs have been shown to be active against HBV replication [268].

1.2.4.1 HIV virology

The HIV infectious viral particle [269] consists of a cell-derived lipid bilayer envelope with embedded surface proteins gp120 and gp41. The matrix protein (MA) lines the inner surface of the envelope enclosing viral proteins P6, Vif, Vpr, Nef and the viral capsid.
The capsid is formed by a capsid protein encasing two viral RNA genomes associated with a nucleocapsid protein (NC), viral protease (PR), reverse transcriptase (RT) and integrase (IN). The most important non-viral component of the capsid is the cellular $tRNA^{Lys}$.

The two envelope proteins gp120 and gp41 mediate fusion of the virion with the cell membrane [270]. gp120 interacts with two host cell surface receptors: the CD4 antigen, expressed on T cells and macrophages, and the chemokine receptor CXCR4 on T cells, or CCR5 on macrophages. This specific interaction determines the CD4+ T lymphocyte or macrophage tropism of the HIV virion. gp120 engagement is followed by a conformational change in gp41, which induces the fusion of the viral envelope with the cell membrane, followed by release of the viral capsid into the cytoplasm [271]. Upon entering the cytoplasm, the viral capsid, a reverse transcription complex (RTC), undergoes partial uncoating mediated by cell factors, allowing for exposure to dNTPs present in the cytoplasm [272, 273]. This exposure is thought to be sufficient for triggering reverse transcription within the RTC [274]. Reverse transcription results in a linear blunt-ended, double-stranded viral DNA contained within a pre-integration

complex (PIC) [275, 276]. HIV-1 can infect non-dividing, terminally differentiated cells (dendritic cells and macrophages), which suggests that disintegration of the nuclear membrane is not required [277]. Though it has been shown that the PIC is actively delivered to the nucleus of the infected cell [278], the exact mechanism of this process remains unclear [274]. Nevertheless, a number of viral [279, 280] and host factors, including tRNAs [274, 281], were shown to mediate PIC transport into the nucleus. In the nucleus, viral DNA is integrated into the host cell genome through the concerted action of viral integrase and cellular enzymes [282, 283].

Transcription from the integrated viral DNA involves a complex interplay between the HIV genomic 5` long terminal repeat (LTR), the viral transactivator of transcription (TAT) [284], the cellular RNA polymerase II machinery and cellular transcription factors [285, 286]. Similar to HBV, the transcribed RNA serves as mRNA for translation into viral proteins or as genomic RNA. Approximately 30 different viral transcripts are generated by alternative splicing of a full-length RNA transcript. These can be grouped as unspliced, singly and multiply spliced mRNA. A peculiarity of HIV is that singly spliced and unspliced RNA transcripts contain introns; hence, they have to be actively exported from the nucleus. This function is mediated by a viral protein REV, which is expressed from multiply spliced RNA [287]. Thus, REV action involves regulation of HIV gene expression such that the early regulatory proteins produced from multiply spliced mRNA (TAT, NEF and REV) are synthesized first, while production of viral proteins encoded by singly spliced (VPU, VPR, VIF and ENV) and unspliced (structural and enzymatic proteins derived from the GAG-POL polyprotein) RNA transcripts is delayed [288].

The self-assembly of a new viral particle is triggered by the translation of the GAG protein complex [289]. GAG and GAG-POL precursors are targeted to the cell membrane through a co-translationally added N-myristic acid and a cluster of basic amino acids within the matrix protein region [290]. C-terminal specific

regions of the capsid protein portions of GAG are responsible for both GAG and GAG-POL dimerization, which is required for their incorporation into the virion [291-293]. GAG recruits viral genomic RNA through a specific interaction between its nucleocapsid domain and the 5` region of the RNA, which initiates the viral genome encapsidation [294]. The GAG-POL precursor and cellular lysyl-tRNA synthetase are responsible for specific selection of cellular $tRNA^{Lys}$ into the forming virion [295-297]. VPR protein is recruited to the virion through interaction with the p6 portion of the GAG precursor [298]. Incorporation of the VIF protein to the virion possibly involves interaction with both viral RNA and the GAG-POL precursor [299, 300]. Similar to the GAG and GAG/POL precursors, recruitment of the NEF protein to the cell membrane is thought to depend on both its myristoylation and its N-terminal basic domain [301], resulting in its incorporation into the virion [302]. In a parallel process, ENV glycoprotein complexes are processed and recruited to the cell surface [303]. The virion assembly involves stimulating the interaction between the ENV glycoproteins and the GAG precursor by a cellular factor [304]. The budding of the viral particle is mediated by the interaction of the p6 domain of the GAG precursor [305], with the host cell endosomal sorting complex required for transport [306]. The protein precursors within the newly released viral particles are cleaved by the viral protease, causing viral particle reorganization, which generates morphologically mature infectious viruses [307, 308].

In the context of the HIV life cycle, two types of viral genome can be distinguished: viral RNA and proviral DNA. Though the genomic organization is very similar, their functional significance is quite different owing to the nature of the nucleic acid sequence and its intracellular location. Proviral DNA is integrated into the host cell genome. It consists of two same-orientation/same-sequence non-coding regions located at the 5`- and 3`-ends of the genome (long terminal repeats, LTR) and the leader sequence, located 3` to the 5`LTR until the 5`-end of the coding region. The coding region is located between the two non-coding LTRs and is used as a template for viral mRNA encoding for viral structural, enzymatic

and auxiliary proteins. Production of these proteins involves alternative splicing and/or post-translational processing by host or viral proteases. The non-coding regions of the proviral DNA are involved in integration into the host genome and activation of the transcription of the coding region by the host RNA polymerase II [283, 285]. Genomic viral RNA is located in the capsid in the form of a (+) single-stranded RNA homodimer. In terms of functional significance, regions of its sequence can be classified as either sequences involved in the synthesis and processing of RNA transcripts (transcription, splicing, nuclear-to-cytosol transport and encapsidation) or sequences mediating reverse transcription.

Viruses face two major mechanical constraints during genome replication: priming and genome endpoints replication. The examples of herpes viruses, HBV and HIV illustrate very different strategies to solve these tasks (Table 1.7). Herpes viruses use a virally encoded primase to generate primers. The primase activity of HBV is encoded within the HBV-RT: the viral polymerase uses the hydroxyl of its tyrosine residue as the functional equivalent of the 3`-hydroxyl of the primer's terminating nucleotide. There is no primase activity associated with HIV; instead, a host cell $tRNA^{Lys3}$, present in the capsid, is used by HIV-1 RT as a primer. $tRNA^{Lys3}$ contains 18 nucleotides that are complementary to the viral primer binding sequence (PBS) located between the 3`-end of the 5` LTR and the leader sequence. In terms of genome endpoint replication, herpes viruses use a rolling circle mechanism of replication that generates viral double-stranded DNA concatamers, which are subsequently cleaved by cellular enzymes to generate single unit genomes. HBV and HIV are similar in that both involve translocation of the RT/primer complex from the 5`- to the 3`-end of the RNA to initiate the (-) DNA strand synthesis and usage of RNase H-resistant sequences as primers for the (+) DNA synthesis. But in the case of HBV, the effective circularization of the (-) DNA strand is the result of a (-) DNA-strand covalently attached RT, while sequence complementarity allows for primer translocation/strand transfer during the (+) DNA synthesis. In this regard, the (+) DNA synthesis by HIV-1 RT also

goes through a circular intermediate, but depends solely on sequence complementarity.

HIV-1 RT uses its RNA- and DNA-dependent DNA polymerase activities and the RNA/DNA-specific ribonuclease H (RNase H) activity [309] to catalyze the reverse transcription of viral RNA into a proviral dsDNA [310]. The redundant sequence R located at both extremities of the RNA genome, as well as four *cis*-acting sequences (PBS, two RNase H-resistant polypurine tracks [central and 3` with respect to the RNA genome, PPTc and PPT3`, respectively] and the central terminal sequence [CTS]) are important in the reverse transcription of HIV RNA. PBS consists of 18 nucleotides complementary to the 3`-terminal nucleotides of the human $tRNA^{Lys3}$. The annealed PBS/ $tRNA^{Lys3}$ generates a 3`-hydroxyl, which is recognized by the HIV-1 RT as a substrate for DNA polymerization. As the (-) DNA synthesis proceeds towards the 5` end of the RNA, the newly formed DNA/RNA hybrid is degraded by the RNase H activity of HIV-1 RT. The PBS region of the DNA/RNA hybrid resists degradation at this point, thereby determining the new 5` end intermediate of the RNA. In addition, the RNase H activity facilitates the release of the newly synthesized (-) ss DNA (5`-[ $tRNALys^3$/PBS/U5/R]-3`), which allows for its transfer to the 3` end of the RNA. The complementarity between the newly synthesized R portion of the (-) ss DNA and the R at the 3` end of the RNA mediates the annealing of the two sequences, thereby generating a free 3`-hydroxyl. Since two copies of the RNA genome are present, this transfer may occur in *cis* or in *trans* with respect to the templating RNA. The (-) strand DNA synthesis resumes and continues until the 5` end of the RNA, thus generating the following intermediate: 5`-[$tRNALys^3$/U5/R/U3/Genome/PBS]-3`. As the (-) DNA/(+) RNA is forming during this step of (-) strand DNA synthesis, the (+) strand RNA is degraded by the RNase H activity of the HIV-1 RT. But two regions are resistant to this degradation: PPTc and PPT3`. These will serve as the RNA primers for the (+) strand DNA synthesis termed *downsteam* (D+) if generated from PPTc, or *upstream* (U+) when generated from PPT3`. U+ DNA strand synthesis generates

5`-[PPT3`/U3/R/U5/PBS]-3` as the result of a strong stop when HIV-1 RT encounters the first methylation-modified base of the tRNA portion of the template strand. The RNase H activity of HIV-1 RT removes the PPT3` from the 5` end of the U+ strand and the tRNA from the 5` end of the (-) strand DNA. The cleavage of PPT3`, as well as of PPTc, occurs exactly at the RNA/DNA and DNA/DNA junction, while the cleavage of the tRNA leaves a single ribonucleotide at the 5` end of the (-) strand DNA. The new intermediates are (-) strand DNA as 5`-[U5/R/U3/Genome/PBS]-3` and U+ as 5`-[U3/R/U5/PBS]-3`. The second strand transfer occurs when PBS^{U+} anneals with $PBS^{(-)DNA}$ in a cis fashion with respect to the templating (-) strand DNA. In addition to D+ primed from PPTc, the PBS^{U+}/$PBS^{(-)DNA}$ annealing generates two additional templated 3`-hydroxyl groups that are used by HIV-1 RT to continue DNA synthesis. HIV-1 RT has been shown to possess a strand displacement activity resulting in the denaturing of DNA/DNA hybrids. This activity is required for continuing the D+ strand synthesis, resulting in displacing the 5` end of the U+ strand and effectively linearizing the DNA/DNA intermediate. The 3`-end product of the D+ synthesis reconstitutes the double-stranded 3` LTR (U3/R/U5). Continuation of the (-) strand DNA synthesis proceeds from its $U+^{strand}$-templated 3`-hydroxyl, resulting in a reconstituted double-stranded 5` LTR (U3/R/U5). Finally, U+ strand synthesis occurs across the (-) strand DNA template until it reaches the CTS, resulting in a second strand displacement event: about 100 base pairs of the 5` end of the D+ strand are disrupted so that the U+ strand synthesis can reach the CTS. The overall product of the reverse transcription of RNA is (1) a linear double-stranded DNA that is longer than the RNA genome (additional U3 and U5 segments at the 5` and 3` ends, respectively), (2) a duplicated terminal LTR and (3) a DNA flap resulting in a discontinued (+) strand DNA.

The viral RNA reverse transcription is catalyzed by the HIV-1 RT [311].

HIV-1 RT, protease and integrase are the three enzymatic proteins encoded by the POL gene [312, 313]. HIV-1 RT is a heterodimer consisting of p66 and p51 subunits [314]. p66 is generated by the proteolytic cleavage of the GAG-POL

polyprotein precursor by viral protease [315]. It can be further cleaved at a specific site in its C-terminal domain to generate the p51 subunit. A p66/p51 heterodimer is required to form a functionally active HIV-1 RT [316]. But all enzymatic activities are exclusive to the p66 subunit [317, 318], leaving the p51 with only a structural role.

On the basis of the HIV-1 RT crystal structures, p66 is subdivided into four functional and one structural domain [319]. The functional domains are subdivided into one RNase H domain, present only in the p66 subunit, and three domains constituting the polymerase activity of HIV-1 RT. The structural domain serves as a spacer that connects the RNase H and polymerase domains; hence, it is called the connection domain. On the basis of the analogy between the three-dimensional organization of the polymerase region of the HIV-1 RT and a right hand, the three polymerase domains were named as fingers (residues 1-85 and 118-155), thumb (237-318) and palm (residues 86-117 and 156-236) [319, 320]. The palm domain contains the three aspartic acid residues that are crucial for the catalysis of nucleotide incorporation (D110, and D185 and D186 as part of the highly conserved YMDD motif). The fingers and thumb of the p66 subunit contain amino acids whose side chains wrap the DNA/DNA hybrid into the nucleic acid binding channel formed by the fingers, thumb and palm subdomains [320]. This channel is absent in the p51 subunit owing to a different spatial orientation of subdomains. In addition, the catalytically important residues of the polymerase active site (the highly conserved polymerase YMDD motif) are buried in p51, which correlates with the absence of enzymatic activity in this subunit [317, 321]. It was noticed by comparing the crystal structures of the HIV-1 RT:DNA/DNA (binary) [320] and HIV-1 RT:DNA/DNA:dNTP (ternary) [322] complexes that upon binding, the incoming dNTP p66 subunit undergoes a conformational change where the finger subdomain closes on the dNTP. This effectively traps the incoming dNTP in the orientation that supports formation of the catalytic complex for nucleotide incorporation.

HIV-1 RT remains the primary target for most of the currently available anti-HIV drugs (Table 1.3). All anti-HIV-1 RT drugs inhibit its polymerase activity by interfering with the basic mechanism of nucleotide incorporation. The catalysis of nucleotide incorporation is an ordered two-substrate reaction [323]. The polymerase forms a relatively stable binary complex with the nucleic acid substrate (template/primer). Formation of a binary complex can generate a conformation that supports the binding of the second substrate, dNTP, to form a relatively unstable ternary complex. The ternary complex can assume a stable conformation that coordinates the catalysis of the phosphodiester bond between the terminating nucleotide of the primer and the incoming dNTP, resulting in incorporation of one nucleotide and a release of the byproduct of the reaction. The newly formed binary complex (RT/template/primer+1nucleotide) again is capable of generating a conformation supporting the binding of the next templated dNTP. A drug that inhibits the formation of the binary complex will inhibit the overall polymerase activity in an uncompetitive manner [324]. None of the currently available anti-HIV-1 RT drugs acts in this way. Instead, they all target either the formation of the ternary complex or the conformational change that makes it compatible with nucleotide incorporation. Drugs that target the former compete with dNTP binding, and hence act competitively. Drugs that target the latter do not compete with dNTP binding, and hence act non-competitively. These drugs belong to two structurally different classes: nucleoside RT inhibitors (NRTI) and non-NRTIs (NNRTI), respectively (Figures 1.1 and 1.5) NRTIs and NNRTIs target two different binding sites within HIV-1 RT.

NRTIs compete with their natural counterpart for dNTP binding (Figure 1.6). On the basis of the crystal structure of the ternary complex [322], the triphosphate moiety of the incoming dNTP is coordinated by the side chains of Lys65, Arg72, the main chain-NH groups of residues Asp113 and Ala114, and two divalent ions, which are required for catalysis [325]. The backbone carbonyl of residue Val111 and the side chains of catalytic aspartates Asp110 and Asp185 are involved in coordinating the metal ion, which is wrapped by the α and β phosphates of the

dNTP. The 3`-hydroxyl of the incoming nucleotide is located in a small pocket formed by the side chains of Asp113, Tyr115, Phe116 and Gln151, and the peptide backbone between residues Asp113 and Tyr115. The size of this pocket is sufficient to accommodate several water molecules in addition to the 3`-hydroxyl, suggesting a structural explanation for the acceptance of AZT into a dNTP binding site. In addition to Lys65 and Gln151, the residues Lys70, Leu74 and Met184 are in the neighborhood of the dNTP and are involved in drug resistance [326]. But resistance to NRTIs cannot be explained solely by interference with the dNTP binding site.

The NNRTI binding site (NNRTI-BS) is located 10 angstroms away from the dNTP binding site (Figure 1.7) [319]. It is a hydrophobic pocket created primarily by the residues of the p66 subunit (L100, K101, K103, V106, T107, V108, V179, Y181, Y188, V189, G190, F227, W229, L234, Y318) and one residue of the p51 subunit (E138) [327, 328]. It was concluded on the basis of the structural data that the NNRTI-BS is created upon NNRTI binding to HIV-1 RT, since this pocket does not exist in the unliganded HIV-1 RT [329]. Formation of the NNRTI-BS results from the displacement of a region between the palm and thumb and the rearrangement of residues Y181 and Y188. The overall effect is that the thumb domain of p66 loses its flexibility by adopting a conformation that is even more extended than in a RT:DNA binary complex [320, 329]. It was noticed by comparing the crystal structures of the ternary complex with NNRTI-liganded HIV-1 RT [330, 331] that formation of the NNRTI-BS forces the YMDD motif to adopt a catalytically unfavorable conformation [328]. Interestingly, because of the sequences difference between HIV-1 and HIV-2, resulting in a loss of aromatic residues at positions 181 and 188, the NNRTI-BS does not exist in HIV-2 RT [332].

Though the selective drug pressure acts only on two functionally closely related sites within HIV-1 RT, the viral response in the form of drug resistance involves more than just altering the drug binding sites. As discussed below, it also includes

(1) repositioning of the template/primer within the binary complex, (2) excision of incorporated drugs that have successfully competed with their natural counterparts or (3) altering of the RNase H activity on the template/primer containing the incorporated drug such as to promote its excision from the 3` end of the primer.

1.2.4.2 HIV therapy: drugs and drug resistance.

Currently available anti-HIV-1 drugs can be classified as acting against either viral enzymatic proteins or viral entry [333]. Though all the viral enzymes have a specific inhibitor, most drugs target viral protease or reverse transcriptase. The anti-HIV-1 RT drugs consist of two structurally different classes, NRTIs and NNRTIs. NRTIs are structural analogues of natural nucleosides, and as such they must be activated to their tri-phosphate form through phosphorylation by cellular enzymes. In this regard, tenofovir differs from other NRTIs in that it is a nucleoside phosphonate and hence requires only two phosphorylation events (Figure 1.1) [334]. Common to all NRTIs is the absence of the 3`-hydroxyl group, or its functional equivalent, on their ribose moiety. Hence, all NRTIs act as obligate chain terminators of DNA synthesis. Other differences from natural nucleosides involve modifications of the ribose moiety and/or of the base of the nucleoside. Tenofovir stands out because it does not have a full ribose ring and is therefore referred to as an acyclic nucleoside phosphonate. Finally, lamivudine and emtricitabine contain L-ribose, as opposed to the D-ribose present in the rest of the cyclic NRTIs and natural nucleosides. NRTIs employ a standard nucleoside analogue mechanism of action that involves (1) competition for binding to the dNTP binding site, (2) recognition by HIV-RT as an alternative substrate for DNA synthesis, resulting in incorporation, (3) chain termination of DNA synthesis and (4) inhibition of HIV-1 RT through forming a dead-end complex with the next incoming nucleotide [335]. NRTIs exhibit variable levels of specificity for HIV-1 RT versus cellular polymerases [336], resulting in a spectrum of toxicities, primarily mitochondrial toxicity [337].

The four NNRTIs currently approved for anti-HIV therapy represent a structurally distinct class of hydrophobic molecules (Figure 1.5). Unlike NRTIs, NNRTIs do not require activation through phosphorylation by cellular enzymes, nor are they incorporated into the growing DNA chain. Binding NNRTI to the NNRTI-BS does not prevent dNTP binding to its respective site; instead, it prevents formation of a catalytically active conformation of the polymerase active site, which results in inhibiting the chemical step of the polymerization reaction [338]. NNRTIs exhibit moderate, predictable and manageable toxic effects [339].

Since the early days of anti-HIV therapy, drug resistance has been recognized as a growing problem [340, 341]. The generation of high viral genetic variation in a given infected person has been attributed to the mutagenic potential of reverse transcription, different selective pressures and their weight on viral fitness [342]. Acknowledging that the term "quasispecies" [68] applies to HIV-1 [343] explained the continuous problem of drug resistance: a rapidly changing spectrum of viral genetic variations correlates with a spectrum of fitness that, under selective drug pressure, temporarily suppresses (but does not eliminate [344]) drug-responsive viruses, while promoting the expansion of viral sequences that are drug resistant.

Two basic mechanisms of resistance to NRTIs have been recognized [345]: increased discrimination against NRTIs [322], thus preventing their binding to the dNTP binding site, and excision of incorporated NRTIs [346, 347], which removes a chain terminator, allowing for DNA synthesis to continue. A classic example of an NRTI resistance-conferring mutation that employs the discrimination mechanism is the M184I/V substitution, which confers resistance to 3TC [348, 349]. It has been proposed that the enhancement of a steric conflict between the side chains of isolucine or valine substitutions and the sulfur atom in the oxathiolane ring of 3TC by the L-configuration of the ribose moiety explains the structural basis for increased discrimination against 3TC [350]. All mutations that function based on the discrimination mechanism are located within the

fingers or the palm of RT and can influence the binding of the incoming dNTP. Among them are K65R, L74V and Q151M and its accompanying mutations, which, it has been suggested, amplify the negative effect of the absence of 3`-hydroxyl on the overall recognition of the NRTIs [351-354]. Mutations that favor the increased discrimination mechanism have been shown to resensitize viruses resistant to AZT because of mutations functioning through the excision mechanism of NRTI resistance [355-358]. The excision of NRTIs is associated with a set of excision enhancing mutations (EEMs: M41L, D67N, K70R, L210W, T215Y/F and K219Q, also known as thymidine-associated resistance mutations, or TAMs). The molecular mechanism of this resistance pathway is similar to the nucleotide incorporation reaction but runs in reverse. Upon formation of a phosphodiester bond between the primer 3`-end nucleotide and the incoming nucleotide, and prior to the release of the PPi byproduct of the reaction, the newly formed 3`-end of the primer is still located in the dNTP binding site of HIV-1 RT. In this conformation, the overall direction of the reaction equilibrium to the nucleotide incorporation can be shifted back by increasing the concentration of PPi. This phosphorolysis reaction (PPi-lysis) regenerates the free dNTP. But once the newly formed 3`-end of the primer translocates to the primer binding site, the PPi-lysis is no longer possible. It has been shown that the 3`-end of the primer oscillates in equilibrium between the primer (P) and nucleotide (N) binding sites, and that this equilibrium can be shifted to the P-site by the increasing concentrations of PPi, and to the N-site by the next incoming nucleotide [35, 359]. Excision enhancing mutations (EEMs) were shown to enhance the excision of the incorporated NRTIs using ATP as a PPi donor; this reaction was inhibited by the next incoming nucleotide owing to the formation of a stable dead-end complex (DEC) [346]. In this regard, mutations involving the insertion of two amino acids between residues 69 and 70 of HIV-1 RT in the background of the EEMs confer an NRTI multidrug resistance by decreasing the stability of the DEC, thereby promoting the EEMs-mediated ATP-lysis [360-362]. Connection domain mutations N348I and A360V in the background of the EEMs were also shown to increase AZT resistance partly through inhibiting the RNase H activity of HIV-1

RT, thereby providing more time for the excision reaction on the $RNA^{template}/DNA^{primer}$ terminated with AZT [363].

Another interesting example of drug resistance involving the dNTP binding site is the E89K mutation. This substitution confers resistance to foscarnet [31]. Foscarnet has been shown to trap the RNA:DNA/DNA binary complex in a conformation where the 3`-end of the primer resides in the N-site of HIV-1 RT [359], thereby competing out the incoming dNTP from its favorable conformation [35]. But E89K acts by repositioning the 3`-end of the primer such that its distribution between the P and N sites is less defined, thereby generating resistance to foscarnet along with reducing the efficiency of nucleotide incorporation [35].

All NNRTI resistance-conferring mutations occur in the context of the NNRTI-BS and directly affect either the hydrophobic pocket itself or access to it [364]. The most common resistance-conferring mutations are K103N, located at the entrance of the pocket (nevirapine, delavirdine and efavirenz but not etravirine), and Y181C, causing a loss of a key hydrophobic interaction (all NNRTIs) [365, 366]. Y181C is a particularly interesting mutation because nevirapine/AZT dual therapy prevents its generation, while introducing this mutation in the background of EEMs was shown to suppress AZT resistance [367]. Other interesting mutations in this regard are P236L and G190A/S, P225H. The former confers resistance to delavirdine but resensitizes to nevirapine [368], while the latter combination resensitizes to delavirdine but generates resistance to nevirapine and efavirenz [369].

The examples of NRTI and NNRTI resistance-conferring mutations illustrate the dichotomy of cross-resistance and non-overlapping drug-resistant mutations within HIV-1 RT, which provided the basis for the initial suggestion of a combination therapy consisting of NRTIs and an NNRTI [370]. The highly active antiretroviral therapy (HAART) for HIV infection was initiated in 1996. Currently

various combination therapies, including NRTIs, NNRTIs, protease and integrase inhibitors, as well as viral entry inhibitors, are available [50].

1.3 Co-infection

Co-infection with several different viruses is a product of the omnipresence of certain viruses, similar routes of acquisition, viral latency and potential interviral synergy. hawse have already mentioned that the viral incidence of herpes viruses can reach 100% for HHV-6 and above 50% for HCMV, implying that any subsequent infection with a heterogeneous virus is in fact a co-infection. As early as the first description and subsequent clinical definition of AIDS, it was recognized that herpes virus infections constitute a substantial portion of the clinical manifestations associated with the syndrome [371, 372].

HSV, HBV, HCV and HIV can initiate systemic infections as a result of blood contact or sexual intercourse between infected and uninfected individuals. On the basis of epidemiologic studies, it has been estimated that infection with HSV-2 is associated with a five-fold increase in per-sexual contact transmission rates, correlating with a significantly increased risk of contracting HIV-1 [44, 373]. A seroepidemiologic study of 180 HIV-infected individuals in north-central Nigeria reported a 7.2% prevalence of triple HIV/HCV/HBV co-infection [374]. All herpes viruses, as well as HBV and HIV, are capable of persistent or latent infections, thereby increasing the chance of sequential co-infection. The incidence of HBV co-infection in HIV-infected patients has been reported to be between 5% and 10% [375].

The aspect of potential interviral synergy is more complex because of the different levels where the synergy can occur: intracellular, immunological or a combination of the two. The viral synergy at the intracellular level gives rise to two basic questions: (1) can the same cell be reinfected with the same virus and (2) can a single cell support multiple co-infections with different viruses. With

regard to the first question, it has been shown that different variants of HSV-1, as well as HCMV, can infect the same cell, resulting in mutually beneficial intraviral trans-complementation [376, 377]. This provides a potential explanation for the clinical observation of an increased viral load and severity of the disease in multiply reinfected HCMV patients [378]. HIV was also shown to be capable of the double infection of a single cell [379]. The positive answer to the first question provides the conceptual basis for the actuality of the second. In fact, it has been shown *in vitro* that a single cell can be doubly (HIV-1/HSV-1) and even triply (HCV/HHV-6/HIV-1) infected [380, 381]. The intracellular synergy between co-infecting viruses was explicitly shown in *in vitro* studies reporting an interaction between HSV regulatory proteins and HIV-1 LTRs, resulting in upregulation of HIV-1 replication [382] and transcription [383]. Similar interviral, intracellular synergistic interactions have been reported for HHV-6 and HCMV [384, 385]. These results are in line with *in vivo* observations of viral co-infections [386] and more rapid progression to AIDS in co-infected patients [387]. But multiple co-infection with different viruses can also be counterproductive from a viral point of view. Recently, it has been reported that acyclovir can be activated into an HIV inhibitor in HIV-infected cells as a result of specific monophosphorylation by the endogenous herpes thymidine kinase [47].

Synergy between co-infecting viruses at the immunological level can exacerbate the consequences of the infection by one of the viruses through its reactivation from latency in an already co-infected individual, and/or can promote infection with a second pathogen in a singly infected patient. HIV/AIDS represents a perfect example of the resurgence and worsening of opportunistic infections, including herpes simplex and cytomegalovirus infections, which may be mild or even subclinical in immunocompetent individuals [388, 389]. On the other hand, HSV-2 infection has been associated with an increased risk of HIV transmission [44, 373], which may result from HSV-2-dependent partial disruption of mucosal immunity and recruitment of CD4+ cells to herpetic ulcers, thereby facilitating HIV infection [390]. Synergistic co-infection is associated with accelerated

disease progression, increased morbidity and mortality. HSV-2/HIV-1 co-infection has been associated with a decrease of survival rates in patients [391]. An increased risk of liver-related mortality has been demonstrated in HIV/HBV and HIV/HCV co-infected patients [392, 393].

Therefore, it can be concluded that viral co-infection and its consequences represent a substantial problem at both the levels of prevention and of treatment of viral infections. This underlines the potential benefit of developing and using drugs with either dual or multiple antiviral activities [394, 395].

1.4 Objectives

Foscarnet is a drug with a broad-spectrum antiviral activity targeting viral polymerases. Recently, its mechanism of action was elucidated in the context of HIV-1 RT. But the mechanism of foscarnet inhibition of the HCMV polymerase remains convoluted. This is primarily because of (1) a lack of functionally relevant structural data on the HCVM polymerase, which results from the impossibility of expressing and purifying the enzyme from bacterial cells, and (2) a lack of biochemical studies characterizing the foscarnet binding site. Hence, with respect to foscarnet my objectives are two-fold: (1) to characterize the foscarnet binding site on the HCMV polymerase, and (2) to reconstitute the polymerase active site of the HCMV polymerase in the background of the Rb69 polymerase, an easily purifiable enzyme with extensive structural and biochemical data reported in the literature. In line with these objectives, I used the phenotypic data on HCMV foscarnet resistance and hypersusceptibility, as well as the structural and biochemical data on the RB69 polymerase. I supplemented these previously available data with my biochemical data on the HCMV polymerase and proposed a model for foscarnet binding to the HCMV polymerase. I also generated an active $HCMV_{active\ site}/Rb69_{background}$ polymerase

chimera that exhibits HCMV phenotypic characteristics. This chimeric protein may be used to generate currently unavailable structural data on $HCMV_{active\ site}$/foscarnet interactions.

Entecavir is a potent selective anti-HBV drug that targets HBV polymerase through a mechanism of delayed chain termination of DNA synthesis. Recently it has been shown to have an anti-HIV activity, which has had profound consequences for the use of this drug in the context of HIV/HBV co-infections. I set my objective to determine the molecular mechanism of entecavir anti-HIV action. On the basis of recent clinical and *in vitro* phenotypical data on entecavir, I chose two HIV-RT substitutions to conduct a biochemical characterization of their effect on HIV-RT functions in the presence or absence of entecavir. I proposed a model for the mechanism of the anti-HIV action of entecavir, which argues that delayed chain termination may be a useful drug characteristic in future mechanism-based drug designs.

Acyclovir is a potent selective anti-HSV drug that targets the HSV polymerase through the mechanism of delayed chain termination of DNA synthesis. Acylovir is specifically activated in herpes virus-infected cells owing to the action of the virally encoded thymidine kinase. But recently acyclovir has been shown to have an anti-HIV activity *in vitro* in HHV-6/HIV-1 co-infected cells. Acyclovir pressure has also been shown to select for the V75I mutation in HIV-1 RT. These findings may be of particular interest in the context of synergic HSV-2/HIV-1 co-infection. Thus, I made it my objective to determine the molecular mechanism of resistance to acyclovir by the V75I-mutant HIV-1 RT. My data argue that discrimination against the inhibitor at the level of incorporation is the dominant mechanism associated with ACV resistance conferred by V75I. Nevertheless, the incorporated ACV-MP is subject to higher levels of excision by the V75I-containing HIV-1 RT. Thus, acyclovir appears to be vulnerable to both major NRTI-associated resistance pathways.

1.5 Figures and tables.

Figure 1. Chemical structures of nucleoside analogues.

Generic name	Chemical structure IUPAC name; simplified chemical name	Natural counterpart, simplified chemical name
Abacavir (ABC)	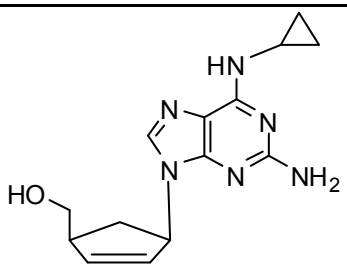 [(1R)-4-[2-amino-6-(cyclopropylamino)purin-9-yl]-1-cyclopent-2-enyl]methanol	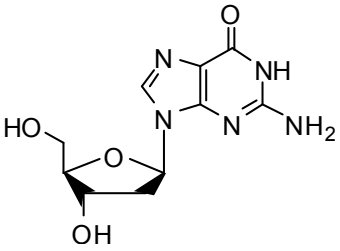 2`deoxyguanosine
Acyclovir (ACV)	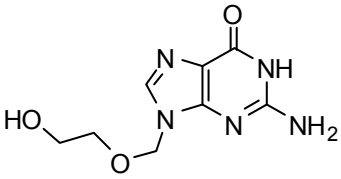 2-amino-9-(2-hydroxyethoxymethyl)-3H-purin-6-one; 9-(2-hydroxyethoxymethyl)guanine	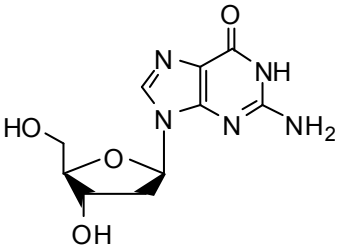 2`deoxyguanosine
Adefovir (PMEA)	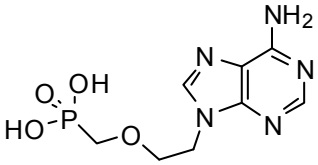 [2-(6-aminopurin-9-yl)ethoxymethyl-(2,2-dimethylpropanoyloxymethoxy)phosphoryl]oxy methyl; 2,2-dimethylpropanoate 9-(2-phosphonylmethoxyethyl)adenine]	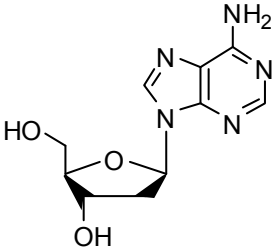 2`deoxyadenosine
Cidofovir (HPMPC)	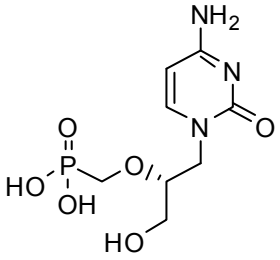 [(2S)-1-(4-amino-2-oxopyrimidin-1-yl)-3-hydroxypropan-2-yl]oxymethylphosphonic acid; (S)-1-[3-hydroxy-2-(phosphonylmethoxy)propyl]cytosine	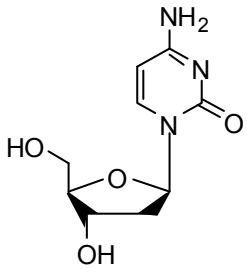 2`deoxycytidine

Didanosine (ddI)	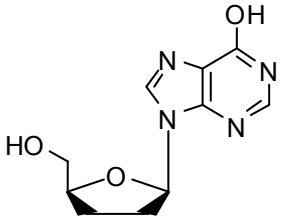 9-[(2R,5S)-5-(hydroxymethyl)oxolan-2-yl]-3H-purin-6-one; 2`,3`-dideoxyinosine	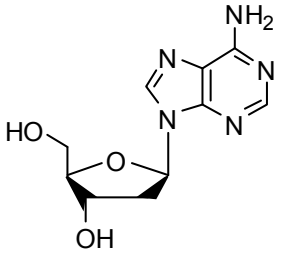 2`-deoxyadenosine
Entecavir (ETV)	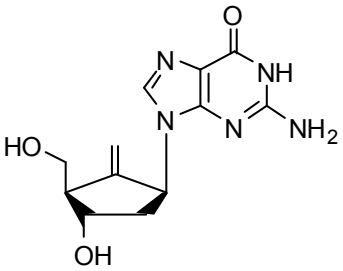 2-amino-9-[(1S,3R,4S)-4-hydroxy-3-(hydroxymethyl)-2-methylidenecyclopentyl]-3H-purin-6-one	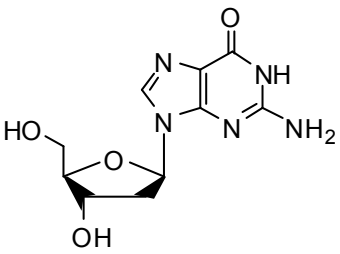 2`-deoxyguanosine
Emtricitabine (FTC)	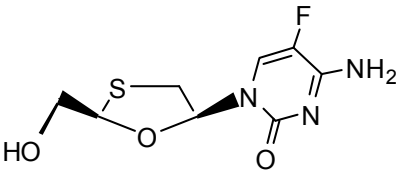 4-amino-5-fluoro-1-[(2R,5S)-2-(hydroxymethyl)-1,3-oxathiolan-5-yl]pyrimidin-2-one; (-)-β-L-3'-thia-2',3'-dideoxy-5-fluorocytidine	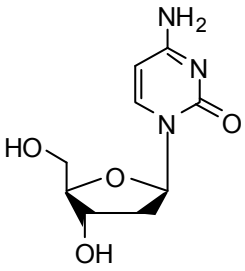 2`-deoxycytidine
Ganciclovir (GCV)	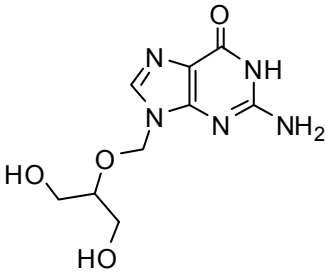 2-amino-9-(1,3-dihydroxypropan-2-yloxymethyl)-3H-purin-6-one; (9-(1,3-dihydroxy-2-propoxymethyl)-guanine)	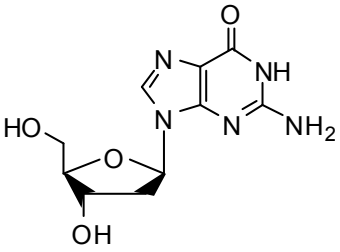 2`-deoxyguanosine

Lamivudine (3TC)	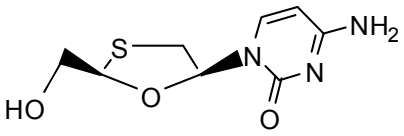 4-amino-1-[(2R,5S)-2-(hydroxymethyl)-1,3-oxathiolan-5-yl]pyrimidin-2-one; (-)β-L-2`,3`-dideoxy-3`thiacytidine	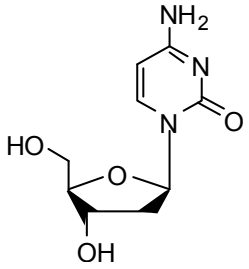 2`-deoxycytidine
Penciclovir (PCV)	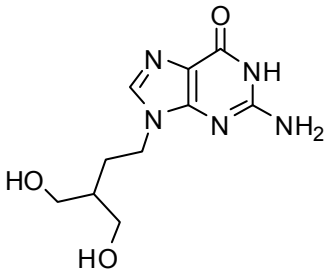 2-amino-9-[4-hydroxy-3-(hydroxymethyl)butyl]-3H-purin-6-one; 9-(4-hydroxy-3-hydroxy-methylbut-1-yl)guanine	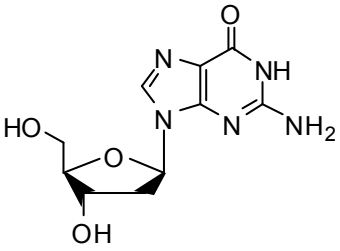 2`-deoxyguanosine
Stavudine (d4T)	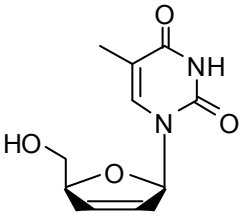 1-[(2R,5S)-5-(hydroxymethyl)-2,5-dihydrofuran-2-yl]-5-methylpyrimidine-2,4-dione; 2',3'- didehydro-2',3'-dideoxythymidine	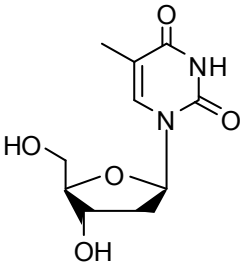 2`-deoxythymidine
Telbivudine (LdT)	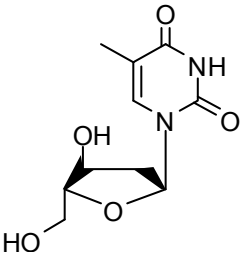 1-[(2S,4R,5S)-4-hydroxy-5-(hydroxymethyl)oxolan-2-yl]-5-methylpyrimidine-2,4-dione; β-L-2`-deoxythymidine	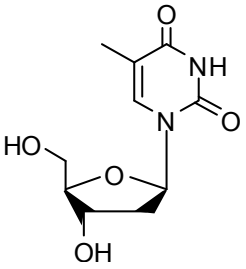 2`-deoxythymidine

Tenofovir (PMPA)	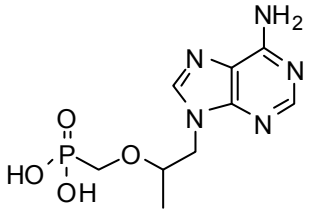 [(2R)-1-(6-aminopurin-9-yl)propan-2-yl]oxymethylphosphonic acid; (*R*)-9-(2-phosphonylmethoxypropyl)adenine	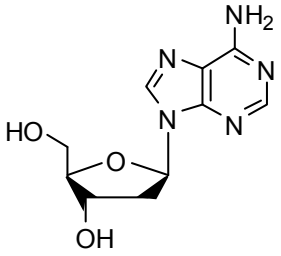 2`-deoxyadenosine
Zalcitabine (ddC)	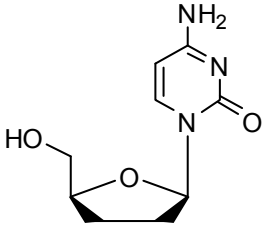 4-amino-1-[(2R,5S)-5-(hydroxymethyl)oxolan-2-yl]pyrimidin-2-one; 2`3`-deoxycytidine	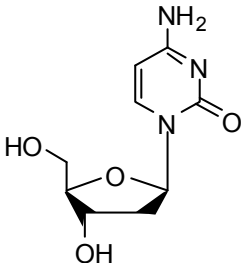 2`-deoxycytidine
Zidovudine (AZT)	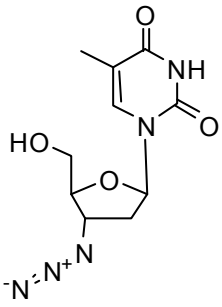 1-[(2R,4S,5S)-4-azido-5-(hydroxymethyl)oxolan-2-yl]-5-methylpyrimidine-2,4-dione; 3'-azido-2',3'-dideoxythymidine	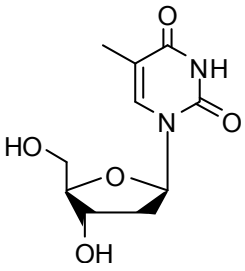 2`-deoxythymidine

Figure 1.2 Schematic representation of a nucleoside.

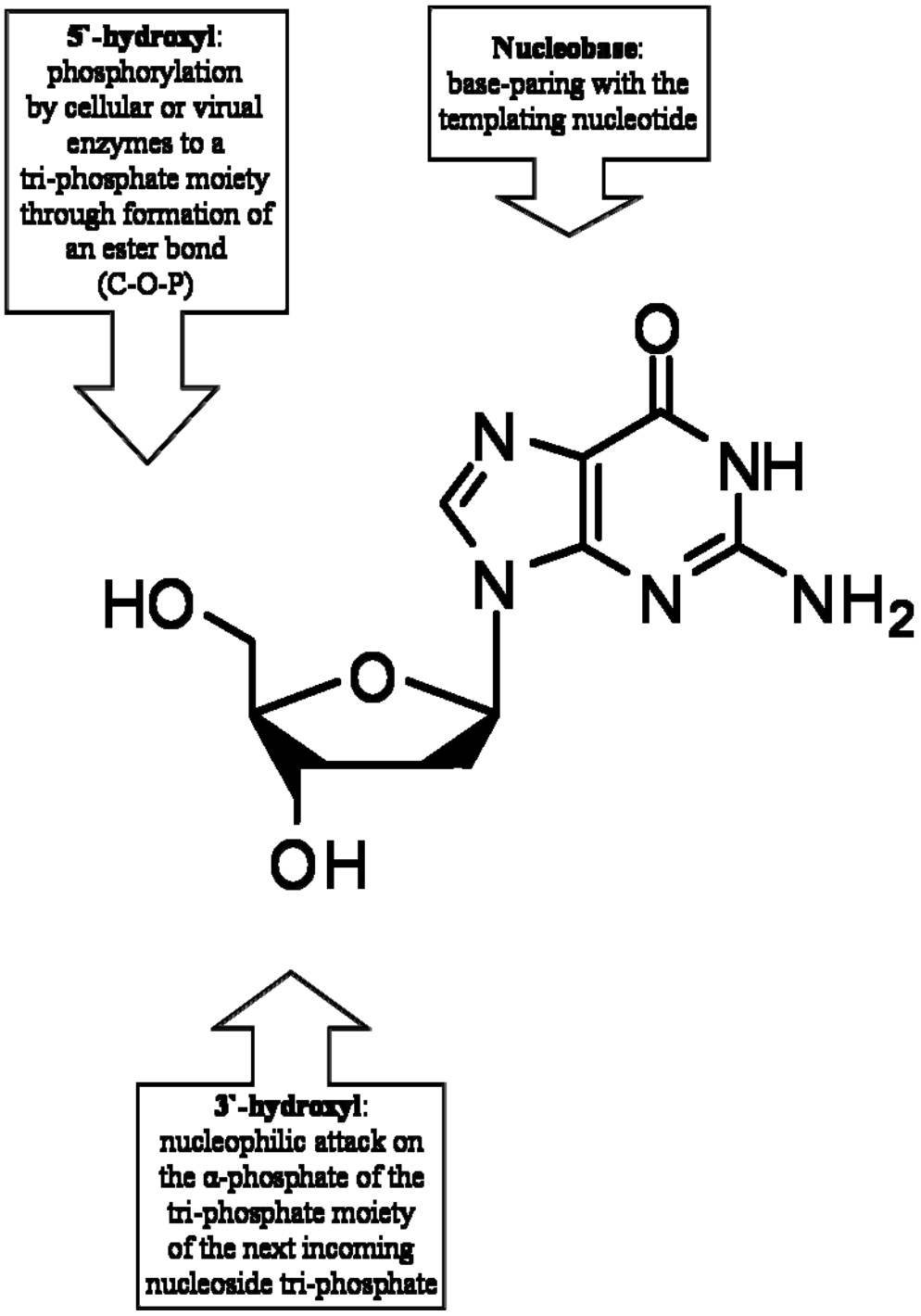
5`-hydroxyl:
phosphorylation
by cellular or virual
enzymes to a
tri-phosphate moiety
through formation of
an ester bond
(C-O-P)
Nucleobase:
base-paring with the
templating nucleotide
O
N
NH
N
N
NH2
HO
O
OH
3`-hydroxyl:
nucleophilic attack on
the α-phosphate of the
tri-phosphate moiety
of the next incoming
nucleoside tri-phosphate

Figure 1.3 Chemical structure of foscarnet

Generic Name	Acronym	Chemical structure simplified chemical name	Natural counterpart
Foscarnet	PFA	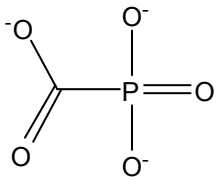 phosphonoformic acid	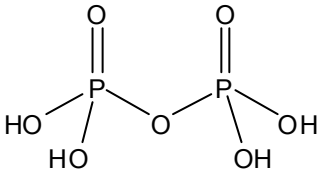 pyrophosphate

Figure 1.4 Summary of modifications on nucleoside analogues

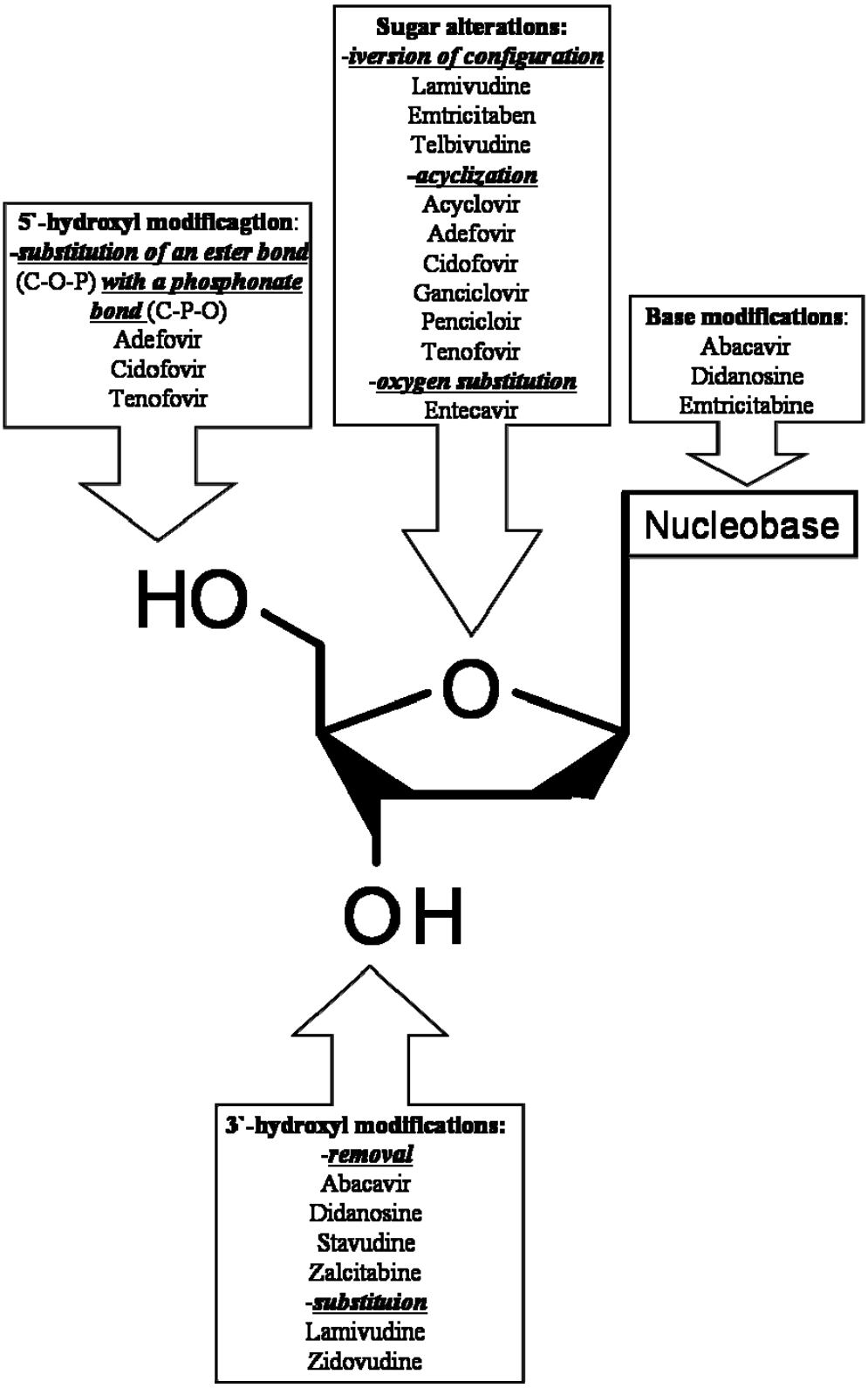
Sugar alterations:
-iversion of configuration
Lamivudine
Emtricitaben
Telbivudine
-acyclization
Acyclovir
Adefovir
Cidofovir
Ganciclovir
Pencicloir
Tenofovir
-oxygen substitution
Entecavir
5`-hydroxyl modificagtion:
-substitution of an ester bond
(C-O-P) with a phosphonate bond (C-P-O)
Adefovir
Cidofovir
Tenofovir
Base modifications:
Abacavir
Didanosine
Emtricitabine
Nucleobase
HO
O
OH
3`-hydroxyl modifications:
-removal
Abacavir
Didanosine
Stavudine
Zalcitabine
-substitution
Lamivudine
Zidovudine

Figure 1.5 Chemical structures of non-nucleoside analogues

Generic Name	Chemical structure, IUPAC name
Nevirapine (NEV)	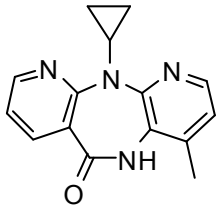 1-cyclopropyl-5,11-dihydro-4-methyl-6H-dipyrido [3,2-b:2',3'-e][1,4] diazepin-6-one
Delavirdine (DLV)	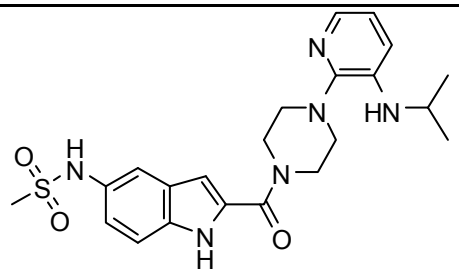 N-[2-[4-[3-(propan-2-ylamino)pyridin-2-yl]piperazine-1-carbonyl]-1H-indol-5-yl]methanesulfonamide
Efavirentz (EFV)	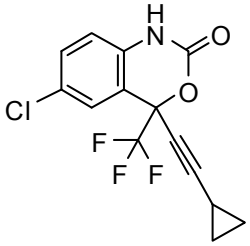 (4S)-6-chloro-4-(2-cyclopropylethynyl)-4-(trifluoromethyl)-1H-3,1-benzoxazin-2-one
Etravirine (ETR)	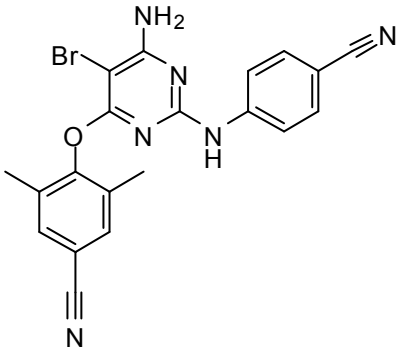 4-[6-Amino-5-bromo-2- [(4-cyanophenyl)amino] pyrimidin-4-yl]oxy-3,5-dimethylbenzonitrile

Figure 1.6 Nucleotide binding site of HIV-1 RT. The dTTP binding site of HIV-1 RT based on crystal structure of HIV-1 RT complexed with DNA/DNA primer/template and the incoming nucleotide by Huang et al., 1998 (PDB code 1RTD). Molecular graphics image was produced using the UCSF Chimera package from the Resource for Biocomputing, Visualization, and Informatics at the University of California, San Francisco (supported by NIH P41 RR-01081), Pettersen et al., 2004. dTTP is shown in black with phosphorous atoms in magenta and the 3`-oxygen atom in yellow. All aminoacids are shown in a stick representaion. Residues colored in red are catalytic aspartic amino acids 110 and 185. Cyan-colored aminoacids illustrate postions involved in resistance to NRTI. These residues are labeled in black. Light green sphere illustrate a magnesium ion. Primer and template are shown in a wire representation.

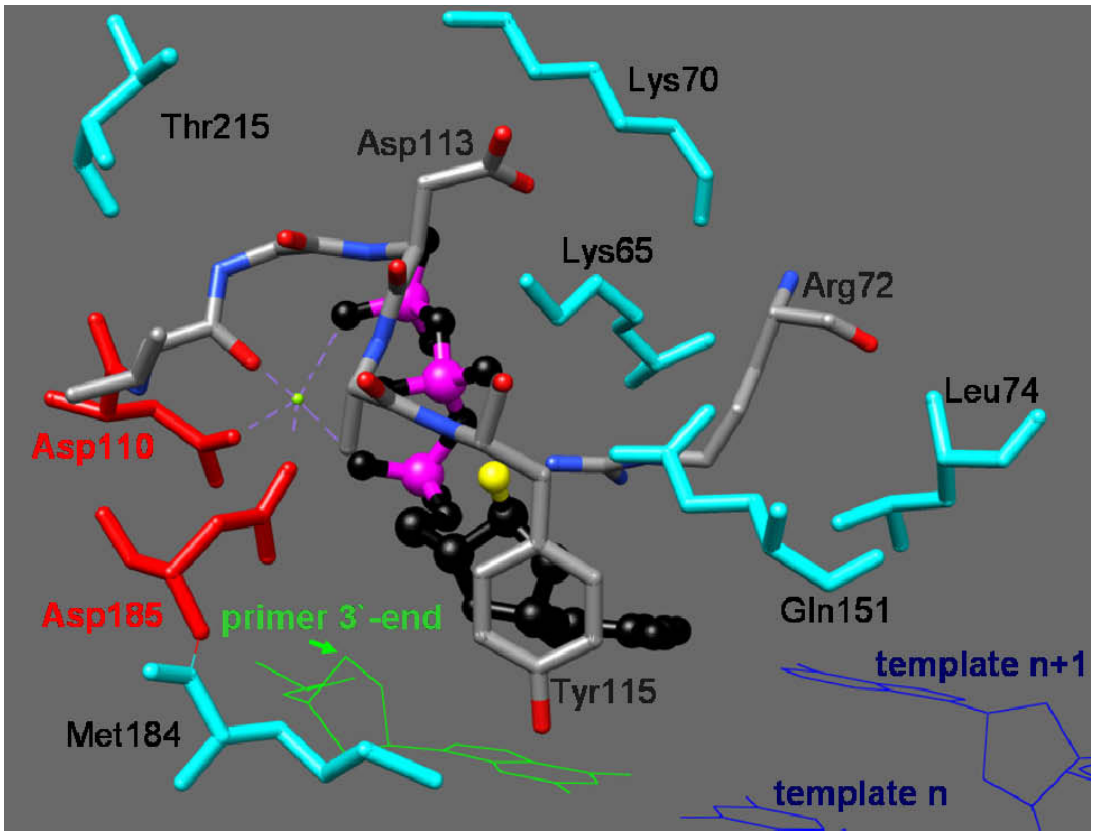
Thr215
Lys70
Asp113
Lys65
Arg72
Leu74
Asp110
Asp185
primer 3`-end
Gln151
template n+1
Tyr115
Met184
template n

Figure 1.7 Non-nucleoside reverse transcriptase inhibitor binding site of HIV-1 RT. The efavirenz binding site of HIV-1 RT based on crystal structure of HIV-1 RT complexed with efavirenz by Ren et al., 2000 (PDB code 1FK9). Molecular graphics image was produced using the UCSF Chimera package from the Resource for Biocomputing, Visualization, and Informatics at the University of California, San Francisco (supported by NIH P41 RR-01081), Pettersen et al., 2004. Efavirenz is shown in black. All aminoacids are shown in a stick representaion. For the reasons of clarity only residues that are 3.5 angstroms away from efavirenz are shown. Cyan-colored aminoacids illustrate postions most frequently involved in resistance to NRTI.

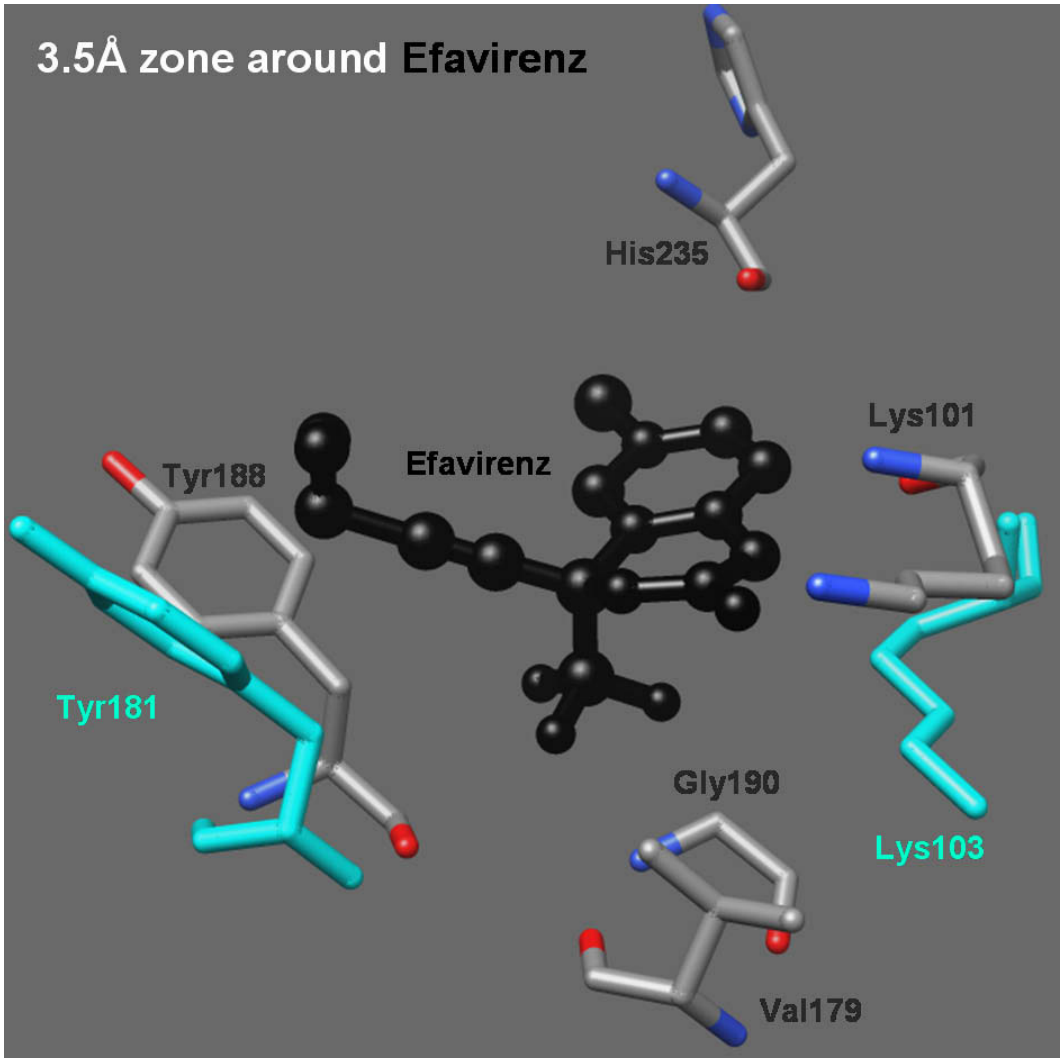
3.5Å zone around Efavirenz
His235
Lys101
Tyr188
Efavirenz
Tyr181
Gly190
Lys103
Val179

Table 1.1 Comparative summary of steps in the viral life cycle employed as targets for currently approved antivirals

Step	Number of drugs	Virus
ENTRY	2	HIV
GENOME EXPRESSION	1	HCMV
GENOME REPLICATION		
Polymerase	25	HSV, HCMV, HBV, HIV
Other proteins	1	HCMV
GENOME INTEGRATION	1	HIV
MATURATION	10	HIV

Table 1.2. Currently approved drugs for anti-HSV therapy

Drug	Approved (year)
Nucleoside analogues	
Acyclovir	1981
Famciclovir	1994
Valacyclovir	1995
Penciclovir	1996

Table 1.3 Currently approved drugs for anti-HIV therapy

Drug	Approved (year)
Nucleoside reverse transcriptase inhibitiors	
Zidovudine	1987
Didanosine	1991
Zalcitabine	1992
Stavudine	1994
Lamivudine	1995
Abacavir	1998
Tenofovir	2001
Emtricitabine	2003
Non-nucleoside reverse transcriptase inhibitiors	
Nevirapine	1996
Delavirdine	1997
Efavirenz	1998
Etravirine	2008
Protease inhibitors	
Saquinavir	1995
Indinavir	1996
Ritonavir	1996
Nelfinavir	1997
Amprenavir	1999
Lopinavir	2000
Fosamprenavir	2003
Atazanivir	2003
Tipranavir	2005
Darunavir	2006
Fusion inhibitor	
Enfuvirtide	2003
Entry inhibitor - CCR5 co-receptor antagonist	
Maraviroc	2007
Integrase strand transfer inhibitor	
Raltegravir	2007

Table 1.4 Currently approved drugs for anti-HBV therapy

Drug	Approved (year)
Nucleoside analogues	
Lamivudine	1998
Adefovir	2002
Entecavir	2005
Telbivudine	2006
Tenofovir	2008
Immunomodulators	
Interferon alpha-2b	1986
Peginterferon alpha-2a	2004

Table 1.5 Location of conserved regions within HSV-1 and HCMV DNA polymerases

Conserved region	HSV-1 (residues)	HCMV (residues)
Exonuclease domain		
Exo I	363 - 373	295 – 312
Exo II	460 - 476	404 – 418
Exo III	572 - 585	533 - 545
Polymerase domain		
δC	531 - 627	492 - 588
I	881 - 896	905 - 919
II	694 - 736	696 – 742
III	805 – 845	805 – 845
IV	437 – 479	379 – 421
V	953 – 963	978 – 988
VI	772 – 791	771 – 790
VII	938 – 946	962 – 970

Table1.6 Currently approved drugs for anti-HCMV therapy

Drug	Approved (year)
Nucleoside analogues	
Ganciclovir	1988
Foscarnet	1991
Cidofovir	1996
Valganciclovir	2000
Anti-sense RNA oligonucleotide	
Fomivirsen	1998
UL97 kinase inhibitor	
Maribavir	2006

Table 7. Comparative summary of viral genome replication

Virus	Template	Primer	Mechanism	Intermediates	Virally Encoded Enzymatic activities involved in genome replication
HSV	DNA	RNA	Rolling circle	Concatameric dsDNA genomes	Helicase, primase, polymerase, exonuclease, thymidine kinase
HCMV	DNA	RNA	Rolling circle	Concatameric dsDNA genomes	Helicase, primase, polymerase, exonuclease, protein kinase
HBV	RNA	Tyrosine residue of HBV-RT	Primer translocation, strand transfer	(1) Circular, covalently closed DNA, (2) pre-genomic RNA, (3) RNA(+)/ DNA(-) hybrid, (4) effectively circular, partially dsDNA	Reverse transcriptase RNase H
HIV	RNA	Cellular $tRNA^{Lys3}$	Primer translocation, strand transfer	(1) RNA(+) /DNA(-) hybrid, (2) circular intermediate, (3) dsDNA with a DNA(+) strand flap in the central region	Reverse transcriptase RNase H

CHAPTER 2

ROLE OF HELIX P OF THE HUMAN CYTOMEGALOVIRUS DNA POLYMERASE IN RESISTANCE AND HYPERSUSCEPTIBILITY TO THE ANTIVIRAL DRUG FOSCARNET

This chapter was adapted from an article authored by E.P.Tchesnokov, C. Gilbert, G. Boivin, and M. Gotte that appeared in the ***Journal of Virology***, 2006, 80(3):1440-1450.

2.1 Abstract.

Mutations in the human cytomegalovirus DNA polymerase (UL54) can not only decrease but also increase susceptibility to the pyrophosphate (PPi) analogue foscarnet. The proximity of L802M, which confers resistance, and K805Q, which confers hypersusceptibility, suggests a possible unifying mechanism that affects drug susceptibility in one direction or the other. We found that the polymerase activities of L802M- and K805Q-containing mutant enzymes were literally indistinguishable from that of wild-type UL54; however, susceptibility to foscarnet was decreased or increased, respectively. A comparison with the crystal structure model of the related RB69 polymerase suggests that L802 and K805 are located in the conserved α-helix P that is implicated in nucleotide binding. Although L802 and K805 do not appear to make direct contacts with the incoming nucleotide, it is conceivable that changes at these residues could exert their effects through the adjacent, highly conserved amino acids Q807 and/or K811. Our data show that a K811A substitution in UL54 causes reductions in rates of nucleotide incorporation. The activity of the Q807A mutant is only marginally affected, while this enzyme shows relatively high levels of resistance to foscarnet. Based on these data, we suggest that L802M exerts its effects through subtle structural changes in α-helix P that affect the precise positioning of Q807 and, in turn, its presumptive involvement in binding of foscarnet. In contrast, the removal of a positive charge associated with the K805Q change may facilitate access or increase affinity to the adjacent Q807.

2.2 Introduction

The human cytomegalovirus (HCMV), which is a DNA virus that belongs to the *Herpesviridae* family, is an important human pathogen [131, 137]. Immunocompromised patients, for instance, transplant recipients or AIDS patients, are especially vulnerable to such infection, although the clinical use of anti-retroviral drugs against human immunodeficiency virus type 1 (HIV-1) has dramatically decreased the incidence of HCMV-related disease for patients who respond to HIV-specific treatment [396]. Antiviral drugs that are used to treat HCMV infection target the viral DNA polymerase [397]. The nucleoside analogue ganciclovir (GCV) and the nucleotide analogue cidofovir (CDV) are approved anti-HCMV drugs. Both drugs were shown to significantly reduce the viral burden; however, antiviral therapy over protracted periods of time can lead to the emergence of resistance-conferring mutations, which is a major factor associated with treatment failure [132]. Resistance to GCV has been associated with mutations in the viral UL97 and UL54 genes [132, 398-400]. The former encodes a kinase that phosphorylates the drug to its monophosphate form, and the latter encodes the viral DNA polymerase that accepts the triphosphate form of this compound. CDV is a phosphonate that requires activation by cellular enzymes to its diphosphate form, which explains why changes in the UL97 gene do not affect susceptibility to this compound [401]. However, many of the mutations found in the DNA polymerase confer cross-resistance to both drugs.

The pyrophosphate analogue foscarnet (PFA; phosphonoformic acid) is the third approved anti-HCMV compound that is frequently administered when first-line agents have failed.

The triphosphate form of GCV and the diphosphate form of CDV compete with their natural counterparts dGTP and dCTP, respectively, for binding to the DNA polymerase and incorporation into the viral DNA [172]. Once incorporated, these

compounds were shown to reduce subsequent polymerization steps [173]. Biochemical studies with the UL54 enzyme and the related herpes simplex virus (HSV) DNA polymerase (UL30) suggested that resistance-conferring mutations appear to diminish drug binding and/or incorporation [402, 403]. The mechanisms of drug action and resistance associated with foscarnet are less well characterized. This compound exhibits a broad spectrum of antiviral activities and has been shown to block replication of related herpesviruses, including HCMV, HSV type 1 (HSV-1), and HSV-2, as well as retroviruses, including HIV-1 [32, 174]. Foscarnet acts noncompetitively with respect to the deoxynucleoside triphosphate (dNTP) substrate [33]. It has been suggested that the pyrophosphate analogue binds to a site in close proximity to the active center that may overlap at least in part with the pyrophosphate binding site [34]. This notion is based on biochemical studies showing that foscarnet blocks pyrophosphate exchange reactions and pyrophosphorolysis, i.e., the reverse reaction, in competitive fashion. However, the precise binding site of foscarnet and the detailed mechanism of drug action remain elusive. Mutations that confer resistance to foscarnet map to different conserved regions in the UL54 gene and do not appear to cluster around a specific site [22]. At the same time, it should be mentioned that crystal structure models of UL54 and UL30 are not available, which makes it difficult to define the active center and the putative binding site for foscarnet.

Clinical data have shown that resistance to foscarnet is associated with mutations T700A, M715V, E756Q, V781I, V787L, L802M, A809V, V812L, and T821I [132, 404, 405]. Of note, it has been reported that prolonged treatment with GCV and PFA can lead to the emergence of a dually resistant phenotype. One particular isolate harbored mutations T821I and K805Q among others [406]. Drug susceptibility measurements with recombinant viruses that contained single point mutations revealed that T821I caused a 21-fold decrease in susceptibility to foscarnet, while K805Q conferred a 5- to 6-fold increase in susceptibility to foscarnet [402]. Drug hypersusceptibility is of potential clinical benefit, which merits further investigation. K805 is also located in the vicinity of other residues

that were shown to reduce susceptibility to foscarnet, e.g., L802M. It is therefore conceivable that this region plays an important role in drug binding and enzymatic activity.

Subtle structural changes may either decrease or increase the affinity to foscarnet, which may translate into resistant or hypersusceptible phenotypes, respectively. Here we generated wild-type (WT) UL54 as well as the K805Q- and L802M-containing mutant enzymes in order to study the biochemical mechanisms associated with these complex phenotypes. We found that the enzymatic activities are not significantly changed in the absence or in the presence of either of the two mutations. However, K805Q increased the inhibitory effects of foscarnet, while L802M decreased its efficacy in cell-free assays, which is in good agreement with published drug susceptibility data [402]. We provide evidence to show that both residues are most likely located within a helical region in close proximity but not in contact distance to the bound dNTP. Mutagenesis studies, based on the structure of the related DNA polymerase (gp43) of the bacteriophage RB69, suggest that both mutations could exert their effects indirectly through the adjacent, highly conserved residue Q807.

2.3 Experimental procedures

Plasmid constructs- Wild-type and mutant enzymes were derived from recombinant viruses generated by overlapping cosmids as described previously (5). The UL54 coding sequence was cloned into pCITE4b (Novagen) by use of the EcoRI and HindIII sites to generate pCITE4b/UL54-WT, -L802M, -Q805A, -Q807A, and -K811A. Amino acid substitutions were introduced with *Pfu* DNA polymerase (Fermentas) according to the manufacturer's recommendations by amplification of the pCITE4b/UL54-WT plasmid with primer pairs that contained the proper changes. All plasmids were sequenced to confirm the presence of the introduced mutation and the absence of undesired changes.

Protein expression- All enzymes were expressed in rabbit reticulocyte lysate by use of a coupled in vitro transcription-translation system (Promega). Reactions were conducted essentially as previously described [407]. In order to assess and compare the yields of the different enzymes, we included 40 mCi [^{35}S]methionine (Amersham Biosciences) in the reaction mixture and analyzed the products through sodium dodecyl sulfate-polyacrylamide gel electrophoresis. The gels were quantified by phosphorimager analysis (Storm 840; Amersham Biosciences). We found that 2.5 to 3% of [^{35}S]methionine was incorporated into the proteins, which corresponds to a protein concentration of approximately 1.5 ng/ml. This amount was similar for wild-type and mutant proteins.

Bioinformatics and structural analyses- Sequence alignments were generated with MacVector software (Accelrys). The structural information of the RB69-associated polymerase gp43 is based on the structure of the ternary complex (PDB no. 1IG9). Figure 2.1C was generated with a Deep View-Swiss PDB viewer.

Filter-based DNA polymerase assay- DNA polymerase activity was tested in the presence of activated calf thymus DNA. The reaction was performed with 25 mM Tris-HCl (pH 8), 90 mM NaCl, 0.5 mM dithiothreitol, 0.2 mg/ml bovine serum albumin, and *5%* glycerol (designated buffer P). dATP, dCTP, and dTTP (10 μM each), 100 μg/ml activated calf thymus DNA (Amersham Biosciences), 1 μM [^{3}H]dTTP, and 0.5 μl of the enzyme-containing transcription-translation mixture (~0.75 ng enzyme) were used in a typical setup. Reactions were carried out in a total volume of 25 ul at 37°C, following the addition of $MgCl_2$ (10 mM). DNA synthesis was stopped after 30 min by addition of 600 μl of cold 10% trichloroacetic acid-1% $NaPP_i$, followed by nucleic acid precipitation on ice for 1 h. The samples were filtered and washed with 10% trichloroacetic acid-1% NaPPi to measure the labeled DNA by scintillation counting.

Gel-based DNA polymerase assay- Unless otherwise indicated, we used the following synthetic heteropolymeric oligonucleotides (Invitrogen) in gel-based

assays to measure the polymerase activity of UL54: 5'-GAGTGGTATAGTGGA GTGAA-3' (P20) and 5'-CCAATATTCACCATCAAGGCTTGACGTCACTTC ACTCCACTATACCACTC-3' (T50). The underlined sequence represents the region of the template that is complementary to the primer (P20). The synthetic oligonucleotides were purified on 12% polyacrylamide-7 M urea gels containing 50 mM Tris-borate, pH 8.0, and 1 mM EDTA. 5'-end labeling of the primer was performed with [γ-^{32}P]ATP and T4 polynucleotide kinase. The labeled products were again electrophoretically purified to obtain homogeneously labeled nucleic acids. Primer/template sequences were annealed prior to the start of the reaction. In a typical reaction, DNA synthesis was conducted with buffer P in the presence of 10 μM of each of the four nucleoside triphosphates, 1.5 pmol of the primer/template substrate, and 1 μl (~0.0125 pmol UL54) of the enzyme preparation. We used a relatively high ratio of nucleic acid/enzyme to ensure that DNA synthesis was monitored in the linear range. Reactions were initiated by the addition of $MgCl_2$ (10 mM) in a total volume of 20 μl and stopped by addition of 20 μl formamide and bromophenol blue/xylene cyanole dyes. The products were heat denatured for 5 min at 95°C, resolved on 8% polyacrylamide-7 M urea gels, and analyzed by phosphorimager analysis.

Measurements of IC_{50} values- Polymerase activity was monitored in the presence of increasing concentrations of foscarnet or pyrophosphate in order to determine the concentrations of inhibitor that were required to block 50% of full-length DNA synthesis (50% inhibitory concentrations [IC_{50}]). The ranges of concentrations used are indicated in the figure legends. The data were analyzed with Prism software (GraphPad Prism version 4.0).

Steady-state kinetics- Steady-state kinetic parameters K_m and V_{max} for single-nucleotide incorporation events were determined through gel-based assays, as described previously [408]. We used four different primer/template combinations, referred to as P20/T33-A, -C, -G, and -T: 5'-GAGTGGTATAGTGGAGTG AA-3' (P20), 5^f-AGAGAGAGAGAGTTTCACTCCACTATACCACTC-3^f (T33-A), 5'-

ACACACACACACGTTCACTCCACTATACCACTC-3' (T33-C), 5'-GTG TGTGTGGTGCTTCACTCCACTATACCACTC-3' (T33-G), and 5'-TCTCTC TCTTCTATTCACTCCACTATACCACTC-3' (T33-T). Each underlined sequence represents the region of the template that is complementary to the primer (P20).

The incorporation of the nucleotide was monitored at a single time point in the presence of increasing concentrations of dATP, dCTP, dGTP, or dTTP. Reactions were allowed to proceed for 10 min at 37°C. Misincorporations have not been observed under these conditions. The data were fitted to Michaelis-Menten equations by use of GraphPad Prism (version 4.0). K_i values were determined on the basis of measurements of multiple incorporation events by using calf thymus DNA as described above. The assay was conducted in the presence of 1 μM [^{3}H]dTTP and increasing concentrations (0, 0.08, 0.16, 0.32, 0.64, 1.3, and 2.5 μM) of dATP, dCTP, and dGTP. This experiment was performed with five different concentrations of foscarnet (0.13, 0.25, 0.5, 1, and 2 μM for WT-UL54; 0.25, 0.5, 1, 2, and 4 μM for the L802M and Q807A mutants; and 0.031, 0.061, 0.13, 0.25, and 0.5 μM for Q805K). The data were fitted to Michaelis-Menten equations to determine K_m and V_{max} values. K_i values and type of inhibition were determined by plotting $1/V_{max}$ and K_m as a function of foscarnet concentration.

2.4 Results

Experimental design- Figure 2.1A shows the distribution of known foscarnet resistance mutations in domain III of HCMV UL54. This region contains numerous residues that are highly conserved among different members of the α-DNA polymerase family, to which the HSV-, HCMV-, and RB69-associated enzymes belong [22]. While structural models of the HSV and HCMV polymerases are not available, the crystal structure of the RB69 enzyme (gp43) has been determined in various forms [101, 409, 410], including the structure of a complex with bound primer/template and nucleotide substrates [103]. This model shows that the highly conserved residues of domain III constitute part of helix P,

which interacts with the template strand and the nucleoside triphosphate (Figure 2.1B and C). K560 in gp43 has been identified as an important residue that contacts the bound nucleotide at its α- and γ-phosphates [411]. Pre-steady-state kinetic analyses have shown that a K560A change in gp43 caused a severe reduction in rates of nucleotide incorporation [411]. The mutant had a much higher K_d value than the wild-type enzyme. The UL54 counterpart of K560 is located at position 811, which is in close proximity to the mutations that are implicated in resistance (L802M) and hypersusceptibility (K805Q) to foscarnet. However, the gp43 structure suggests that the equivalent residues, A551 and T554, respectively, reside at a distance of approximately 12 Å away from γ-phosphate (Figure 2.1C). Thus, one could consider two different explanations to reconcile these observations. The structures of UL54 and gp43 could differ to such an extent that L802 and K805 are actually located closer to the bound nucleotide, where the two mutations may directly affect binding of foscarnet. Alternatively, the structures are indeed very similar and L802M and K805Q may exert their effects indirectly over a longer distance. An HSV-1 recombinant that contains the K805Q change shows the same hypersusceptible phenotype as described for HCMV, which points to a high degree of structural homology in this region, at least among UL54 and UL30 [412]

.

To better assess to which degree the structures of the RB69 and UL54 enzymes resemble one another, in particular around the dNTP/PPi binding site, we generated two UL54 mutant enzymes that contain alanine residues at positions K811 and Q807. The glutamine is also conserved among various members of the α-like polymerases; however, Q556 in gp43 still resides at a distance of approximately 6 Å away from the γ-phosphate. This may not suffice for direct contacts, although Q556 is located on the same side of the helix as the phosphate. Thus, one would predict that the effects of changes at Q556 (gp43) and Q807 (UL54) on the rates of polymerization are likely to be less pronounced than changes at K560 and K811, respectively. In order to shed light on the molecular mechanisms involved in resistance and hypersusceptibility to foscarnet, we

characterized the two UL54-associated mutants K811A and Q807A together with enzymes that contain mutations L802M and K805Q.

Steady-state kinetics- Throughout this study, we used a coupled *in vitro* transcription-translation system to generate UL54 and its mutant variants (see Materials and Methods). This expression system has proven successful for the determination of steady-state kinetic parameters [153, 185]. In order to compare the efficiency of DNA synthesis of wild-type UL54 and that of the four mutant enzymes, we initially looked at multiple nucleotide incorporation events by using a defined primer/template system in gel-based assays (Figure 2.2). The activities of wild-type UL54 and the Q807A mutant appeared almost identical in this experiment; however, DNA synthesis with K811A was compromised. The two mutants L802M and K805Q displayed wild-type-like activities as well (data not shown). To translate these observations into quantitative terms, we next determined K_m and V_{max} values with regards to the incorporation of a single nucleotide. For this purpose, we incrementally increased the concentrations of the first nucleotide and omitted the three other dNTPs from the reaction mixture (Figure 2.3). Overall, we found that the efficiency of the reaction (V_{max}/K_m) was similar for wild-type UL54 and the three mutants Q807A, L802M, and K805Q, while K811A was again compromised (Table 2.1). We measured the following reductions in the efficiency of a single-nucleotide incorporation event when K811A was compared with the wild-type enzyme: 15-fold (dATP), 12-fold (dCTP), 20-fold (dGTP), and 30-fold (dTTP). In contrast, Q807A caused only relatively minor changes: 2.3-fold (dATP), 2-fold (dCTP), 1.7-fold (dGTP), and 3-fold (dTTP). We determined similar relatively small changes with the other two mutants, L802M and K805Q (Table 2.1).

These data provide strong evidence to suggest that the two conserved residues in helix P of gp43 and UL54 exhibit similar functions with regards to dNTP binding and catalysis. With the exception of dATP, the reduced efficiency of nucleotide incorporation seen with the K811A mutant was largely attributable to higher K_m values. For yet-unknown reasons, the incorporation of dAMP, relative to that of

the three other nucleotides, was generally associated with elevated K_m values for each of the enzymes studied. The relatively small effects on single-nucleotide incorporation events seen with the Q807A mutant suggest that the distance between the side chain of the conserved glutamine and the γ-phosphate of the incoming nucleotide might be too long to allow direct contacts. This notion is supported by the fact that mutations L802M and K805Q showed similar minor changes with respect to the efficiency of incorporation of a single nucleotide.

Inhibitory effects of foscarnet and pyrophosphate- We utilized the same primer/template substrate as shown in Figure 2.2 to analyze the effects of L802M- and K805Q-containing mutant enzymes on DNA synthesis in the presence of increasing concentrations of foscarnet. In this context, we measured the concentration of foscarnet that is required to inhibit 50% of the production of full-length DNA (Figure 2.4). The L802M mutant showed a threefold-increased IC_{50} value, while the K805Q mutant showed a fivefold-decreased IC_{50} value. These biochemical data are remarkably consistent with drug susceptibility measurements based on plaque reduction assays [402]. It would be of interest to conduct the kinetic measurements also in the presence of UL44, which acts as a processivity factor [413]; however, our data suggest that resistance- or hypersusceptibility-conferring mutations affect intrinsic properties of the polymerase UL54. It is unlikely that L802M and K805Q may directly affect binding of foscarnet. Our data with mutants K811A and Q807A suggest that positions 802 and 805 are too far away from the presumptive binding site of the drug. This site may partially overlap with the PPi binding site, considering that foscarnet inhibits pyrophosphorolysis in a competitive fashion. Crystal structures of complexes of T7 RNA polymerase with and without PPi or dNTP substrates show that PPi binds to the same location that was formerly occupied by the β-and γ-phosphates of the bound nucleotide [414].

L802M and K805Q may exert their effects indirectly through structural changes of other residues that are located in close proximity to the nucleotide binding site.

Q807 might be a good candidate in this regard. Thus, we included the Q807A mutant in this set of experiments and found that this change caused a sixfold-increased IC_{50} value, which is twice as high as the change we measured with the naturally occurring resistance mutation L802M. These data support the notion that L802M may exert its resistance-conferring effects through structural perturbations at or around position 807. However, these data do not explain the hypersusceptible phenotype associated with K805Q.

If the binding site for foscarnet indeed overlaps with the binding site for PP_i, one can predict that the three mutations L802M, K805Q, and Q807A affect the inhibition of DNA synthesis in the presence of PPi in a fashion similar to that described for foscarnet. To address this problem, we utilized a polymerase assay that is based on measurements of DNA synthesis with activated calf thymus DNA (see Materials and Methods). This assay differs from our gel-based setup, as it involves longer heteropolymeric DNA templates, which potentially provides higher sensitivity since the inhibitory effects of the drug can theoretically affect each of the multiple nucleotide incorporation events. We found that the resistance values (*n*-fold) for foscarnet are similar for both assays (Table 2.2): L802M (3.5-fold), K805Q (0.3-fold), and Q807M (5.3-fold). The measurements with PPi do not reveal any significant differences between wild-type UL54 and enzymes that contain mutations L802M and Q807A, which increase the IC_{50} for foscarnet. Although we observed subtle increases in IC_{50} values, these increases are by far not as pronounced as those seen with foscarnet.

These data suggest that the binding sites for foscarnet and PPi may not be identical. It appears that Q807A can affect binding of foscarnet but not binding of PPi. These data are consistent with the crystal structure of gp43, which shows the functional equivalent of Q807 at a distance that does not allow contacts with the β- and γ-phosphates of the incoming nucleotide. Unlike mutations L802M and Q807A, K805Q, which decreased the IC_{50} for foscarnet (0.3-fold), also decreased the IC_{50} for PPi (0.6-fold). Thus, it appears that K805Q diminishes the inhibitory

effects of PPi and the PPi analogue through a similar mechanism. This mechanism does not appear to involve increased drug binding through 805Q, because position 805 is too far away from the β- and γ-phosphates of the bound nucleotide.

Type of inhibition- Previous biochemical studies have shown that foscarnet is a noncompetitive inhibitor with respect to the nucleotide substrate [33]. Thus, we next determined steady-state kinetic parameters (K_{max}, K_m, and K_i) in the presence of increasing concentrations of foscarnet in order to analyze whether the same or a different type of inhibition is seen with the resistance- and hypersusceptibility-conferring mutants (Figure 2.5 and Table 2.3). With respect to all four enzymes, i.e., wild-type UL54, L802M, K805Q, and Q807A, we found that changes for K_m values were insignificant, while V_{max} values decreased dramatically with increasing concentrations of the drug. These data show that foscarnet acts as a noncompetitive inhibitor in each case, regardless of whether the phenotype shows resistance or hypersusceptibility. As expected, the extent of the decrease in V_{max} values depends on the phenotype. K_i values were determined by plotting $1/V_{max}$ against the different concentrations of foscarnet (Table 2.3). K_i values higher than those for wild-type UL54 are consistent with a resistant phenotype (L802M and Q807A), while the lower K_i value determined for K805Q is consistent with the hypersusceptible phenotype.

2.5 Discussion

The pyrophosphate analogue foscarnet is clinically used to treat infection with HSV, HCMV, and related herpesviruses. As with other antiviral drugs, success in therapy is sometimes severely compromised in the presence of resistance-conferring mutations that eventually emerge over longer periods of treatment. Specific mutations have been identified for various conserved domains of the HCMV DNA polymerase and do not appear to cluster around a single site [132]. In this study, we focused on the biochemical characterization of relevant mutations that are found in helix P (A786 to N825). Changes in this region have

also been associated with resistance to nucleoside/nucleotide inhibitors (Figure 2.1A), and in this context it is interesting to note that a V823A change was also shown to decrease susceptibility to a non-nucleoside analogue inhibitor [415]. These combined data suggest that α-helix P plays important roles in enzymatic function.

The structure of the related RB69-associated polymerase gp43 shows that N564, K560, and Q556 of helix P reside in the vicinity of the incoming dNTP [411]. The functional equivalents in UL54 are N815, K811, and Q807. Several mutations that confer either reduced (L802M, A809V, V812L, and T821I) or increased (K805Q) susceptibility to foscarnet are located in close proximity to the conserved residues that are implicated in nucleotide binding. Based on our biochemical studies, we propose a model that helps to explain the role of helix P in mechanisms involved in foscarnet drug action and drug resistance. We suggest that the presumptive binding site for foscarnet is located in close proximity to the γ-phosphate of the bound nucleotide and that Q807 provides important contacts (Figure 2.6). The development of this model is discussed next.

Nucleotide binding characteristics. Previous biochemical and crystallographic data for gp43 suggested that K560 is involved in nucleotide binding [411]. Here we propose a similar function for K811 of UL54. The notion that this residue is involved in nucleotide binding is supported by steady-state kinetic analyses showing that DNA synthesis with the K811A mutant is compromised. This effect is largely attributable to increases in K_m values, which is reminiscent of the higher K_d values obtained with the functionally equivalent RB69 mutant. The K_m and K_d values are not necessarily identical [416]; however, given the established position of K560 in the RB69 enzyme [411], it is reasonable to assume that K811 is likewise involved in nucleotide binding. In contrast, the function of the conserved residue Q807 is less well defined, because the model of gp43 shows the equivalent amino acid at a distance of approximately 6 Å away from the γ-phosphate, which appears to be too far to permit direct contacts with the bound

nucleotide. In fact, the polymerase activity of the Q807A mutant of UL54 was not significantly altered. These data provide strong evidence to suggest that the structures and functions of helix P of enzymes gp43 and UL54 are very similar. It remains to be elucidated why the glutamine at position 807 is actually conserved among the various members of the α-polymerase family. Given the proximity to the phosphates of the bound nucleotide, this residue might be involved in the release of PPi, which is difficult to study under steady-state conditions. Pre-steady-state kinetic analyses along with cell culture-based fitness measurements may help to shed light on this problem.

Binding of foscarnet. Here we have shown that the Q807A mutant confers sixfold resistance to foscarnet, which suggests that Q807 might be directly involved in binding of foscarnet. Previous studies of related polymerases have shown that foscarnet acts as a competitive inhibitor with respect to the reverse reaction, i.e., pyrophosphorolysis [34]. These findings indicate that the binding sites for PPi and foscarnet may overlap to a certain degree. Such overlap is unlikely to be extensive, since foscarnet acts as a noncompetitive inhibitor with respect to the nucleotide substrate [33]. Moreover, high levels of resistance to foscarnet are usually not associated with high levels of resistance to PPi (Table 2.2) [34], which is what one would predict were the binding sites identical. Together, these data provide evidence to suggest that the binding site for foscarnet is located in close proximity to the position of the γ-phosphate and that Q807 provides important contacts (Figure 2.6). Both the carboxyl and phosphonate moieties may interact either with Q807 or with residues that are normally in contact with the γ-phosphate. Of note, residue K65 in HIV-1 reverse transcriptase (RT) contacts the γ-phosphate of the bound nucleotide and a K65R change confers resistance to foscarnet [417]. In UL54, K811 could be seen as a functional equivalent in this regard; however, the activity of the K811A mutant is impaired per se, which makes it difficult to accurately measure changes in IC_{50} values. Drug binding in the proposed mode may prevent simultaneous binding of PPi, particularly if one considers the high IC_{50} values compared to those for foscarnet (Table 2.2). In

contrast, the noncompetitive mode of inhibition of DNA synthesis suggests that the incoming dNTP may still bind to its designated binding site; thus, simultaneous binding of foscarnet could affect the precise positioning of the dNTP substrate rather than its affinity to the enzyme. Binding of the dNTP substrate and foscarnet may also involve different complexes, as previously suggested for HIV-1 RT [418]. Site-specific foot-printing experiments revealed that the nucleotide substrate can bind only to a posttranslocation complex, in which the dNTP binding site is freely accessible [359]. In contrast, foscarnet may (also) bind to the pretranslocation complex, in which the newly incorporated nucleoside monophosphate occupies the dNTP binding site.

Other residues that are not necessarily part of helix P may likewise provide contacts to the bound foscarnet. For instance, the gp43 structure suggests that basic amino acids R785 and R789 in UL54 are found within 6 Å of the γ-phosphate [103]. Of note, changes at the adjacent amino acid V781 have been associated with resistance to foscarnet, and changes at positions D780 and L782 of the related herpes simplex virus DNA polymerase (UL30) reduce susceptibility to foscarnet and to acyclovir and adefovir [22]. All of these residues belong to helix N, which was also shown to provide important contacts to the bound dNTP binding [103, 411]. As for helix P, many mutations that affect susceptibility to foscarnet and nucleoside/nucleotide analogue inhibitors are found in close proximity to highly conserved residues. It is thus likely that some of these mutations exert their effects indirectly, possibly through subtle rearrangements of the side chains of adjacent highly conserved residues.

Resistance and hypersusceptibility. In this study, we have focused on mutations L802M and K805Q. Our model predicts that the distance between L802M and the bound foscarnet might be too long to allow contacts. Drug binding in close proximity to the highly conserved residues K811 and Q807, as shown in Figure 2.6, literally excludes direct interactions with L802. The L802M substitution may affect the precise positioning of Q807, which in turn affects binding of foscarnet.

In this model, subtle rearrangements of the side chain do not necessarily affect the affinity to PPi. Based on crystal structures of other polymerase complexes, it is reasonable to assume that PPi occupies the positions of the β- and γ-phosphates of a nucleoside triphosphate substrate [414]. This region is not within contact distance of Q807, which is supported by our data that show that Q807A- and L802M-associated mutations increase IC_{50} values for foscarnet, while no discernible differences were measured with PPi.

In contrast to the data obtained with L802M, the K805Q mutant that confers hypersusceptibility to foscarnet also reduces the IC_{50} value for PPi. It is unlikely that the K805Q change can directly affect binding of foscarnet or PPi, because the distance to the presumptive binding sites would be too long, as outlined above. However, the natural K805 could affect the precise orientation of foscarnet and/or its interaction with Q807. The net loss of positive charge in K805Q may counteract such an effect, which would provide an explanation for the hypersusceptible phenotype. Mechanisms that are not based on affinity changes cannot be excluded at this point. Previous biochemical and crystallographic data have shown that the K103N mutation in HIV-1 RT acts as a "gate keeper" and restricts the access of certain non-nucleoside analogue RT inhibitors to their designated target site [419]. Conversely, it is conceivable that hypersusceptibility-conferring mutations, such as the K805Q change, may facilitate drug access.

The mechanisms by which mutations V812L, A809V, and T821I confer resistance to the drug can also differ from the mechanisms discussed in this study. V812L and A809V are located in close proximity to the incoming nucleotide and may thus directly affect binding of foscarnet. In contrast, T821I, which confers relatively high levels of resistance to foscarnet, is too far away from the bound nucleotide. However, the structural equivalent in RB69 contacts the template, which may provide an alternative mechanism of drug resistance. Resistance-conferring mutations in HIV-1 RT were also found to map to various regions [418], which likewise points to different mechanisms. One of these mutations,

e.g., E89K, may affect the interaction with the template, as suggested for T821I in HCMV UL54, but many other changes do not make direct contacts with the active site, the bound dNTP, or the nucleic acid substrate, which is again reminiscent of the mutational patterns described for HSV and HCMV. Several studies have shown that mutations in the conserved region II (around positions 696 and 724) of the related HSV-1, HSV-2, and bacteriophage T4 DNA polymerases can increase or decrease susceptibility to foscarnet or to its derivative phosphonoacetic acid [412, 420-422]. Given that this region is likewise implicated in nucleotide binding, it would be interesting to study the effects of corresponding mutations in this region of HCMV UL54.

Taken together, the data presented in this study provide strong evidence to suggest that the structures and functions of helix P of RB69 gp43 and HCMV UL54 are highly related, at least in the vicinity of the nucleotide binding site. The characterization of enzymes with mutations at highly conserved residues sheds light on the possible binding site for the pyrophosphate analogue foscarnet. We propose a model that places foscarnet in close proximity to Q807 and the position of the γ-phosphate of the bound dNTP. In this model, mutations L802M and K805Q exert their effects indirectly through structural changes that affect the interaction between foscarnet and Q807.

2.6 Acknowledgements

E.T. performed this work in partial fulfillment of the requirements for a Ph.D. degree, Faculty of Graduate Studies and Research, McGill University, Montreal, Quebec, Canada. We thank Thomas Cihlar for providing some of the HCMV recombinant mutants. This research was supported by grants to M.G. and G.B. from the Canadian Institutes of Health Research (CIHR). M.G. is recipient of a career award from the CIHR.

2.7 Abbreviations

HCMV, human cytomegalovirus; UL54, catalytic subunit of the HCMV DNA polymerase; CDV, cidofovir; GCV, ganciclovir; ACV, acyclovir; PPi, pyrophosphate; PFA, foscarnet; HSV, herpes simplex virus; RT, reverse transcriptase HIV-1, human immunodeficiency virus, type 1; dNTP, deoxyribonucleotide; UL30, catalytic subunit of the HSV DNA polymerase; gp43, catalytic subunit of the RB69 DNA polymerase; DTT, dithiothreitol.

2.8 Figures and tables

Figure 2.1. Location of resistance-conferring mutations in helix P. *A.* Amino acid sequence of conserved domain III of the HCMV DNA polymerase UL54. Highlighted are residues that have been associated with changes in drug susceptibility: cidofovir (CDV), ganciclovir (GCV), and foscarnet (PFA). Superscript R and HS indicate resistant and hypersusceptible phenotypes, respectively. *B.* Amino acid sequence of helix P of the RB69-associated DNA polymerase gp43 aligned against corresponding sequences of UL54 (HCMV) and UL30 (HSV-1). Bold letters indicate amino acid residues that are conserved in both UL54 and UL30. Underlined letters indicate amino acid residues conserved among all three related DNA polymerases. Highly conserved residues are found between positions 807 and 822. *C.* Interaction between helix P and the bound nucleotide, based on the structure of the ternary complex of gp43 [423]. Divalent metal ions are shown as gray spheres. The bound nucleotide is shown in green, the position of the 3' end of the primer is shown in yellow, and the complementary template positions $i + 1$ and i are shown in white. Helix P (A535 to G571) is shown in blue, and residues that are relevant to this work are highlighted: A551 (red; changes at this position in UL54 are associated with resistance to foscarnet), T554 (green; changes at this position in UL54 are associated with hypersusceptibility to foscarnet), Q556 (yellow), and K560 (magenta). The last two amino acids are highly conserved among a-DNA polymerases. Amino acids in parentheses indicate the structural equivalents in UL54.

A

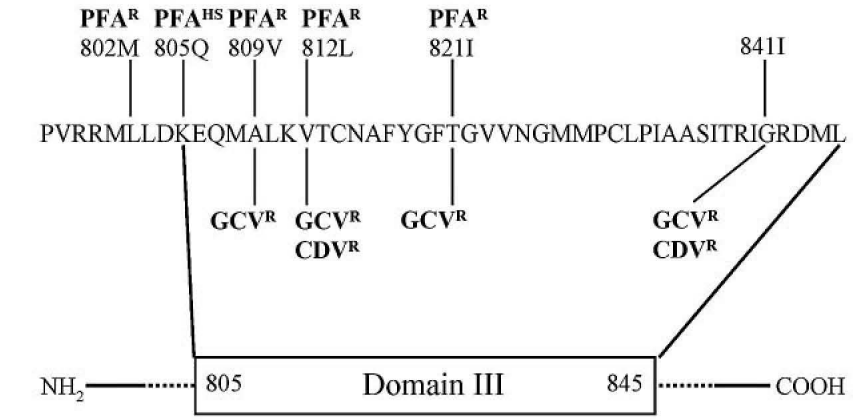
PFA^R 802M
PFA^HS 805Q
PFA^R 809V
PFA^R 812L
PFA^R 821I
841I
PVRRMLLDKEQMALKVTCNAFYGFTGVVNGMMPCLPIAASITRIGRDML
GCV^R
GCV^R CDV^R
GCV^R
GCV^R CDV^R
NH2
805
Domain III
845
COOH

B

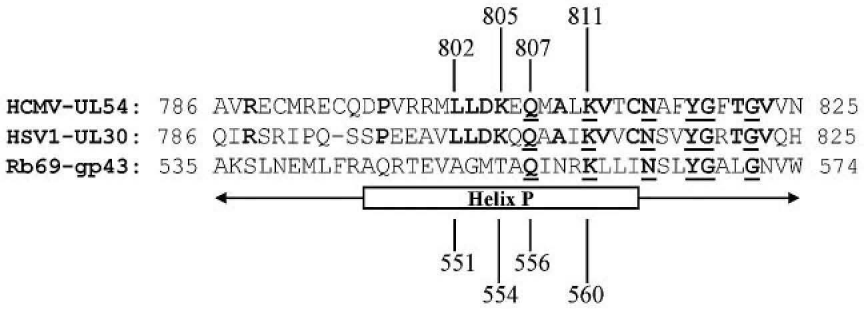
805
811
802
807
HCMV-UL54: 786 AVRECMRECQDPVRRMLLDKEQMALKVTCNAFYGFTGVVN 825
HSV1-UL30: 786 QIRSRIPQ-SSPEEAVLLDKQQAAIKVVCNSVYGRTGVQH 825
Rb69-gp43: 535 AKSLNEMLFRAQRTEVAGMTAQINRKLLINSLYGALGNVW 574
Helix P
551
556
554
560

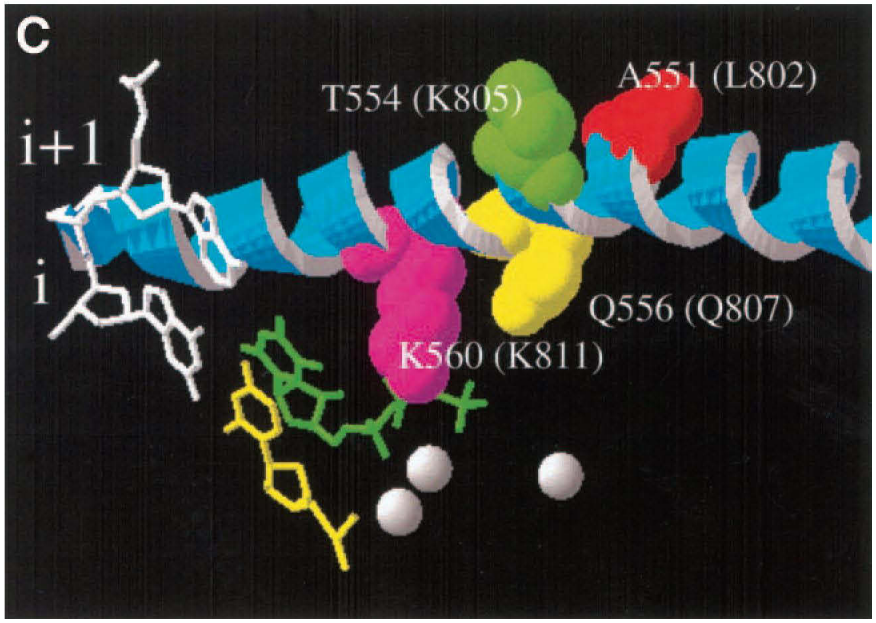
C
i+1
i
T554 (K805)
A551 (L802)
Q556 (Q807)
K560 (K811)

Figure 2.2. Efficiency of DNA synthesis with WT and mutant enzymes. The levels of DNA synthesis were measured with the heteropolymeric primer/template substrate P20/T50 DNA as a function of time. FL denotes the full-length product, and P20 denotes the unextended primer. The asterisk points to the exonuclease activity of UL54 enzymes. This band is less pronounced in the control without enzyme (left, primer only) and in reaction mixtures that contain plasmid pCITE4b without the coding sequence for UL54 (right).

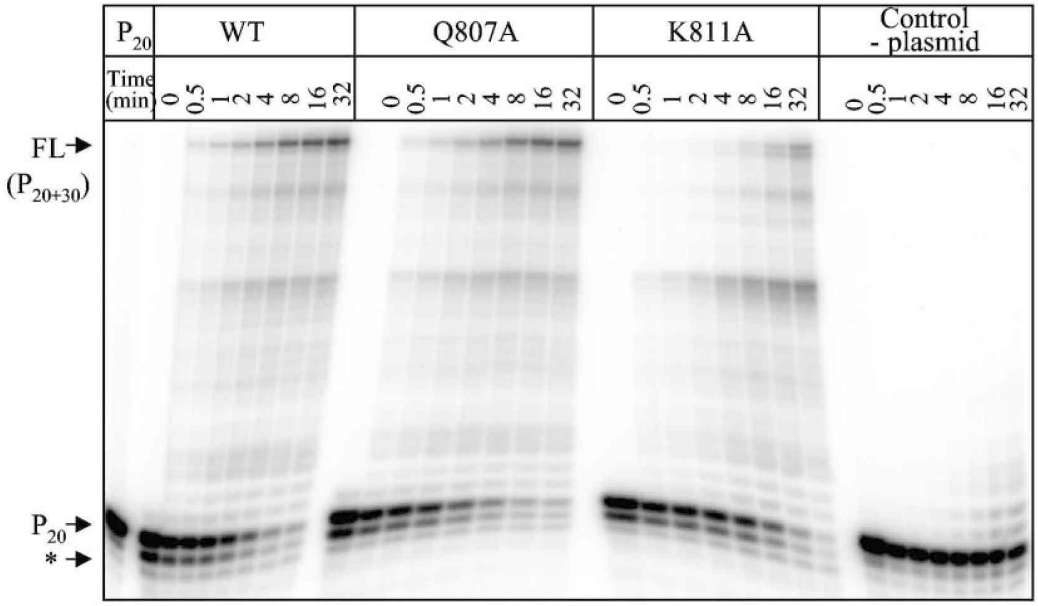
P20
WT
Q807A
K811A
Control - plasmid
Time (min)
0 0.5 1 2 4 8 16 32
FL
(P20+30)
P20
*

Figure 2.3. Steady-state kinetic analyses. *A.* Graphic representation of the experimental setup used to monitor single-nucleotide incorporations. The substrate P20/T33-T DNA allows the incorporation of dTTP, which extends primer P20 by a single nucleotide to yield P20 + 1. Complete sequences are shown in Materials and Methods. *B.* Incorporation of dTMP by WT UL54. efficiency of single-nucleotide incorporations was monitored in the presence of increasing concentrations of dTTP, while all other deoxyribonucleotides were omitted from the reaction. The reaction was allowed to proceed for 10 min. Under these conditions, no significant extensions in the control reactions that contain plasmid pCITE4b without the coding sequence for UL54 were seen. This approach was used to determine the kinetic parameters that are listed in Table 1.

A

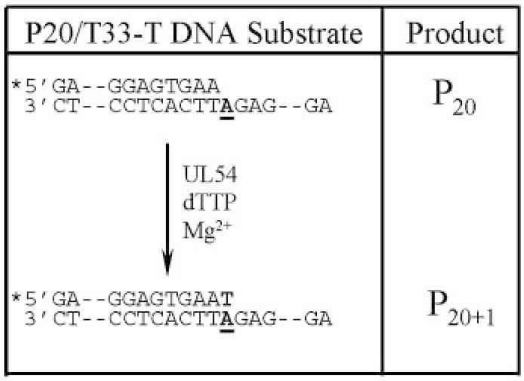
P20/T33-T DNA Substrate
Product
*5′GA--GGAGTGAA
3′CT--CCTCACTTAGAG--GA
P20
UL54
dTTP
Mg2+
*5′GA--GGAGTGAAT
3′CT--CCTCACTTAGAG--GA
P20+1

B

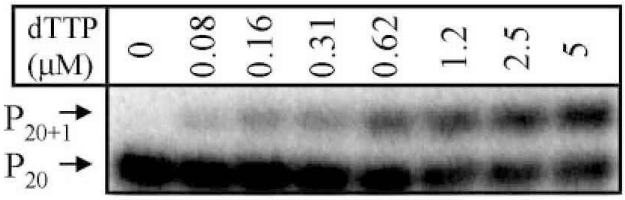
dTTP (μM)
0
0.08
0.16
0.31
0.62
1.2
2.5
5
P20+1
P20

Figure 2.4. Measurements of IC_{50} values for inhibition of DNA synthesis in the presence of foscarnet. *A.* The amount of full-length (FL) DNA synthesis was measured in the presence of increasing concentrations of foscarnet as indicated. Reactions were allowed to proceed for 30 min. *B.* Dose-response curves and measurements of IC_{50} values for inhibition of DNA synthesis by WT and mutant enzymes. Changes in the ratios of the full-length product and the unextended primer were quantified to generate dose-response curves. Dotted lines point to the concentration of the inhibitor that reduces the activity of the enzyme by 50% (IC_{50}).

A

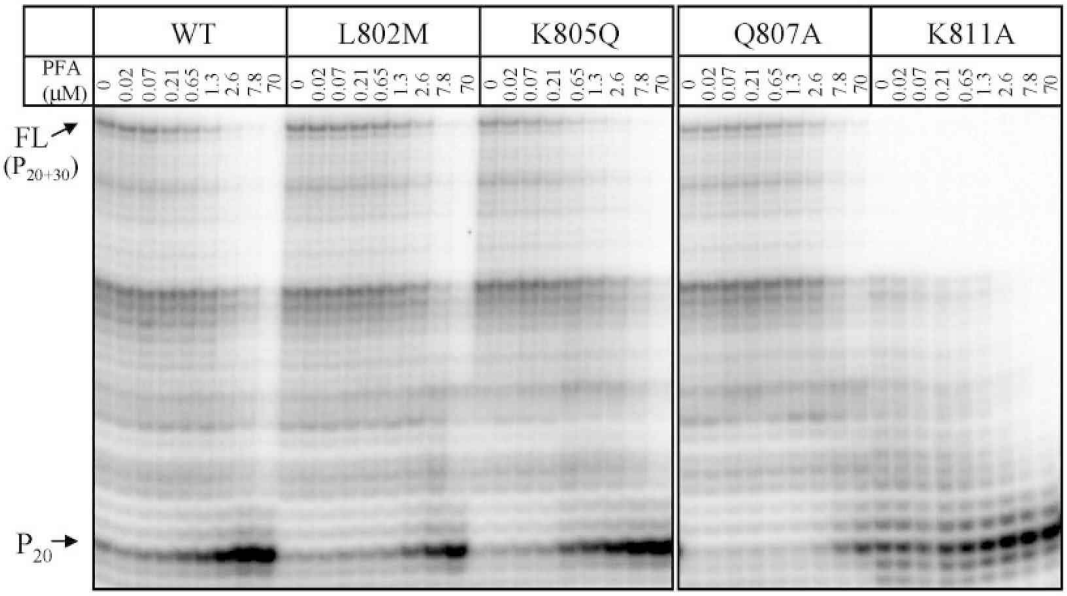
WT
L802M
K805Q
Q807A
K811A
PFA (μM)
0 0.02 0.07 0.21 0.65 1.3 2.6 7.8 70
FL (P20+30)
P20

B

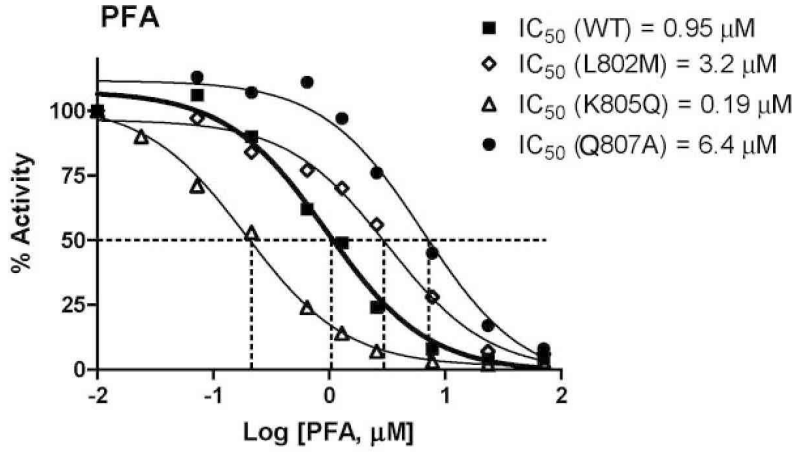
PFA
IC50 (WT) = 0.95 μM
IC50 (L802M) = 3.2 μM
IC50 (K805Q) = 0.19 μM
IC50 (Q807A) = 6.4 μM
% Activity
100
75
50
25
0
-2
-1
0
1
2
Log [PFA, μM]

Figure 2.5. Type of inhibition and measurements of K_i values. *A.* DNA synthesis was measured at a single time point (30 min) in the presence of increasing concentrations of each the four nucleotides. This experiment was repeated with different concentrations of foscar-net to determine K_i values as described in Materials and Methods. This figure shows changes in V_{max} and K_m for WT UL54 as an example. *v,* velocity of the reaction. The data for WT and mutant enzymes are summarized in Table 3. *B.* Replot of $1/V_{max}$ and K_m values determined as for panel A, shown here as a function of foscarnet concen tration. The *x* intercept provides the K_i value. Changes in V_{max} at constant K_m point to a noncompetitive type of inhibition. This is shown for WT UL54 as an example. *C.* Values of $1/V_{max}$ determined as for panel A and replotted as for panel *B*, shown here for WT and mutant enzymes.

A

WT						
Foscarnet, (μM)	0	0.125	0.25	0.5	1	2
Vmax, (pmol/min)	0.036	0.028	0.022	0.017	0.011	0.006
Km, (μM)	0.37	0.37	0.27	0.34	0.49	0.33

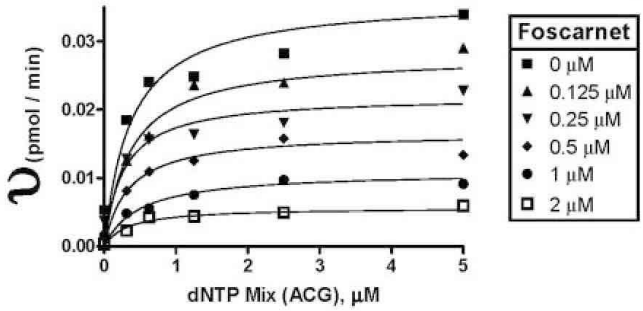

B

WT		
	1 / Vmax	Km
X-intercept	-0.3443	-24.65

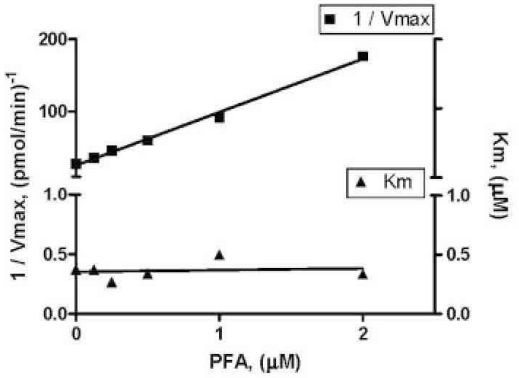

C

	WT	L802M	K805Q	Q807A
X-intercept	-0.30	-1.9	-0.12	-1.8

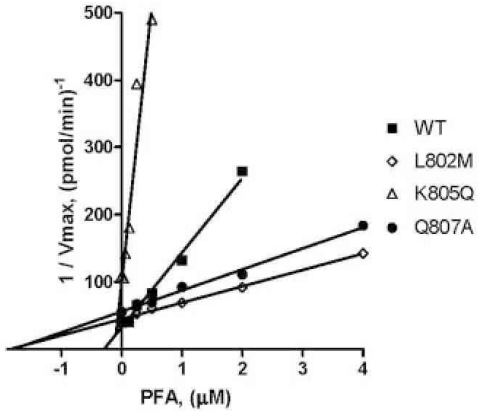

Figure 2.6. Possible interactions between helix P and foscarnet. This simplified model shows side chains of important residues in helix P that are either highly conserved (boxed) among α-DNA polymerases or associated with changes in susceptibility to the drug (R, resistant; HS, hypersusceptible). Helix P of UL54 is shown here in an orientation to the bound nucleotide similar to that shown for helix P of gp43 in Figure 1C. The structural data suggest that positions 805 and 802 are likely to be too far away to provide direct contacts with the drug. Our data suggest that foscarnet may bind in close proximity to Q807. The gray circle indicates the possible location of the bound drug relative to the nucleotide. The orientation of the bound foscarnet cannot be predicted on the basis of the data presented in this study. Dotted lines illustrate possible interactions between the negatively charged foscarnet and the side chain of Q807. There might be a partial overlap with the position of the γ-phosphate (large open circle), which would help to explain previous data that suggested a competitive mode of inhibition of pyrophosphorolysis. Dashed lines illustrate contacts between the structural equivalent of K811 (K560) in gp43 and the α- and γ-phosphates of the bound dNTP. Possible interaction between K811 and foscarnet cannot be confirmed, because mutations at this position were shown to affect dNTP binding at the same time.

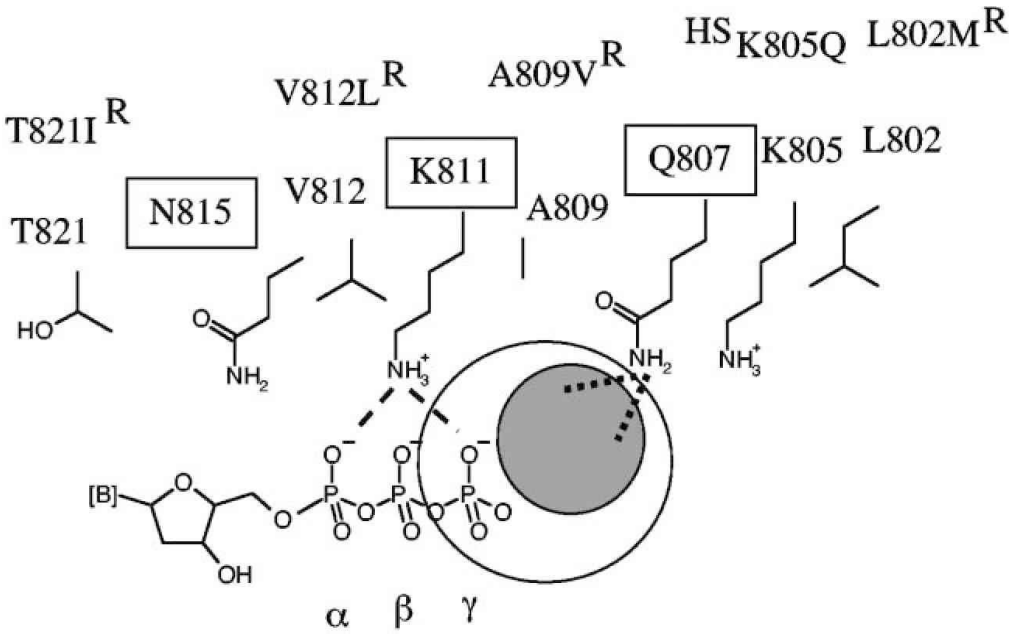
HS K805Q L802M R
V812L R
A809V R
T821I R
Q807
K805
L802
K811
V812
A809
N815
T821
HO
NH2
NH3+
NH2
NH3+
[B]
OH
α β γ

Table 2.1 Kinetic parameters for DNA polymerization[a].

Enzyme	dATP			dCTP			dGTP			dTTP		
	K_m (μM)	V_{max} (pmol/min)	K_m/V_{max}	K_m (μM)	V_{max} (pmol/min)	K_m/V_{max}	K_m (μM)	V_{max} (pmol/min)	K_m/V_{max}	K_m (μM)	V_{max} (pmol/min)	K_m/V_{max}
WT	0.79 ± 0.03	0.07 ± 0.003	0.09	0.10 ± 0.02	0.12 ± 0.08	1.2	0.11 ± 0.01	0.11 ± 0.002	1.0	0.31 ± 0.04	0.10 ± 0.005	0.3
L802M	1.01 ± 0.11	0.07 ± 0.002	0.07	0.10 ± 0.03	0.07 ± 0.005	0.7	0.22 ± 0.03	0.06 ± 0.004	0.3	0.24 ± 0.02	0.06 ± 0.002	0.3
K805Q	0.57 ± 0.05	0.07 ± 0.004	0.13	0.16 ± 0.02	0.05 ± 0.001	0.3	0.21 ± 0.02	0.04 ± 0.006	0.2	0.20 ± 0.01	0.06 ± 0.003	0.3
Q807A	1.16 ± 0.09	0.04 ± 0.020	0.04	0.19 ± 0.05	0.12 ± 0.08	0.6	0.17 ± 0.01	0.11 ± 0.005	0.6	0.76 ± 0.45	0.10 ± 0.008	0.1
K811A	1.65 ± 0.66	0.01 ± 0.002	0.006	0.65 ± 0.07	0.08 ± 0.03	0.1	2.09 ± 0.38	0.10 ± 0.01	0.05	3.55 ± 0.6	0.05 ± 0.03	0.01

[a] DNA synthesis reactions of one nucleotide incorporation were performed using P20/T33 DNA substrates as described in Materials and Methods. Data were fitted to the Michaelis-Menten equation in order to determine K_m and V_{max} constants. Values are means of at least three determinations ± standard deviations.

Table 2.2. Inhibition of DNA synthesis in the presence of foscarnet and pyrophosphate.

Enzyme	Foscarnet		Pyrophosphate	
	IC_{50} (μM)[a]	Fold resistance[b]		Fold resistance[b]
WT	0.47 ± 0.17	1	1.03 ± 0.22	1
L802M	1.68 ± 0.15	3.5	1.11 ± 0.02	1.1
K805Q	0.16 ± 0.05	0.3	0.62 ± 0.04	0.6
Q807A	2.98 ± 0.73	5.3	1.18 ± 0.23	1.1

[a] IC_{50} values were determined in the presence of activated calf thymus DNA as described in Materials and Methods. Values are means of at least three independent determinations ± standard deviations.
[b] Values of less than 1 represent hypersusceptibility.

Table 2.3. K_i values for foscarnet-mediated inhibition of DNA synthesis[a]

	Foscarnet	
Enzyme	K_i (μM)[b]	Fold resistance[c]
WT	0.30 ± 0.08	1
L802M	2.0 ± 0.4	6.7
K805Q	0.14 ± 0.03	0.47
Q807A	1.9 ± 0.7	6.3

[a] As described in Materials and Methods.
[b] Values are means of at least three independent determinations ± standard deviations.
[c] Values of less than 1 represent hypersusceptibility.

CHAPTER 3

ENGINEERING OF A CHIMERIC RB69 DNA POLYMERASE SENSITIVE TO DRUGS TARGETING THE CYTOMEGALOVIRUS ENZYME

This chapter was adapted from an article authored by E.P. Tchesnokov, A. Obikhod, I. R. F. Schinazi and M. Götte recently submitted to the ***Journal of Biological Chemistry***.

3.1 Preface to chapter 3

HCMV polymerase (UL54) expression and purification remain the bottleneck for the extensive biochemical, structural and high throughput screening studies of drug/target interactions. Interestingly, the RB69 DNA polymerase, whose crystal structures are frequently used as a template for molecular modeling studies of UL54, is in fact an easily expressible and purifiable protein. In addition, this enzyme is largely insensitive to foscarnet inhibition.

In previous studies I validated my structure-based alignment between RB69 and HCMV polymerases, identified the catalytically important residues of the UL54 helix P and proposed the presumptive UL54 binding site for foscarnet. The role of the UL54 helix N in foscarnet binding remained to be determined. Therefore, in an attempt to engineer an enzyme with properties that facilitate protein expression while preserving the UL54 foscarnet/acyclovir profile, I replaced critical regions of the nucleotide binding site of gp43 with equivalent regions of the HCMV enzyme.

Such a chimera should be a useful tool in biochemical and structural studies of drug-target interactions in the context of the HCMV polymerase.

3.2 Abstract

The DNA polymerase of the human cytomegalovirus (HCMV UL54) is the target for antiviral drugs. The crystal structure of the related RB69 DNA polymerase (gp43) is often used as a model system to explain mechanisms of inhibition of DNA synthesis and drug resistance. However, here we demonstrate that gp43 is literally resistant to the pyrophosphate analog foscarnet, while UL54 is sensitive to this drug. The RB69 enzyme is also able to discriminate against the nucleotide analog inhibitor acyclovir. In contrast, the HCMV polymerase is able to incorporate this compound with similar efficiency as observed with its natural counterpart, although detailed structural and biochemical studies with UL54 are hampered by difficulties to obtain this enzyme in large quantities. In an attempt to engineer an enzyme with properties that facilitate protein expression, we replaced critical regions of the nucleotide binding site of gp43 with equivalent regions of the HCMV enzyme. We show that chimeric gp43-UL54 enzymes that contain important regions of helix N and helix P of UL54 are resensitized against foscarnet and acyclovir. Changing a region of three amino acids of helix N showed the strongest effects, and changes of two segments of three amino acids in helix P further contributed to the reversal of the phenotype. The data suggest that the chimeric enzyme can be used as a tool in drug discovery and development efforts, and to study the structural basis for mechanisms associated with drug action and resistance.

3.3 Introduction

Infection with the human cytomegalovirus (HCMV), which belongs to the *herpesviridae*, remains an important health problem in immunocompromised persons [131, 132, 424-428]. Several drugs that target the viral DNA polymerase (UL54) have been developed to treat the infection [71, 155, 183, 429, 430]. Cidofovir (CDV), ganciclovir (GCV) or its prodrug valganciclovir (VGCV) are nucleotide or nucleoside analogue inhibitors, respectively, that are intracellularly phosphorylated to their triphosphate form and compete with natural nucleotide pools for incorporation [140, 160, 164, 167-171]. These compounds are characterized by an acyclic sugar moiety with the equivalent of a 3'-hydroxyl group that is required for the next nucleotide incorporation event [431]. Thus, once incorporated, these compounds interfere with DNA synthesis at various positions downstream [168, 173, 432]. In contrast, compounds that lack the 3'-hydroxyl group, such as the antiherpetic drug acyclovir (ACV), act as chain-terminators [10, 21]. Although active against HCMV, ACV is not approved for treatment of HCMV infection and its efficacy is inferior to GCV or CDV [155, 433, 434]. The pyrophosphate (PPi) analog foscarnet (phosphonoformic acid, PFA) is a third approved anti-HCMV drug that inhibits UL54 [23, 24]. However, toxicity, problems with oral bioavailability, and the rapid development of resistance can limit the clinical utility of each of the approved drugs.

PFA is a broad-spectrum antiviral that was shown to inhibit various polymerases, including enzymes encoded by herpes simplex virus (HSV), human herpesvirus (HHV), HCMV, and the reverse transcriptase (RT) of the human immunodeficiency virus type 1 (HIV-1) [23, 24]. Progress has been made in elucidating the mechanism of inhibition of HIV-1 RT [35, 435]. Site-specific footprinting experiments revealed that the enzyme can oscillate between two conformations, referred to as pre- and post-translocation [359]. The 3'-end of the primer still occupies the nucleotide binding site in the pre-translocated complex [345, 436]. Binding of the next nucleotide requires translocation of the enzyme

relative to its nucleic acid substrate [437]. The dNTP substrate can bind to and is incorporated in this post-translocated complex. In contrast, PFA binds specifically to the pre-translocational complex [35, 359]. The inhibitor traps the pre-translocational state, which provides a plausible mechanism for inhibition. The mechanism of action might be similar with the HCMV enzyme; however, the limited solubility of UL54 makes it difficult to produce the purified enzyme in sufficient amounts required for detailed biochemical and structural studies [438, 439]. Combined *in vitro* transcription/translation systems and the baculovirus expression system have proven successful for the expression of UL54 and the related HSV polymerase (UL30) [185, 402, 440-443]. The UL30 apoenzyme has been crystallized [104]; however, crystallographic data for UL54 are not available [147].

Like the related phage RB69 DNA polymerase (gp43), UL54 and UL30 belong to the polymerase α family [100]. The RB69 polymerase can be expressed in its soluble form in *Escherichia coli (E. coli)*, which facilitates protein production at high yields [101, 410]. This enzyme has also been crystallized in various forms, with and without the bound primer/template and the nucleotide substrate [101-103]. The ternary complex serves as a model system that is often used to explain mechanisms of drug action and resistance associated with UL54 [147]. The structure of the ternary complex shows that helix N and helix P provide important contacts that help to trap the incoming nucleotide [103]. Enzyme kinetic data confirmed the roles played by conserved amino acids in nucleotide binding and catalysis [411, 444]. Phenotypic drug susceptibility assays suggest that the equivalent regions in UL54 can affect susceptibility to GCV, CDV and also to PFA [132, 445]. Our recent biochemical data have shown that changes at residues of helix P implicated in PFA resistance or hypersusceptibility can either increase or decrease the inhibitory effects of this compound [442]. A comparison with the crystal structure of gp43 suggests that the binding sites for PFA and the γ-phosphate of the bound nucleotide might overlap. However, although the existence of conserved residues within helix P suggests a similar functional role in

both enzymes, several residues in this region are different in nature, which may in turn affect sensitivity to PFA (Figure 1A). Moreover, the contribution of helix N in PFA binding remains to be determined.

In light of the limitations with respect to the expression of UL54, and the general shortcomings of surrogate system such as the RB69 enzyme, we engineered a chimeric RB69 DNA polymerase in which critical components of helix N and helix P were replaced by equivalent regions of the related HCMV enzyme. The chimeric enzyme retained properties that facilitate expression and purification, and, at the same time, the enzyme facilitates the study of mechanisms involved in drug action and drug resistance associated with the clinically relevant HCMV system. Most importantly, we show that gp43 is literally resistant to PFA and ACV, while the chimeric gp43-UL54 enzyme is almost as sensitive to both drugs as observed with UL54. The chimeric enzyme may serve in the future as a tool to study the structural requirements for inhibition of UL54 by and resistance to anti-HCMV drugs.

3.4 Experimental Procedures

Plasmid constructs- wild-type HCMV polymerase (UL54) was derived from recombinant viruses generated by overlapping cosmids as described previously [402]. The UL54 coding sequence was kindly provided by Dr. Guy Boivin (Laval University). The UL54 coding sequence was cloned into pCITE4b (Novagen) by use of the *EcoRI* and *HindIII* sites to generate pCITE4b/UL54. We also generated a 3`-5` exonuclease negative construct that contains the D542A substitution. The RB69 DNA polymerase (gp43) coding sequence was kindly provided by Dr. Sylvie Doublié (University of Vermont) and Dr. Jim Karam (Tulane University). The gp43 coding sequence was cloned into pPR-IBA1 (IBA) using the *BsaI* site to generate pPR-IBA1/gp43. This construct facilitates protein purification through Strep-tag affinity chromatography (IBA). D222A and D327A substitutions were introduced to remove the 3`-5` exonuclease activity. Constructs for the production

of mutant enzymes were generated by site-directed mutagenesis. The amino acid substitutions were introduced with *PfuUltra* DNA polymerase (Stratagene) according to the manufacturer's recommendations.

Protein expression- the HCMV polymerase UL54 was expressed in rabbit reticulocyte lysate with a coupled *in vitro* transcription-translation system (Promega). Reactions were conducted essentially as previously described [185, 442]. The RB69 DNA polymerase and chimeric RB69/HCMV enzymes were expressed as previously described [410]. All enzymes were purified using Strep-tag affinity chromatography (IBA) according to the manufacturer's recommendations. Heterodimeric reverse transcriptase p66/p51 was expressed and purified as described [446].

Nucleic Acids and chemicals- Oligo-deoxynucleotides used in this study were chemically synthesized and purchased from InVitrogen Life Technologies. The following sequences were used as templates T1: 5`GTAACTAGAGATCCCTCAGACCCTTTTAGTCAGAAT and T2: 5`CCAATATTCACCATCAAGGCTTGATGAAACTTCACTCCACTATACCA CTC. The underlined nucleotides are the portion of the templates annealed to the primer. The following primers were used in this study: P1: 5` TTCTGACTAAAAGGGTCTGAGGGAT and P2: 5`GAGTGGTATAGTGGAGTGAA. Deoxynucleotides were purchased from Fermentas life sciences and PFA was purchased from Sigma.

Synthesis of ACV-TP- ACV (1.5 mmol) was dissolved in 200 µl of dry 1,3-dimethyl-2-oxohexahydropyrimidine *N,N'*-dimethylpropylene urea (DMPU) with 12-15 molecular sieves under nitrogen, stirred for 24 h. The mixture was chilled with ice-water bath and stirred for 1 h, followed by slow addition of phosphorus oxychloride 3 eq. and stirred for additional 25 min. A solution of tributylammonium pyrophosphate (4 eq.) in 200 µL of DMPU and tributyl amine (15 eq.) were simultaneously added to the reaction. After 45 min. reaction was

quenched with ice-cold water. The reaction was washed with chloroform, and the aqueous layer collected and co-evaporated with deionized water three times. The residue was re-suspended in 100 µL of deionized water and purified on ion-exchange column by HPLC $\lambda_{(max)}$= 253 nm. The final product was co-evaporated with water five times, giving total yield of ACV-TP $(NH_3)_4$ of 18% with purity ≥ 95%. The molecular weight of the ACV-TP was confirmed by LC-MS/MS *m/z* (M+1) 466→152 [447].

Enzyme kinetics- 100 nM DNA/DNA template/primer hybrid T1/P1 (100 nM) was pre-incubated for 5-10 min at 37°C with a given DNA polymerase in a buffer containing 25 mM Tris-HCl (pH 8), 50 mM NaCl, 0.5 mM dithiothreitol (DTT), 0.2 mg/ml bovine serum albumin, and 5% glycerol. To compare different enzymes in single nucleotide incorporation assays, we adjusted the enzyme concentration and the time point of the reaction such that ~40% of the primer was used at the saturating concentration of dNTP. For K_m and K_i measurements, the range of the dNTP substrate and/or inhibitor was chosen such that the values were in the middle of the chosen concentration range. Nucleotide incorporation was initiated by the addition of $MgCl_2$ to a final concentration of 10 mM, and the reactions were allowed to proceed for 5 minutes. The reactions were stopped by the addition of 3 reaction volumes of formamide containing traces of bromophenol blue and xylene cyanol. Samples were then subjected to 15% denaturing polyacrylamide gel electrophoresis followed by phosphorimaging. The incorporation of single nucleotides was quantified as the fraction of the DNA substrate (primer n) converted to product (primer n+1).

K_m and K_i experiments- The rate of the reaction was plotted versus the concentration of nucleotide substrate. The data points of a 42-data-point K_m/K_i experiment were fit to the general mixed-model of inhibition using GraphPad Prism (version 5.0) in order to calculate k_{cat}, K_m and K_i values. k_{cat} is defined as the enzyme turnover number which is calculated by normalizing the maximum rate of the single nucleotide incorporation reaction to the enzyme concentration.

K_m is defined as the dNTP substrate concentration at half maximum rate of the reaction. K_i is the inhibitor dissociation constant [448, 449]. Significant figures for the fitted data of all experiments are as reported by the software. Standard deviations for all experiments were determined on the basis of at least three independent replicates.

IC_{50} experiments- The incorporation of dCTP was determined by plotting the percentage of incorporation against the concentration of PFA. IC_{50} values were calculated by fitting at least 10 data points to a sigmoidal dose response (variable slope) equation using GraphPad Prism (version 5.0). Significant figures for the fitted data of all experiments are as reported by the software. Standard deviations for all experiments were determined on the basis of at least three independent replicates.

Bioinformatics- The amino acid sequence of UL54 was aligned against the amino acid sequence of the crystal structure of RB69 (PDB code 1IG9 [103]) using Cn3D software [450]. The sequence alignment output was graphically prepared with ESPRIPT software [451]. Conserved residues are highlighted in black while similar residues are boxed [452].

3.5 Results

Experimental design– The goal of this study was to engineer and to characterize a chimeric RB69/UL54 enzyme that facilitate the study of PFA-mediated inhibition of DNA synthesis and drug resistance. We focused on segments of helix N and helix P that are located in close proximity to the phosphates of the bound dNTP substrate in the ternary complex with gp43 [103]. Several amino acids in these regions are likewise implicated in binding of PFA by UL54. Phenotypic susceptibility assays, and our previous biochemical data suggest that the region between 807 and 815 in helix P (556 to 564 in gp43) plays an important role in

this regard [132, 442]. Some of the amino acids of this segment can interact with the bound nucleotide, while others appear to be involved in interhelical interaction with residues 779 to 784 (477 to 482 in gp43) of helix N [102, 103] (Figure 1B, left). In an attempt to closely mimic the structure of the UL54, we replaced all amino acids that differ at equivalent positions in gp43 according to the sequence alignment shown in Figure 1A. These changes involve the block of three amino acids between the conserved residues K477 and Q481/K482 of helix N, referred to as block A, and two blocks of three amino acids between conserved residues Q556 and N564 of helix P, referred to as block B and block C, respectively. All enzymes designed and characterized in this study are listed in Table 1.

We generated chimeric gp43-based enzymes in which block A of helix N, and blocks B/C of helix P have been replaced by equivalent regions of UL54. Several conserved amino acids within these regions interact with the phosphates of the nucleotide (Figure 1B, right). R482 of helix N, as well as Q556 of helix P appear to contact the γ-phosphate of the bound nucleotide. The same region is also implicated in PFA binding. The Q807A mutation in helix P in UL54 increases the IC_{50} value for PFA [442]. However, a potential role of helix N in PFA resistance remains to be defined. Of note, F479 of helix N in gp43 is equivalent to V781 in UL54, and the V781I substitution in the HCMV enzyme shows decreased phenotypic susceptibility to PFA [453]. This residue is likewise located in the vicinity of the γ-phosphate, and this region appears to be important for PFA binding. Thus, to test how close the chimeric enzyme may mimic the natural HCMV polymerase, we introduced V781I, and alanine substitutions at conserved residues R784 (helix N) and Q807 (helix P), respectively, against the background of the chimera.

Efficiency of nucleotide incorporation– We initially determined steady-state kinetic parameters for single nucleotide incorporation events, and compared several chimeric enzymes with WT gp43 (Table 2). Throughout this study, we used 3'-5' exonuclease negative mutants to prevent potentially confounding

effects through the editing activity. Replacing block A (helix N) with the equivalent UL54 region caused approximately 2 to 3-fold reductions in the efficiency of single nucleotide incorporation events. Introducing the V781I mutation against this background caused similar reduction in kinetic parameters. Chimeric enzymes containing block A (helix N), as well as blockB/C (helix P) of UL54 showed 10-fold reductions in the same assay. Alanine mutations at conserved positions R784 and Q807 that were introduced against this mutational background did not cause further significant reductions in the efficiency of nucleotide incorporation. Overall, these findings show that replacing critical element of helix N and helix P with their UL54 counterparts can cause reductions in enzymatic activity. Due to the lack of a corresponding expression/purification protocol for UL54, it is at this point difficult to assess whether the activity of the HCMV enzyme is intrinsically reduced or whether the chimeric nature of the enzyme may cause such deficits. However, the enzymatic activities are sufficiently high to measure potential changes in drug sensitivity, provided that the concentration of each of the enzymes to be compared are appropriately adjusted.

Sensitivity to PFA– The ability to inhibit single nucleotide incorporation events with PFA was expressed in both IC_{50} and K_i values (Table 3). Figure 2 shows an example of the assay used to evaluate the extent of inhibition. We compared gp43 with UL54, and HIV-1 RT as another control. UL54 and HIV-1 RT are sensitive to inhibition with PFA and have IC_{50} values between 0.6 and 0.9 μM. In contrast, gp43 has an IC_{50} value greater than 300 μM, which renders the enzyme approximately 400-fold less susceptible to PFA when compared with UL54. Thus, despite the evidence for structural and functional links between gp43 and UL54, these data point to important differences between the two enzymes.

IC_{50} and K_i- measurements show that helix N is a critical structural determinant that mediates PFA sensitivity. The chimeric enzyme containing block A (helix N) from UL54 shows a ≈ 50-fold reduction in IC_{50} values when compared with WT

gp43. This value is 3-fold increased when the V781I mutation is introduced against this mutational background. A similar trend is observed for the K_i values. The enzyme with blocks A (helix N), and B/C (helix P) of UL54 showed further subtle increases in sensitivity to PFA. Overall, we measured a 100-fold increase as compared to WT gp43. Moreover, alanine changes at conserved residues Q807 and R784 confer 8- to 11-fold resistance in the context of our biochemical measurements. Together, these findings identify helix N as an important determinant for PFA sensitivity, while helix P, in relation to helix N, appears to be a minor contributor. However, the resistance data unambiguously indicated that changes in either one of the two helices can affect PFA susceptibility.

To confirm these phenotypes, we devised a gel-based assay that allowed us to monitor the effects of PFA over multiple template positions (Figure 3). We focused on the chimeric enzyme with blocks A and B/C of UL54, referred to as gp43-UL54ABC, that showed the lowest IC_{50} values. In agreement with the aforementioned data, we demonstrated that both HIV-1 RT and UL54 were sensitive to PFA. Concentrations as low a 1 μM had significant levels of inhibition as judged by full-length product formation, while gp43 is not inhibited at concentrations of 10 μM. The chimeric enzyme gp43-UL54ABC shows a similar inhibition profile as observed with HIV-1 RT and UL54. Mutations Q807A and R784A, introduced against this mutational background, confer significant levels of resistance to PFA. Each of the aforementioned changes at positions V781, Q807, and R784 that are located in close proximity to the γ-phosphate of an incoming nucleotide can in turn affect binding of PFA. Thus, the data obtained under conditions that allow either single or multiple nucleotide incorporation events are in good agreement and demonstrate that critical elements of helix N and helix P in UL54 can sensitize the RB69 enzyme to PFA.

Efficiency of incorporation of ACV-MP– The large difference in PFA sensitivity between WT gp43 and the gp43-UL54ABC mutant enzyme suggests that the critical helical elements of UL54 may also affect the precise positioning of the

triphosphate moiety of an incoming nucleotide. Such effects may be exacerbated with nucleotide analog inhibitors. To test this hypothesis, we asked whether gp43, UL54, and gp43-UL54ABC showed differences in efficiency of incorporation of ACV-TP. In order to assess the ability of viral enzymes to use ACV-TP as a substrate for DNA synthesis we determined the steady-state parameters for incorporation of ACV-MP and its natural counterpart dGMP (Figure 4 and Table 4). The ratio of V_{max}/K_m is indicative for the efficiency of nucleotide incorporation, and the ratio of $V_{max}/K_{m\ (dGTP)}$ and $V_{max}/K_{m\ (ACV\text{-}TP)}$ defines the selectivity for the inhibitor. Amongst the three enzymes, the RB69 enzyme demonstrated the highest efficiency for incorporation of dGMP but the lowest for ACV-MP. The gp43-UL54ABC showed significantly reduced rates of incorporation of dGMP as compared to UL54. The selective advantage of incorporation of the natural nucleotide over the inhibitor was > 300. Of significance, the gp43-UL54ABC mutant enzyme does not show such a selective advantage. The mutant enzyme behaved almost exactly like UL54. The selectivity values for UL54 and gp43-UL54ABC were close to 1, suggesting that these enzymes accept ACV-TP and dGTP as substrates for DNA synthesis with similar efficiencies.

3.6 Discussion

In light of the problems associated with the development of an expression system for the HCMV DNA polymerase (UL54) [439], we engineered and characterized chimeric enzymes derived from the related RB69 polymerase (gp43) with critical elements of its viral counterpart. We replaced regions of helix N and helix P that are located in close proximity to the triphosphate moiety of a bound nucleotide, according to the crystallographic data obtained with gp43. Our biochemical data point to profound differences in sensitivity and selectivity to antiviral drugs when UL54 was compared with gp43. The phage enzyme appears to be resistant to PFA and ACV, respectively, while the HCMV enzyme was sensitive to inhibition with either one of the two drugs. These findings reveal limitations of the ternary gp43

complex as a model system to study mechanisms associated with drug action and drug resistance [147]. In general, mutations that affect susceptibility to antiviral drugs often involve subtle structural changes that do not include conserved amino acids, which makes it difficult to model such effects if only the structures of related enzymes are available. The chimeric enzymes designed in this study may help to tackle this problem.

Replacing the critical regions of helix N of gp43 with the equivalent region of UL54 caused marked increases in sensitivity to PFA (Table 3). The introduction of a naturally occurring, resistance-conferring mutation against this mutational background translated this phenotype in biochemical terms. Thus, a limited number of amino acids can be changed to produce a chimeric gp43-UL54 enzyme that shows a similar behavior to an antiviral drug as observed with WT UL54. The substitution of the three amino acids of helix N showed the strongest PFA resensitization effects, while the contribution of changes in helix P are minor. However, helix P contains various amino acids that are involved in HCMV resistance to PFA, CDV, and GCV [132]. Changes at these amino acids may directly affect binding of these inhibitors, or indirectly through intermolecular interactions between helix N and helix P. Thus, future studies aimed at elucidating mechanisms of resistance to the approved anti-HCMV enzymes may be performed with the gp43-UL54ABC enzyme in which important regions of both helices are replaced.

We have further demonstrated that changes of residues that are located in close proximity to the γ-phosphate of a bound nucleotide, either as part of helix N or as part of helix P, diminish the inhibitory effects of PFA. These findings are consistent with our previous mutational studies on UL54, and point to this region as a possible binding site for PFA [442]. Binding of PFA to the pre-translocated complex of HIV-1 RT depends on the presence of Mg^{2+} ions, which suggests that the inhibitor binds in close proximity to the location that occupies the β- and γ-phosphates of the bound nucleotide in the post-translocated complex [35, 359,

437]. Like the nucleotide, the presence of PFA stabilizes the complex, presumably as a result of a conformational change that traps the ligand. The structures of binary and ternary complexes of the RB69 enzyme show a similar conformational change that involves helix N and helix P [102, 103]. Thus, the differences between gp43 and UL54 in sensitivity to PFA may also be linked to potential differences in the ability of the two enzymes to trap the inhibitor.

The incorporation of nucleotides and nucleotide analogs follow the sequence of binding, conformational change, and catalysis [338, 454-456]. Sensitivity to a certain nucleotide analog can likewise be affected by these parameters [328, 345, 431, 457-459]. Our results show that gp43 is literally resistant to ACV, while UL54 and gp43-UL54ABC are both – to the same degree - sensitive to the inhibitor.

Taken together, the chimeric gp43-UL54 enzyme can provide a valuable tool to study the mechanisms of action and resistance to PFA and to nucleotide analog inhibitors. Although various other regions of the enzyme, including its 3'-5' exonuclease activity can also contribute to differences in drug susceptibility, helix N and helix P play an important role in this context [132, 402]. Gp43-UL54ABC and the various resistant mutant enzymes can be expressed and purified at high yields, which facilitates detailed structural and biochemical studies.

3.7 Acknowledgements

We would like to thank Suzanne McCormick for excellent technical assistance. This study was supported by the Canadian Institutes for Health Research (CIHR). MG is recipient of a national career award from the CIHR. RFS is supported in part by NIH grants 5R37-AI-041980, 4R37-AI-025899, 5P30-AI-50409 (CFAR), and by the US Department of Veterans Affairs.

3.8 Abbreviations

HCMV, human cytomegalovirus; UL54, catalytic subunit of the HCMV DNA polymerase; CDV, cidofovir; GCV, ganciclovir; VGCV, valganciclovir; ACV, acyclovir; PPi, pyrophosphate; PFA, foscarnet; HSV, herpes simplex virus; HHV, human herpes virus; RT, reverse transcriptase HIV-1, human immunodeficiency virus, type 1; dNTP, deoxyribonucleotide; UL30, catalytic subunit of the HSV DNA polymerase; gp43, catalytic subunit of the RB69 DNA polymerase; DTT, dithiothreitol; DMPU, *N,N′*-dimethylpropylene urea; HPLC, high performance liquid chromatography; LC-MS/MS, liquid chromatography-mass spectrometry/tandem MS.

3.9 Figures and tables

Figure 3.1 Structure-based correlation between the nucleotide binding sites of related RB69 and HCMV polymerases. *A.* Sequence alignment of critical regions of helix N and helix P of DNA polymerases from HCMV and RB69. The amino acid sequence of UL54 was aligned against the amino acid sequence of the crystal structure of RB69 (PDB code 1IG9) using C3nD software [103, 450, 451]. Conserved residues are highlighted in black while similar residues are boxed [452]. The amino acid substitutions V781I and Q807A illustrate the previously reported foscarnet resistant mutations [442, 453]. The black brackets and the corresponding caption "block A, B and C" underline the three amino acids of the HCMV polymerase that were replaced in this study. *B.* The crystal structure of RB69 DNA polymerase in complex with incoming nucleotide and primer/template (PDB code 3CFP). Conserved residues of helices N and P are highlighted in green. Residues involved in generating the gp43-UL54 chimeric enzyme are highlighted in yellow. The figure on the right is a simplified version of the figure shown on the left to highlight the role of residues in the vicinity of the γ-phosphate of the incoming nucleotide.

A

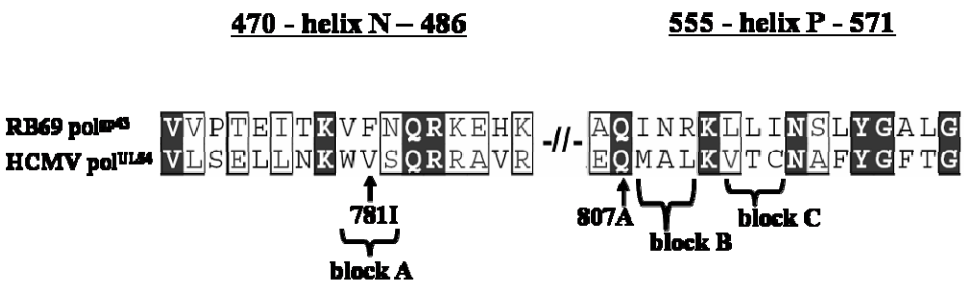
470 - helix N – 486
555 - helix P - 571
RB69 pol^gp43
HCMV pol^UL54
VVPTEITKVFNQRKEHK
VLSELLNKWVSQRRAVR
-//-
AQINRKLLINSLYGALG
EQMALKVTCNAFYGFTG
781I
block A
807A
block B
block C

B

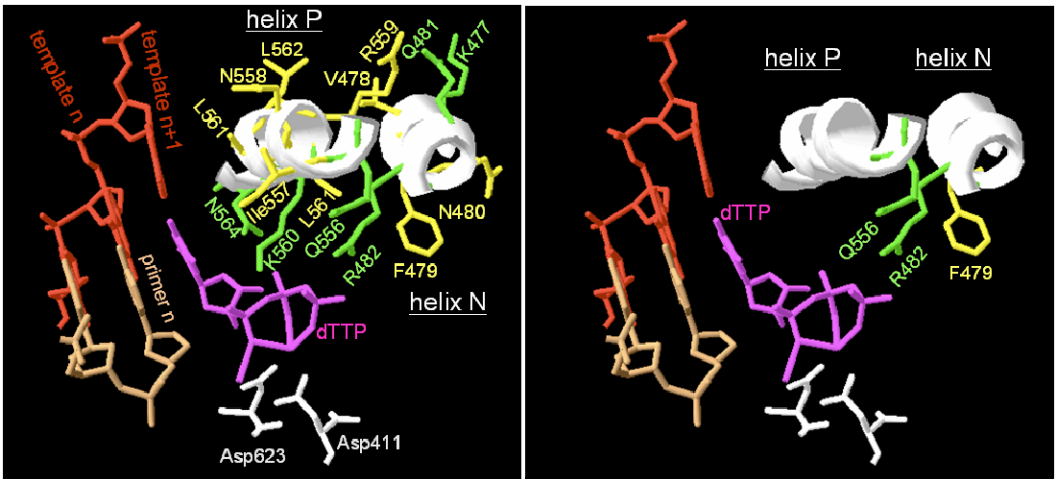
helix P
L562
N558
V478
R559
Q481
K477
L561
template n
template n+1
primer n
Ile557
N564
K560
L561
Q556
R482
F479
N480
helix N
dTTP
Asp623
Asp411
helix P
helix N
dTTP
Q556
R482
F479

Figure 3.2 PFA inhibition of DNA synthesis by viral polymerases under steady state conditions for single nucleotide incorporation events. *A.* Chemical structure of PFA *B.* Single nucleotide incorporation events in the presence of constant concentrations of dCTP and increasing concentrations of PFA. The migration pattern of the 5`end radioactively labelled primer (s) and product (p) is illustrated by corresponding arrows. *C.* Graph of data shown under *A*. IC_{50} values for PFA were calculated by fitting the data points to a sigmoidal dose response. Dotted lines illustrate the respective IC_{50} values for PFA.

A

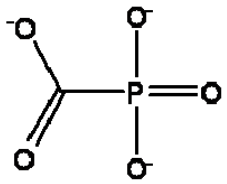

B

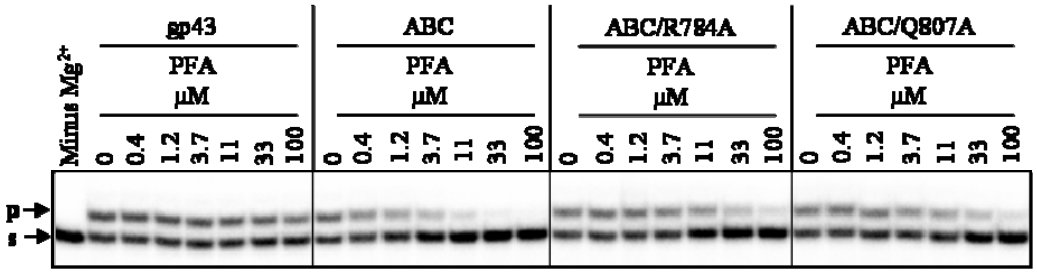

C

	gp43	ABC	ABC/R784A	ABC/Q807A
IC_{50}, μM	> 100	2.9	27	29

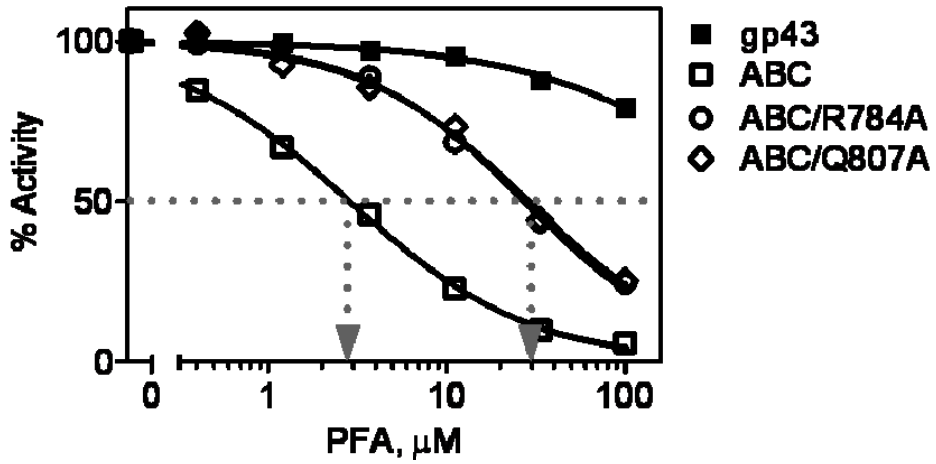

Figure 3.3 PFA inhibition of DNA synthesis for multiple nucleotide incorporation events. Reactions were monitored in the presence of constant concentrations of dNTPs and increasing concentrations of PFA. The reactions conditions were chosen such that the maximum of the available primer/template substrate was used in the absence of PFA. PFA-mediated inhibition of DNA synthesis is illustrated by the disappearance of a band corresponding to the migration pattern of a full length product (fl) which is indicated by the corresponding arrow. The migration pattern of the 5`end radioactively labelled primer (s) and the product of the terminal transferase activity (tt) is illustrated by corresponding arrows. The *asterisk* points to the exogenous background exonuclease activity present in samples with HCMV polymerase UL54 expressed *in vitro* transcription/translation system.

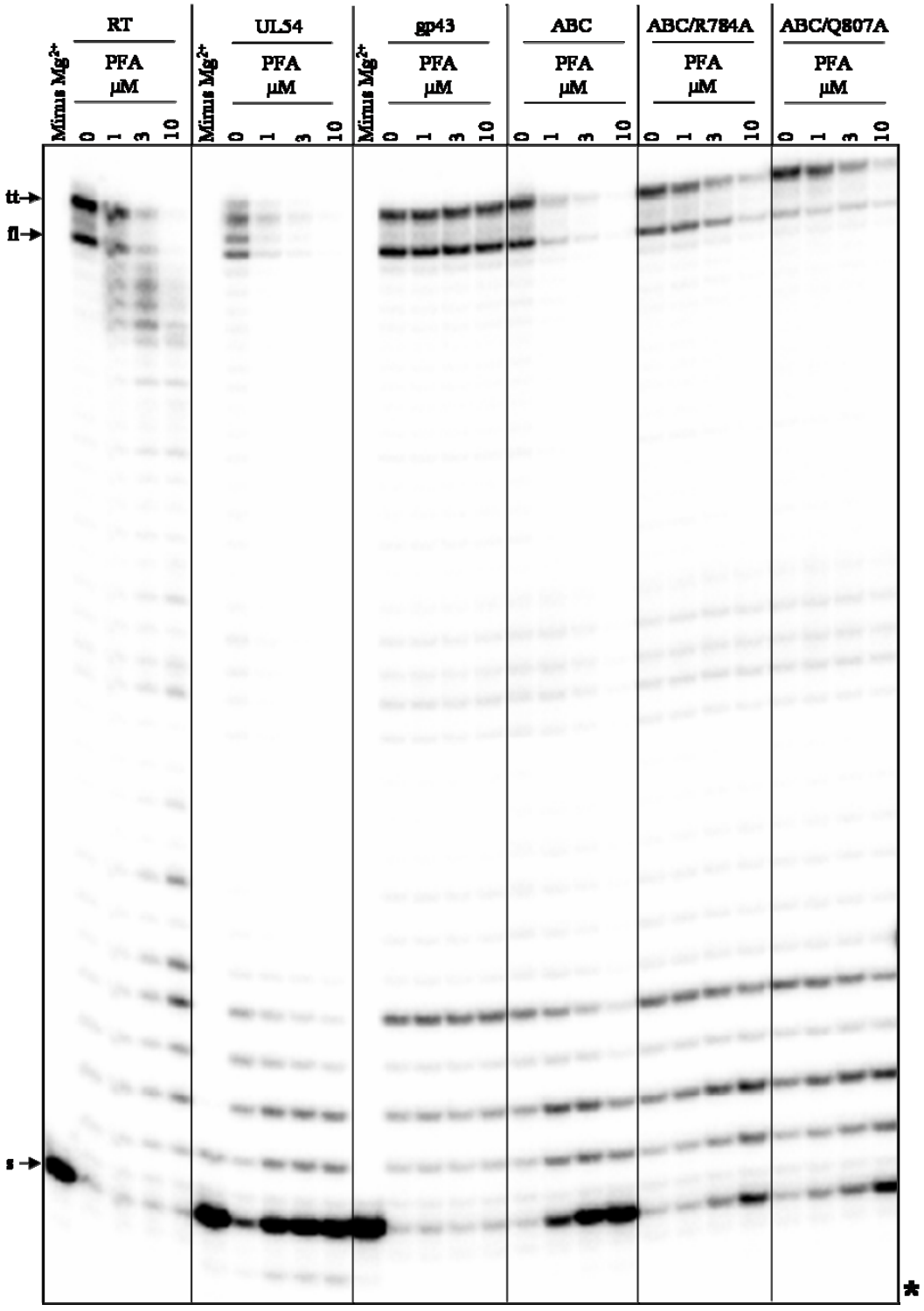
RT
UL54
gp43
ABC
ABC/R784A
ABC/Q807A
Minus Mg2+
PFA
μM
0
1
3
10
tt
fl
s
*

Figure 3.4 Efficiency of nucleotide incorporation for ACV-TP and dGTP. *A.* Chemical structure of acyclovir. *B.* Graphical representation of single nucleotide incorporation events monitored in the presence of increasing concentrations of dGTP or ACV-TP.

A

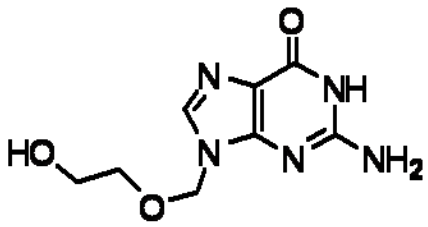
O
N
NH
HO
N
N
NH2
O

B

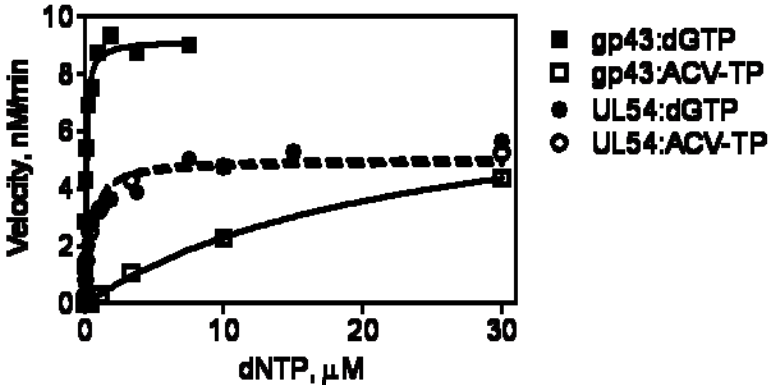
10
8
6
4
2
0
Velocity, nM/min
0
10
20
30
dNTP, μM
gp43:dGTP
gp43:ACV-TP
UL54:dGTP
UL54:ACV-TP

Table 3.1 RB69 - HCMV DNA polymerase chimera.

Nomenclature for chimera (block)	Region	RB69 residues	HCMV residues	Comments
A	helix N	V478 F479 N480	W780 V781 S782	none
A/V781I	helix N	chimera A V479I	chimera A V781I	foscarnet resistance conferring mutation[1]
B	helix P	I557 N558 R559	M808 A809 L810	none
C	helix P	L601 L602 I603	V812 T813 C814	none
ABC/R784A	helix N helix P	chimera A R482A chimera BC	chimera A R784A chimera BC	conserved residue
ABC/Q807A	helix N helix P	chimera A chimera BC Q556A	chimera A chimera BC Q807A	conserved residue conferring resistance to foscarnet[2]

[1] 5.2-fold increase in foscarnet resistance [453]
[2] 6-fold increase in foscarnet resistance [442]

Table 3.2 Kinetic constants for dCTP incorporation.[1]

Enzyme	k_{cat}[2] sec-1	K_m[3] µM	k_{cat} / K_m
gp43*	0.61[4]	0.49	1.25
A	0.39	0.92	0.42
A/V781I	0.51	0.92	0.55
ABC	0.46	2.7	0.17
ABC/R784A	0.39	3.3	0.12
ABC/Q807A	0.50	3.6	0.14

[1] Values were calculated by fitting the data points to Michaelis-Menten equation using GraphPad Prism (version 5.0).
[2] k_{cat} is the enzyme turnover number which is calculated by normalizing the maximum velocity of the reaction to the enzyme concentration.
[3] K_m is the substrate concentration at half maximum velocity of the reaction.
[4] Standard deviations were determined on the basis of at least three independent experiments and represent a maximum of 12% of the reported value.
* The previously reported gp43 values for dCTP k_{cat} and K_m are 1.0 sec^{-1} and 0.57 µM, respectively [444].

Table 3.3 Kinetic constants for inhibition of nucleotide incorporation by PFA.

Enzyme	IC_{50}[1] µM	Fold[2] change	K_i[3] µM	Fold change
UL54*	0.87[4]	reference[5]	0.076	reference
RT	0.60	1.4 S	1.1	14
gp43	333	380 R	na[6]	na
gp43	333	reference	na	na
A	7.5	44 S	na	na
ABC	3.3	100 S	na	na
A	7.5	reference	0.99	reference
A/V781I	19.7	2.6 R	1.8	1.8 R
ABC	3.3	reference	0.55	reference
ABC/R784A	37	11 R	5.9	11 R
ABC/Q807A	27	8.2 R	6.1	11 R

[1] IC_{50} is the inhibitory concentration of PFA that reduced the nucleotide incorporation activity of enzyme by 50%. Values were calculated by fitting the at least 10 data points to to a sigmoidal dose response (variable slope) equation using GraphPad Prism (version 5.0).

[2] Fold change is calculated as a ratio of the IC_{50} or K_i values of the reference and the query enzyme in the subgroup such that the ratio is more than 1.

[3] K_i is the inhibitor dissociation constant. Values were calculated by globally fitting the 42-data-point K_i experiment to the general mixed-model of inhibition using GraphPad Prism (version 5.0).

[4] Standard deviations were determined on the basis of at least three independent experiments and represent a maximum of 25% of the reported value.

[5] *Reference* defines the enzyme whose inhibitory constants were used as a reference value in the subgroup. Subgroups of enzymes are separated by extra rows.
[6] na, *not available.*
[R,S] R and S stand for resistance and sensitivity, respectively, and illustrate fold changes in resistance or sensitivity to PFA with respect to the reference enzyme in the subgroup.
[*] The HCMV polymerase UL54 was expressed *in vitro* transcription/translation system.

Table 3.4 Kinetic constants for dGTP and ACV-TP incorporation.[1]

Enzyme	dGTP			ACV-TP			
	V_{max}[2] nM/min	K_m[3] µM	V_{max}/K_m	V_{max} nM/min	K_m µM	V_{max}/K_m	SEL[4]
UL54[*] and [**]	2.2 ± 0.086[6]	0.041 ± 0.0067	54	1.2 ± 0.13	0.039 ± 0.023	31	1.7
gp43[***]	9.2 ± 0.12	0.079 ± 0.0053	117	8.6 ± 0.45	24 ±2.8	0.36	325
ABC	5.1 ± 0.23	0.47 ± 0.10	11	5.1 ± 0.14	0.41 ± 0.059	12.4	0.87

[1] Values were calculated by fitting the data points to Michaelis-Menten function using using GraphPad Prism (version 5.0).
[2] V_{max} is the the maximum velocity of the reaction.
[3] K_m is the substrate concentration at half maximum velocity of the reaction.
[4] SEL, selectivity, is calculated as a ratio of k_{pol}/ K_d for dGTP over k_{pol}/ K_d for ACV-TP.
[5] Standard deviations were determined on the basis of at least two independent experiments.
[*] UL54, the HCMV polymerase, was expressed *in vitro* transcription/translation system.
[**] The previously reported UL54 value for dGTP K_m is 0.11 µM [442].
[***] The previously reported gp43 value for dGTP K_m is 0.17 µM [444].

CHAPTER 4

MECHANISMS ASSOCIATED WITH HIV-1 RESISTANCE TO ACYCLOVIR BY THE V75I MUTATION IN REVERSE TRANSCRIPTASE

This chapter was adapted from an article authored by E.P. Tchesnokov, A. Obikhod, I. Massud, A. Lisco, C. Vanpouille, B. Brichacek, J. Balzarini, C. McGuigan, M. Derudas, L. Margolis, R. F. Schinazi and M. Götte recently submitted to the ***Journal of Biological Chemistry***.

4.1 Preface to chapter 4.

In the early days of antiviral treatment and prior to the discovery of the anti-HIV specific drug zidovudine, foscarnet and acyclovir were commonly used to treat HCMV and HSV infections in HIV-infected individuals. Recent reports of the anti-HIV activity of acyclovir and the selection of the V75I mutation in HIV-1 RT under the pressure of the drug placed acyclovir in the category of regimens with multiple antiviral activities. In addition, recent clinical studies have suggested an apparent benefit of acyclovir therapy in persons with synergistic herpesvirus-HIV co-infection. In this regard, the efficient clinical application of acyclovir in the context of herpesvirus-HIV co-infection depends on knowing the precise molecular mechanism of drug resistance associated with V75I substitution.

4.2 Abstract

It has recently been demonstrated that the antiherpetic drug acyclovir (ACV) also displays antiviral activity against the human immunodeficiency virus type 1 (HIV-1). The triphosphate form of ACV is accepted by HIV-1 reverse transcriptase (RT), and subsequent incorporation leads to classical chain-termination. Like all approved nucleoside analogue RT inhibitors (NRTIs), the selective pressure of ACV is associated with the emergence of resistance. The V75I mutation in HIV-1 RT appears to be dominant in this regard. By itself, this mutation is usually not associated with resistance to currently approved NRTIs. Here we studied the underlying biochemical mechanism. We demonstrate that V75I is also selected under the selective pressure of a monophosphorylated prodrug that was designed to bypass the bottleneck in drug activation to the triphosphate form (ACV-TP). Pre-steady-state kinetics reveal that V75I discriminates against the inhibitor at the level of catalysis, while binding of the inhibitor remains largely unaffected. The incorporated ACV-monophosphate (ACV-MP) is vulnerable to excision in the presence of the pyrophosphate donor ATP. V75I compromises binding of the next nucleotide that can otherwise provide a certain degree of protection from excision. Collectively, the results of this study suggest that ACV is sensitive to two different resistance pathways, which warrants further investigation regarding the detailed resistance profile of ACV. Such studies will be crucial in assessing the potential clinical utility of ACV and its derivatives in combination with established NRTIs.

4.3 Introduction

Acyclovir (ACV) (Figure 1A, right) was developed decades ago as one of the first selective antiviral agents and it is still used in the clinic to treat infections caused by herpes simplex virus 1 and 2 (HSV-1 and HSV-2) [11, 22, 110]. As its valyl prodrug, and to a lesser extent as parent ACV, it is also used in treating varicella zoster infections. The drug is an acyclic guanosine analogue that needs to be selectively converted to its triphosphate form (ACV-TP) that is accepted by the viral polymerase and acts as a chain terminator. The herpesviruses provide the kinases that generate the monophophate (ACV-MP), while cellular enzymes are required to synthesize the triphosphate form [13, 15, 16]. ACV-TP competes with intracellular dGTP pools for incorporation. Once incorporated, it acts as a chain-terminator due to the lack of a structural equivalent of the 3'-hydroxyl group of the sugar moiety of a natural nucleotide [10, 19]. The next complementary nucleotide, immediately downstream of the ACV-terminated 3'-end of the primer, can still bind to the HSV DNA polymerase and triggers formation of a stable Dead-End Complex (DEC) [21].

It has recently been demonstrated that ACV also exhibits, under certain conditions, antiviral activity against the human immunodeficiency virus type 1 (HIV-1) [47, 48]. ACV was shown to suppress HIV-1 replication in human tissues co-infected with HIV-1 and human herpesviruses (HHV) [47]. The latter provide the viral kinase that facilitates production of ACV-MP. This bottleneck in the production of the active antiviral agent can also be bypassed with a monophosphorylated prodrug (CF2648) (Figure 1A, left), that shows anti-HIV activity in HSV-free cells [13, 17, 18]. Cell-free assays revealed HIV-1 reverse transcriptase (RT) as the target [47, 48]. ACV-TP binds to the nucleotide binding site, and the incorporated ACV-MP causes DNA chain-termination following the release of pyrophosphate (PPi). Like most other nucleoside analogues [328, 346, 436], the incorporated ACV-MP can be excised from the 3'-end of the primer in the presence of PPi or the PPi-donor ATP [47]. This reaction can reduce the

overall inhibitory effect; however, the removal of the chain-terminator can be blocked through formation of a DEC [347]. DEC formation depends critically on the chemical nature of the inhibitor [335]. High concentrations (> 100 μM) of the next nucleotide are required to form a DEC with a primer terminated with zidovudine (AZT), while submicromolar concentrations are often sufficient to form a DEC with ddNTPs [346]. ACV-MP shows a behavior in the middle of the spectrum; approximately 25μM of the next nucleotide inhibits excision by 50% [47].

In vitro selection experiments revealed that ACV drug pressure is linked to the emergence of mutation V75I in the RT gene [48]. A similar change, i.e. V75T, has earlier been associated with resistance to stavudine (d4T) [460]. Mutations M184V and T69N are other previously known resistance conferring mutations that emerged under the selective pressure of ACV; however, V75I outgrew the culture over protracted periods of time, suggesting that this mutation is strongly associated with ACV resistance. HIV variants containing V75I showed marked increases in 50% effective antiviral concentrations (EC_{50}), which confirms the selection experiments [48].

Here we studied the underlying biochemical mechanism of HIV resistance to ACV associated with V75I. Two major mechanisms of resistance to nucleoside analogue RT inhibitors (NRTIs) have been described [345, 461-464]. The first mechanism is based on substrate discrimination. In this case, the mutant enzyme can selectively diminish binding and/or incorporation of the nucleotide analogue, while the properties of the natural counterpart remain largely unaffected. M184V that confers high-level resistance to 3TC is a prominent example in this regard. The second major resistance mechanism associated with NRTIs is based on excision. In this case, the mutant enzyme can increase the rate of excision of the incorporated inhibitor. Thymidine analogue associated mutations (TAMs) were shown to be able to recruit ATP as a PPi-donor and increase excision of incorporated AZT-MP [347]. In this study, we demonstrate that V75I discriminates against ACV-TP at the level of incorporation. Excision of the

incorporated nucleotide is also increased when compared with wild type RT; however, the effect is less pronounced as seen with the excision of ACV-MP against a background of TAMs. V75I does not provide further protection from excision through DEC formation. Collectively, the data suggest that ACV is vulnerable to both major resistance mechanisms.

4.4 Experimental Procedures

Enzymes and Nucleic Acids- Heterodimeric reverse transcriptase p66/p51 was expressed and purified as described [446]. Mutant enzymes were generated through site-directed mutagenesis using the Stratagene QuikChange kit according to the manufacturer's protocol. TAM2 refers to HIV1-RT containing the following substitutions: D67N, K70R, T215F, and K219Q. Oligo-deoxynucleotides used in this study were chemically synthesized and purchased from InVitrogen Life Technologies and from Integrated DNA Technologies. The following sequence was used as template T50A6:

5`CCAATATTCACCATCAAGGCTTGATGAAACTTCACTCCACTATACCA CTC

The underlined nucleotides are the portion of the templates annealed to the primer.

The following primer was used in this study: P1: 5`GAGTGGTATAGTGGAGTGAA

Synthesis of ACV-TP- ACV (1.5 mmol) was desolved in 200 µl of dry 1,3-dimethyl-2-oxohexahydropyrimidine *N,N′*-dimethylpropylene urea (DMPU) with 12-15 molecular sieves under nitrogen, stirred for 24 h. The mixture was chilled with ice-water bath and stirred for 1 h, followed by slow addition of phosphorus oxychloride 3 eq. and stirred for additional 25 min. A solution of tributylammonium pyrophosphate (4 eq.) in 200 µL of DMPU and tributyl amine (15 eq.) were simultaneously added to the reaction. After 45 min. reaction was quenched with ice-cold water and then it was slowly brought to the room

temperature. The reaction was washed with chloroform, and the aqueous layer collected and co-evaporated with deionized water three times. The residue was re-suspended in 100 μL of deionized water and purified on ion-exchange column by HPLC $\lambda_{(max)}$=253. In order to reduce the amount of excess salt, the final product was co-evaporated with water five times, giving total yield of ACV-TP $(NH_3)_4$ of 18% with purity ≥ 95%. The molecular weight of the ACV-TP was confirmed by LC-MS/MS *m/z* (M+1) 466→152 [447].

Synthesis of CF2648- The ACV prodrug CF2648 was prepared by the coupling of suitably base protected ACV with the appropriate phosphorochloridate reagent under anhydrous coinditions, followed by base deprotection, according to procedures we have previously reported [465].

Competition between ACV-TP and dGTP- DNA synthesis was monitored with 5'-end-labeled primers, unless otherwise indicated. 150 nM DNA/DNA (T50A6/P1) was incubated with 30 nM of HIV-1 RT in a buffer containing 50 mM Tris-HCl pH7.8, 50 mM NaCl, of constant concentrations of dGTP (1 μM) and ddTTP (2 μM), or dNTP mix (1 μM) and increasing concentrations of ACV-TP. Nucleotide incorporation was initiated by the addition of $MgCl_2$ to a final concentration of 10 mM, and the reactions were allowed to proceed for 5 minutes. The reactions were stopped by the addition of 3 reaction volumes of formamide containing traces of bromophenol blue and xylene cyanol. The samples were then subjected to 15% denaturing polyacrylamide gel electrophoresis (PAGE) followed by phosphorimaging. Inhibitory concentration of ACV-TP required to inhibit DNA synthesis at position +2 by 50% (IC_{50}) was determined by normalizing the product fraction formed at position +2 in the presence of ACV-TP to the corresponding value in the absence of inhibitor. Data points were fit to a sigmoidal dose response (variable slope) function using GraphPad Prism (version 5.0).

ATP-dependent excision- The T50A6/P1 DNA/DNA substrate was extended by a single nucleotide to generate an oligonucleotide with ACV-MP at the 3'-end. The extended primer was gel-purified, and annealed with template

T50A6. 50 nM of the substrate was then incubated with 500 nM of HIV-1 RT in a buffer containing 50 mM Tris-HCl pH7.8, 50 mM NaCl, 10 mM $MgCl_2$ and 3.5 mM ATP (pyrophosphotase treated). Aliquots were taken at different time points and analyzed as described.

Site-specific Footprinting- In preparation of the footprinting experiments, template T50A6 was 5'-end-labeled and heat-annealed with primer P1. 50 nM DNA/DNA hybrid was incubated with 750 nM HIV-RT for 10 min in a reaction mixture containing sodium cacodylate pH 7 (120 mM), NaCl (20 mM), DTT (0.5 mM), $MgCl_2$ (10 mM) and 25 μM ddGTP or 5 μM ACV-TP in a final volume of 15 μL. In control reactions ddGTP and ACV-TP were either omitted or substituted with 100 μL phosphonoformic acid (PFA or foscarnet). Following complete complex formation and/or nucleotide incorporation, increasing concentrations of dTTP were added to the reactions followed by an incubation of 5 minutes at 37^0C. For the actual footprinting, complexes were treated with 0.1 mM ammonium iron (II) sulphate hexahydrate [359]. The reactions were allowed to proceed for 5 min and were processed and analysed as described.

DEC formation- DNA synthesis at template position +1 was conducted in similar fashion as described above except that a chain terminator (ddGTP, 25 μM or ACV-TP, 2.5 μM) was incorporated at this position. A time course of incorporation of the chain terminator at position +1 in the absence or in the presence of increasing concentrations of the nucleotide at the following position +2 was monitored. The reactions were processed and analysed as described. Slopes of the linear portion of product formation illustrate the velocities of the reaction which, when normalized to the enzyme concentration, determine the turnover number (k_{cat}). Inhibition of DNA synthesis by DEC formation is illustrated by a decrease in k_{cat}.

Pre-steady-state kinetics for nucleotide incorporation - Nucleotide incorporation under single-turnover conditions was monitored using a rapid quench-flow instrument (KinTek RQF-3). Reactions involved rapid mixing of a solution containing preincubated 100 nM DNA/DNA template/primer hybrid with 500 nM of HIV-1 RT in a buffer consisting of 50 mM Tris-HCl pH7.8, 50 mM

NaCl and 10 mM $MgCl_2$ at 37ºC with a solution of the same buffer composition except that template/primer and RT were substituted with a given concentration of dGTP or ACV-TP. Nucleotide incorporation was monitored at time points of 0.015, 0.025, 0.05, 0.075, 0.1, 0.2, 0.3, 0.5, 1 seconds. The reactions were processed and analysed as described. Data points from time courses were fit by nonlinear regression (GraphPad Prism (version 5.0)) to a single exponential equation, [product]=A(1-exp(-$k_{observed}t$)), where A represents the amplitude, and $k_{observed}$ is the first order rate constant for dGTP or ACV-TP incorporation. $k_{observed}$ were reploted versus increasing concentrations of dGTP or ACV-TP to determine the respective $k_{observed}$. Data points were fit to a hyperbolic function, $k_{observed}=k_{pol}$[dNTP]/($K_{d,dNTP}$+[dNTP]), where k_{pol} is the maximum first-order rate constant for dGMP or ACV-MP incorporation, and $K_{d,dNTP}$ is the equilibrium dissociation constant for the interaction of dGTP or ACV-TP with the RT:template/primer complex**.**

Selection of resistance- MT-4 cells were obtained from the NIH AIDS Research & Reference Reagent Program and infected with HIV-$1_{LAI.04}$ in the absence or presence of CF2648. Every 3 to 5 days, 3% of the culture supernatant was used to infect fresh cells. Cultures were maintained in the absence or presence of gradually escalating concentrations of CF2648. HIV-1 replication in infected cultures was assessed by measuring $p24_{gag}$ from culture supernatants, as previously described [47]. Phenotypic resistance of viruses serially passed in the absence or in the presence of the CF2648 was evaluated in MT-4 cell cultures using drug concentrations ranging from 0 to 150 μM. The effective concentration that inhibits 50% replication was calculated by fitting the data points to a sigmoidal dose-response curve using GraphPad Prism (version 4.0).

Genotyping of the drug-exposed HIV-1 strains- Viral RNA was extracted from plasma using the QIAamp Viral RNA Mini Kit (Qiagen, Hilden, Germany). HIV-1 RNA was reverse transcribed into cDNA and a 2878-bp nucleotide fragment, encompassing protease and reverse transcriptase, was amplified in an outer PCR using SuperScript III One-Step RT-PCR System with Platinum Taq High Fidelity (Invitrogen, Merelbeke, Belgium) and outer primers AV190-1 and

CR1 [466]. A 2853-bp nucleotide fragment was amplified using Expand High Fidelity PCR System (Roche Diagnostics, Mannheim, Germany) and the inner primers AV190-2 and CR2. Amplification products were separated on a 1% agarose gel and visualized by ethidium bromide staining. PCR products were purified with Microspin S-400 (GE Healthcare, Roosendaal, The Netherlands). Sequencing was performed using the ABI PRISM BigDye Terminator v3.1 Ready Reaction Cycle Sequencing Kit as described before [466]. The reactions were run on an ABI3100 Genetic Analyzer and analysis was performed using Sequence Analysis version 3.7 and SeqScape version 2.0 (Applied Biosystems, Nieuwerkerk a/d Ijssel, The Netherlands).

4.5 Results

Selection of resistance with CF2648. The V75I mutation in HIV-1 RT was shown to emerge rapidly under the selective pressure of ACV [48]. The poor production of ACV-MP, and, in turn, the poor production of ACV-TP, is a possible factor that diminishes the efficacy of ACV and facilitates the selection of resistance. It is currently unknown whether monophosphorylated prodrugs can prevent or significantly delay the development of resistance. To address this problem, we attempted to select for resistance with the monophosphorylated prodrug CF2648. HIV-1 was propagated in MT-4 cells in the presence of increasing concentrations of CF2648. The antiviral activity of CF2648 after 39 serial passages (approximately 120 days) in the presence of the compound was reduced relative to the control propagated in the absence of the drug. Sequencing of HIV-1 RT revealed the emergence of V75I, and phenotypic resistance measurements revealed a 15-fold increase in the EC_{50} value (Table 1). Overall, the data suggest that the selection of V75I in the RT enzyme may not be prevented with prodrugs that bypass the first phosphorylation step. Given the potential relevance of this mutation in clinical settings, we studied the underlying biochemical mechanisms.

Discrimination against ACV-TP. We initially studied substrate discrimination as a possible mechanism for resistance. Classic protocols that

address this problem include steady-state kinetics that measure efficiencies of incorporation of the inhibitor and its natural counterpart in separate experiments. However, with this approach, we were unable to detect significant differences between purified wild type (WT) RT and the mutant enzyme containing V75I (data not shown). We considered two potential problems associated with this assay. First, incorporation of the inhibitor was measured in the absence of the natural counterpart dGTP. Therefore, we devised an assay that monitors incorporation of ACV-MP in the presence of both ACV-TP and dGTP (Figure 2A). The primer/template was designed to monitor incorporation of ACV-MP at the next template position (n+1) following the 3'end of the primer (n). Incorporation of ACV-MP causes chain-termination, while incorporation of dGMP allows the addition of a second nucleotide that is provided as a "stop nucleotide", which limits DNA synthesis and reduces complexity of the assay. The natural dGTP was provided at a constant concentration of 1μM and ACV-TP was provided at varying concentrations (Figure 2B). We found that the concentrations required to diminish dinucleotide extensions by 50% were significantly higher with the mutant enzyme, which suggests that the V75I mutant increases discrimination against the inhibitor (Figure 2C). We obtained essentially the same result with a different primer/template sequence that allowed us to monitor ACV-MP incorporation at template position +7 (Figure 3).

A second common problem associated with classic steady-state kinetics is that the multiple turnovers can mask differences in substrate binding or catalysis [338]. To address this problem, we measured kinetic parameters under pre-steady-state conditions, which provides at the same time mechanistic insight (Table 2). WT RT binds ACV-TP and dGTP with similar affinity as evidenced by K_d values of 2.2 μM, and 1.3 μM, respectively. However, the rate of incorporation is significantly higher for dGMP (k_{pol} = 66 s^{-1}) as compared to ACV-TP (k_{pol} = 14 s^{-1}), which translates in an 8-fold selective advantage of the natural nucleotide over the inhibitor with regards to the efficiency of nucleotide incorporation (k_{pol}/K_d).

The efficiency of incorporation of the natural nucleotide is not largely affected by the V75I mutation. The subtle increase in the K_d value is neutralized by a subtle

increase in the k_{pol} value, and these variations are not considered to be relevant. However, we measured a marked decline in the rate of incorporation for ACV-MP when V75I is compared with WT RT (k_{pol} = 1.5 s^{-1} versus k_{pol} = 14 s^{-1}), while the K_d value is not significantly increased. The selective effect on the rate constant suggests that V75I affects the catalytic step. Nucleotide binding of ACV-TP is not significantly changed. Overall, the data point to a 10-fold increase in discrimination against the inhibitor at single nucleotide resolution.

Excision of ACV-MP. An increased rate of excision is yet another possible mechanism that could help to explain the resistance phenotype associated with V75I. We devised a primer that was terminated with ACV-MP and studied the efficiency of the ATP-dependent excision reaction with WT RT, V75I and a mutant enzyme that contains four TAMs (D67N, K70R, T215F, and K219Q). This particular combination represents the TAM2 pathway. Like other combinations of TAMs, this cluster facilitate the recruitment of ATP as a PPi-donor. In agreement with previous reports, excision with WT RT is inefficient (Figure 4). However, V75I appears to increase the efficiency of ACV-MP excision over time, and the TAMs-containing enzyme shows further significant increases. Thus, increases in excision of the incorporated ACV-MP may be considered as another possible factor that contributes to ACV resistance.

Positioning of RT on ACV-terminated primers. The precise positioning of RT on its primer/template, and, in turn, enzymatic function, can be influenced by the chemical nature of the 3'-end of the primer [467, 468]. Prior to nucleotide incorporation the enzyme needs to translocate a single position further downstream, which liberates the nucleotide binding site from the 3'-end of the primer [330, 359, 437]. In contrast, excision can only take place when the 3'-end of the primer occupies the nucleotide binding site [345, 436, 437]. The two conformations are referred to as post- and pre-translocational states, and the RT enzyme is able to shuttle between the two conformations. We have recently developed site-specific footprinting techniques that allow us to distinguish between the two complexes [359, 468]. Incubation of RT-DNA/DNA primer/template complexes with Fe^{2+} generates specific cuts on the template

strand. These cuts are mediated through the RT-associated ribonuclease H (RNase H) active site at the C-terminal domain of the enzyme. Cleavage at position -17 is indicative for post-translocated complexes, while cleavage at position -18 is indicative for pre-translocated complexes. Here we compared footprints obtained with WT RT and V75I in complex with either ddGMP or ACV-terminated primers (Figure 5). Complexes with the bound nucleotide can only exist in the post-translocational state, while complexes with the PPi-analogue PFA exist pre-translocation (see controls). In an attempt to gradually stabilize the complex (DEC formation), we increased concentrations of the next complementary nucleotide, i.e. dTTP, which correlated with an increase in signal intensity. Complexes with WT RT and ddGMP-terminated primers exist predominantly in the post-translocated state even in the absence of nucleotide substrate. The signal is increased in the presence of increasing concentrations of the next nucleotide, which confirms formation of a DEC in the post-translocational state. In contrast, corresponding complexes with ACV-terminated primers are difficult to identify. Much higher concentrations of the next nucleotide are required to trap the complex in the post-translocational state. We obtained very similar results with the V75I mutant. The trend is the same, although the overall band intensity appears slightly diminished when compared with WT RT. Overall, these findings suggest that DEC formation is compromised with ACV-MP, and the V75I mutation may further contribute to this effect. The diminished signal points to increased complex dissociation .

DEC formation- In order to compare and quantify the ability of WT RT and V75I to form a DEC, we measured the turnover following incorporation of ACV-MP and ddGMP, respectively. The simultaneous inclusion of the next nucleotide, at different concentrations, allows formation of the ternary DEC (Figure 6). In this set-up, increases in the turnover number (k_{cat}) correlate inversely with DEC formation (Table 3). WT RT shows a decline in the turnover with ddGMP-terminated primers and increasing concentration of the next nucleotide. DEC formation is approximately 8-fold enhanced at concentrations of 100 μM dTTP when compared with the control in the absence of the nucleotide

substrate. Under the same conditions, DEC formation is compromised with ACV-terminated primers (only 2-fold increases with 100 μM dTTP), and V75I further enhances this effect. These findings suggest that DEC formation is likely to be insignificant under physiologically relevant conditions with dNTP concentrations below 100 μM. Thus, the ACV-terminated primer is unlikely to be protected from excision in the mutational context of V75I.

4.6 Discussion

The potential clinical benefit of ACV or the prodrug version valacyclovir in treating HIV/HSV-2 co-infection has been tested in large clinical trials [46, 394, 469]. HIV co-infection with HSV-2 can exacerbate disease progression [44, 391]. In support of this notion, several trials have shown that ACV-mediated suppression of HSV-2 is associated with reductions in HIV viral load [45, 46]. In contrast other trials failed to show that anti-herpetic therapy prevents infection with HIV-1 [470, 471]. Two subsequent studies demonstrated that ACV can also directly inhibit HIV-1 replication by targeting the RT enzyme [47, 48]. However, the development of resistance can compromise the antiviral activity in clinical settings. Three different mutations in HIV-1 RT were shown to emerge under the selective pressure of ACV *in vitro*: M184V, T69N, and V75I, respectively [48]. Experiments with constructs that were generated by site-directed mutagenesis confirmed the selection experiments and revealed that each of the three mutations can reduce susceptibility to ACV. V75I shows by far the strongest effect in this regard. Moreover, here we demonstrate that V75I is likewise selected in the presence of a monophosphorylated prodrug derivative of ACV that was developed to bypass the bottleneck in the metabolic conversion of ACV to ACV-TP. Although other mutations, independent of or in conjunction with V75I, may also contribute to HIV-1 resistance to ACV or its prodrugs, here we focused on the characterization of the effect of V75I on the function of RT.

Residue V75 is located in close proximity to template position n+1 opposite the incoming nucleotide (Figure 7)[472]. Thus, a direct effect of a

mutation at this position on binding and/or incorporation of nucleoside analogues is not evident. V75I is part of the "Q151M cluster" that is associated with multiple resistance to NRTIs [473, 474]. However, in this context, V75I does not appear to contribute to the resistance phenotype, the mutation rather compensates for enzymatic deficits that are introduced by Q151M [475]. A related mutation, i.e. V75T, has been associated with low level (3- to 4-fold) resistance to stavudine (d4T), which is an 2',3'-unsaturated thymidine analogue and therefore structurally distinct from ACV [460, 475]. The increase of approximately one-two orders of magnitude in resistance to ACV is by far the strongest effect that has been reported for changes at this position [48]. We consider three complementary mechanisms that help to explain the resistant phenotype.

Discrimination against ACV-TP. Competition experiments under steady-state conditions and pre-steady state kinetics suggest that V75I further discriminates against the inhibitor. The selective advantage for the natural nucleotide over the inhibitor that is seen with WT RT is 10-fold increased with the V75I mutant. The difference can be assigned to equivalent changes in k_{pol} values. Thus, the V75I mutation appears to compromise the chemical step, while affinities to substrate and inhibitor, respectively, remain largely unchanged. This result is unexpected, given considerable distance between V75 and the active site or the incoming nucleotide (Figure 7). The V75I change may therefore indirectly affect the catalytic step. Specific decreases in k_{pol} values have been reported for other NRTI resistance associated mutations [353, 476]. K65R and Q151M are important examples in this regard [353, 417, 476, 477]. K65 is located in close proximity to the γ-phosphate of the incoming nucleotide, which indicates that changes at this position may affect its proper alignment with the attacking 3'-end of the primer. The side chains of Q151 and also R72 are seen in the vicinity of the α-phosphate of the incoming nucleotide, which suggests a direct role in the catalytic step [478, 479]. By extension, changes at this position can directly compromise catalysis at the center of the reaction. It is therefore conceivable that changes at position V75 can affect the precise positioning of one of the two residues, or both, which could help explain the observed decreases in k_{pol} values.

The backbone of V75 is in contact distance with the backbone of Q151, and subtle structural alterations at V75, i.e. V75I, can impact on the positioning of R72 that are both part of the flexible β3-β4 hairpin loop that traps the incoming nucleotide. Regardless of the precise mechanism, the effect of V75I on ACV-MP incorporation appears to be indirectly mediated through other amino acids. In contrast, classic NRTI-associated mutations, such as M184V, K65R, and Q151M discriminate against the inhibitor directly at the active site.

Previous studies have shown that changes at V75 can also affect the affinity to the substrate. V75T showed increases in K_d values for stavudine without affected k_{pol} [475]. Moreover, mispair extension experiments with the V75I mutant enzyme showed likewise significant increases in K_d values, without affecting k_{pol} [480]. Together the results suggest that changes at position V75 can affect nucleotide incorporation through different mechanisms. Mutations at this position can affect substrate binding or the catalytic step. Whether the effects of V75I on the catalytic step of ACV-MP incorporation can be ascribed to the acyclic nature of the inhibitor remains to be seen. However, in this context, it is interesting to note that the acyclic phosphonate tenofovir, which is an important component in currently used drug regimens, is sensitive against the Q151M cluster that includes V75I [481].

Excision of ACV-MP. Excision of incorporated NRTIs is a second major mechanism for NRTI resistance. TAMs increase the excision of AZT-MP when compared with WT RT [346, 436]; however, the reaction is not restricted to thymidine analogues. The efficiency of the ATP-dependent excision reaction is relatively high with AZT-MP at the 3'-end of the primer. In contrast, ddNMPs and 3TC-MP terminated primer strands are poor substrates for the reaction, although these nucleotides analogues are not completely resistant to excision [482]. Here we demonstrate that a mutant enzyme containing 4 TAMs can also markedly increase excision of ACV-MP. Of note, purine analogues are usually poorly excised when compared with their pyrimidine counterparts, which indicates that the base moiety is an important determinant for the reaction [483]. However, the acyclic purine analogues tenofovir [468], and ACV-MP are both

efficiently removed from the primer terminus, suggesting that the increased flexibility of the acyclic linker between the base and the phosphate or phosphonate of these compounds can facilitate the reaction.

The V75I mutation shows an intermediate phenotype when the excision of ACV-MP is compared with WT RT and TAMs, respectively. However, the mechanism associated with such increase in efficiency of the excision reaction is likely to be different as described for TAMs. TAMs were shown to facilitate binding of ATP in a catalytically competent fashion [436]. The aromatic side chains of T215Y/F, i.e. the hallmark for AZT resistance, are implicated in stacking interaction with the base moiety of ATP, which facilitates its binding in an orientation that allows its use as a PPi-donor (Figure 7). In contrast, the position of V75 in close proximity to template position n+1 and the nature of the amino acid substitution do not support such interaction. The mutation may indirectly affect the excision reaction in similar manner as proposed for the incorporation of ACV-MP; however, such interaction would be counterproductive. Thus, we also consider an alternative interpretation. Excision of ACV-MP with ATP generates the ACV-(5')-tetraphospho-(5')-A (ACVp4A) that is eventually released from the complex. The tetraphosphate can be used as a substrate [346, 484], resulting in re-incorporation of ACV-MP. At this level, the V75I mutant has a disadvantage over WT RT, which leads to an accumulation of the excised product. In contrast, TAMs containing enzymes do not significantly affect the efficiency of incorporation of nucleotide analogues [485-487].

Dead-End-Complex (DEC) formation. The formation of a DEC with the next complementary nucleotide following the chain-terminator at the 3'end of the primer has two major consequences. First, the bound nucleotide stabilizes the complex, which translates in a diminished turnover of the reaction under steady-state conditions [454]. This experimental set-up allowed us to compare and to quantify DEC formation of WT RT with mutant V75I RT. ACV-MP generally diminishes DEC formation when compared with ddGTP, and V75I increased this effect. A similar effect has been observed when comparing tenofovir with ddATP, suggesting that the acyclic linker can negatively influence nucleotide binding

[468]. V75I may further affect DEC formation through structural alterations at template position n+1 that is complementary to the next nucleotide. Of note, our data show at the same time that neither the ACV-terminated primer, nor the V75I mutation affect the distribution of pre- and post-translocated complexes.

The second major consequence of a stable DEC is that the 3'-end of the primer is protected from excision [346]. The nucleotide traps the complex in its post-translocational state, which prevents excision to occur [437]. This observation is of potential biological relevance considering that WT RT can excise ACV-MP, although the reaction is inefficient.

Conclusion. The results of this study suggest that discrimination against the inhibitor at the level of incorporation is the dominant mechanism associated with ACV resistance conferred by V75I. Protection against excision is compromised through diminished formation of a ternary DEC, and TAMs can directly increase efficiency of excision of ACV-MP. Thus, ACV appears to be vulnerable to both major NRTI-associated resistance pathways. It is therefore essential to characterize the detailed resistance profile of this compound, to better assess its potential clinical utility in combination with established antiretrovirals. The use of ACV might be compromised in persons who were recently infected with resistant HIV variants. In addition, the clinical use of ACV may cause the emergence of resistance mutation that can decrease susceptibility to established antiretroviral agents.

4.7 Acknowledgements

We would like to thank Suzanne McCormick for excellent technical assistance. This study was supported by the Canadian Institutes for Health Research (CIHR). MG is recipient of a national career award from the CIHR. RFS is supported in part by NIH grants 5R37-AI-041980, 4R37-AI-025899, 5P30-AI-50409 (CFAR), and by the US Department of Veterans Affairs. JB received a grant from the K.U.Leuven (GOA no. 05/19). AL, CV, BB and LM were supported by the NICHD Intramural Program.

4.8 Abbreviations

ACV, acyclovir; ACV-MP, acyclovir-monophosphate; ACV-TP, acyclovir-triphosphate; HIV-1, human immunodeficiency virus, type 1; HSV-1, herpes simplex virus, type 1; TK, thymidine kinase; RT, reverse transcriptase; NRTI, nucleoside-analogue RT inhibitor; DEC, dead-end complex; HHV, human herpes virus; PPi, pyrophosphate; AZT, zidovudine; d4T, stavudine; TAM, thymidine analogue-associated mutation; PFA, foscarnet; DMPU, *N,N′*-dimethylpropylene urea; HPLC, high performance liquid chromatography; LC-MS/MS, liquid chromatography-mass spectrometry/tandem MS; DTT, dithiothreitol.

4.9 Figures and tables

Figure 4.1 Resistance to ACV and CF2648. Structures of ACV and the monophosphorylated prodrug CF2648.

CF2648

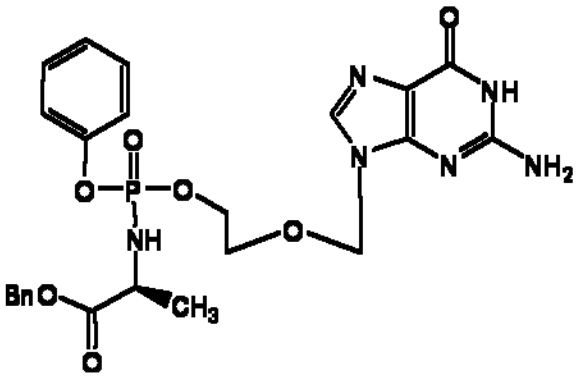

Acyclovir

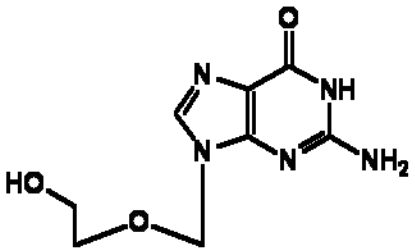

Figure 4.2 Competition between ACV-TP and dGTP. *A*. Reaction scheme. Nucleotide incorporation was monitored at positions +1 and +2. Letters in bold italic illustrate the incorporated nucleotide(s). *X* illustrates an incorporated ACV-MP. The *asterisk* points to the 5'-end radio-labelled primer. *B*. Two nucleotide incorporation events in the presence of constant concentrations of dGTP and ddTTP and increasing concentrations of ACV-TP. ACV-mediated inhibition of DNA synthesis is monitored at position +2, and corresponding arrows illustrate the migration pattern of non-extended substrate and extended primers. *C*. Graph of data shown under B. Dotted lines illustrate a shift in IC_{50}.

A

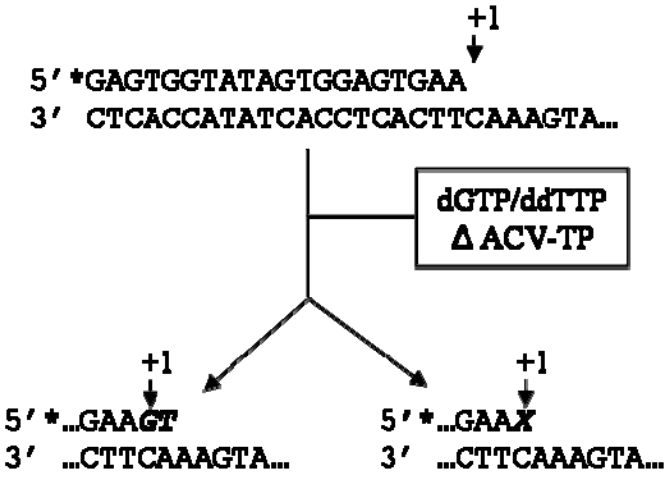
+1
5′ *GAGTGGTATAGTGGAGTGAA
3′ CTCACCATATCACCTCACTTCAAAGTA...
dGTP/ddTTP
Δ ACV-TP
+1
+1
5′ *...GAAGT
3′ ...CTTCAAAGTA...
5′ *...GAAX
3′ ...CTTCAAAGTA...

B

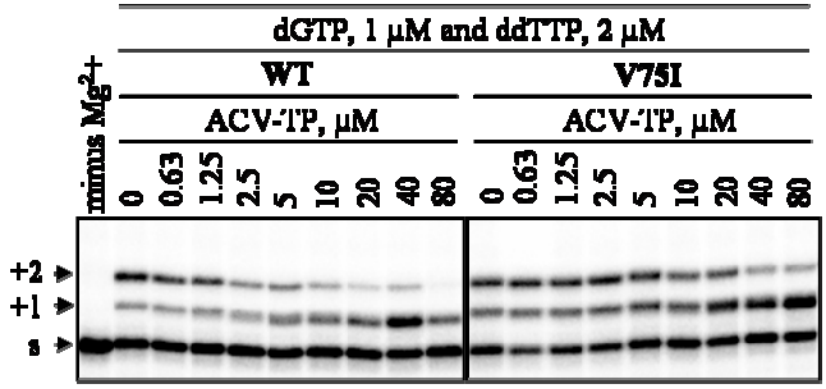
dGTP, 1 μM and ddTTP, 2 μM
WT
V75I
minus Mg2+
ACV-TP, μM
ACV-TP, μM
0 0.63 1.25 2.5 5 10 20 40 80
0 0.63 1.25 2.5 5 10 20 40 80
+2
+1
s

C

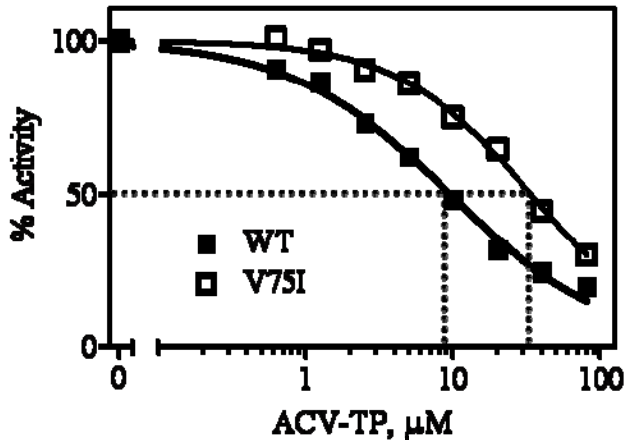
100
50
0
% Activity
WT
V75I
0
1
10
100
ACV-TP, μM

Figure 4.3. Competition between ACV-TP and dGTP during later stages of DNA synthesis. *A*. DNA/DNA primer/template substrate used in the experiment. ACV-MP incorporation was monitored at position +7. The *asterisk* points to the 5'-end radio-labelled primer. *B*. Multiple nucleotide incorporation events in the presence of constant concentration of dNTP mix and increasing concentrations of ACV-TP. Arrows illustrate the migration pattern of non-extended substrate, extended primers by 7 nucleotides and full length product. Dashed lines point to 50% product formation; however, we were unable to accurately determine IC50 values under these conditions. Incorporation of ACV-MP is generally diminished when compare with the sequence used in Figure 2.

A

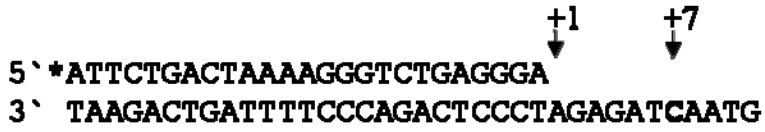
+1
+7
5`*ATTCTGACTAAAAGGGTCTGAGGGA
3` TAAGACTGATTTTCCCAGACTCCCTAGAGATCAATG

B

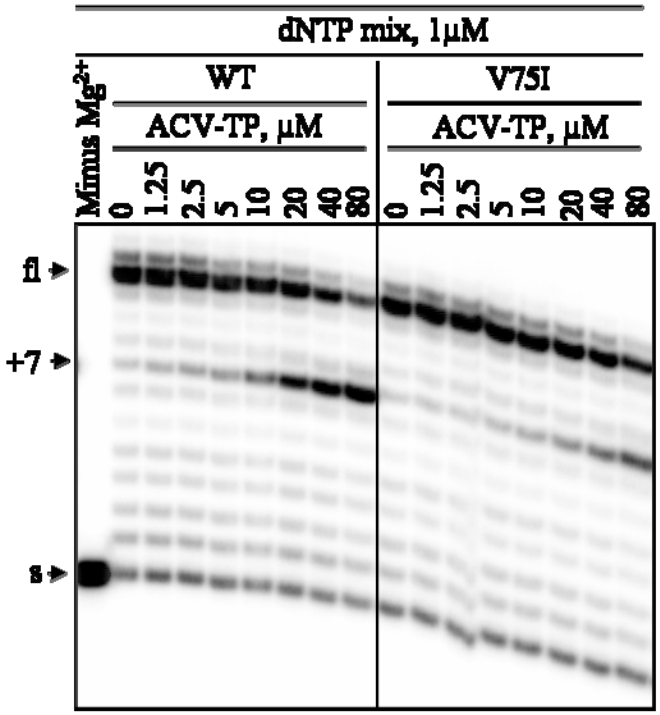
dNTP mix, 1μM
WT
V75I
Minus Mg2+
ACV-TP, μM
ACV-TP, μM
0 1.25 2.5 5 10 20 40 80
0 1.25 2.5 5 10 20 40 80
fl
+7
s

C

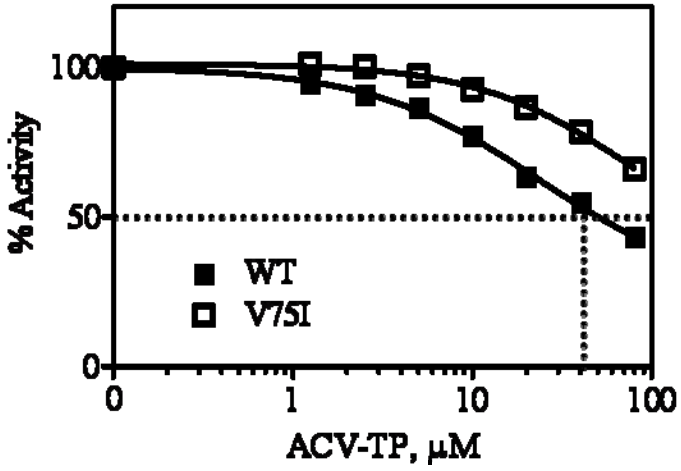
100
50
0
% Activity
WT
V75I
0
1
10
100
ACV-TP, μM

Figure 4.4 ATP-dependent excision of ACV-MP containing primers. Time course of ATP-dependent excision of ACV-MP from the 3'-end of the primer. The migration pattern of the 5`end radioactively labelled primer (s) and reaction product (p) is illustrated by corresponding arrows.

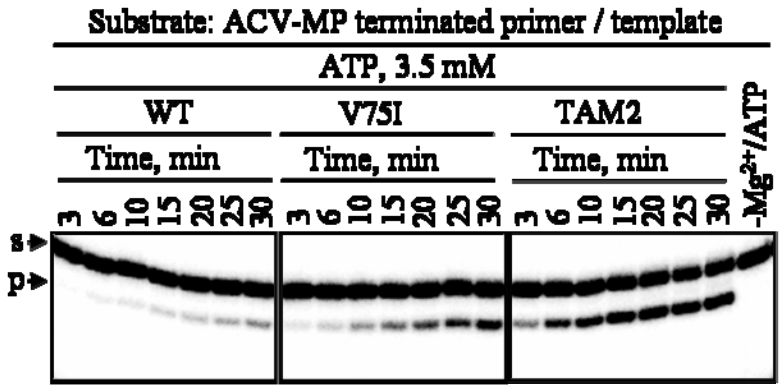
Substrate: ACV-MP terminated primer / template
ATP, 3.5 mM
WT
V75I
TAM2
Time, min
Time, min
Time, min
3 6 10 15 20 25 30
3 6 10 15 20 25 30
3 6 10 15 20 25 30
-Mg2+/ATP
s
p

Figure 4.5 Site-specific footprinting of HIV1 RT-DNA substrate complexes. *A*. Reaction scheme. Complexes were treated with Fe^{2+} following incorporation of ACV-MP or ddGMP. The additional presence of PFA or dTTP provides conditions to trap the pre- or post-translocated complex, respectively. The *asterisk* illustrates a 5'-end radioactively labelled template. *B*. Footprinting patterns with ddGMP or ACV-MP terminated primers. *Minus* Fe^{2} represents a control experiment in the absence of Fe^{2+}. *Plus* Fe^{2+} represents treatment of binary complexes with Fe^{2+} prior to nucleotide incorporation. *PFA 100 μM* represents the footprint in the presence of 100 μM PFA that traps the pre-translocated complex.

A

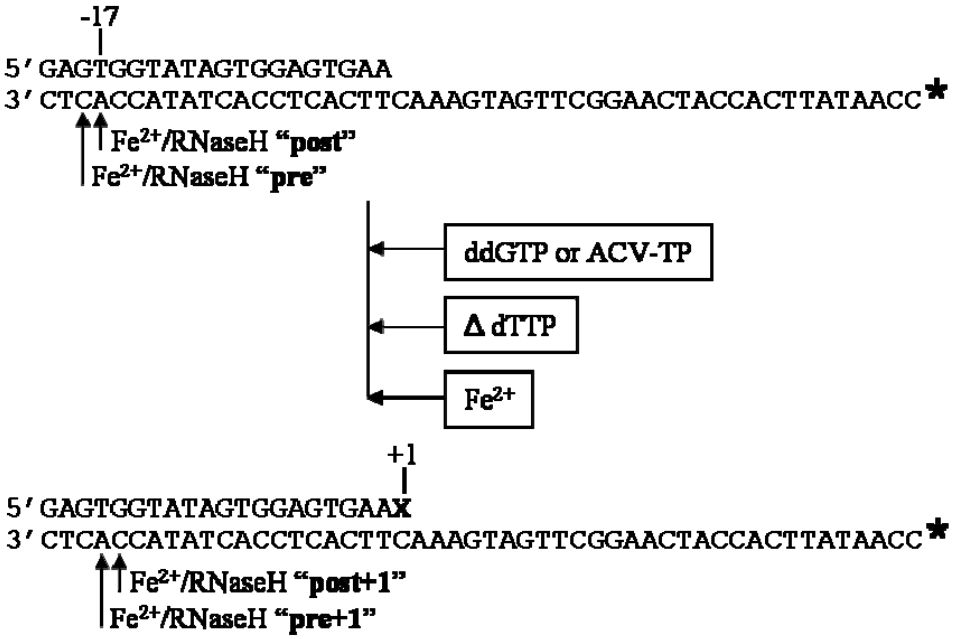
-17
5′ GAGTGGTATAGTGGAGTGAA
3′ CTCACCATATCACCTCACTTCAAAGTAGTTCGGAACTACCACTTATAACC*
Fe2+/RNaseH "post"
Fe2+/RNaseH "pre"
ddGTP or ACV-TP
Δ dTTP
Fe2+
+1
5′ GAGTGGTATAGTGGAGTGAAX
3′ CTCACCATATCACCTCACTTCAAAGTAGTTCGGAACTACCACTTATAACC*
Fe2+/RNaseH "post+1"
Fe2+/RNaseH "pre+1"

B

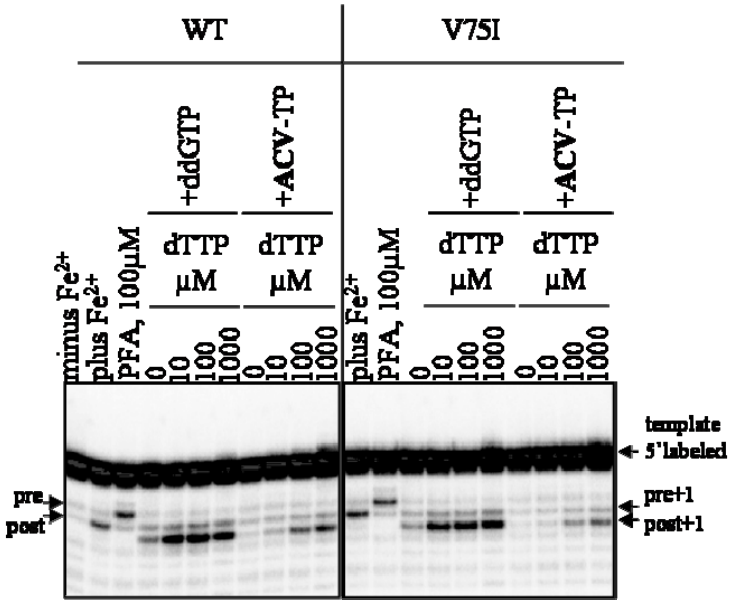
WT
V75I
+ddGTP
+ACV-TP
dTTP µM
minus Fe2+
plus Fe2+
PFA, 100µM
0
10
100
1000
template 5'labeled
pre
post
pre+1
post+1

Figure 4.6 Dead-end complex formation (DEC). *A*. Graphical representation of a time course of incorporation of a ddGTP chain terminator at position +1 in the absence (closed squares) or in the presence of increasing concentrations of the nucleotide (dTTP) for the binding at position +2 (open symbols). Left and right graphs of the panel represent ddGTP incorporation by WT RT and V75I, respectively. Slopes of the linear portion of the normalized product formation illustrate the turn over number (k_{cat}) (Table 2).

A

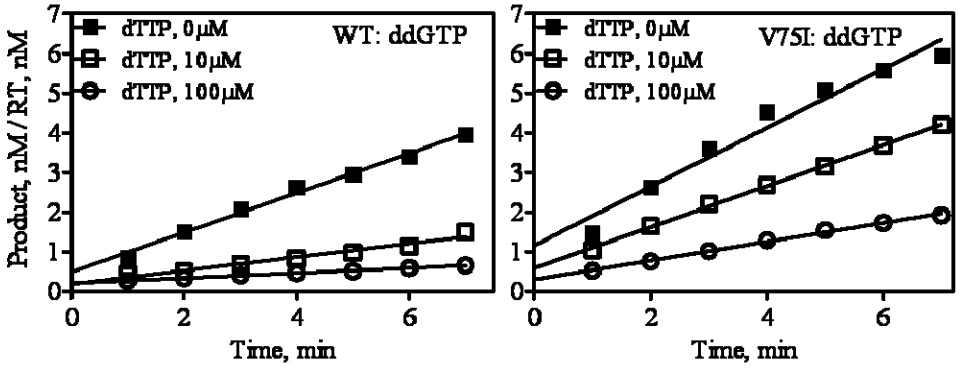
dTTP, 0μM
dTTP, 10μM
dTTP, 100μM
WT: ddGTP
V75I: ddGTP
Product, nM/RT, nM
Time, min

B

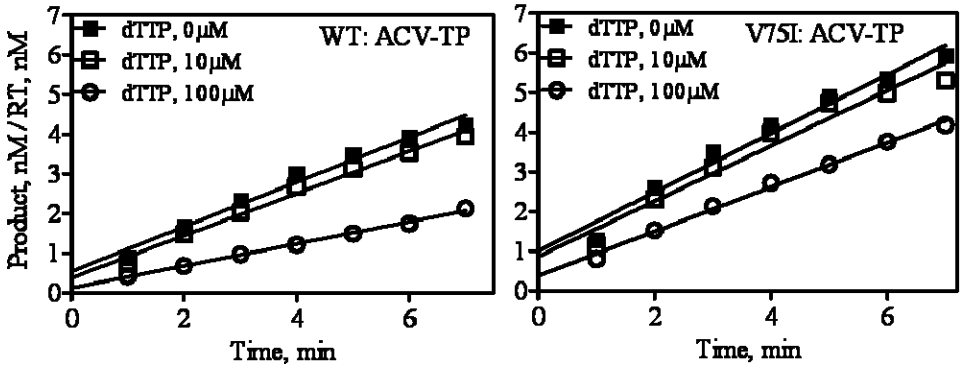
dTTP, 0μM
dTTP, 10μM
dTTP, 100μM
WT: ACV-TP
V75I: ACV-TP
Product, nM/RT, nM
Time, min

Figure 4.7 Relative location of V75 and critical other amino acid residues in HIV-1 RT. The crystal structure of HIV-1 RT in complex with tenovovir and primer/template (PDB code 1r0a) [488]. Tenofovir is shown in cyan, primer position n is in red, and template positions n and n+1 are highlighted in green. Residues implicated in resistance are labelled (see text).

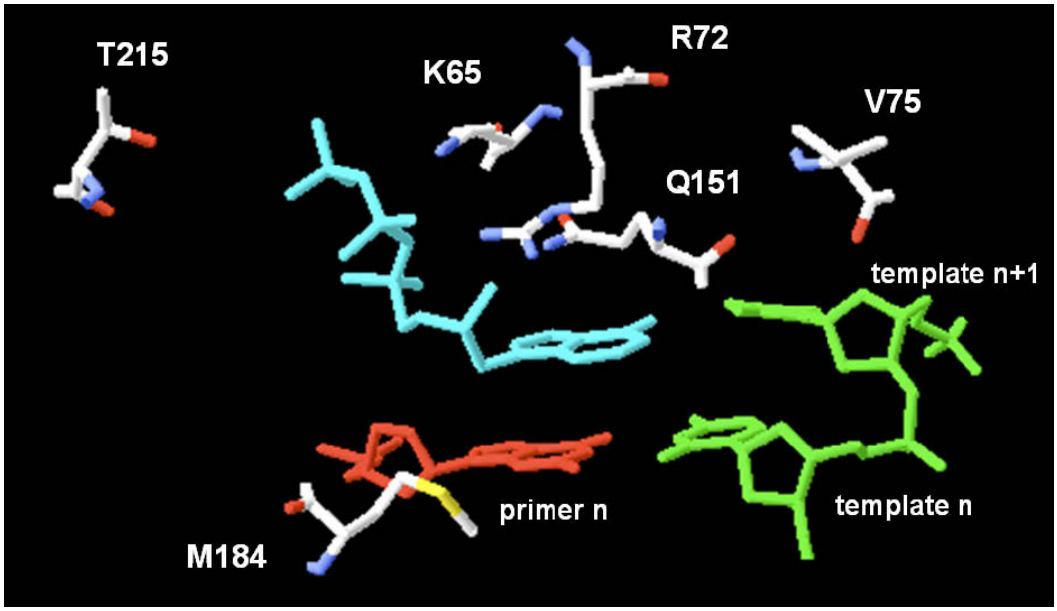
T215
K65
R72
V75
Q151
template n+1
primer n
template n
M184

Figure S1. Effect of HIV-1 NCp7 on the competition between ACV-TP and dGTP during DNA synthesis. *A*. Multiple nucleotide incorporation events in the presence of constant concentration of dNTPs and increasing concentrations of ACV-TP and NCp7 (kindly provided by Dr. Chen Liang, Lady Davis Institute for Medical Research, Montreal, Quebec, Canada), respectively. Based on the ratio of 1 molecule of NCp7 per 7 single-stranded oligonucleotides, a 1 μM concentration of NCp7 represents a saturating concentration with respect to the single-stranded portion of the primer-template used in the experiment. Reaction conditions are the same as in Figure 3. ACV-MP incorporation was monitored at position +7, and corresponding arrows illustrate the migration pattern of non-extended substrate, extended primers by 7 nucleotides and full length product. *B*. Graph of data shown under B.

A

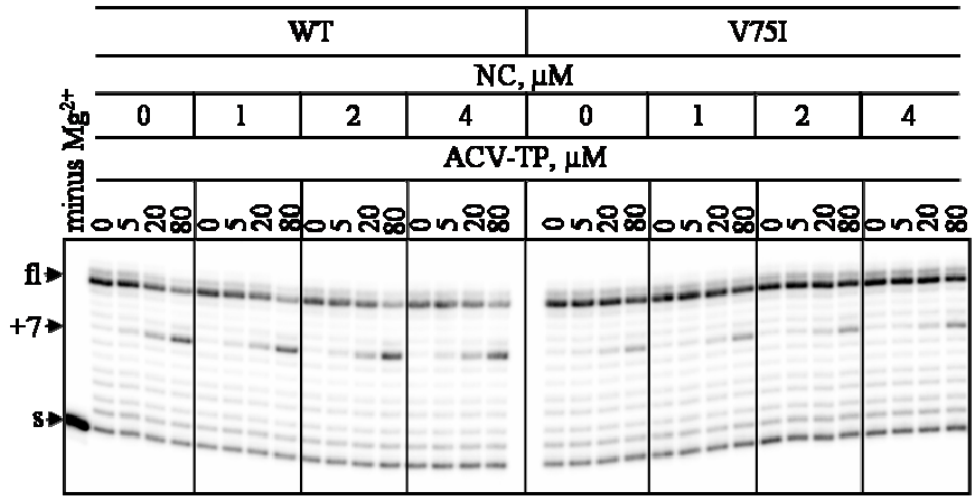
WT
V75I
NC, μM
0
1
2
4
0
1
2
4
minus Mg^{2+}
ACV-TP, μM
0 5 20 80
fl
+7
s

B

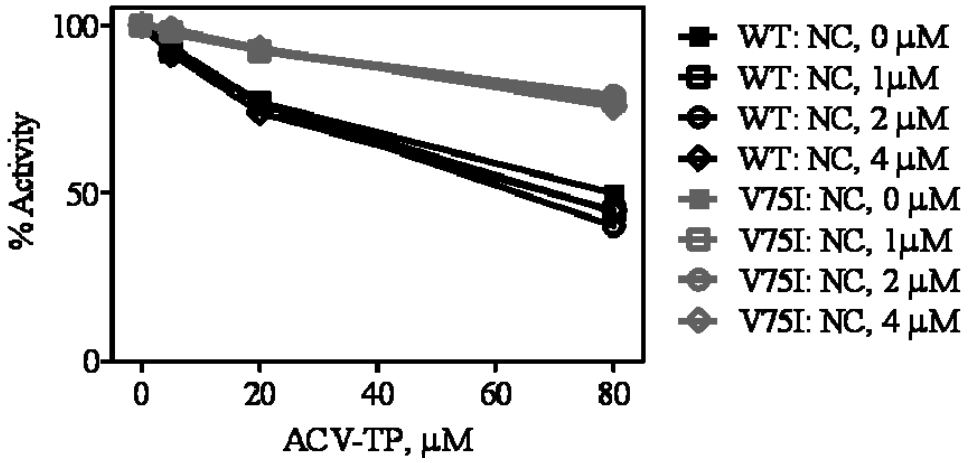
100
50
0
% Activity
0
20
40
60
80
ACV-TP, μM
WT: NC, 0 μM
WT: NC, 1μM
WT: NC, 2 μM
WT: NC, 4 μM
V75I: NC, 0 μM
V75I: NC, 1μM
V75I: NC, 2 μM
V75I: NC, 4 μM

Table 4.1 Inhibitory activity of ACV ProTide CF2648 against HIV-$1_{Lai.04}$ in MT-4 cells.

	Wild-Type (WT)	CF2648 Selected (15V)	Fold increase
EC_{50} ± SE (μM)[a]	3.4 ± 2.8	51 ± 2.3	15

[a] EC50, effective concentration that inhibits 50% of HIV-$1_{LAI.04}$ replication ± standard error

Table 4.2 Pre-steady state parameters for nucleotide incorporation by WT and V75I mutant RT.

	Substrate							
	dGTP			ACV-TP				
Enzyme	k_{pol} sec^{-1}	K_d μM	k_{pol} / K_d	k_{pol} sec^{-1}	K_d μM	k_{pol} / K_d	SEL[1]	RES[2]
WT	66 ±3.0[3]	1.3 ±0.16	51	14 ±0.39	2.2 ±0.18	6.4	8.0	1.0
V75I	114 ±2.9	3.7 ±0.18	31	1.5 ±0.071	3.8 ±0.43	0.40	78	9.8

[1]SEL, selectivity, is calculated as a ratio of k_{pol}/ K_d for dGTP over k_{pol}/ K_d for ACV-TP. [2]RES, resistance, is calculated as a ratio of selectivity of WT over the selectivity of V75I mutant RT.
[3]Errors reported represent the deviation of points from the curve fit generated by GraphPad Prism (version 5.0).

Table 4.3 Inhibition of DNA synthesis by WT RT and V75I mutant RT through DEC formation

		Enzyme					
		WT			V75I		
		k_{cat} min^{-1}	DEC[3]	Fold Change[4]	k_{cat} min^{-1}	DEC	Fold Change
ddGTP[1]	dTTP[2] 0 μM	0.46 ±0.057[5]			0.77 ±0.078		
	dTTP 10 μM	0.16 ±0.014	2.9	1.0	0.51 ±0.021	1.5	1.9
	dTTP 100 μM	0.060 ±0.0057	7.7	1.0	0.23 ±0.014	3.3	2.0
ACV-MP	dTTP[2] 0 μM	0.63 ±0.028			0.64 ±0.15		
	dTTP 10 μM	0.54 ±0.0071	1.2	1.0	0.65 ±0.078	1.0	1.2
	dTTP 100 μM	0.27 ±0.014	2.3	1.0	0.55 ±0.021	1.2	1.9

[1] The 3'-end of the primer was terminated in the presence of ddGTP or ACV-TP to prevent incorporation of the next nucleotide during DEC formation.
[2] Next complementary nucleotide
[3] DEC formation is calculated as a ratio of k_{cat} in the absence of dTTP over k_{cat} in the presence of dTTP.
[4]Fold change reflects differences in DEC formation by WT RT overV75I mutant RT.
[5]Standard deviations were determined on the basis of at least three independent experiments.

CHAPTER 5

DELAYED CHAIN-TERMINATION PROTECTS THE ANTI-HBV DRUG ENTECAVIR FROM EXCISION BY HIV-1 REVERSE TRANSCRIPTASE

This chapter was adapted from an article authored by E.P.Tchesnokov, A. Obikhod, R.F. Schinazi and M. Götte that appeared in the ***Journal of Biological Chemistry***, 2008, 283(49): 34218-28.

5.1 Preface to chapter 5

Almost parallel to the discovery of the dual antiviral activity of acyclovir, a similar pattern was reported for entecavir, an anti-HBV drug. But the anti-HIV activity of entecavir in HBV/HIV co-infected patients represented a major challenge to its safe clinical use in such persons, owing to the selection of the M184V mutation in the HIV-1 RT under pressure of the drug. M184V substitution is a classic mutation that confers resistance to nucleoside analogues. Therefore, in HBV-HIV co-infected patients who do not require initiation of an anti-HIV specific therapy, entecavir can select for resistance to such therapy prior to its administration.

Entecavir is a unique compound from a structural point of view: it is the first nucleoside analogue that is not an obligate chain terminator clinically active against HIV-1. Entecavir was shown to cause a delayed chain termination in the context of the HBV polymerase. The delayed chain termination's mechanism for inhibiting HIV-1 RT would represent a novel mechanism of action. Therefore, I sought to determine the precise molecular mechanism of entecavir action in the context of HIV-1 RT.

5.2 Abstract

Entecavir (ETV) is a potent antiviral nucleoside analogue that is used to treat hepatitis B virus (HBV) infection. Recent clinical studies have demonstrated that ETV is also active against the human immunodeficiency virus type 1 (HIV-1). Unlike all approved nucleoside analogue RT inhibitors (NRTIs), ETV contains a 3'-hydroxyl group that allows further nucleotide incorporation events to occur. Thus, the mechanism of inhibition likely differs from classic chain-termination. Here, we show that the incorporated ETV-monophosphate (MP) can interfere with three distinct stages of DNA synthesis. First, incorporation of the next nucleotide at position n+1 following ETV-MP is compromised, although DNA synthesis eventually continues. Second, strong pausing at position n+3 suggests a long range effect, referred to as "delayed chain-termination". Third, the incorporated ETV-MP can also act as a "base-pair confounder" during synthesis of the second DNA strand, when the RT enzyme needs to pass the inhibitor in the template. Enzyme kinetics revealed that delayed chain-termination is the dominant mechanism of action. High-resolution footprinting experiments suggest that the incorporated ETV-MP "repels" the 3'-end of the primer from the active site of HIV-1 RT, which, in turn, diminishes incorporation of the natural nucleotide substrate at position n+4. Most importantly, delayed chain-termination protects ETV-MP from phosphorolytic excision, which represents a major resistance mechanism for approved NRTIs. Collectively, these findings provide a rationale and important tools for the development of novel, more potent delayed chain-terminators as anti-HIV agents.

5.3 Introduction

Co-infection with the hepatitis B virus (HBV) and the human immunodeficiency virus type-1 (HIV-1) is common and complicates treatment [62]. Although both viruses share a highly related target for pharmaceutical intervention, there are few drugs that are approved to treat HBV and HIV-1 infection simultaneously [50, 62]. HBV and HIV replicate through a reverse transcription step, carried out by the virally encoded HBV DNA polymerase and the HIV-1 reverse transcriptase (RT), respectively [489, 490]. Lamivudine (3TC) and emtricitabine (FTC) are cytidine analogues that exert potent antiviral effects against HBV and HIV-1 targeting their DNA polymerase [55, 491, 492]. Once intracellularly phosphorylated to their triphosphate forms, these drugs act as chain-terminators. However, the development of resistance can limit their clinical utility [348, 349, 493]. In HIV-1, both 3TC and FTC can select for the M184V mutation in the conserved YMDD motif at the active site of RT [494]. A structurally and functionally equivalent mutation, i.e., M204V, is selected in HBV [240, 493, 495-498]. This mutation is often accompanied with other mutations, including L180M, that appear to compensate for fitness deficits that are introduced by the primary mutation [499]. The incidence of 3TC-resistance is high in part because 3TC has been for a long time the only small molecule approved for the treatment of HBV, and 3TC has also been and remains an important component in recommended drug regimens for the treatment of HIV [50]. The acyclic phosphonate tenofovir is active against 3TC resistant HIV and HBV strains [481, 500-502], while the structurally related compound adefovir has been approved for HBV treatment only, even though it has activity against HIV [503, 504].

Entecavir (ETV) belongs to the few available drugs that retain potency against 3TC-resistant HBV [505, 506]. This compound does not appear to select for M204 and L180M in HBV, although the pre-existence of the two mutations can decrease susceptibility to ETV [59, 252]. Additional other mutations can further amplify clinically relevant levels of resistance to this drug [507]. In contrast, it has

recently been demonstrated that ETV can select for the M184V mutation in HBV/HIV co-infected individuals [60]. These data showed unambiguously that ETV can exert antiretroviral effects, which led to the recommendation that ETV should not be administered in co-infected individuals unless these persons are simultaneously on highly active antiretroviral therapy (HAART) [60, 508]. Subsequent case reports and clinical studies with smaller cohorts are consistent with the original study, and *in vitro* selection experiments as well as phenotypic susceptibility measurements with HIV-1 strains containing the M184V mutation confirmed the clinical data [509-513]. Moreover, pre-steady state kinetics with wild type (WT) HIV-1 RT demonstrated that the enzyme can incorporate ETV-monophosphate (MP) [61]. The M184V mutant appears to be able to discriminate against the inhibitor, as the efficiency of incorporation of ETV-MP is severely diminished.

Aside of the clinical importance of these findings, the observation that ETV exhibits antiretroviral activity has potential implications for the development of novel drugs that may evade major resistance pathways in HIV. Unlike all approved nucleoside analogue RT inhibitors that lack the 3'-hydroxyl group of the sugar moiety and act as chain-terminators, ETV contains this group that can attack the next incoming nucleotide on its α-phosphate (Figure 1). Thus, DNA synthesis may be inhibited at several steps after incorporation of ETV-MP. *In vitro* studies with HBV replication complexes [57] and purified HIV-1 RT [61], respectively, indicated pausing of DNA synthesis immediately following incorporation of ETV-MP and later following incorporation of up to three additional nucleotides. Such late pausing is referred to as "delayed chain-termination". Very few nucleotide analogues have been described that show this type of inhibition of HIV-1 RT [64]; however, these compounds are toxic and/or are not converted intracellularly into their triphosphate form [514]. ETV may therefore be exploited as a model compound for the study of delayed chain-termination and its implications in current drug development efforts. Of note, ETV is fully susceptible against a background of thymidine analogue associated mutations

(TAMs) [61], that reduce susceptibility to literally all approved nucleotide analogue RT inhibitors (NRTIs), albeit at different degrees [462]. TAMs include changes at positions 41, 67, 70, 210, 215, and 219 that were shown to increase the phosphorolytic excision of incorporated nucleotide analogues [346, 461]. These mutations are able to recruit ATP as a pyrophosphate (PPi) donor, which ultimately removes the inhibitor from the primer terminus and leads to the rescue of DNA synthesis. ETV may evade this resistance mechanism through delayed chain-termination.

Here, we demonstrate that delayed chain-termination at position n+3, i.e. three nucleotides following incorporation of ETV-MP, is the major mechanism of inhibition. Although ETV-MP is efficiently excised with TAMs containing RT enzymes, the inhibitor is not excised when the primer was extended by three additional nucleotides. These proof-of-principle studies show that delayed chain-terminators are protected from excision.

5.4 Experimental procedures

Enzymes and Nucleic Acids- Heterodimeric reverse transcriptase p66/p51 was expressed and purified as described [446]. Mutant enzymes were generated through site-directed mutagenesis using the Stratagene QuikChange kit according to the manufacturer's protocol. TAM refers to HIV1-RT containing the following substitutions: M41L, D67N, L210W, and T215Y. Oligo-deoxynucleotides used in this study were chemically synthesized and purchased from InVitrogen Life Technologies and from Integrated DNA Technologies. The following sequences were used as templates:

T45:

5`ATTGAGTATGAAGGATTGATATCTATTCACTCCACTATACCACTC

T50:

5`CCAATATTCACCATCAAGGCTTGACGTCACTTCACTCCACTATACCACTC

T50A:

5`CCAATATTCACCATCAAGGCTTGACGTGACTTCACTCCACTATACCA
CTC

T50A6:

5`CCAATATTCACCATCAAGGCTTGATGAAACTTCACTCCACTATACCA
CTC

The underlined nucleotides are the portion of the templates annealed to the primer.

The following primers were used in this study:

P1: 5`GAGTGGTATAGTGGAGTGAA

P1b: 5`GAGTGGTATAGTGGAGTGAATA

P2: 5`ATTGAGTATGAAGGATTGAT

Synthesis of ETV-TP- 2-Amino-9-[4-hydroxy-3-(hydroxymethyl)-2-methylidene-cyclopentyl]-3*H*-purin-6-one (4.71 mg, 1.7 mmol) was dissolved in 200 ml of dry 1,3-Dimethyl-2-oxohexahydropyrimidine *N,N′*-dimethylpropylene urea with 15 molecular sieves under nitrogen and stirred for 24 h. The mixture was chilled with ice-water bath and stirred for 1h followed by slow addition of phosphorus oxychloride 3 eq. and stirred for another 50 min. A solution of tributylammonium pyrophosphate 4 eq. in 200 uL of DMPU and tributyl amine 15 eq. were simultaneously added to the reaction. After 2 h., the reaction was quenched with ice-cold water and slowly brought to room temperature. The solution was washed with chloroform, aqueous layer collected and co-evaporated with water three times. The product was re-suspended in 100 mL of water and purified on HPLC followed by co-evaporation with water, giving a total yield of 9% with 98% purity. ETV-TP was finally purified by ion-exchange High Performance Liquid Chromotagraphy (HPLC).

DNA Synthesis at Position n- 150 nM DNA/DNA template/primer hybrid T50A/P1, was incubated with 50 nM of HIV-1 RT in a buffer containing 50 mM Tris-HCl pH7.8, 50 mM NaCl, in the presence of increasing concentrations of

dGTP or ETV-TP or both. The concentrations of dGTP ranged from 0.008 to 2 μM and the concentrations of ETV-TP covered the range of 0.039 to 10 μM in a series of two-fold dilutions. In the experiments where both nucleotides were present only ETV-TP concentrations were varied from 0.16 to 50 μM in the series of two-fold dilutions, while the concentration of dGTP was kept constant at 0.05 or 0.1 or 0.5 μM.

Nucleotide incorporation was initiated by the addition of $MgCl_2$ to a final concentration of 10 mM, and the reactions were allowed to proceed for 3 minutes. The reaction conditions were optimized such that the rate of the product formation was within its linear range with respect to the enzyme concentration and time point, which is consistent with steady-state approach.The reactions were stopped by the addition of 3 reaction volumes of formamide containing traces of bromophenol blue and xylene cyanol. The samples were then subjected to 18% denaturing polyacrylamide gel electrophoresis (PAGE) followed by phosphorimaging. The incorporation of single nucleotides was quantified as the fraction of the DNA substrate (template/primer) converted to product (template/primer+1 nucleotide). The rate of the reaction was plotted versus the concentration of nucleotide substrate. The data were fitted to Michaelis-Menten equation by use of GraphPad Prism (version 4.0) to determine K_m and k_{cat} values for dGTP and ETV-TP. Significant figures for the fitted data are as reported by the software. k_{cat} was defined as maximal rate of single nucleotide incorporation. K_m was defined as the concentration of dNTP at which the rate of single nucleotide incorporation equals half of the maximal rate. In the experiments where both dGTP and ETV-TP were present for the incorporation at position n, the concentration of ETV-TP at which the incorporation of dGTP was reduced by 50% (IC_{50}) was determined by plotting the per cent incorporation of dGTP *vs.* the concentration of ETV-TP. The data were fit to a sigmoidal curve (variable slope).

DNA Synthesis at Position n+1- The reactions were conducted as described above, except that (i) T50A/P1 was used as the DNA/DNA hybrid, (ii) 1 μM

dGTP or 10 μM ETV-TP was used for the incorporation at position n and (iii) the time point was extended to 30 minutes to ensure maximum product formation at position n. Then, increasing concentrations of dTTP from 0.02 to 2 μM with *n* = dGMP and 0.078 to 10 μM were allowed to proceed for 4 min.

DNA Synthesis at Position n+4- The reactions were conducted as described, except that (i) T50A6/P1 was used as the DNA/DNA hybrid and (ii) increasing concentrations of dCTP from 0.03 to 256 μM were added in a series of two-fold dilutions. Reactions were allowed to proceed for 4 min. In the experiment where dGTP, ETV-TP, dTTP and dCTP were present at the same time only dGTP concentrations were varied from 0.03 to 2 μM while the concentrations of ETV-TP, dTTP and dCTP were kept constant at 5 and 0.5 μM, respectively. In addition, the concentrations of HIV-RT and DNA substrate were adjusted to 100 nM and the reactions were stopped after 5 min to enhance the signal at the pausing sites.

Site-specific Footprinting- In preparation of the footprinting reaction, the 5'end-labelled template T50A was heat annealed with the primer P1. 50 nM DNA/DNA hybrid was incubated with 750 nM HIV-RT for 10 min in a reaction mixture containing sodium cacodylate pH 7 (120 mM), NaCl (20 mM), DTT (0.5 mM), $MgCl_2$ (10 mM) and 25 μM ddGTP or ETV-TP in a final volume of 15 μL. At the 10 min time point, increasing concentrations of PFA or dTTP from 0.8 to 500 μM were added to the reactions in a series of five fold dilutions followed by an incubation of 5 minutes at 37^0C. The complex was treated with 0.1 mM ammonium iron (II) sulphate hexahydrate [359]. The reactions were allowed to proceed for 5 min and were processed and analysed as described.

RNase H Activity Assays- Primer P1, annealed to T50A or T50A6 templates, was extended by 2 or 4 nucleotides, respectively, such that dGMP or ETV-MP were incorporated at position n followed by 1 or 3 more nucleotides. These primers with n = dGMP or ETV-MP were gel purified and re-annealed to T50A or T50A6 RNA templates, respectively. 3`-end-labeling with [^{32}P]pCp and T4 RNA ligase

was carried out as described [515]. The RNA/DNA hybrid (50 nM) was incubated with 750 nM HIV-RT in a reaction buffer containing 50 mM Tris-HCl pH7.8, 50 mM NaCl and 0.3 mM EDTA at 37^0C for 10 minutes. Heparin (4 mg/ml, final) was added to the reaction mixture and allowed to incubate for variable time ranging from 0 to 60 sec after which $MgCl_2$ (10 mM, final) was added to initiate the RNase H activity. The reactions were stopped by the addition of 3 reaction volumes of formamide containing traces of bromophenol blue and xylene cyanol. The samples were subjected to 18% denaturing PAGE followed by phosphorimaging. RNaseH activity was monitored and quantified based on the appearance of the 3`-end labelled RNA template degradation products. RNaseH specific products were identified based on the experiments controlling for the efficiency of the heparin trap as well as for RNaseH activity in the absence of $MgCl_2$. The rate of the dissociation of the RNA/DNA hybrid from the RNase H active site of the HIV1-RT (k_{off}) was determined by plotting the percent remaining RNase H activity *vs.* incubation time with heparin and fitting the data points to a single exponential decay function.

Inhibition of DNA synthesis with primer/templates containing dGMP, ddGMP or ETV-MP at the 3`-end of the primer- The rate constant (k_{cat}) for dGTP incorporation using 150 nM T50A/P1 primer/template was determined from the slope of the linear portion of product formation vs. time. Reactions were carried ou in the presence of 50 nM HIV-RT and 1 μM dGTP. The effect of the addition of 300 nM of primer/templates containing already dGMP, ddGMP or ETV-MP at the 3`-end of the primer on the k_{cat} was monitored to assess potential differences in relative affinities of dGMP-, ddGMP- or ETV-containing primer/templates.

DNA synthesis across a template containing ETV-MP- The T45/P1 RNA/DNA hybrid was used to generate a template containing ETV-MP. The RT-associated RNase H activity degraded the original T45 RNA template. The newly synthesized DNA template containing ETV-MP was annealed to 5`-end labeled primer P2 and incubated with 500 nM HIV1-RT in the presence of $MgCl_2$ (10

mM) and dNTP mix (0.5 μM). Aliquots were taken at time points 1, 2, 5, 20 min and data were processed and analyzed as described.

ATP-dependent Phosphorolysis- The radiolabeled T50A6/P1 DNA/DNA hybrid was extended by a single nucleotide to generate an oligonucleotide with ETV-MP or dGMP at the 3' end. Primers were also further extended by three residues, gel purified, and annealed with T50A6. The 50 nM DNA/DNA template/primer hybrid with ETV-MP at the 3`-end of the primer or ETV-MP followed by 3 more nucleotides was incubated with 750 nM of HIV-1 RT in a buffer containing 50 mM Tris-HCl pH7.8, 50 mM NaCl, 10 mM $MgCl_2$ and 3.5 mM ATP (pyrophosphotase treated). Aliquots were taken at time points 1, 3, 6, 12, 25, 40, 60 min and analyzed as described.

5.5 Results

ETV-TP is Able to Compete with dGTP- In order to assess the efficiency with which ETV-MP is incorporated in comparison to its natural counterpart dGMP, we determined the concentration of ETV-TP required for 50% inhibition (IC_{50}) of incorporation of dGMP (Figure S1). High-resolution polyacrylamide gels allowed us to distinguish between primers extended by dGMP or respectively ETV-MP (Figure S1A). As expected for a competitive inhibitor, we found that the IC_{50} (ETV-TP) value increased with increasing concentrations of dGTP (Figure S1B). Concentrations of dGTP as low as 0.5 μM, which is within the physiologically relevant range, require relatively high concentrations of 19 μM ETV-TP to obtain 50% inhibition. These data are in good agreement with steady-state kinetic that show 14- to 18-fold differences in efficiencies of incorporation (Table 1).

Incorporation of ETV-MP Causes Pausing at Positions n and n+3- The effects of incorporation of ETV-MP at position n was analyzed by studying the efficiency of subsequent nucleotide incorporation events (Figure 2). Enzyme pausing is evident at positions n and n+3, and to a lesser extent also at position n+2 (Figure 2B).

Pausing at positions n and n+2 can be overcome, while pausing at position n+3 represents the final product when DNA synthesis was limited to four nucleotide incorporation events (Figure 2C). Increasing the concentrations of dCTP reduced pausing and resulted in increased product formation at position n+4 (Figure 2D). Thus, incorporation of ETV-MP appears to exert an immediate effect on the next nucleotide at position n+1, and pausing at position n+3 points to long range effects of the inhibitor that can affect nucleotide incorporation at position n+4.

To translate these findings into quantitative terms, we devised primer/template substrates that allowed us to determine the efficiency of nucleotide incorporation at positions n+1 and n+4. The primer strands contained either ETV-MP or dGMP at position n. Steady-state kinetics revealed that the incorporation of the next complementary nucleotide was approximately 7-fold reduced when the primer was terminated with ETV-MP (Table 2). Nucleotide incorporation at position n+4 was measured with primers that were further extended by 3 nucleotides to yield the n+3 substrate. The measurements revealed substantially higher reductions, i.e. > 1000-fold, in efficiency of nucleotide incorporation with ETV-MP at position n. Thus, inhibition at position n+4 was more than two orders of magnitude more efficient when compared to inhibition at position n+1.

Effects of ETV-MP when Present in the Template- Given that increasing the concentrations of natural dNTP substrates can overcome RT pausing (Figure 2D), it is conceivable that the incorporated ETV-MP may also exert inhibitory effects when located in the template strand. In order to identify positions that could be affected, we devised a primer/template substrate that contained the inhibitor two nucleotides away from the primer terminus in the template (Figure 3A). A primer extensions assay revealed specific pausing opposite the incorporated ETV-MP, also referred to as position n, and at position n+1 (Figure 3B). Together, the data point to three distinct mechanism of inhibition: (i) inhibition of nucleotide incorporation at position n+1 immediately following the inhibitor, (ii) inhibition at

later stages, predominantly at position n+4, and (iii) inhibition during synthesis of the second strand, opposite the templated ETV-MP.

Inhibition at Position n+1 Correlates with Diminished Translocation of RT- We considered two possible scenarios that could lead to inhibition of DNA synthesis by the incorporated ETV-MP. First, the inhibitor may increase dissociation of the RT-primer/template complex. Second, the incorporated ETV-MP may affect the positioning of RT on its primer/template. Binding and/or incorporation of the next nucleotide would be affected in either case, which ultimately results in enzyme pausing. To address this issue, we focused on inhibition at position n+1, i.e. the equivalent of classic chain-termination, and position n+4, i.e. delayed chain-termination.

We have recently developed site-specific footprinting tools that allowed us to determine the positioning of HIV-1 RT on DNA/DNA templates at single nucleotide resolution [35, 359, 467, 468]. One of these methods takes advantage of the RT-associated ribonuclease H (RNase H) domain that trails the polymerase active site by approximately 18 base pairs [515]. The RNase H active site accommodates Fe^{2+} ions that cleave the DNA template in oxidative fashion. Specific cuts were seen at positions -17 and -18. The cut at -18 was indicative of a pre-translocation complex that exists immediately following nucleotide incorporation. In this configuration, the nucleotide binding site is still occupied with the 3'-end of the primer, and the polymerase needs to translocate to allow binding of the next incoming nucleotide. The cut at -17 was indicative of such a post-translocation complex. The PPi-analogue foscarnet (PFA) was shown to trap the pre-translocational state [35, 359], while the nucleotide substrate traps the post-translocational state (Figure 4A). Termination caused by ETV-MP incorporation resulted in different patterns. While the pre-translocated complex can still be identified in the presence of PFA, the post-translocated complex was only seen as a faint band even in the presence of the next nucleotide (Figure 4B). These findings indicated that ETV-MP reduces the population of post-translocated

complexes that are available for nucleotide incorporation, which may help to explain the subtle inhibitory effects at position n+1 (Table 2). Increasing concentrations of the next nucleotide will eventually result in its incorporation; however, the bands remain faint because this complex is not sufficiently stabilized due to the lack of the following dNTP substrate. In contrast, reactions with the ddGMP-terminated primer contain the correct next nucleotide (dTTP) that can stabilize the complex.

To study potential differences in complex dissociation with ETV-MP *versus* dGMP-terminated primers, we measured RNase H activity directly in the presence of increasing concentrations of substrate (Materials and Methods). However, the dissociation rate constants k_{off} (ETV-MP) = 0.27 sec^{-1} and k_{off} (dGMP) = 0.22 sec^{-1} were almost identical (Figure 4C), which argues against such a contribution to inhibition. Moreover, ETV-MP and dGMP-terminated primer and template substrates show the same inhibitory effects when added to reaction mixtures containing preformed ternary complexes (Figure 4D).

Inhibition at Position n+4 Correlates with a Misplacement of RT- We were unable to obtain specific cleavage in our footprinting experiments when using the ETV-MP containing primer that was further extended by three nucleotides. Since the intrinsic RNase H activity provides a more robust pattern, we used this activity again directly to identify potential differences between the substrates (Figure 5). The pattern with the natural primer with dGMP at position n and additional three nucleotides up to position +3 shows three distinct cuts (Figure 5B). The central RNase H cut was seen 18 nucleotides upstream of the 3'-end of the primer, which is indicative of the post-translocated configuration (Figure 5A). The two cuts upstream and downstream did not depend on a specific position of the primer terminus, and are therefore referred to as polymerase-independent. These two cuts are likewise observed with the primer that contains ETV-MP at position n (Figure 5B). However, specific polymerase-dependent cuts were missing. The controls in the absence of inhibitor with and without PFA identified

cuts that represent pre- and post-translocated complexes, and neither of these bands were seen with the ETV-modified primer. These findings suggested that ETV-MP at position n misplaces the 3'end of the primer at position n+3. The sum of RNase H activity at the three cleavage events was identical with both primers, which resulted in very similar k_{off} values that argued again against a contribution of complex dissociation to inhibition (Figure 5C).

ETV-MP is Efficiently Excised at Position n and Delayed Chain-Termination Provides Protection from Excision- While binding and incorporation of nucleotides can only occur in the post-translocated state, excision of incorporated nucleotides can only occur in the pre-translocated state that allows productive binding of PPi or the PPi-donor ATP [437]. The site-specific footprinting data suggested that ETV-MP may not affect formation and/or stability of the pre-translocated complex (Figure 4), which is a pre-requisite for the excision reaction. To address this question directly, we compared efficiencies of excision of ETV-MP and dGMP with WT RT and a mutant enzyme that contained major TAMs: M41L, D67N, L210W, and T215Y (Figure 6). ATP-dependent excision of dGMP and ETV-MP with WT RT was generally low (Figure 6B). In contrast, TAMs showed significant increases in the efficiency of the removal of ETV-MP (Figure 6A, B). Based on these data, one would predict that TAMs decrease susceptibility to ETV; however, *in vitro* susceptibility experiments have shown that TAMs-containing viruses are fully sensitive to this compound [61].

To reconcile these findings, we further analyzed the excision reaction at the level of delayed chain-termination that may provide a certain degree of protection (Figure 6C, D). The natural primer without the inhibitor is readily cleaved with the TAMs-containing enzyme. Cleavage products are seen down to position n. In contrast, excision of the ETV-MP modified primer was considerably less efficient, which is consistent with our RNase H mapping studies that did neither detect pre- nor post-translocated complexes (Figure 5). Thus, the combined data provide strong evidence that delayed chain-termination provides protection from

excision and is therefore identified as a major mechanism for inhibition of HIV-1 RT by ETV.

5.6 Discussion

The structure of the anti-HBV drug ETV differs from all approved anti-HIV NRTIs in that the sugar moiety contains a 3'-hydroxyl group. The lack of the 3'-hydroxyl group of established NRTIs cause chain-termination, whereas the presence of this group allows in principle the nucleophilic attack on the α-phosphate of the next dNTP substrate. Thus, the mechanism of inhibition associated with this type of nucleoside analogues can differ from classic chain-terminators. In this study, we identified three distinct mechanisms of inhibition of HIV-1 RT with ETV: (i) inhibition of nucleotide incorporation at position n+1 immediately following the incorporated ETV-MP at position n, (ii) inhibition of nucleotide incorporation at position n+4, and (iii) inhibition of nucleotide incorporation opposite the templated ETV-MP.

Inhibition at position n+1 has been described before for several compounds that target the hepatitis C virus (HCV) RNA-dependent RNA polymerase [516]. 2'-C-Methylated ribonucleotides are readily incorporated by HCV RNA polymerase and prevent binding of the next complementary nucleotide. As a consequence, this nucleotide is not incorporated and RNA synthesis is literally terminated. Thus, these compounds act as chain-terminators, despite the presence of the 3'-hydroxyl group. It has been suggested that some 2'-C-Methylated ribonucleotides may block RT translocation, which provides a mechanism for the inability to accommodate the next incoming nucleotide [517]. Modeling studies with ETV-TP bound to an HIV-1 RT derived structure of HBV polymerase point to a similar scenario [58]. A putative steric clash between Y203 in the vicinity of the active site of the HBV enzyme and the exocyclic double bond of the inhibitor can disfavour the post-translocated complex. This model is consistent with our site-specific footprinting experiments with HIV-1 RT that showed marked reductions

in the population of post-translocated complexes, while the stability of the pre-translocated complex was not affected. However, kinetic measurements revealed the inhibition of nucleotide incorporation at position n+1 was inefficient and classic chain-termination was, therefore, unlikely a major mechanism of action for ETV.

Inhibition of nucleotide incorporation at position n+4 was two to three orders of magnitude more efficient than inhibition at n+1, suggesting that delayed chain-termination represented an important mechanism of action. Mapping the RT-associated RNase H activity on the RNA template strand provided snap-shots of complexes that exist at this advanced stage of DNA synthesis. The location of primary RNase H cuts revealed the existence of pre- and post-translocated configurations solely in the absence of ETV-MP. With primers containing ETV-MP at position n, the RNase H pattern lacked these polymerase-dependent cuts, while polymerase-independent cleavage increased concomitantly. The incorporated inhibitor does not appear to increase enzyme dissociation, the data rather show that the 3'-end of the primer was not properly positioned at the polymerase active site to allow binding and incorporation of the next nucleotide. Based on these findings we propose a model in which the various complexes co-exist in equilibrium (Figure 7). The incorporated ETV-MP appears to "repel" the 3'-end of the primer from the active site, which causes a bias toward polymerase-independent conformations.

Crystal structures of HIV-1 RT bound to primer/template substrates show important contacts with the first six 3'-terminal residues of the primer [518-520]. ETV-MP, as part of the extended primer, interacts with residues that form the "minor grove binding track" or "translocation track" of HIV-1 RT. K263, G262, and K259 are specific amino acids that may collide with the inhibitor when the primer is extended by three more residues. Modeling studies suggest that ETV-MP may induce structural distortions within the helix that could likewise affect productive interaction with the enzyme [61]. Moreover, nucleotide analogues that

are conformationally locked in the A-form show similar pausing patterns at positions n+2 and n+3 [64]. Thus, this region appears to be sensitive to subtle structural differences of the nucleic acid substrate although the underlying mechanisms may not necessarily be identical. The structural reasons that help to explain the inhibitory effects of ETV-MP when present in the template strand are likewise unknown. RT pausing opposite ETV-MP suggests that the inhibitor may affect proper base-pairing. However, structural studies are required to address these issues.

The resistance profile of ETV provided independent support for our conclusion that delayed chain-termination was a dominant mechanism of inhibition. Resistance to NRTIs is based on two major mechanisms: substrate discrimination and ATP-dependent excision, respectively [461, 462]. M184V discriminates against NRTIs, including ETV [61], (Table 3). M184V can cause significant decreases in susceptibility to most approved NRTIs, with few exceptions including AZT and tenofovir [481, 500-502]. In contrast, TAMs were shown to decrease susceptibility to all approved NRTIs, albeit at different degrees [461, 462]. Increases in resistance often correlate with increases in excision. AZT is efficiently excised and TAMs confer high level resistance to this drug, while 3TC and FTC are to some degree protected from excision and multiple TAMs are required to cause relevant levels of resistance in these cases [521]. However, ETV appears to be fully susceptible in the context of HIV-1 variants containing four TAMs [61]. Conversely, we show that ETV-MP was effectively excised at the point of incorporation with TAMs-containing HIV-1 RT. A possible explanation is that excision of ETV-MP does not play a significant role in biological settings.

We identified several factors that provide protection from excision of the incorporated ETV-MP. In contrast to classic chain-termination, the subtle 7-fold reduction in the efficiency of nucleotide incorporation at position n+1 does not appear to give sufficient time for excision to occur. ATP-dependent excision of terminal nucleotides is at least three orders of magnitude slower than rates of nucleotide incorporation [487]. Second, delayed chain-termination at position n+3

diminishes the forward reaction as well as the reverse. Nucleotide incorporation can only occur post-translocation, while excision can only occur pre-translocation; however, neither of the two complexes can be detected at point of DNA synthesis (Figure 7). Nucleotide incorporation and also excision eventually occurs at the terminal two residues, but re-incorporation is again much more efficient than subsequent excision events that are required to remove ETV-MP at position n.

Together, these results demonstrate that efficient delayed chain-termination paired with insignificant inhibition at the point of incorporation can provide protection from a major resistance pathway, i.e., excision. Several studies have shown that ETV selects for M184V [60, 509-511], while TAMs do not appear to play a role in resistance [61]. Thus, the combined biochemical and clinical findings warrant further investigation on the development of novel delayed chain-terminators - related and unrelated to ETV - that show antiretroviral activity against a background of TAMs.

5.7 Acknowledgements

We would like to thank Suzanne McCormick for excellent technical assistance. This study was supported by the Canadian Institutes for Health Research (CIHR). MG is recipient of a national career award from the CIHR. RFS is supported in part by NIH grants 5R37-AI-041980, 4R37-AI-025899, 5P30-AI-50409 (CFAR), and by the US Department of Veterans Affairs

5.8 Abbreviations

The abbreviations used are: HIV-1, human immunodeficiency virus type 1; HBV, Hepatitis B virus; RT, reverse transcriptase; NRTIs, nucleoside-analogue RT inhibitors; dNTP, deoxynucleotide triphosphate; ETV, entecavir; TAM, thymidine analogue associated mutations

5.9 Figures and tables

Figure 5.1. Chemical structures of selected NRTIs and ETV

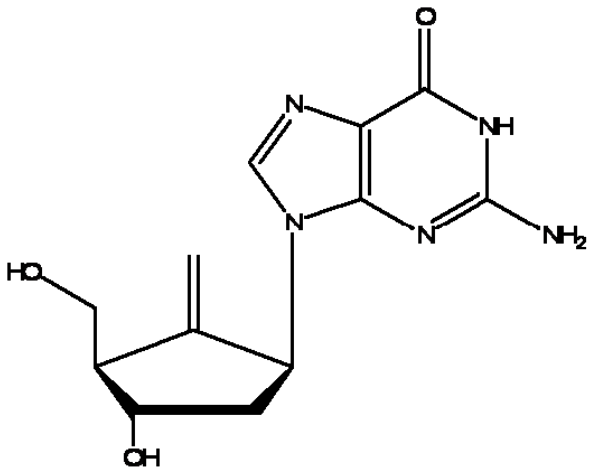

ETV

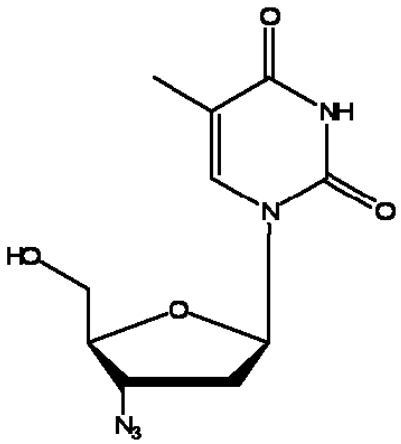

AZT

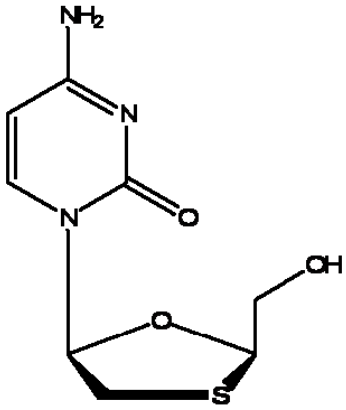

3TC

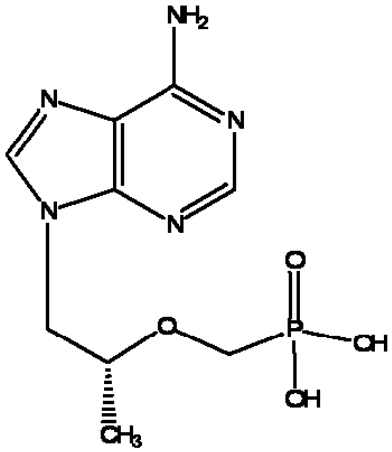

PMPA

Figure 5.2. Effects of incorporation of ETV-MP at position n on subsequent nucleotide incorporation events. (A) DNA/DNA primer/template substrates used in this assay. (B) Multiple nucleotide incorporation events in the presence of a constant concentrations of dNTPs and increasing concentrations of ETV-TP. We used primer/template T45/P1b that provides a single site of incorporation for the inhibitor. ETV-mediated pausing is observed at the site of incorporation and at position n+3. The asterisk shows inhibitor independent pausing. (C) DNA synthesis was here limited to position n+4 with primer/template T50A6/P1 in the presence of a constant concentration of ETV-TP, dCTP and dTTP and increasing concentrations of dGTP. Lane C represents a control experiment where ETV-TP was omitted while dCTP and dTTP were present at 0.5 μM in order to control for possible misincorporation events at position n. Arrows serve the same purpose as in panel B. (D) DNA synthesis as in panel C except that a constant concentration of ETV-TP and dTTP and increasing concentrations of dCTP were present in the reaction mixture. Lane c1 represents a control experiment where Mg^{2+} was omitted. Lane c2 represents a control experiment where ETV-TP was omitted in order to control for possible misincoporation events at position n. Lane c3 represents a control experiment where ETV-TP was substituted with 0.5 μM dGTP in the presence of 0.5 μM dTTP and dCTP. Arrows serve the same purpose as in panel B. The product fraction was calculated as the ratio of product at position n+4 over the sum of remaining substrate and intermediate products in the same lane.

A

T45 / P1b

5′ GAGTGGTATAGTGGAGTGAATA

3′ CTCACCATATCACCTCACTTATCTATAGTTAGGAAGTATGAGTTA

T50A6 / P1

5′ GAGTGGTATAGTGGAGTGAA

3′ CTCACCATATCACCTCACTTCAAAGTAGTTCGGAACTACCACTTATAACC

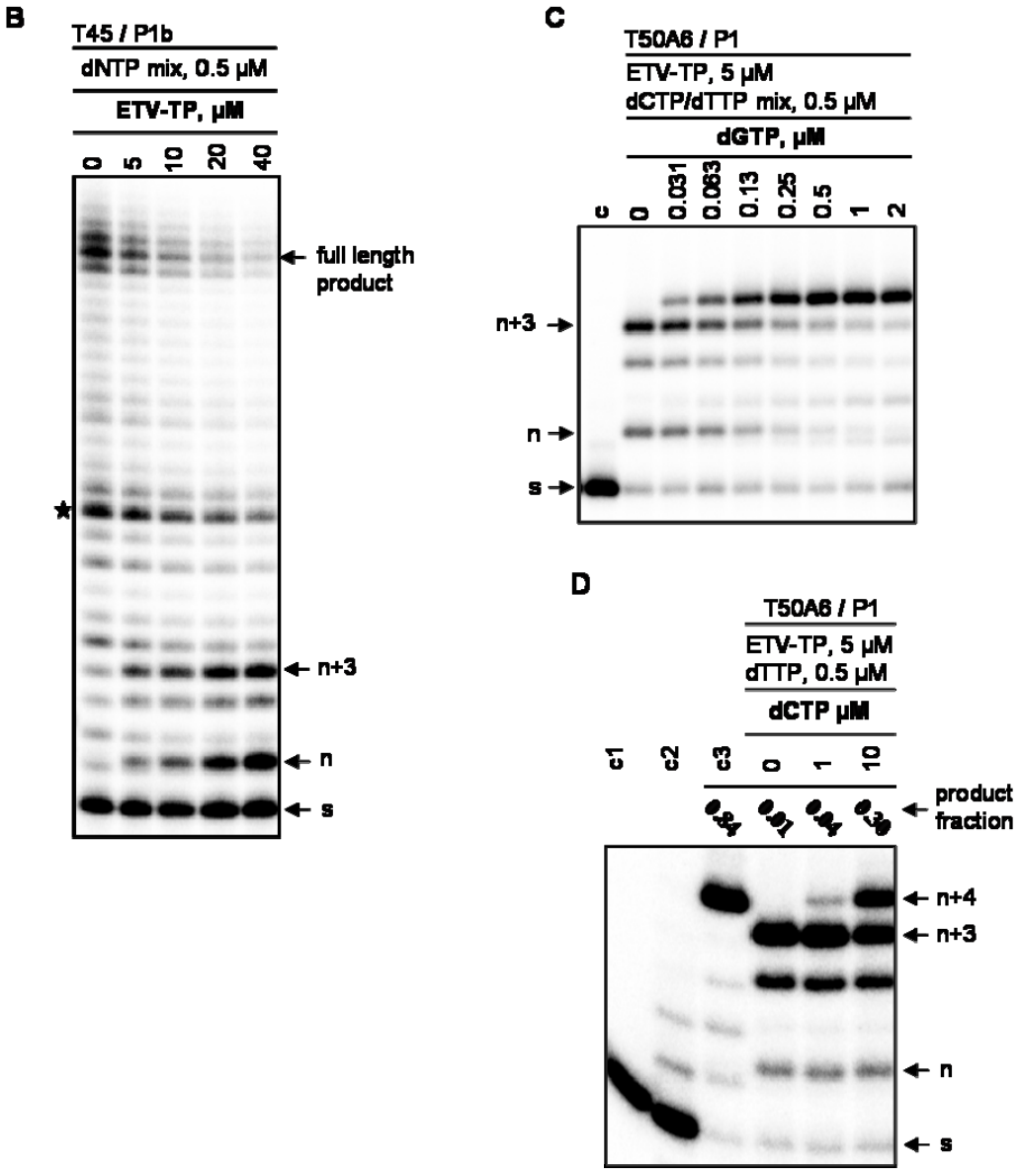

Figure 5.3. Effect of ETV-MP in the template strand. (A) DNA/DNA primer/template substrate used in the reaction. "E" illustrates ETV-MP incorporation. (B) DNA synthesis along a template containing either dGMP (left) or ETV-MP (right). Lane c1 represents a control experiment where $MgCl_2$ was omitted. Lane c2 represents a control experiment where dATP, dTTP and ddCTP were added in order to terminate DNA synthesis opposite ETV-MP. Lane c3 represents a control experiment where dATP and ddTTP were added as an additional marker. The star on the left shows pausing in the absence of inhibitor, while the asterisks illustrate ETV-mediated inhibition of DNA synthesis.

A

5`ATTGAGTATGAAGGATTGAT

3'TAACTCATACTTCCTAACTATAEATAAGTGAGGTGATATGGTGAG

B

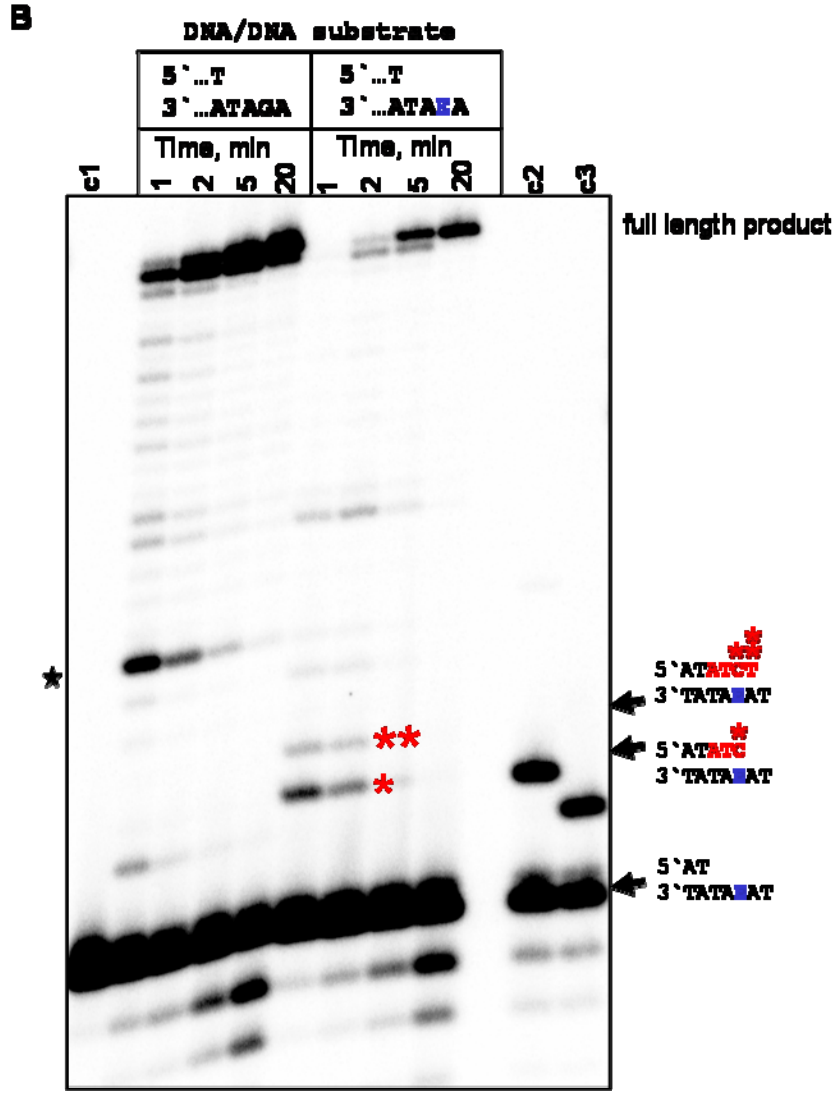

Figure 5.4. Site-specific footprinting of HIV1-RT/DNA substrate complexes containing ddGMP or ETV-MP at the 3`-end of the primer. (A) Reaction scheme. Complexes were treated with Fe^{2+} following incorporation of ETV-MP or ddGMP. The additional presence of PFA or dTTP provide conditions to trap the pre- or post-translocated complex, respectively. Fe^{2+}/RNaseH cleavage at positions -18 or -17 distinguish between the conformations. (B) Footprinting patterns with ddGMP or ETV-MP terminated primers. The –Fe lane represents a control experiment in the absence of Fe^{2+} . The +Fe lane represents treatment of the binary complexes with Fe^{2+} prior to nucleotide incorporation. +Fe/+PFA represents the footprint in the presence of 100 μM PFA that shows a bias toward pre-translocation. (C) Rate of dissociation of RNA/DNA template/primer. The rate constant k_{off} was determined with an RNA/DNA version of the template/primer shown in panel A. The primer were terminated with ETV-MP or ddGMP at position n and RNase H cleavage products were quantified at different time points following the addition of trap. (D) Inhibition of DNA synthesis with primer/templates containing dGMP (G), ddGMP (ddG) or ETV-MP (E) at the 3`-end of the primer.

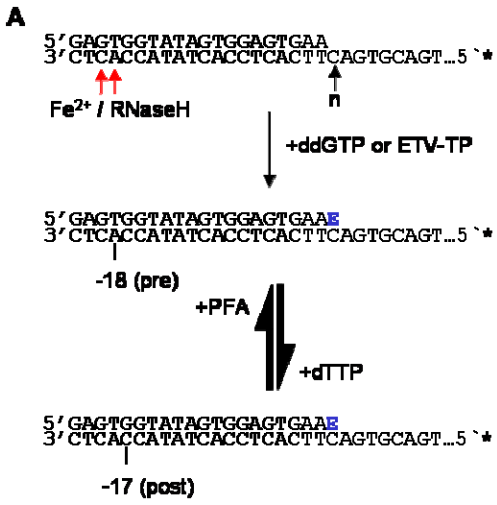
A
5′GAGTGGTATAGTGGAGTGAA
3′CTCACCATATCACCTCACTTCAGTGCAGT…5 `*
Fe2+ / RNaseH
n
+ddGTP or ETV-TP
5′GAGTGGTATAGTGGAGTGAAE
3′CTCACCATATCACCTCACTTCAGTGCAGT…5 `*
-18 (pre)
+PFA
+dTTP
5′GAGTGGTATAGTGGAGTGAAE
3′CTCACCATATCACCTCACTTCAGTGCAGT…5 `*
-17 (post)

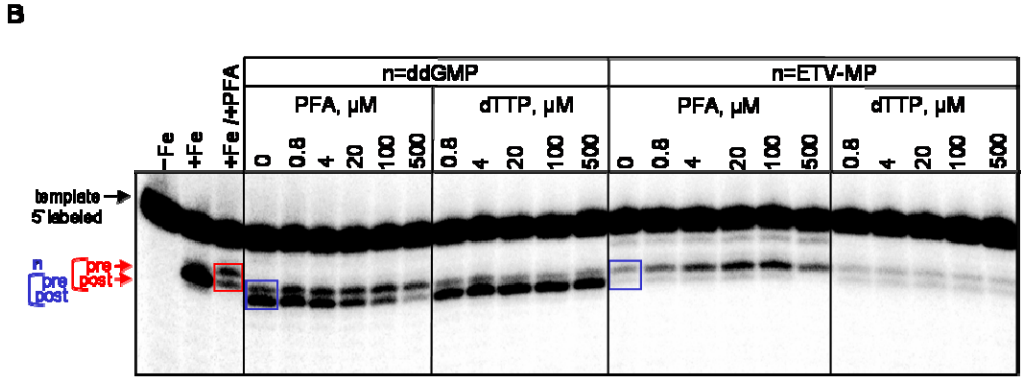
B
n=ddGMP
n=ETV-MP
PFA, μM
dTTP, μM
-Fe
+Fe
+Fe /+PFA
0
0.8
4
20
100
500
template
5'labeled
n
pre
post

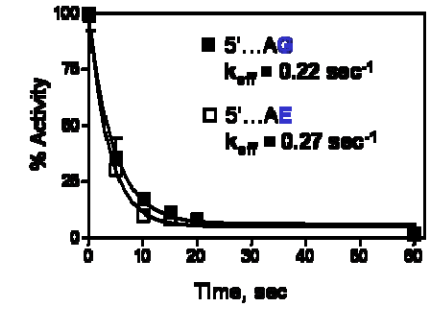
C
% Activity
5'…AG
keff = 0.22 sec-1
5'…AE
keff = 0.27 sec-1
Time, sec

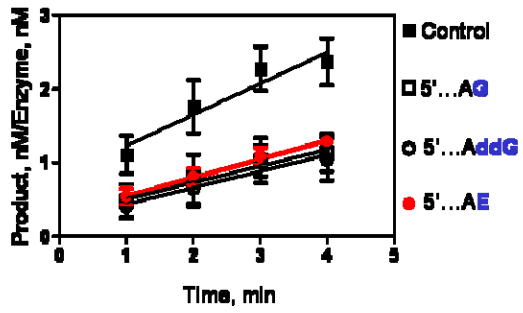
D
Product, nM/Enzyme, nM
Control
5'…AG
5'…AddG
5'…AE
Time, min

**Figure 5.5 RNase H activity on RNA/DNA template/primer substrates containing dGMP or ETV-MP 4 nucleotides upstream the 3`-end of the primer**. (A) RNase H activity monitored with 3`-end labeled RNA/DNA template/primer following incubation with heparin for variable time. Lane c1 represents a control experiment where heparin was omitted. Lane c2 represents a control experiment where $MgCl_2$ was omitted. Lane c3 represents a control experiment where trap was added prior to the addition of HIV1-RT in order to assess the efficiency of the trap. Arrows point to the specific polymerase-dependent RNase H cleavage products that are indicative for pre- and post-translocated conformations. Lane c4 represents a control experiment where RNA template was subjected to alkaline hydrolysis to produce a ladder. Asterisks show polymerase independent RNase H cleavage. (B) RNA/DNA substrate used in the reaction. Position -19 illustrates the distance in nucleotides between the polymerase and RNase H active sites of HIV1-RT with respect to 3`end of the primer. ETV-MP or dGMP is incorporated at position n. Arrows and asterisks assign the RNase H cuts to the sequence of the template. (C) Rate of the dissociation of the RNA/DNA template/primer was determined as described in Figure 4.

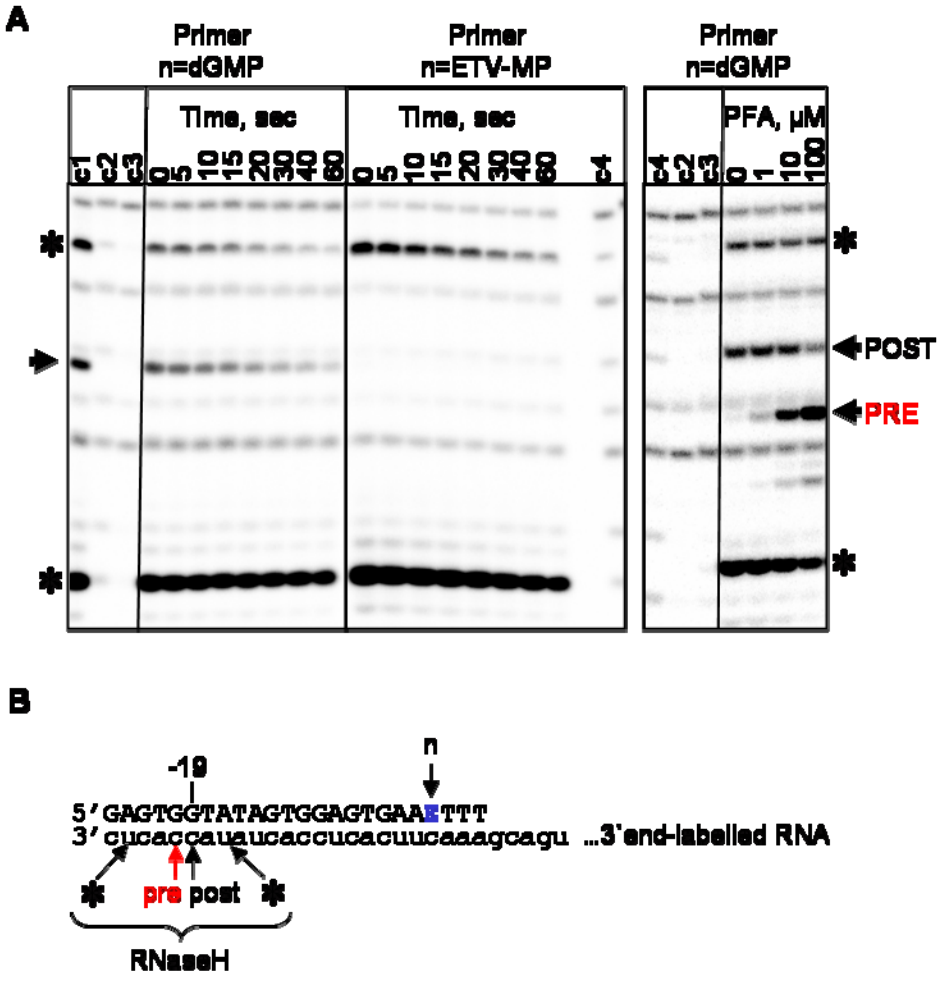
A
Primer
n=dGMP
Primer
n=ETV-MP
Primer
n=dGMP
Time, sec
Time, sec
PFA, μM
c1 c2 c3 0 5 10 15 20 30 40 60 0 5 10 15 20 30 40 60 c4
c4 c2 c3 0 1 10 100
POST
PRE
B
-19
n
5′ GAGTGGTATAGTGGAGTGAAETTT
3′ cucaccauaucaccucacuucaaagcagu ...3'end-labelled RNA
pre post
RNaseH
C
% Activity
100
75
50
25
0
5'...AGTTT
k_off = 0.027 sec-1
5'...AETTT
k_off = 0.021 sec-1
0 10 20 30 40 50 60
Time, sec

Figure 5.6 ATP-dependent excision on dGMP or ETV-MP containing primers. (A) Time course of ATP-dependent excision of dGMP (left) or ETV-MP (right) at the 3'-end of the primer (position n). The gel shows reactions with HIV-1 RT containing the TAMs cluster used in this study. Lane c represents a control experiment where $MgCl_2$ was omitted. The asterisk points to side reactions that reflect misincorporation events. (B) Graphic representation of data shown under A. (C) Time course experiments with primers containing dGMP and ETV-MP, respectively at position n and three additional nucleotides at position n+1 to n+3. (D) Graphic representation of data shown under C.

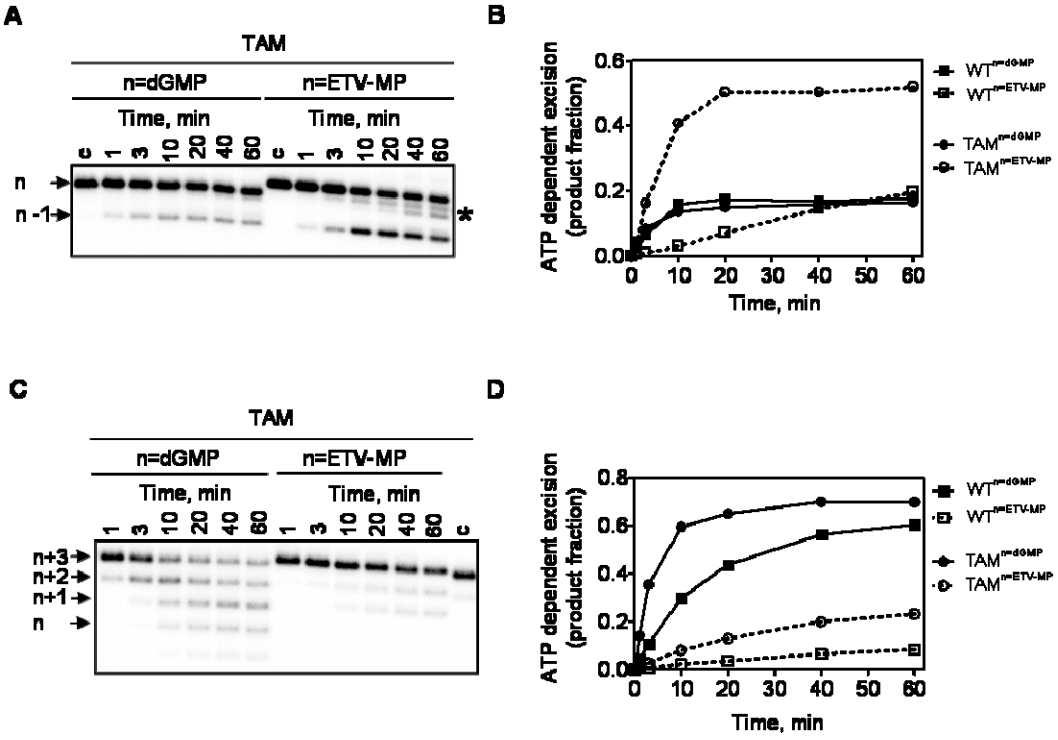
A
TAM
n=dGMP
n=ETV-MP
Time, min
Time, min
c 1 3 10 20 40 60 c 1 3 10 20 40 60
n
n -1
*
B
ATP dependent excision (product fraction)
0.0 0.2 0.4 0.6
0 10 20 30 40 50 60
Time, min
WT n=dGMP
WT n=ETV-MP
TAM n=dGMP
TAM n=ETV-MP
C
TAM
n=dGMP
n=ETV-MP
Time, min
Time, min
1 3 10 20 40 60 1 3 10 20 40 60 c
n+3
n+2
n+1
n
D
ATP dependent excision (product fraction)
0.0 0.2 0.4 0.6 0.8
0 10 20 30 40 50 60
Time, min
WT n=dGMP
WT n=ETV-MP
TAM n=dGMP
TAM n=ETV-MP

Figure 5.7 Model of ETV-mediated delayed chain-termination. Green cylinders show the template strand, while blue cylinders show the primer strand DNA. Red cylinder represents the incorporated ETV-MP. The larger blue-lined cylinder points to the nucleotide binding site of HIV-1 RT and the arrow represents the RNaseH active site schematically. The RNase H mapping studies of Figure 5 suggest that the RT enzyme can bind its nucleic acid substrate at various positions. Nucleotide binding can only occur when the complex exists in its post-translocated configuration, while the pyrophosphate analogue PFA stabilizes the pre-translocated complex. The data show that these polymerase-dependent conformations are in equilibrium with various polymerase-independent conformations. A primer containing ETV-MP at position n followed by three natural nucleotides affects this equilibrium and favors polymerase or excision independent binding, which is indicated by the larger sized arrows.

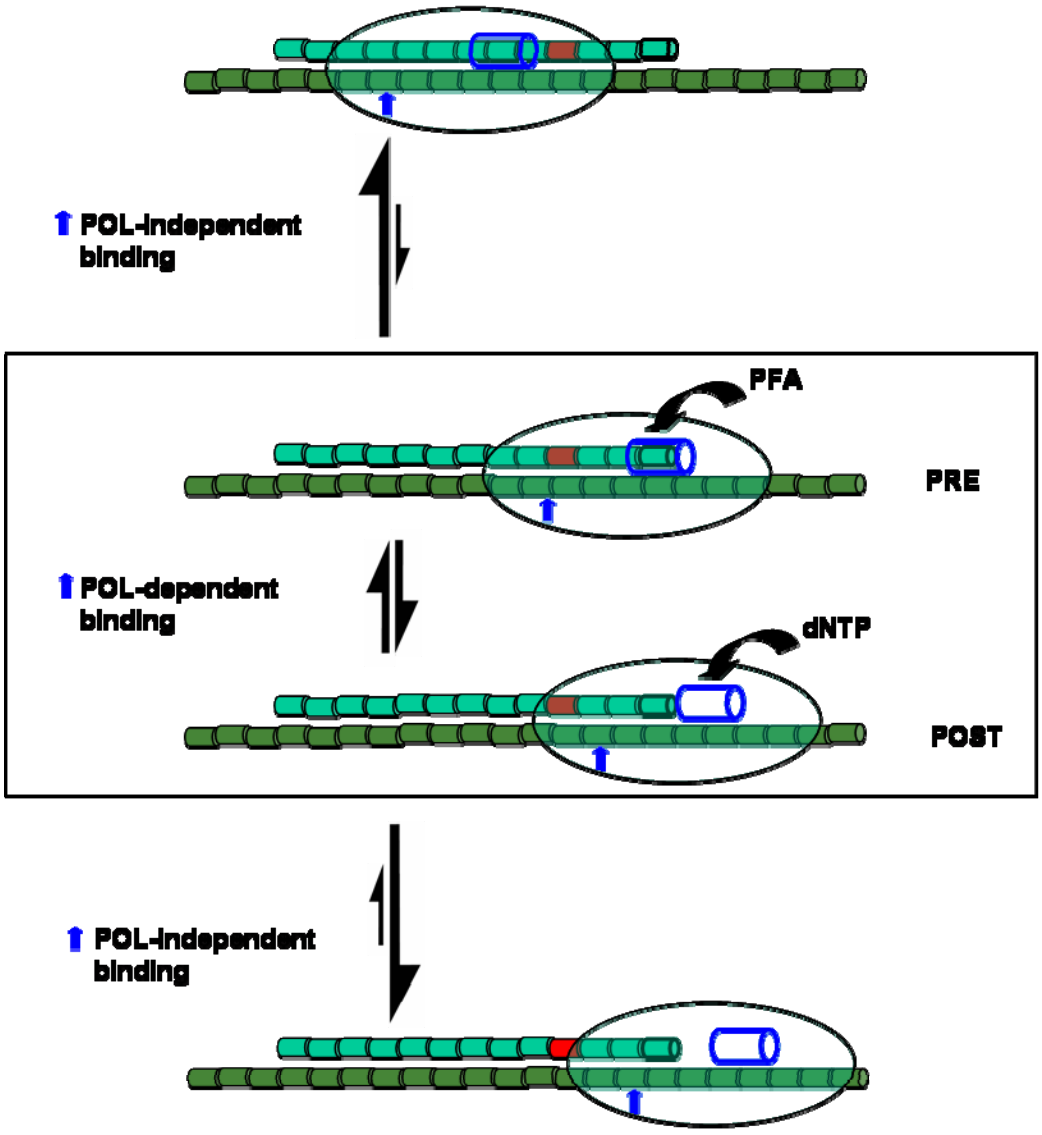
POL-independent binding
PFA
PRE
POL-dependent binding
dNTP
POST
POL-independent binding

Figure 5.S1. Competition between ETV-TP and dGTP. (A) Inhibition of incorporation of dGMP in the presence of increasing concentrations of ETV-TP. Single nucleotide incorporation events were assayed in the presence of constant concentration of dGTP and increasing concentrations of ETV-TP. The arrows point to the migration patterns of primers extended with dGMP and ETV-MP, respectively. "s" indicates the substrate, i.e. the un-extended primer. Lane C represents the control experiment in the absence of MgCl2. (B) Inhibitory concentrations of ETV-TP that reduce incorporation of dGMP by 50% (IC50).

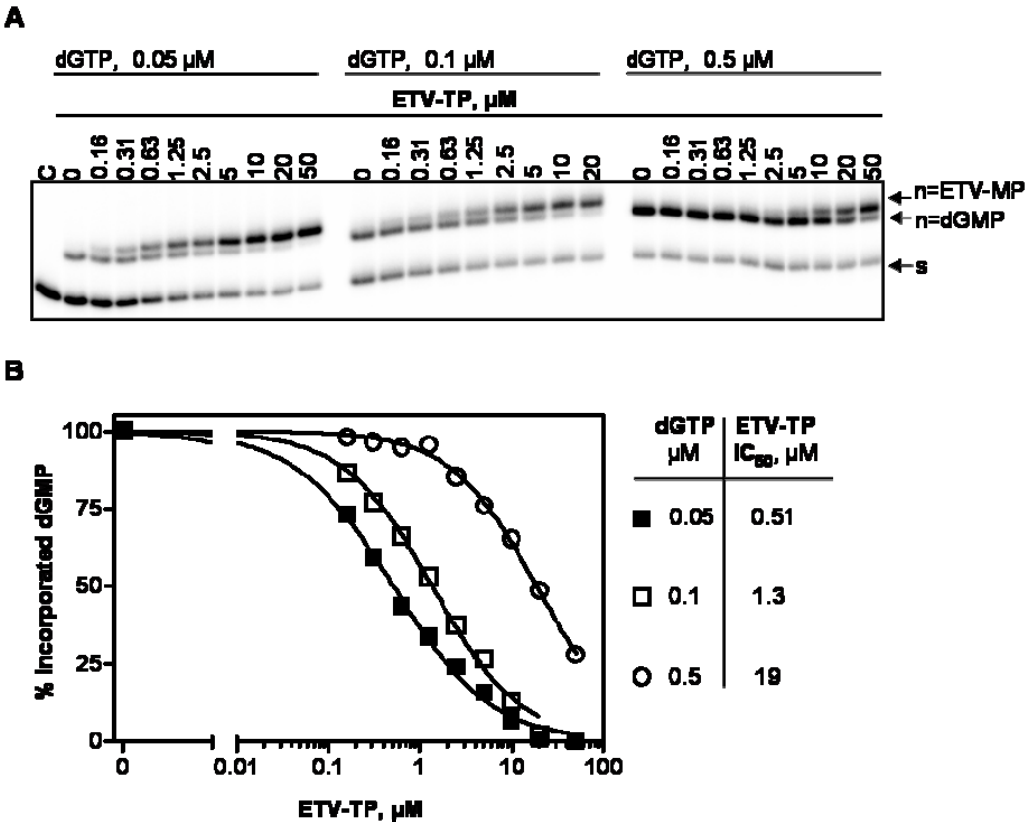
A
dGTP, 0.05 µM
dGTP, 0.1 µM
dGTP, 0.5 µM
ETV-TP, µM
C
0
0.16
0.31
0.63
1.25
2.5
5
10
20
50
n=ETV-MP
n=dGMP
s
B
% Incorporated dGMP
100
75
50
25
0
0
0.01
0.1
1
10
100
ETV-TP, µM
dGTP µM
ETV-TP IC50, µM
0.05
0.51
0.1
1.3
0.5
19

Table 5.1. Summary of the single nucleotide incorporation kinetic constants for HIV-RT at position n

Substrate						
dGTP			**ETV-TP**			
k_{cat}	**K_m**	**k_{cat}/K_m**	**k_{cat}**	**K_m**	**k_{cat}/K_m**	**Selectivity**
0.51 ±0.068	0.041 ±0.0075	13	0.34 ±0.11	0.45 ±0.075	0.74	18

K_m is in μM dGTP or ETV-TP. k_{cat} is in min^{-1}. Selectivity is defined as a ratio of k_{cat}/K_m for dGTP over k_{cat}/K_m for ETV-TP. Standard deviation was determined on the basis of at least three independent experiments.

Table 5.2. Summary of the single nucleotide incorporation kinetic constants for HIV-RT at position n+1 and n+4

		Primer						
		n=dGMP			n=ETV-MP			
Site	**Nucleotide**	**k_{cat}**	**K_m**	**k_{cat}/K_m**	**k_{cat}**	**K_m**	**k_{cat}/K_m**	**Fold change**
n+1	dTTP	0.38 ±0.07	0.057 ±0.007	6.7	0.36 ±0.06	0.38 ±0.04	0.95	7
n+4	dCTP	0.30 ±0.01	0.10 ±0.02	3.0	0.076 ±0.01	33 ±8.3	0.002	1300

K_m is in μM dTTP or dCTP. k_{cat} is in min^{-1}. Fold change reflects fold differences between k_{cat}/K_m with n=dGMP and k_{cat}/K_m with n=ETV-MP. Standard deviation was determined on the basis of at least three independent experiments.

Table 5.3. Summary of the single nucleotide incorporation kinetic constants for HIV-RT wild type and mutants at position n

	Substrate							
	dGTP			ETV-TP				
Enzyme	**k_{cat}**	**K_m**	**k_{cat}/K_m**	**k_{cat}**	**K_m**	**k_{cat}/K_m**	**SEL**	**RES**
WT	0.51 ±0.068	0.041 ±0.0075	13	0.34 ±0.11	0.45 ±0.075	0.74	18	1
TAM	0.23 ±0.0095	0.022 ±0.0039	11	0.15 ±0.0068	0.23 ±0.042	0.65	17	1
M184V	0.33 ±0.012	0.047 ±0.0072	7.0	0.095 ±0.020	4.7 ±1.6	0.020	3500	19

K_m is in μM dGTP or ETV-TP. k_{cat} is in min^{-1}. SEL stands for selectivity and defined as a ratio of k_{cat}/K_m for dGTP over k_{cat}/K_m for ETV-TP. RES stands for resistance and defined as a ratio of selectivity of WT over the selectivity of a mutant.
Standard deviation was determined on the basis of at least three independent experiments.

CHAPTER 6

CONCLUSIONS

The research project described in this thesis provides novel findings that contribute to our overall understanding of the molecular mechanisms of drug action and drug resistance in the context of viral polymerases. The study focused on the drugs foscarnet, entecavir and acyclovir because of their dual or multiple antiviral activities. Foscarnet is a broad spectrum antiviral agent effective against DNA and RNA viruses, including HSV-1, HSV-2, HCMV and HIV-1 [32, 33]. Acyclovir is a classic anti-herpes drug that draws its specificity from the action of virally encoded thymidine kinase [10-14]. Recent reports have shown that acyclovir can be activated into an anti-HIV agent *in vitro* in cells co-infected with HHV-6 and HIV-1 [47, 48]. Entecavir is a potent drug for treating HBV infections and was recently shown to exhibit anti-HIV-1 activity [56-58, 60].

6.1 Antiviral effects of foscarnet

The example of foscarnet illustrates the potential benefits of drugs with multiple antiviral activities in the context of drug resistance. Despite toxic side effects, foscarnet is sometimes used as a second-line agent for the salvage therapy of acyclovir-resistant HSV infections, ganciclovir-resistant HCMV infections and nucleoside analogue-resistant HIV infections [25, 26, 397]. Importantly, foscarnet resistance resensitizes HIV to nucleoside analogues [30, 31].

The recent study by Marchand et al., 2007, to which I contributed the biochemical data on the kinetics of nucleotide incorporation by pre- and post-translocational HIV-1 RT/DNA substrate binary complexes, put forward a precise molecular mechanism of foscarnet action and resistance. According to this model, foscarnet traps the binary complex in its pre-translocational conformation, which is incompetent for incorporating the next nucleotide. This model provides the basis for a conceptually new strategy in designing antiviral drugs that would target a specific conformational state of a viral protein in complex with its substrate.

The understanding of foscarnet-HCMV polymerase interactions requires knowledge of the foscarnet binding site within the HCMV polymerase. The first step in this direction implies the identification of the amino acid residues that are directly involved in foscarnet binding. To this end, this study supplemented a structure-based alignment of the Rb69 and HCMV DNA polymerases with Michaelis-Menten enzyme kinetics analysis. It characterized DNA synthesis catalyzed by both wild-type and mutant HCMV polymerases in either the presence or absence of foscarnet.

The HCMV polymerase belongs to the family B or α-like polymerases based on the sequence conservation within highly conserved regions [100]. The RB69 DNA polymerase is also a member of this family. Several crystal structures of the RB69 DNA polymerase have supported extensive biochemical and enzyme kinetics data in the apo, editing and polymerase modes to allow the description of polymerase and 3`-5` exonuclease active sites [101-103, 411, 444]. Here I conducted a structure-based alignment between the RB69 and HCMV polymerases in an attempt to transpose the location of the RB69 polymerase residues involved in dNTP binding onto the sequence of the HCMV polymerase. On the basis of this alignment, I identified a region within the HCMV polymerase that corresponds to helix P of the RB69 polymerase. Helix P is located within the conserved region III of the polymerase domain of the HCMV polymerase; it also contains a cluster of highly conserved amino acid residues [132, 445]. In the context of the γ-phosphate of the incoming nucleotide, the highly conserved residues K811 and Q807 are of particular interest.

Previous biochemical and crystallographic data for gp43 have suggested that K560 is directly involved in nucleotide binding, while Q556 is located in the vicinity of the incoming nucleotide [103, 411, 444]. The corresponding amino acid residues within the HCMV polymerase are Q807 and K811, which are located within a cluster of amino acid residues involved in generating an altered response to foscarnet [132, 445]. The close proximity of two amino acid

substitutions, L802M and K805Q, which generate resistance and hypersusceptibility to foscarnet, respectively, as well as their location with respect to the highly conserved residues Q807 and K811, suggested possible involvement of the HCMV polymerase helix P residues in direct interaction with foscarnet.

I generated an expression construct for the HCMV polymerase synthesis using an *in vitro* coupled transcription-translation system [185, 442]. I also reconstituted the L802M, K805Q, Q807A and K811A mutations within the HCMV polymerase. The Michaelis-Menten enzyme kinetics analysis of the effect of these substitutions on the polymerase activity of the HCMV polymerase identified K811 as a catalytically critical residue for nucleotide incorporation. In contrast, the effect on polymerase function by the Q807A substitution was only marginal. These findings correlated with the enzymatic and crystallographic data on the corresponding RB69 polymerase residues Q556 and K560 [103, 411, 444], thereby validating my structure-based alignment between the RB69 and HCMV polymerases.

I also analyzed the patterns of foscarnet inhibition of DNA synthesis catalyzed by both wild-type and mutant enzymes. My biochemical data on the foscarnet profile of the L802M and K805Q substitutions correlated with previously reported clinical and *in vitro* observations [132]. The novelty of this study is that the Q807A substitution generated a 6-fold resistance to foscarnet, suggesting a possible direct implication of this residue in foscarnet binding. My data also confirmed the previously reported non-competitive character of the foscarnet inhibition of DNA synthesis with respect to the nucleotide substrate [32, 33].

Foscarnet is a pyrophosphate analogue. The crystallographic data on the T7 RNA polymerase/pyrophosphate complex suggest that foscarnet may occupy the positions of the β- and γ-phosphates of the incoming nucleotide [414]. In support of this notion, it has been reported that foscarnet competitively inhibits the pyrophosphorolysis reaction—the reverse reaction of nucleotide incorporation

[34]. This evidence indicates that the pyrophosphate and foscarnet may share the same binding site, thus contradicting their simultaneous binding to the polymerase.

According to my model for the foscarnet/HCMV polymerase interaction, the presumptive binding site for foscarnet is located in close proximity to the γ-phosphate of the incoming nucleotide, while Q807 provides important contacts. Foscarnet binding does not prevent the binding of the incoming nucleotide. Instead, it may alter its catalytic orientation, resulting in a non-competitive mode of inhibiting DNA synthesis. This notion is supported by the observation that the extent of resistance to foscarnet does not correlate with that to pyrophosphate, which would be expected if the binding sites were mutually exclusive. My model assigns an indirect role for L802M and K805Q in modulating the foscarnet resistance phenotype of the HCMV polymerase. I propose that the L802M substitution may affect the precise positioning of Q807, which in turn would negatively affect the binding of foscarnet. Such an effect would explain the resistant phenotype of L802M. On the other hand, the hypersusceptible phenotype of the K805Q substitution may be explained by the net loss of the positive charge at this position. Consequently, the orientation of the overall negatively charged foscarnet will be altered in the context of its interaction with Q807.

Taken as a whole, this study of foscarnet/HCMV DNA polymerase interactions is the first I know of to provide experimental evidence for the correlation between helices P of RB69 and the HCMV DNA polymerases in their structural and enzymatic characteristics with respect to the nucleotide binding site. This is also the first study to propose a structurally relevant model for the foscarnet binding site within the HCMV polymerase based on the mutational and enzymatic analysis of highly conserved residues, as well as residues involved in the altered foscarnet phenotype.

To date, the main difficulty in biochemical and crystallographic studies of the HCMV DNA polymerase has been the lack of a robust expression system [439]. Therefore, I attempted to circumvent this limitation by generating a chimeric RB69-HCMV enzyme (gp43-UL54). The following four considerations provided the rational for such a chimera: (i) my previous study of HCMV DNA polymerase, which identified critical residues involved in nucleotide and foscarnet binding [442], (ii) my experimental observation that the RB69 DNA polymerase was essentially insensitive to foscarnet and acyclovir, (iii) previously reported HCMV-polymerase secondary-structure modeling efforts based on the crystal structure of the RB69 DNA polymerase [147], and (iv) a robust expression system for the RB69 DNA polymerase, which has provided sufficient amounts of enzyme for a number of biochemical and crystallographic studies [101-103, 444]. I hypothesized that transferring the HCMV DNA polymerase critical residues of helix N and helix P, which are located close to the triphosphate moiety of a bound nucleotide on the background of the RB69 DNA polymerase, would impart the HCMV foscarnet/acyclovir phenotype on the chimera. Furthermore, such a chimera should preserve the ease of protein expression and purification associated with the RB69 DNA polymerase.

The experimental results show that the chimeric gp43-UL54 enzyme gained sensitivity to both foscarnet and acyclovir as compared with the RB69 DNA polymerase background, which was resistant to both drugs. The foscarnet/acyclovir sensitivity profile of the chimera paralleled the HCMV DNA polymerase phenotype. Most importantly, reconstituting the amino acid substitutions that have been previously reported to generate resistance to foscarnet in the context of the HCMV DNA polymerase produced the same effect on the chimera. The protein expression and purification of the chimeric proteins mimicked the RB69 DNA polymerase.

As a whole, this is the first proof-of-principle study of which I am aware to show that changing a limited number of critical residues within the RB69 DNA

polymerase to generate a chimeric gp43-UL54 enzyme can reproduce the foscarnet/acyclovir phenotype of the wild-type HCMV polymerase. Since these amino acid substitutions involve non-conserved residues, these findings stress the limitations of using the RB69 DNA polymerase crystal structures as a template to model the structural components of the HCMV DNA polymerase in the context of drug action and drug resistance [147]. Therefore, the chimeric enzymes present an opportunity to avoid this problem. The findings of this study argue that chimeric enzymes have potential as a tool for studying the biochemical and structural aspects of drug action and drug resistance in the context of viral enzymes that have not yet been purified.

6.2 Antiviral effects of acyclovir

The example of acyclovir in the herpes/HIV-1 context stresses the important implications of co-infection with heterogeneous viruses: on one hand, HSV-2/HIV-1 co-infections have been shown to be synergetic in terms of disease progression, outcome and incidence [44, 391]; on the other hand, the ubiquitous character of the HHV-6 and herpes viruses in general can be exploited by an antiviral regimen in combating both viruses at the same time [71, 129]. Recent clinical reports have documented the benefit of anti-herpes treatment on the progression of HIV infection [46, 394, 469]. In addition, it has been suggested that the anti-HIV co-lateral effect of the anti-herpes treatment may reduce the probability of HIV superinfection in HSV-2 infected individuals [45, 46]. But the exact clinical significance of such an effect remains controversial [470, 471].

Two major experimental findings have recently provided important insights into the molecular mechanism of the anti-HIV activity of acyclovir in the context of herpes/HIV-1 co-infection [47, 48]. It has been shown that acyclovir is activated into an inhibitor of HIV-1 replication at the level of HIV-1 RT through a specific α-phosphorylation catalyzed by the HHV-6 thymidine kinase present in HHV-6/HIV-1 co-infected cells. A V75I substitution within HIV-1 RT has also been

identified as being selected under acyclovir pressure and conferring a high level of resistance to the drug. But the precise molecular mechanism of acyclovir resistance generated by the V75I substitution remains to be elucidated.

Two major mechanisms of resistance to the NRTIs exploited by HIV-1 RT have been described [345, 461-464]. The first mechanism involves substrate discrimination by the mutant enzyme such that the overall catalytic efficiency of incorporating the nucleotide analogue is compromised, as compared with the natural counterpart. The second mechanism is based on an increased rate of ATP-dependent excision of the incorporated nucleotide analogue catalyzed by the mutant enzyme as compared with the wild type. I hypothesized that the V75I substitution may be subject to both mechanisms.

To address the molecular mechanism of the increased substrate discrimination, I used the pre-steady state approach to catalyzing nucleotide incorporation by HIV-1 RT. This approach allowed separating the consequences of the V75I substitution into effects on the binding versus effects on the catalysis of nucleotide incorporation. My data showed that the V75I substitution affected specifically the catalytic step of ACV-TP incorporation. On the basis of the available crystallographic data on HIV-1 RT in complex with the DNA and nucleotide substrates, as well as the resistance profile of major mutations involved in the resistance mechanism to substrate discrimination, I proposed that V75I exerts its effect indirectly through repositioning the neighboring residues (K65, Q151 and R72) with respect to the tri-phosphate moiety of the inhibitor.

To address the molecular mechanism of the increased rate of the ATP-dependent excision, I used (i) ATP-dependent hydrolysis of 3`-end terminating nucleotides, (ii) site-specific chemical footprinting of the HIV-1 RT/DNA binary and HIV-1 RT/DNA/nucleotide ternary complexes, and (iii) the steady-state approach to the enzymatic aspects of immediate chain termination in the context of dead-end complex formation. These techniques allowed me to investigate the interactions

between HIV-1 RT and acyclovir based on the effects of incorporating ACV-MP into DNA on the rate of the ATP-dependent hydrolysis, as well as on the conformational status of the HIV-1 RT in complex with the ACV-MP-containing DNA substrate. My data showed that the incorporated ACV-MP did not benefit in protection from excision either through affecting the translocational status of HIV-1 RT or through increased dead-end complex formation. In fact, the incorporated ACV-MP was subject to an increased rate of ATP-dependent excision exhibited by V75I-containing HIV-1 RT, though the increase was only intermediate as compared with the classical set of mutations (EEMs, or TAMs) involved in the excision mechanism.

Taken together, my data on acyclovir/HIV-1 RT interaction show that acyclovir resistance involves both major mechanisms of NRTI-associated resistance. But the discrimination against acyclovir at the level of incorporation exhibited by the V75I-containing HIV-1 RT appears to be the dominant mechanism. My experimental findings constitute a significant contribution in that they provide the molecular mechanism for the previously observed anti-HIV activity of acyclovir in the context of herpes/HIV-1 infection. This is the first study I know of that addresses the molecular mechanism of acyclovir resistance in the context of HIV-1.

6.3 Antiviral effects of entecavir

The example of entecavir stresses the potential complexities of applying treatment regimens with dual antiviral activity. Recent experimental and clinical evidence clearly shows that entecavir treatment in HBV/HIV co-infected patients that do not require an anti-HIV treatment does generate an anti-HIV treatment resistance prior to its initiation in those patients [60, 522]. In line with this evidence, recent biochemical investigation of the entecavir/HIV-1 RT interaction has shown that ETV-TP is used by HIV-1 RT as a substrate for DNA synthesis [61]. Incorporating ETV-MP into a growing primer was shown to inhibit DNA

synthesis immediately, as well as several nucleotides after the ETV-MP incorporation site. The clinically observed M184V substitution within HIV-1 RT under ETV-TP pressure generated resistance to entecavir through a discrimination mechanism [60, 61]. On the basis of this clinical and experimental evidence, it was subsequently recommended that ETV should not be administered in HBV/HIV co-infected individuals unless these persons are simultaneously on highly active antiretroviral therapy [60, 508]. But several intriguing questions remain unanswered. First, the relative contribution of immediate versus delayed inhibition of DNA synthesis needs to be quantified. Second, HIV-1 RT mutant viruses carrying thymidine analogue resistance-conferring mutations (TAMs), or also known as excision enhancing mutations (EEMs) were reported to be fully susceptible to entecavir [61]. In this context it should be noted that EEMs constitute the basis for the excision pathway that generates resistance to literally all approved NRTIs [462].

I used a combination of four independent biochemical techniques to study the ETV-TP/HIV-1 RT: (i) a steady-state approach to the enzymatic aspects of the DNA synthesis by HIV-1 RT, (ii) site-specific chemical footprinting of HIV-1 RT/DNA binary and HIV-1 RT/DNA/nucleotide (or foscarnet) ternary complexes, (iii) HIV-1 RT RNase H hydrolytic footprinting of binary and ternary complexes, and (iv) ATP-dependent hydrolysis of 3`-end terminating nucleotides. These techniques allowed me to investigate ETV-TP/HIV-1 RT interactions, based on the effects of incorporating ETV-MP into DNA, on the catalysis of the subsequent incorporation events, as well as on the conformational status of the HIV-1 RT binary and ternary complexes.

On the basis of my experimental data, I identified three distinct mechanisms of inhibition of HIV-1 RT with ETV: (i) inhibition of nucleotide incorporation at position n+1 immediately following the incorporated ETV-MP at position n, (ii) inhibition of nucleotide incorporation at position n+4, and (iii) inhibition of nucleotide incorporation opposite the templated ETV-MP. My data provide a

quantitative basis on which to argue that delayed chain termination at position *n*+3 (i.e., three nucleotides following incorporation of ETV-MP) is the major mechanism for inhibiting DNA synthesis by entecavir.

My mutational analysis revealed that the incorporated ETV-MP was fully susceptible to ATP-dependent excision by EEMs-containing HIV-1 RT. Interestingly, once the incorporated ETV-MP was further extended by 3 nucleotides, it became inaccessible to the ATP-dependent excision. My conformational studies provided a possible explanation for this phenomenon by suggesting that the incorporated ETV-MP at position *n* inhibited formation of the post- and pretranslocational complexes required respectively for both ATP-dependent excision and dNTP-dependent nucleotide incorporation at position *n*+3. Thus, eventual excision at *n*+3 and *n*+2 would generate a 3`-end primer at positions *n*+2 and *n*+1, respectively. But at these positions the nucleotide incorporation is much more efficient than the subsequent excision events that are required to remove ETV-MP at position *n*. On the basis of my overall data, I proposed a model for an entecavir-mediated delayed chain termination, according to which the delayed chain termination shields ETV-MP from ATP-dependent excision, thereby explaining why the excision of ETV-MP does not play a significant role in biological settings.

Taken as a whole, my study of ETV-MP/HIV-1 RT interactions is the first I know of to provide a quantitative measure for the delayed chain termination in the context of HIV-1 RT. My experimental findings constitute a significant contribution to previous attempts to dissect the exact molecular mechanism of the entecavir-dependent inhibition of DNA synthesis by HIV-1 RT. My data provide additional support for the discrimination mechanism of resistance to entecavir displayed by M184V-containing HIV-1 RT. Most importantly, this is the first proof-of-principle study of a clinically approved (anti-HBV) drug to show that the delayed chain terminators are protected from ATP-dependent excision. My findings thus provide experimental evidence for the potential clinical benefits of

the concept of delayed chain termination as an important characteristic in the development of novel drugs with either dual or multiple antiviral activities.

6.4 Perspectives

The study of the mechanisms of the action of drugs with dual or multiple antiviral activities presented in this thesis defines new concepts and provides novel tools for discovering and developing future antiviral drugs.

Drug-related structural and biochemical studies of a number of viral enzymes, including the HBV, HSV and HCMV polymerases, have been hampered by the poor expression and purification characteristics of these proteins. In this regard, chimeric enzymes represent an attractive solution to the expression/purification difficulties while retaining the drug-related phenotype of the target protein. The gp43/UL54 chimeric enzyme retained the excellent expression/purification qualities of the RB69 DNA polymerase, but clearly showed the HCMV phenotype with respect to acyclovir and foscarnet. Therefore, this chimeric enzyme may be used in the future for high throughput screening of novel anti-HCMV compounds. In addition, chimeric enzymes in general may in the future prove to be a valuable tool in studying the detailed structural and biochemical mechanisms of drug action and drug resistance in the context of viral proteins that are difficult to purify.

The clinical use of all current antiviral drugs faces two major complexities: drug toxicity and drug resistance. Therefore, conceptually new strategies are required to tackle these problems.

The recent study by Lisco et al., 2008 [47], to which I contributed the biochemical data on the anti-HIV-1 RT effect of acyclovir, illustrated a new concept in the context of intracellular prodrug activation. The anti-herpes drug acyclovir was shown to be specifically activated into an anti-HIV agent in HHV-6/HIV-1 co-

infected cells. The significance of this observation is that it puts forward a conceptual possibility of transferring the low toxicity characteristic of one drug, such as acyclovir, into the context of a totally new viral target, such as HIV-1 RT. The subsequent report by MacMahon et al., 2008 [48], reported the selection of the V75I mutation within the HIV-1 RT under the pressure of acyclovir. My own study of the biochemical mechanisms of the V75I-associated resistance to acyclovir further showed that this mutation can be selected in the presence of the monophosphorylated acyclovir analogue CF2648. The significance of this observation is that it provides the rationale for the concept of designing phosphorylated prodrugs. Such prodrugs would provide a bypass to the rate-limiting step (monophosphorylation) in producing the active antiviral agent.

In the context of nucleoside analogues, which are incorporated into the viral genome, two major mechanisms explain the viral resistance to a given drug: drug discrimination and drug excision. My study of the antiviral effect of entecavir in the context of the HIV-1 RT showed that the delayed chain termination, which is caused by the incorporated ETV-MP, protects the incorporated drug from excision. This observation argues for delayed chain termination as a new concept in drug design. The remaining challenge in this direction, however, is to prevent the selection of the M184V mutation that discriminates against entecavir, and that could therefore possibly do the same against future delayed chain terminators.

The three above-mentioned examples of drugs with multiple antiviral activities illustrate the potential complexities of the clinical usage of these agents in the context of viral co-infection. The treatment of herpesvirus/HIV co-infection with acyclovir appears to be beneficial [46, 394, 469]. But a similar approach to HBV/HIV co-infection using entecavir represents an important challenge because M184V, a classical nucleoside analogue resistance-conferring mutation, can be selected in HIV-1 prior to initiating anti-HIV therapy [60, 522]. This would compromise the eventual anti-HIV-1 therapy when initiated. Therefore, extracting potential benefits and avoiding problems associated with the clinical usage of

therapeutic agents with multiple antiviral activities depends on knowing the precise molecular mechanism of drug-target interactions.

REFERENCES

1. *FDA notifications. Maraviroc approved as a CCR5 co-receptor antagonist.* AIDS Alert, 2007. **22**(9): p. 103.
2. Dorr, P., et al., *Maraviroc (UK-427,857), a potent, orally bioavailable, and selective small-molecule inhibitor of chemokine receptor CCR5 with broad-spectrum anti-human immunodeficiency virus type 1 activity.* Antimicrob Agents Chemother, 2005. **49**(11): p. 4721-32.
3. Prusoff, W.H., *Synthesis and biological activities of iododeoxyuridine, an analog of thymidine.* Biochim Biophys Acta, 1959. **32**(1): p. 295-6.
4. Hughes, W.F., *Treatment of herpes simplex keratitis. A review.* Am J Ophthalmol, 1969. **67**(3): p. 313-28.
5. De Clercq, E., et al., *Antiviral Chemistry & Chemotherapy's current antiviral agents FactFile 2006 (1st edition).* Antivir Chem Chemother, 2006. **17**(3): p. 113-66.
6. Kaufman, H.E., *Clinical cure of herpes simplex keratitis by 5-iodo-2-deoxyuridine.* Proc Soc Exp Biol Med, 1962. **109**: p. 251-2.
7. Schabel, F.M., Jr., *The antiviral activity of 9-beta-D-arabinofuranosyladenine (ARA-A).* Chemotherapy, 1968. **13**(6): p. 321-38.
8. Schaeffer, H.J., et al., *Novel substrate of adenosine deaminase.* J Med Chem, 1971. **14**(4): p. 367-9.
9. Elion, G.B., *Nobel Lecture. The purine path to chemotherapy.* Biosci Rep, 1989. **9**(5): p. 509-29.
10. Derse, D., et al., *Inhibition of purified human and herpes simplex virus-induced DNA polymerases by 9-(2-hydroxyethoxymethyl)guanine triphosphate. Effects on primer-template function.* J Biol Chem, 1981. **256**(22): p. 11447-51.
11. Elion, G.B., et al., *Selectivity of action of an antiherpetic agent, 9-(2-hydroxyethoxymethyl) guanine.* Proc Natl Acad Sci U S A, 1977. **74**(12): p. 5716-20.
12. Furman, P.A., et al., *Inhibition by acyclovir of cell growth and DNA synthesis of cells biochemically transformed with herpesvirus genetic information.* Virology, 1980. **102**(2): p. 420-30.
13. Fyfe, J.A., et al., *Thymidine kinase from herpes simplex virus phosphorylates the new antiviral compound, 9-(2-hydroxyethoxymethyl)guanine.* J Biol Chem, 1978. **253**(24): p. 8721-7.
14. Schaeffer, H.J., et al., *9-(2-hydroxyethoxymethyl) guanine activity against viruses of the herpes group.* Nature, 1978. **272**(5654): p. 583-5.
15. Miller, W.H. and R.L. Miller, *Phosphorylation of acyclovir (acycloguanosine) monophosphate by GMP kinase.* J Biol Chem, 1980. **255**(15): p. 7204-7.
16. Miller, W.H. and R.L. Miller, *Phosphorylation of acyclovir diphosphate by cellular enzymes.* Biochem Pharmacol, 1982. **31**(23): p. 3879-84.
17. Keller, P.M., S.A. McKee, and J.A. Fyfe, *Cytoplasmic 5'-nucleotidase catalyzes acyclovir phosphorylation.* J Biol Chem, 1985. **260**(15): p. 8664-7.

18. Furman, P.A., et al., *Metabolism of acyclovir in virus-infected and uninfected cells.* Antimicrob Agents Chemother, 1981. **20**(4): p. 518-24.
19. Furman, P.A., et al., *Inhibition of herpes simplex virus-induced DNA polymerase activity and viral DNA replication by 9-(2-hydroxyethoxymethyl)guanine and its triphosphate.* J Virol, 1979. **32**(1): p. 72-7.
20. St Clair, M.H., et al., *Inhibition of cellular alpha and virally induced deoxyribonucleic acid polymerases by the triphosphate of acyclovir.* Antimicrob Agents Chemother, 1980. **18**(5): p. 741-5.
21. Furman, P.A., M.H. St Clair, and T. Spector, *Acyclovir triphosphate is a suicide inactivator of the herpes simplex virus DNA polymerase.* J Biol Chem, 1984. **259**(15): p. 9575-9.
22. Gilbert, C., J. Bestman-Smith, and G. Boivin, *Resistance of herpesviruses to antiviral drugs: clinical impacts and molecular mechanisms.* Drug Resist Updat, 2002. **5**(2): p. 88-114.
23. Oberg, B., *Antiviral effects of phosphonoformate (PFA, foscarnet sodium).* Pharmacol Ther, 1989. **40**(2): p. 213-85.
24. Wagstaff, A.J. and H.M. Bryson, *Foscarnet. A reappraisal of its antiviral activity, pharmacokinetic properties and therapeutic use in immunocompromised patients with viral infections.* Drugs, 1994. **48**(2): p. 199-226.
25. Canestri, A., et al., *Foscarnet salvage therapy for patients with late-stage HIV disease and multiple drug resistance.* Antivir Ther, 2006. **11**(5): p. 561-6.
26. Mathiesen, S., et al., *Foscarnet used in salvage therapy of HIV-1 patients harbouring multiple nucleotide excision mutations.* AIDS, 2004. **18**(7): p. 1076-8.
27. Mellors, J.W., et al., *Novel mutations in reverse transcriptase of human immunodeficiency virus type 1 reduce susceptibility to foscarnet in laboratory and clinical isolates.* Antimicrob Agents Chemother, 1995. **39**(5): p. 1087-92.
28. Meyer, P.R., et al., *Effects of dipeptide insertions between codons 69 and 70 of human immunodeficiency virus type 1 reverse transcriptase on primer unblocking, deoxynucleoside triphosphate inhibition, and DNA chain elongation.* J Virol, 2003. **77**(6): p. 3871-7.
29. Tachedjian, G., et al., *Characterisation of foscarnet-resistant strains of human immunodeficiency virus type 1.* Virology, 1995. **212**(1): p. 58-68.
30. Hammond, J.L., et al., *Alkylglycerol prodrugs of phosphonoformate are potent in vitro inhibitors of nucleoside-resistant human immunodeficiency virus type 1 and select for resistance mutations that suppress zidovudine resistance.* Antimicrob Agents Chemother, 2001. **45**(6): p. 1621-8.
31. Tachedjian, G., et al., *Zidovudine resistance is suppressed by mutations conferring resistance of human immunodeficiency virus type 1 to foscarnet.* J Virol, 1996. **70**(10): p. 7171-81.
32. Oberg, B., *Antiviral effects of phosphonoformate (PFA, foscarnet sodium).* Pharmacol Ther, 1982. **19**(3): p. 387-415.

33. Eriksson, B., B. Oberg, and B. Wahren, *Pyrophosphate analogues as inhibitors of DNA polymerases of cytomegalovirus, herpes simplex virus and cellular origin.* Biochim Biophys Acta, 1982. **696**(2): p. 115-23.
34. Derse, D., K.F. Bastow, and Y. Cheng, *Characterization of the DNA polymerases induced by a group of herpes simplex virus type I variants selected for growth in the presence of phosphonoformic acid.* J Biol Chem, 1982. **257**(17): p. 10251-60.
35. Marchand, B., E.P. Tchesnokov, and M. Gotte, *The pyrophosphate analogue foscarnet traps the pre-translocational state of HIV-1 reverse transcriptase in a Brownian ratchet model of polymerase translocation.* J Biol Chem, 2007. **282**(5): p. 3337-46.
36. Shepherd, F.A., et al., *A guide to the investigation and treatment of patients with AIDS and AIDS-related disorders.* CMAJ, 1986. **134**(9): p. 999-1008.
37. Furio, M.M. and C.J. Wordell, *Treatment of infectious complications of acquired immunodeficiency syndrome.* Clin Pharm, 1985. **4**(5): p. 539-54.
38. Crumpacker, C.S., *Treatment of opportunistic viral infections.* AIDS, 1988. **2 Suppl 1**: p. S191-3.
39. Barre-Sinoussi, F., et al., *Isolation of a T-lymphotropic retrovirus from a patient at risk for acquired immune deficiency syndrome (AIDS).* Science, 1983. **220**(4599): p. 868-71.
40. Gallo, R.C., et al., *Frequent detection and isolation of cytopathic retroviruses (HTLV-III) from patients with AIDS and at risk for AIDS.* Science, 1984. **224**(4648): p. 500-3.
41. Yarchoan, R., et al., *Anti-retroviral therapy of human immunodeficiency virus infection: current strategies and challenges for the future.* Blood, 1991. **78**(4): p. 859-84.
42. Resnick, L., *Antiviral chemotherapies directed against HTLV-III/LAV*. Mt Sinai J Med, 1986. **53**(8): p. 648-56.
43. Resnick, L., et al., *In vitro suppression of HTLV-III/LAV infectivity by a combination of acyclovir and suramin.* J Infect Dis, 1986. **154**(6): p. 1027-30.
44. Corey, L., et al., *The effects of herpes simplex virus-2 on HIV-1 acquisition and transmission: a review of two overlapping epidemics.* J Acquir Immune Defic Syndr, 2004. **35**(5): p. 435-45.
45. Cooper, D.A., et al., *The efficacy and safety of zidovudine alone or as cotherapy with acyclovir for the treatment of patients with AIDS and AIDS-related complex: a double-blind randomized trial. European-Australian Collaborative Group.* AIDS, 1993. **7**(2): p. 197-207.
46. Nagot, N., et al., *Reduction of HIV-1 RNA levels with therapy to suppress herpes simplex virus.* N Engl J Med, 2007. **356**(8): p. 790-9.
47. Lisco, A., et al., *Acyclovir is activated into a HIV-1 reverse transcriptase inhibitor in herpesvirus-infected human tissues.* Cell Host Microbe, 2008. **4**(3): p. 260-70.
48. McMahon, M.A., et al., *The antiherpetic drug acyclovir inhibits HIV replication and selects the V75I reverse transcriptase multidrug resistance mutation.* J Biol Chem, 2008. **283**(46): p. 31289-93.

49. Mitsuya, H., et al., *3'-Azido-3'-deoxythymidine (BW A509U): an antiviral agent that inhibits the infectivity and cytopathic effect of human T-lymphotropic virus type III/lymphadenopathy-associated virus in vitro.* Proc Natl Acad Sci U S A, 1985. **82**(20): p. 7096-100.
50. De Clercq, E., *The design of drugs for HIV and HCV.* Nat Rev Drug Discov, 2007. **6**(12): p. 1001-18.
51. Dore, G.J., et al., *Dual efficacy of lamivudine treatment in human immunodeficiency virus/hepatitis B virus-coinfected persons in a randomized, controlled study (CAESAR). The CAESAR Coordinating Committee.* J Infect Dis, 1999. **180**(3): p. 607-13.
52. Baker, R., *FDA approves 3TC and saquinavir. Food and Drug Administration.* BETA, 1995: p. 5, 9.
53. Josefson, D., *Oral treatment for hepatitis B gets approval in the United States.* BMJ, 1998. **317**(7165): p. 1034.
54. Schinazi, R.F., et al., *Activities of the four optical isomers of 2',3'-dideoxy-3'-thiacytidine (BCH-189) against human immunodeficiency virus type 1 in human lymphocytes.* Antimicrob Agents Chemother, 1992. **36**(3): p. 672-6.
55. Severini, A., et al., *Mechanism of inhibition of duck hepatitis B virus polymerase by (-)-beta-L-2',3'-dideoxy-3'-thiacytidine.* Antimicrob Agents Chemother, 1995. **39**(7): p. 1430-5.
56. Innaimo, S.F., et al., *Identification of BMS-200475 as a potent and selective inhibitor of hepatitis B virus.* Antimicrob Agents Chemother, 1997. **41**(7): p. 1444-8.
57. Seifer, M., et al., *In vitro inhibition of hepadnavirus polymerases by the triphosphates of BMS-200475 and lobucavir.* Antimicrob Agents Chemother, 1998. **42**(12): p. 3200-8.
58. Langley, D.R., et al., *Inhibition of hepatitis B virus polymerase by entecavir.* J Virol, 2007. **81**(8): p. 3992-4001.
59. Colonno, R.J., et al., *Entecavir resistance is rare in nucleoside naive patients with hepatitis B.* Hepatology, 2006. **44**(6): p. 1656-65.
60. McMahon, M.A., et al., *The HBV drug entecavir - effects on HIV-1 replication and resistance.* N Engl J Med, 2007. **356**(25): p. 2614-21.
61. Domaoal, R.A., et al., *Pre-steady-state kinetic studies establish entecavir 5'-triphosphate as a substrate for HIV-1 reverse transcriptase.* J Biol Chem, 2008. **283**(9): p. 5452-9.
62. Sulkowski, M.S., *Viral hepatitis and HIV coinfection.* J Hepatol, 2008. **48**(2): p. 353-67.
63. De Clercq, E., et al., *Acyclic/carbocyclic guanosine analogues as anti-herpesvirus agents.* Nucleosides Nucleotides Nucleic Acids, 2001. **20**(4-7): p. 271-85.
64. Boyer, P.L., et al., *Fixed conformation nucleoside analogs effectively inhibit excision-proficient HIV-1 reverse transcriptases.* J Mol Biol, 2005. **345**(3): p. 441-50.
65. Marquez, V.E., *Chemical and biological consequences of locking the conformation of nucleosides at the two antipodal extremes of the pseudorotational cycle.* Nucleic Acids Symp Ser (Oxf), 2004(48): p. 11-2.

66. Mazzucco, C.E., et al., *Entecavir for treatment of hepatitis B virus displays no in vitro mitochondrial toxicity or DNA polymerase gamma inhibition.* Antimicrob Agents Chemother, 2008. **52**(2): p. 598-605.
67. Ying, C., et al., *Ribavirin and mycophenolic acid markedly potentiate the anti-hepatitis B virus activity of entecavir.* Antiviral Res, 2007. **73**(3): p. 192-6.
68. Eigen, M., et al., *The origin of genetic information.* Sci Am, 1981. **244**(4): p. 88-92, 96, et passim.
69. Locarnini, S., *Molecular virology of hepatitis B virus.* Semin Liver Dis, 2004. **24 Suppl 1**: p. 3-10.
70. Munoz, J.L., et al., *HIV-1 reverse transcriptase. A diversity generator and quasispecies regulator.* Ann N Y Acad Sci, 1993. **693**: p. 65-70.
71. Coen, D.M. and P.A. Schaffer, *Antiherpesvirus drugs: a promising spectrum of new drugs and drug targets.* Nat Rev Drug Discov, 2003. **2**(4): p. 278-88.
72. Karayiannis, P., *Hepatitis B virus: old, new and future approaches to antiviral treatment.* J Antimicrob Chemother, 2003. **51**(4): p. 761-85.
73. Schafer, S., et al., *Animal models and experimental systems in hepatitis B virus research.*, in *Hepatitis B Virus: Molecular Mechanisms in Disease and Novel Strategies for Therapy*, R.C. Koshy and W.H. Caselmann, Editors. 1998, Imerial College Press: London. p. 51 - 74.
74. Cherry, E. and M.A. Wainberg, *The structure and biology of HIV-1: introduction*, in *The human immunodeficiency virus: biology, immunology, and therapy*, E.A. Emini, Editor. 2002, Princeton University Press. p. 1 - 43.
75. Yeung-Yue, K.A., et al., *Herpex Simplex Virus*, in *Viral Infections and Treatment*, H. Rubsamen-Waigmann, et al., Editors. 2003, Marcel Dekker: New York. p. 165-192.
76. Roizman, B. and A.E. Sears, *Herpes symplex viruses and their replication*, in *Fundamental Virology*, B.N. Fields, D.M. Knipe, and P.M. Howley, Editors. 1996, Lippincott-Raven: Philadelphia. p. 1043-1107.
77. Rock, D.L. and N.W. Fraser, *Latent herpes simplex virus type 1 DNA contains two copies of the virion DNA joint region.* J Virol, 1985. **55**(3): p. 849-52.
78. Taylor, T.J., et al., *Herpes simplex virus.* Front Biosci, 2002. **7**: p. d752-64.
79. McGeoch, D.J., et al., *The complete DNA sequence of the long unique region in the genome of herpes simplex virus type 1.* J Gen Virol, 1988. **69 (Pt 7)**: p. 1531-74.
80. Dolan, A., et al., *The genome sequence of herpes simplex virus type 2.* J Virol, 1998. **72**(3): p. 2010-21.
81. Honess, R.W. and B. Roizman, *Regulation of herpesvirus macromolecular synthesis. I. Cascade regulation of the synthesis of three groups of viral proteins.* J Virol, 1974. **14**(1): p. 8-19.
82. Nishiyama, Y., *Herpes simplex virus gene products: the accessories reflect her lifestyle well.* Rev Med Virol, 2004. **14**(1): p. 33-46.

83. Hill, A., et al., *Herpes simplex virus turns off the TAP to evade host immunity.* Nature, 1995. **375**(6530): p. 411-5.
84. Haarr, L. and S. Skulstad, *The herpes simplex virus type 1 particle: structure and molecular functions. Review article.* APMIS, 1994. **102**(5): p. 321-46.
85. Challberg, M.D., *A method for identifying the viral genes required for herpesvirus DNA replication.* Proc Natl Acad Sci U S A, 1986. **83**(23): p. 9094-8.
86. Purifoy, D.J., R.B. Lewis, and K.L. Powell, *Identification of the herpes simplex virus DNA polymerase gene.* Nature, 1977. **269**(5629): p. 621-3.
87. Elias, P., et al., *A DNA binding protein specific for an origin of replication of herpes simplex virus type 1.* Proc Natl Acad Sci U S A, 1986. **83**(17): p. 6322-6.
88. Conley, A.J., et al., *Molecular genetics of herpes simplex virus. VII. Characterization of a temperature-sensitive mutant produced by in vitro mutagenesis and defective in DNA synthesis and accumulation of gamma polypeptides.* J Virol, 1981. **37**(1): p. 191-206.
89. Elias, P. and I.R. Lehman, *Interaction of origin binding protein with an origin of replication of herpes simplex virus 1.* Proc Natl Acad Sci U S A, 1988. **85**(9): p. 2959-63.
90. Tanguy Le Gac, N., G. Villani, and P.E. Boehmer, *Herpes simplex virus type-1 single-strand DNA-binding protein (ICP8) enhances the ability of the viral DNA helicase-primase to unwind cisplatin-modified DNA.* J Biol Chem, 1998. **273**(22): p. 13801-7.
91. Chiou, H.C., S.K. Weller, and D.M. Coen, *Mutations in the herpes simplex virus major DNA-binding protein gene leading to altered sensitivity to DNA polymerase inhibitors.* Virology, 1985. **145**(2): p. 213-26.
92. Boehmer, P.E., M.S. Dodson, and I.R. Lehman, *The herpes simplex virus type-1 origin binding protein. DNA helicase activity.* J Biol Chem, 1993. **268**(2): p. 1220-5.
93. Crute, J.J., E.S. Mocarski, and I.R. Lehman, *A DNA helicase induced by herpes simplex virus type 1.* Nucleic Acids Res, 1988. **16**(14A): p. 6585-96.
94. Crute, J.J. and I.R. Lehman, *Herpes simplex-1 DNA polymerase. Identification of an intrinsic 5'----3' exonuclease with ribonuclease H activity.* J Biol Chem, 1989. **264**(32): p. 19266-70.
95. Gallo, M.L., et al., *Purification of the herpes simplex virus type 1 65-kilodalton DNA-binding protein: properties of the protein and evidence of its association with the virus-encoded DNA polymerase.* J Virol, 1988. **62**(8): p. 2874-83.
96. Knopf, K.W., *Properties of herpes simplex virus DNA polymerase and characterization of its associated exonuclease activity.* Eur J Biochem, 1979. **98**(1): p. 231-44.
97. Gibbs, J.S., et al., *Polymerization activity of an alpha-like DNA polymerase requires a conserved 3'-5' exonuclease active site.* Mol Cell Biol, 1991. **11**(9): p. 4786-95.

98. Gottlieb, J., et al., *The herpes simplex virus type 1 UL42 gene product: a subunit of DNA polymerase that functions to increase processivity.* J Virol, 1990. **64**(12): p. 5976-87.
99. Boehmer, P.E. and I.R. Lehman, *Herpes simplex virus DNA replication.* Annu Rev Biochem, 1997. **66**: p. 347-84.
100. Braithwaite, D.K. and J. Ito, *Compilation, alignment, and phylogenetic relationships of DNA polymerases.* Nucleic Acids Res, 1993. **21**(4): p. 787-802.
101. Wang, J., et al., *Crystal structure of a pol alpha family replication DNA polymerase from bacteriophage RB69.* Cell, 1997. **89**(7): p. 1087-99.
102. Shamoo, Y. and T.A. Steitz, *Building a replisome from interacting pieces: sliding clamp complexed to a peptide from DNA polymerase and a polymerase editing complex.* Cell, 1999. **99**(2): p. 155-66.
103. Franklin, M.C., J. Wang, and T.A. Steitz, *Structure of the replicating complex of a pol alpha family DNA polymerase.* Cell, 2001. **105**(5): p. 657-67.
104. Liu, S., et al., *Crystal structure of the herpes simplex virus 1 DNA polymerase.* J Biol Chem, 2006. **281**(26): p. 18193-200.
105. Hodge, R.A. and R.M. Perkins, *Mode of action of 9-(4-hydroxy-3-hydroxymethylbut-1-yl)guanine (BRL 39123) against herpes simplex virus in MRC-5 cells.* Antimicrob Agents Chemother, 1989. **33**(2): p. 223-9.
106. *Drugs for non-HIV viral infections.* Treat Guidel Med Lett, 2007. **5**(59): p. 59-70.
107. Boyd, M.R., et al., *Antiherpesvirus activity of 9-(4-hydroxy-3-hydroxy-methylbut-1-yl)guanine (BRL 39123) in cell culture.* Antimicrob Agents Chemother, 1987. **31**(8): p. 1238-42.
108. Ilsley, D.D., et al., *Acyclic guanosine analogs inhibit DNA polymerases alpha, delta, and epsilon with very different potencies and have unique mechanisms of action.* Biochemistry, 1995. **34**(8): p. 2504-10.
109. Lowe, D.M., et al., *Mode of action of (R)-9-[4-hydroxy-2-(hydroxymethyl)butyl]guanine against herpesviruses.* Antimicrob Agents Chemother, 1995. **39**(8): p. 1802-8.
110. Bacon, T.H., et al., *Herpes simplex virus resistance to acyclovir and penciclovir after two decades of antiviral therapy.* Clin Microbiol Rev, 2003. **16**(1): p. 114-28.
111. Datema, R., et al., *Critical determinants of antiherpes efficacy of buciclovir and related acyclic guanosine analogs.* Antiviral Res, 1987. **7**(6): p. 303-16.
112. Earnshaw, D.L., et al., *Mode of antiviral action of penciclovir in MRC-5 cells infected with herpes simplex virus type 1 (HSV-1), HSV-2, and varicella-zoster virus.* Antimicrob Agents Chemother, 1992. **36**(12): p. 2747-57.
113. Bacon, T.H., et al., *Surveillance for antiviral-agent-resistant herpes simplex virus in the general population with recurrent herpes labialis.* Antimicrob Agents Chemother, 2002. **46**(9): p. 3042-4.

114. Danve-Szatanek, C., et al., *Surveillance network for herpes simplex virus resistance to antiviral drugs: 3-year follow-up.* J Clin Microbiol, 2004. **42**(1): p. 242-9.
115. Chen, Y., et al., *Resistant herpes simplex virus type 1 infection: an emerging concern after allogeneic stem cell transplantation.* Clin Infect Dis, 2000. **31**(4): p. 927-35.
116. Reyes, M., et al., *Acyclovir-resistant genital herpes among persons attending sexually transmitted disease and human immunodeficiency virus clinics.* Arch Intern Med, 2003. **163**(1): p. 76-80.
117. Pottage, J.C., Jr. and H.A. Kessler, *Herpes simplex virus resistance to acyclovir: clinical relevance.* Infect Agents Dis, 1995. **4**(3): p. 115-24.
118. Gaudreau, A., et al., *Phenotypic and genotypic characterization of acyclovir-resistant herpes simplex viruses from immunocompromised patients.* J Infect Dis, 1998. **178**(2): p. 297-303.
119. Graham, D., B.A. Larder, and M.M. Inglis, *Evidence that the 'active centre' of the herpes simplex virus thymidine kinase involves an interaction between three distinct regions of the polypeptide.* J Gen Virol, 1986. **67 (Pt 4)**: p. 753-8.
120. Safrin, S. and L. Phan, *In vitro activity of penciclovir against clinical isolates of acyclovir-resistant and foscarnet-resistant herpes simplex virus.* Antimicrob Agents Chemother, 1993. **37**(10): p. 2241-3.
121. Coen, D.M. and P.A. Schaffer, *Two distinct loci confer resistance to acycloguanosine in herpes simplex virus type 1.* Proc Natl Acad Sci U S A, 1980. **77**(4): p. 2265-9.
122. Sacks, S.L., et al., *Progressive esophagitis from acyclovir-resistant herpes simplex. Clinical roles for DNA polymerase mutants and viral heterogeneity?* Ann Intern Med, 1989. **111**(11): p. 893-9.
123. Collins, P., et al., *Characterization of a DNA polymerase mutant of herpes simplex virus from a severely immunocompromised patient receiving acyclovir.* J Gen Virol, 1989. **70 (Pt 2)**: p. 375-82.
124. Betz, U.A., et al., *Potent in vivo antiviral activity of the herpes simplex virus primase-helicase inhibitor BAY 57-1293.* Antimicrob Agents Chemother, 2002. **46**(6): p. 1766-72.
125. Crute, J.J., et al., *Herpes simplex virus helicase-primase inhibitors are active in animal models of human disease.* Nat Med, 2002. **8**(4): p. 386-91.
126. Kleymann, G., et al., *New helicase-primase inhibitors as drug candidates for the treatment of herpes simplex disease.* Nat Med, 2002. **8**(4): p. 392-8.
127. Duan, J., et al., *Oral bioavailability and in vivo efficacy of the helicase-primase inhibitor BILS 45 BS against acyclovir-resistant herpes simplex virus type 1.* Antimicrob Agents Chemother, 2003. **47**(6): p. 1798-804.
128. Spruance, S.L., et al., *Application of a topical immune response modifier, resiquimod gel, to modify the recurrence rate of recurrent genital herpes: a pilot study.* J Infect Dis, 2001. **184**(2): p. 196-200.
129. Pass, R.F., *Epidemiology and transmission of cytomegalovirus.* J Infect Dis, 1985. **152**(2): p. 243-8.

130. Griffiths, P.D., *Cytomegalovirus*, in *Principles and Practice of Clinical Virology*, A.J. Zuckermann, J.E. Banatvala, and J.R. Pattison, Editors. 2000, John Wiley and Sons: London. p. 79 - 116.
131. Gandhi, M.K. and R. Khanna, *Human cytomegalovirus: clinical aspects, immune regulation, and emerging treatments.* Lancet Infect Dis, 2004. **4**(12): p. 725-38.
132. Gilbert, C. and G. Boivin, *Human cytomegalovirus resistance to antiviral drugs.* Antimicrob Agents Chemother, 2005. **49**(3): p. 873-83.
133. De Bolle, L., L. Naesens, and E. De Clercq, *Update on human herpesvirus 6 biology, clinical features, and therapy.* Clin Microbiol Rev, 2005. **18**(1): p. 217-45.
134. Pass, R.F., *Cytomegalovirus*, in *Fields Virology*, D.M. Knipe and P.M. Howley, Editors. 2001, Lippincott, Williams & Wilkins: Philadelphia. p. 2675-2705.
135. Bissinger, A.L., et al., *Human cytomegalovirus as a direct pathogen: correlation of multiorgan involvement and cell distribution with clinical and pathological findings in a case of congenital inclusion disease.* J Med Virol, 2002. **67**(2): p. 200-6.
136. Bresnahan, W.A. and T. Shenk, *A subset of viral transcripts packaged within human cytomegalovirus particles.* Science, 2000. **288**(5475): p. 2373-6.
137. Landolfo, S., et al., *The human cytomegalovirus.* Pharmacol Ther, 2003. **98**(3): p. 269-97.
138. Chee, M.S., et al., *Analysis of the protein-coding content of the sequence of human cytomegalovirus strain AD169.* Curr Top Microbiol Immunol, 1990. **154**: p. 125-69.
139. Estes, J.E. and E.S. Huang, *Stimulation of cellular thymidine kinases by human cytomegalovirus.* J Virol, 1977. **24**(1): p. 13-21.
140. Biron, K.K., et al., *Metabolic activation of the nucleoside analog 9-[(2-hydroxy-1-(hydroxymethyl)ethoxy]methyl)guanine in human diploid fibroblasts infected with human cytomegalovirus.* Proc Natl Acad Sci U S A, 1985. **82**(8): p. 2473-7.
141. Kalejta, R.F. and T. Shenk, *Manipulation of the cell cycle by human cytomegalovirus.* Front Biosci, 2002. **7**: p. d295-306.
142. Mar, E.C., et al., *Human cytomegalovirus-induced DNA polymerase and its interaction with the triphosphates of 1-(2'-deoxy-2'-fluoro-beta-D-arabinofuranosyl)-5-methyluracil, -5-iodocytosine, and -5-methylcytosine.* J Virol, 1985. **56**(3): p. 846-51.
143. Heilbronn, R., et al., *Genomic localization, sequence analysis, and transcription of the putative human cytomegalovirus DNA polymerase gene.* J Virol, 1987. **61**(1): p. 119-24.
144. Ertl, P.F. and K.L. Powell, *Physical and functional interaction of human cytomegalovirus DNA polymerase and its accessory protein (ICP36) expressed in insect cells.* J Virol, 1992. **66**(7): p. 4126-33.
145. Pari, G.S., M.A. Kacica, and D.G. Anders, *Open reading frames UL44, IRS1/TRS1, and UL36-38 are required for transient complementation of*

human cytomegalovirus oriLyt-dependent DNA synthesis. J Virol, 1993. **67**(5): p. 2575-82.
146. Nishiyama, Y., K. Maeno, and S. Yoshida, *Characterization of human cytomegalovirus-induced DNA polymerase and the associated 3'-to-5', exonuclease.* Virology, 1983. **124**(2): p. 221-31.
147. Shi, R., et al., *Three-dimensional modeling of cytomegalovirus DNA polymerase and preliminary analysis of drug resistance.* Proteins, 2006. **64**(2): p. 301-7.
148. Ollis, D.L., et al., *Structure of large fragment of Escherichia coli DNA polymerase I complexed with dTMP.* Nature, 1985. **313**(6005): p. 762-6.
149. Brautigam, C.A. and T.A. Steitz, *Structural and functional insights provided by crystal structures of DNA polymerases and their substrate complexes.* Curr Opin Struct Biol, 1998. **8**(1): p. 54-63.
150. Hwang, C.B., K.L. Ruffner, and D.M. Coen, *A point mutation within a distinct conserved region of the herpes simplex virus DNA polymerase gene confers drug resistance.* J Virol, 1992. **66**(3): p. 1774-6.
151. Zhang, J., et al., *Primary structure of the catalytic subunit of calf thymus DNA polymerase delta: sequence similarities with other DNA polymerases.* Biochemistry, 1991. **30**(51): p. 11742-50.
152. Bernad, A., et al., *A conserved 3'----5' exonuclease active site in prokaryotic and eukaryotic DNA polymerases.* Cell, 1989. **59**(1): p. 219-28.
153. Ye, L.B. and E.S. Huang, *In vitro expression of the human cytomegalovirus DNA polymerase gene: effects of sequence alterations on enzyme activity.* J Virol, 1993. **67**(11): p. 6339-47.
154. Hanks, S.K., A.M. Quinn, and T. Hunter, *The protein kinase family: conserved features and deduced phylogeny of the catalytic domains.* Science, 1988. **241**(4861): p. 42-52.
155. Mercorelli, B., et al., *Human cytomegalovirus DNA replication: antiviral targets and drugs.* Rev Med Virol, 2008. **18**(3): p. 177-210.
156. Biron, K.K., et al., *Potent and selective inhibition of human cytomegalovirus replication by 1263W94, a benzimidazole L-riboside with a unique mode of action.* Antimicrob Agents Chemother, 2002. **46**(8): p. 2365-72.
157. Wolf, D.G., et al., *Distinct and separate roles for herpesvirus-conserved UL97 kinase in cytomegalovirus DNA synthesis and encapsidation.* Proc Natl Acad Sci U S A, 2001. **98**(4): p. 1895-900.
158. Krosky, P.M., M.C. Baek, and D.M. Coen, *The human cytomegalovirus UL97 protein kinase, an antiviral drug target, is required at the stage of nuclear egress.* J Virol, 2003. **77**(2): p. 905-14.
159. Krosky, P.M., et al., *The human cytomegalovirus UL44 protein is a substrate for the UL97 protein kinase.* J Virol, 2003. **77**(14): p. 7720-7.
160. Littler, E., A.D. Stuart, and M.S. Chee, *Human cytomegalovirus UL97 open reading frame encodes a protein that phosphorylates the antiviral nucleoside analogue ganciclovir.* Nature, 1992. **358**(6382): p. 160-2.

161. Michel, D., et al., *The UL97 gene product of human cytomegalovirus is an early-late protein with a nuclear localization but is not a nucleoside kinase.* J Virol, 1996. **70**(9): p. 6340-6.
162. Markham, A. and D. Faulds, *Ganciclovir. An update of its therapeutic use in cytomegalovirus infection.* Drugs, 1994. **48**(3): p. 455-84.
163. Cvetkovic, R.S. and K. Wellington, *Valganciclovir: a review of its use in the management of CMV infection and disease in immunocompromised patients.* Drugs, 2005. **65**(6): p. 859-78.
164. De Clercq, E. and A. Holy, *Acyclic nucleoside phosphonates: a key class of antiviral drugs.* Nat Rev Drug Discov, 2005. **4**(11): p. 928-40.
165. Trofe, J., et al., *Maribavir: a novel antiviral agent with activity against cytomegalovirus.* Ann Pharmacother, 2008. **42**(10): p. 1447-57.
166. Mulamba, G.B., et al., *Human cytomegalovirus mutant with sequence-dependent resistance to the phosphorothioate oligonucleotide fomivirsen (ISIS 2922).* Antimicrob Agents Chemother, 1998. **42**(4): p. 971-3.
167. Sullivan, V., et al., *A protein kinase homologue controls phosphorylation of ganciclovir in human cytomegalovirus-infected cells.* Nature, 1992. **358**(6382): p. 162-4.
168. Reid, R., et al., *Insertion and extension of acyclic, dideoxy, and ara nucleotides by herpesviridae, human alpha and human beta polymerases. A unique inhibition mechanism for 9-(1,3-dihydroxy-2-propoxymethyl)guanine triphosphate.* J Biol Chem, 1988. **263**(8): p. 3898-904.
169. Pescovitz, M.D., et al., *Valganciclovir results in improved oral absorption of ganciclovir in liver transplant recipients.* Antimicrob Agents Chemother, 2000. **44**(10): p. 2811-5.
170. Cihlar, T. and M.S. Chen, *Identification of enzymes catalyzing two-step phosphorylation of cidofovir and the effect of cytomegalovirus infection on their activities in host cells.* Mol Pharmacol, 1996. **50**(6): p. 1502-10.
171. Ho, H.T., et al., *Intracellular metabolism of the antiherpes agent (S)-1-[3-hydroxy-2-(phosphonylmethoxy)propyl]cytosine.* Mol Pharmacol, 1992. **41**(1): p. 197-202.
172. Xiong, X., et al., *Kinetic analysis of the interaction of cidofovir diphosphate with human cytomegalovirus DNA polymerase.* Biochem Pharmacol, 1996. **51**(11): p. 1563-7.
173. Xiong, X., J.L. Smith, and M.S. Chen, *Effect of incorporation of cidofovir into DNA by human cytomegalovirus DNA polymerase on DNA elongation.* Antimicrob Agents Chemother, 1997. **41**(3): p. 594-9.
174. Crumpacker, C.S., *Mechanism of action of foscarnet against viral polymerases.* Am J Med, 1992. **92**(2A): p. 3S-7S.
175. Razonable, R.R. and V.C. Emery, *Management of CMV infection and disease in transplant patients. 27-29 February 2004.* Herpes, 2004. **11**(3): p. 77-86.
176. Marschall, M., et al., *The protein kinase pUL97 of human cytomegalovirus interacts with and phosphorylates the DNA polymerase processivity factor pUL44.* Virology, 2003. **311**(1): p. 60-71.

177. Drew, W.L., et al., *Maribavir sensitivity of cytomegalovirus isolates resistant to ganciclovir, cidofovir or foscarnet.* J Clin Virol, 2006. **37**(2): p. 124-7.
178. Chou, S. and G.I. Marousek, *Maribavir antagonizes the antiviral action of ganciclovir on human cytomegalovirus.* Antimicrob Agents Chemother, 2006. **50**(10): p. 3470-2.
179. Komazin, G., et al., *Resistance of human cytomegalovirus to the benzimidazole L-ribonucleoside maribavir maps to UL27.* J Virol, 2003. **77**(21): p. 11499-506.
180. Azad, R.F., et al., *Antiviral activity of a phosphorothioate oligonucleotide complementary to RNA of the human cytomegalovirus major immediate-early region.* Antimicrob Agents Chemother, 1993. **37**(9): p. 1945-54.
181. Jabs, D.A., et al., *Cytomegalovirus retinitis and viral resistance: ganciclovir resistance. CMV Retinitis and Viral Resistance Study Group.* J Infect Dis, 1998. **177**(3): p. 770-3.
182. Boivin, G., et al., *Rate of emergence of cytomegalovirus (CMV) mutations in leukocytes of patients with acquired immunodeficiency syndrome who are receiving valganciclovir as induction and maintenance therapy for CMV retinitis.* J Infect Dis, 2001. **184**(12): p. 1598-602.
183. Biron, K.K., *Antiviral drugs for cytomegalovirus diseases.* Antiviral Res, 2006. **71**(2-3): p. 154-63.
184. Chou, S., et al., *Mutation in region III of the DNA polymerase gene conferring foscarnet resistance in cytomegalovirus isolates from 3 subjects receiving prolonged antiviral therapy.* J Infect Dis, 1998. **178**(2): p. 526-30.
185. Cihlar, T., et al., *A point mutation in the human cytomegalovirus DNA polymerase gene selected in vitro by cidofovir confers a slow replication phenotype in cell culture.* Virology, 1998. **248**(2): p. 382-93.
186. Cherrington, J.M., et al., *In vitro antiviral susceptibilities of isolates from cytomegalovirus retinitis patients receiving first- or second-line cidofovir therapy: relationship to clinical outcome.* J Infect Dis, 1998. **178**(6): p. 1821-5.
187. Chou, S., L.C. Wechel, and G.I. Marousek, *Cytomegalovirus UL97 kinase mutations that confer maribavir resistance.* J Infect Dis, 2007. **196**(1): p. 91-4.
188. Chou, S. and G.I. Marousek, *Accelerated evolution of maribavir resistance in a cytomegalovirus exonuclease domain II mutant.* J Virol, 2008. **82**(1): p. 246-53.
189. Chou, S., *Cytomegalovirus UL97 mutations in the era of ganciclovir and maribavir.* Rev Med Virol, 2008. **18**(4): p. 233-46.
190. Lee, W.M., *Hepatitis B virus infection.* N Engl J Med, 1997. **337**(24): p. 1733-45.
191. Moyer, L.A. and E.E. Mast, *Hepatitis B: virology, epidemiology, disease, and prevention, and an overview of viral hepatitis.* Am J Prev Med, 1994. **10 Suppl**: p. 45-55.

192. Malik, A.H. and W.M. Lee, *Chronic hepatitis B virus infection: treatment strategies for the next millennium.* Ann Intern Med, 2000. **132**(9): p. 723-31.
193. Mast, E.E., et al., *A comprehensive immunization strategy to eliminate transmission of hepatitis B virus infection in the United States: recommendations of the Advisory Committee on Immunization Practices (ACIP) Part II: immunization of adults.* MMWR Recomm Rep, 2006. **55**(RR-16): p. 1-33; quiz CE1-4.
194. Ferir, G., et al., *Antiviral treatment of chronic hepatitis B virus infections: the past, the present and the future.* Rev Med Virol, 2008. **18**(1): p. 19-34.
195. Dane, D.S., C.H. Cameron, and M. Briggs, *Virus-like particles in serum of patients with Australia-antigen-associated hepatitis.* Lancet, 1970. **1**(7649): p. 695-8.
196. Ganem, D. and R.J. Schneider, *Hepadnaviridae: the viruses and thier replciation*, in *Fields Virology*, D.M. Knipe, et al., Editors. 2001, Lippincott-Raven: Philadelphia. p. 2921 - 69.
197. Evans, A.A. and W.T. London, *Epidemiology of hepatitis B*, in *Viral Hepatitis*, A.J. Zuckerman and H.C. Thoms, Editors. 1998, Churchill Livingstone: London, UK. p. 107 - 114.
198. Lavanchy, D., *Hepatitis B virus epidemiology, disease burden, treatment, and current and emerging prevention and control measures.* J Viral Hepat, 2004. **11**(2): p. 97-107.
199. Valenzuela, P., et al., *Nucleotide sequence of the gene coding for the major protein of hepatitis B virus surface antigen.* Nature, 1979. **280**(5725): p. 815-9.
200. Kim, C.M., et al., *HBx gene of hepatitis B virus induces liver cancer in transgenic mice.* Nature, 1991. **351**(6324): p. 317-20.
201. Radziwill, G., W. Tucker, and H. Schaller, *Mutational analysis of the hepatitis B virus P gene product: domain structure and RNase H activity.* J Virol, 1990. **64**(2): p. 613-20.
202. Bartenschlager, R. and H. Schaller, *The amino-terminal domain of the hepadnaviral P-gene encodes the terminal protein (genome-linked protein) believed to prime reverse transcription.* EMBO J, 1988. **7**(13): p. 4185-92.
203. Tuttleman, J.S., C. Pourcel, and J. Summers, *Formation of the pool of covalently closed circular viral DNA in hepadnavirus-infected cells.* Cell, 1986. **47**(3): p. 451-60.
204. Newbold, J.E., et al., *The covalently closed duplex form of the hepadnavirus genome exists in situ as a heterogeneous population of viral minichromosomes.* J Virol, 1995. **69**(6): p. 3350-7.
205. Beck, J. and M. Nassal, *Hepatitis B virus replication.* World J Gastroenterol, 2007. **13**(1): p. 48-64.
206. Osamu Yokosuka, M.O.F.I.K.O.J.S., *Changes of hepatitis B virus DNA in liver and serum caused by recombinant leukocyte interferon treatment: Analysis of intrahepatic replicative hepatitis B virus DNA.* Hepatology, 1985. **5**(5): p. 728-734.

207. Moraleda, G., et al., *Lack of effect of antiviral therapy in nondividing hepatocyte cultures on the closed circular DNA of woodchuck hepatitis virus.* J Virol, 1997. **71**(12): p. 9392-9.
208. Dean, J., S. Bowden, and S. Locarnini, *Reversion of duck hepatitis B virus DNA replication in vivo following cessation of treatment with the nucleoside analogue ganciclovir.* Antiviral Res, 1995. **27**(1-2): p. 171-8.
209. Luscombe, C., et al., *Long-term ganciclovir chemotherapy for congenital duck hepatitis B virus infection in vivo: effect on intrahepatic-viral DNA, RNA, and protein expression.* Hepatology, 1996. **24**(4): p. 766-73.
210. Yang, W. and J. Summers, *Integration of hepadnavirus DNA in infected liver: evidence for a linear precursor.* J Virol, 1999. **73**(12): p. 9710-7.
211. Summers, J. and W.S. Mason, *Replication of the genome of a hepatitis B--like virus by reverse transcription of an RNA intermediate.* Cell, 1982. **29**(2): p. 403-15.
212. Kramvis, A. and M.C. Kew, *Structure and function of the encapsidation signal of hepadnaviridae.* J Viral Hepat, 1998. **5**(6): p. 357-67.
213. Stuyver, L.J., et al., *Nomenclature for antiviral-resistant human hepatitis B virus mutations in the polymerase region.* Hepatology, 2001. **33**(3): p. 751-7.
214. Poch, O., et al., *Identification of four conserved motifs among the RNA-dependent polymerase encoding elements.* EMBO J, 1989. **8**(12): p. 3867-74.
215. Zoulim, F. and C. Seeger, *Reverse transcription in hepatitis B viruses is primed by a tyrosine residue of the polymerase.* J Virol, 1994. **68**(1): p. 6-13.
216. Nassal, M. and A. Rieger, *A bulged region of the hepatitis B virus RNA encapsidation signal contains the replication origin for discontinuous first-strand DNA synthesis.* J Virol, 1996. **70**(5): p. 2764-73.
217. Nassal, M. and H. Schaller, *Hepatitis B virus replication--an update.* J Viral Hepat, 1996. **3**(5): p. 217-26.
218. Thomas, H., G. Foster, and D. Platis, *Mechanisms of action of interferon and nucleoside analogues.* J Hepatol, 2003. **39 Suppl 1**: p. S93-8.
219. Lau, G.K., et al., *Peginterferon Alfa-2a, lamivudine, and the combination for HBeAg-positive chronic hepatitis B.* N Engl J Med, 2005. **352**(26): p. 2682-95.
220. Wursthorn, K., et al., *Peginterferon alpha-2b plus adefovir induce strong cccDNA decline and HBsAg reduction in patients with chronic hepatitis B.* Hepatology, 2006. **44**(3): p. 675-84.
221. Cammack, N., et al., *Cellular metabolism of (-) enantiomeric 2'-deoxy-3'-thiacytidine.* Biochem Pharmacol, 1992. **43**(10): p. 2059-64.
222. Zoulim, F., *Mechanism of viral persistence and resistance to nucleoside and nucleotide analogs in chronic hepatitis B virus infection.* Antiviral Res, 2004. **64**(1): p. 1-15.
223. Chang, C.N., et al., *Biochemical pharmacology of (+)- and (-)-2',3'-dideoxy-3'-thiacytidine as anti-hepatitis B virus agents.* J Biol Chem, 1992. **267**(31): p. 22414-20.

224. Merta, A., et al., *Phosphorylation of 9-(2-phosphonomethoxyethyl)adenine and 9-(S)-(3-hydroxy-2-phosphonomethoxypropyl)adenine by AMP(dAMP) kinase from L1210 cells.* Biochem Pharmacol, 1992. **44**(10): p. 2067-77.
225. Seigneres, B., et al., *Effects of pyrimidine and purine analog combinations in the duck hepatitis B virus infection model.* Antimicrob Agents Chemother, 2003. **47**(6): p. 1842-52.
226. Werle-Lapostolle, B., et al., *Persistence of cccDNA during the natural history of chronic hepatitis B and decline during adefovir dipivoxil therapy.* Gastroenterology, 2004. **126**(7): p. 1750-8.
227. Yamanaka, G., et al., *Metabolic studies on BMS-200475, a new antiviral compound active against hepatitis B virus.* Antimicrob Agents Chemother, 1999. **43**(1): p. 190-3.
228. Levine, S., et al., *Efficacies of entecavir against lamivudine-resistant hepatitis B virus replication and recombinant polymerases in vitro.* Antimicrob Agents Chemother, 2002. **46**(8): p. 2525-32.
229. Hernandez-Santiago, B., et al., *Pharmacology of beta-L-thymidine and beta-L-2'-deoxycytidine in HepG2 cells and primary human hepatocytes: relevance to chemotherapeutic efficacy against hepatitis B virus.* Antimicrob Agents Chemother, 2002. **46**(6): p. 1728-33.
230. Bryant, M.L., et al., *Antiviral L-nucleosides specific for hepatitis B virus infection.* Antimicrob Agents Chemother, 2001. **45**(1): p. 229-35.
231. Keam, S.J., *Telbivudine.* Drugs, 2007. **67**(13): p. 1917-29.
232. Kim, J.W., S.H. Park, and S.G. Louie, *Telbivudine: a novel nucleoside analog for chronic hepatitis B.* Ann Pharmacother, 2006. **40**(3): p. 472-8.
233. Delaney, W.E.t., et al., *Intracellular metabolism and in vitro activity of tenofovir against hepatitis B virus.* Antimicrob Agents Chemother, 2006. **50**(7): p. 2471-7.
234. Birkus, G., et al., *Tenofovir diphosphate is a poor substrate and a weak inhibitor of rat DNA polymerases alpha, delta, and epsilon*.* Antimicrob Agents Chemother, 2002. **46**(5): p. 1610-3.
235. Birkus, G., M.J. Hitchcock, and T. Cihlar, *Assessment of mitochondrial toxicity in human cells treated with tenofovir: comparison with other nucleoside reverse transcriptase inhibitors.* Antimicrob Agents Chemother, 2002. **46**(3): p. 716-23.
236. Benhamou, Y., et al., *Anti-hepatitis B virus efficacy of tenofovir disoproxil fumarate in HIV-infected patients.* Hepatology, 2006. **43**(3): p. 548-55.
237. Lada, O., et al., *In vitro susceptibility of lamivudine-resistant hepatitis B virus to adefovir and tenofovir.* Antivir Ther, 2004. **9**(3): p. 353-63.
238. Ratziu, V., et al., *Successful rescue therapy with tenofovir in a patient with hepatic decompensation and adefovir resistant HBV mutant.* Comp Hepatol, 2006. **5**: p. 1.
239. Lok, A.S., et al., *Long-term safety of lamivudine treatment in patients with chronic hepatitis B.* Gastroenterology, 2003. **125**(6): p. 1714-22.
240. Allen, M.I., et al., *Identification and characterization of mutations in hepatitis B virus resistant to lamivudine. Lamivudine Clinical Investigation Group.* Hepatology, 1998. **27**(6): p. 1670-7.

241. Das, K., et al., *Molecular modeling and biochemical characterization reveal the mechanism of hepatitis B virus polymerase resistance to lamivudine (3TC) and emtricitabine (FTC).* J Virol, 2001. **75**(10): p. 4771-9.
242. Delaney, W.E.t., et al., *The hepatitis B virus polymerase mutation rtV173L is selected during lamivudine therapy and enhances viral replication in vitro.* J Virol, 2003. **77**(21): p. 11833-41.
243. Fu, L. and Y.C. Cheng, *Role of additional mutations outside the YMDD motif of hepatitis B virus polymerase in L(-)SddC (3TC) resistance.* Biochem Pharmacol, 1998. **55**(10): p. 1567-72.
244. Schiff, E.R., et al., *Adefovir dipivoxil therapy for lamivudine-resistant hepatitis B in pre- and post-liver transplantation patients.* Hepatology, 2003. **38**(6): p. 1419-27.
245. Hadziyannis, S.J., et al., *Long-term therapy with adefovir dipivoxil for HBeAg-negative chronic hepatitis B for up to 5 years.* Gastroenterology, 2006. **131**(6): p. 1743-51.
246. Osiowy, C., et al., *Detection of rtN236T and rtA181V/T mutations associated with resistance to adefovir dipivoxil in samples from patients with chronic hepatitis B virus infection by the INNO-LiPA HBV DR line probe assay (version 2).* J Clin Microbiol, 2006. **44**(6): p. 1994-7.
247. Angus, P., et al., *Resistance to adefovir dipivoxil therapy associated with the selection of a novel mutation in the HBV polymerase.* Gastroenterology, 2003. **125**(2): p. 292-7.
248. Villeneuve, J.P., et al., *Selection of a hepatitis B virus strain resistant to adefovir in a liver transplantation patient.* J Hepatol, 2003. **39**(6): p. 1085-9.
249. Lee, Y.S., et al., *Increased risk of adefovir resistance in patients with lamivudine-resistant chronic hepatitis B after 48 weeks of adefovir dipivoxil monotherapy.* Hepatology, 2006. **43**(6): p. 1385-91.
250. van der Poorten, D., et al., *Combination adefovir-lamivudine prevents emergence of adefovir resistance in lamivudine-resistant hepatitis B.* J Gastroenterol Hepatol, 2007. **22**(9): p. 1500-5.
251. Daniel J. Tenney, R.E.R.C.J.B.K.A.P.B.J.E.J.F.M.J.W.D.X.J.Y.R.B.W.R., *Long-term monitoring shows hepatitis B virus resistance to entecavir in nucleoside-naïve patients is rare through 5 years of therapy.* Hepatology, 2009. **9999**(9999): p. NA.
252. Tenney, D.J., et al., *Two-year assessment of entecavir resistance in Lamivudine-refractory hepatitis B virus patients reveals different clinical outcomes depending on the resistance substitutions present.* Antimicrob Agents Chemother, 2007. **51**(3): p. 902-11.
253. Lai, C.L., et al., *Telbivudine versus lamivudine in patients with chronic hepatitis B.* N Engl J Med, 2007. **357**(25): p. 2576-88.
254. Lok, A.S. and B.J. McMahon, *Chronic hepatitis B.* Hepatology, 2007. **45**(2): p. 507-39.
255. Yang, H., et al., *Cross-resistance testing of next-generation nucleoside and nucleotide analogues against lamivudine-resistant HBV.* Antivir Ther, 2005. **10**(5): p. 625-33.

256. Lai, C.L., et al., *A 1-year trial of telbivudine, lamivudine, and the combination in patients with hepatitis B e antigen-positive chronic hepatitis B.* Gastroenterology, 2005. **129**(2): p. 528-36.
257. Sheldon, J., et al., *Selection of hepatitis B virus polymerase mutations in HIV-coinfected patients treated with tenofovir.* Antivir Ther, 2005. **10**(6): p. 727-34.
258. Tillmann, H.L., *The treatment of chronic hepatitis B: Focus on adefovir-like antivirals.* Ther Clin Risk Manag, 2008. **4**(4): p. 797-802.
259. Keeffe, E.B., et al., *Chronic hepatitis B: preventing, detecting, and managing viral resistance.* Clin Gastroenterol Hepatol, 2008. **6**(3): p. 268-74.
260. Dienstag, J.L., et al., *Lamivudine as initial treatment for chronic hepatitis B in the United States.* N Engl J Med, 1999. **341**(17): p. 1256-63.
261. Hadziyannis, S.J., et al., *Adefovir dipivoxil for the treatment of hepatitis B e antigen-negative chronic hepatitis B.* N Engl J Med, 2003. **348**(9): p. 800-7.
262. Chang, T.T., et al., *A comparison of entecavir and lamivudine for HBeAg-positive chronic hepatitis B.* N Engl J Med, 2006. **354**(10): p. 1001-10.
263. Sasadeusz, J.J., S.L. Locarnini, and G. Macdonald, *Why do we not yet have combination chemotherapy for chronic hepatitis B?* Med J Aust, 2007. **186**(4): p. 204-6.
264. Deres, K., et al., *Inhibition of hepatitis B virus replication by drug-induced depletion of nucleocapsids.* Science, 2003. **299**(5608): p. 893-6.
265. Butz, K., et al., *Peptide aptamers targeting the hepatitis B virus core protein: a new class of molecules with antiviral activity.* Oncogene, 2001. **20**(45): p. 6579-86.
266. Li, Y., et al., *Inhibition of hepatitis B virus gene expression and replication by helioxanthin and its derivative.* Antivir Chem Chemother, 2005. **16**(3): p. 193-201.
267. Yeo, H., et al., *Synthesis and antiviral activity of helioxanthin analogues.* J Med Chem, 2005. **48**(2): p. 534-46.
268. McCaffrey, A.P., et al., *Inhibition of hepatitis B virus in mice by RNA interference.* Nat Biotechnol, 2003. **21**(6): p. 639-44.
269. Gelderblom, H.R., et al., *Fine structure of human immunodeficiency virus (HIV) and immunolocalization of structural proteins.* 1987. **156**(1): p. 171-6.
270. Doms, R.W. and S.C. Peiper, *Unwelcomed guests with master keys: how HIV uses chemokine receptors for cellular entry.* 1997. **235**(2): p. 179-90.
271. Stein, B.S., et al., *pH-independent HIV entry into CD4-positive T cells via virus envelope fusion to the plasma membrane.* 1987. **49**(5): p. 659-68.
272. Braaten, D., E.K. Franke, and J. Luban, *Cyclophilin A is required for an early step in the life cycle of human immunodeficiency virus type 1 before the initiation of reverse transcription.* 1996. **70**(6): p. 3551-60.
273. Luban, J., et al., *Human immunodeficiency virus type 1 Gag protein binds to cyclophilins A and B.* 1993. **73**(6): p. 1067-78.
274. Goff, S.P., *Host factors exploited by retroviruses.* 2007. **5**(4): p. 253-63.

275. Farnet, C.M. and W.A. Haseltine, *Determination of viral proteins present in the human immunodeficiency virus type 1 preintegration complex.* 1991. **65**(4): p. 1910-5.
276. Miller, M.D., C.M. Farnet, and F.D. Bushman, *Human immunodeficiency virus type 1 preintegration complexes: studies of organization and composition.* 1997. **71**(7): p. 5382-90.
277. Weinberg, J.B., et al., *Productive human immunodeficiency virus type 1 (HIV-1) infection of nonproliferating human monocytes.* 1991. **174**(6): p. 1477-82.
278. Bukrinsky, M.I., et al., *Active nuclear import of human immunodeficiency virus type 1 preintegration complexes.* 1992. **89**(14): p. 6580-4.
279. Gallay, P., et al., *HIV-1 infection of nondividing cells: C-terminal tyrosine phosphorylation of the viral matrix protein is a key regulator.* 1995. **80**(3): p. 379-88.
280. Heinzinger, N.K., et al., *The Vpr protein of human immunodeficiency virus type 1 influences nuclear localization of viral nucleic acids in nondividing host cells.* 1994. **91**(15): p. 7311-5.
281. Zaitseva, L., R. Myers, and A. Fassati, *tRNAs promote nuclear import of HIV-1 intracellular reverse transcription complexes.* 2006. **4**(10): p. e332.
282. Kulkosky, J. and A.M. Skalka, *Molecular mechanism of retroviral DNA integration.* 1994. **61**(1-2): p. 185-203.
283. Roth, M.J., P.L. Schwartzberg, and S.P. Goff, *Structure of the termini of DNA intermediates in the integration of retroviral DNA: dependence on IN function and terminal DNA sequence.* 1989. **58**(1): p. 47-54.
284. Yankulov, K. and D. Bentley, *Transcriptional control: Tat cofactors and transcriptional elongation.* 1998. **8**(13): p. R447-9.
285. Pereira, L.A., et al., *A compilation of cellular transcription factor interactions with the HIV-1 LTR promoter.* 2000. **28**(3): p. 663-8.
286. Wu, Y., *HIV-1 gene expression: lessons from provirus and non-integrated DNA.* 2004. **1**: p. 13.
287. Malim, M.H., et al., *The HIV-1 rev trans-activator acts through a structured target sequence to activate nuclear export of unspliced viral mRNA.* 1989. **338**(6212): p. 254-7.
288. Cullen, B.R., *Regulation of HIV-1 gene expression.* 1991. **5**(10): p. 2361-8.
289. Gottlinger, H.G., J.G. Sodroski, and W.A. Haseltine, *Role of capsid precursor processing and myristoylation in morphogenesis and infectivity of human immunodeficiency virus type 1.* 1989. **86**(15): p. 5781-5.
290. Bryant, M. and L. Ratner, *Myristoylation-dependent replication and assembly of human immunodeficiency virus 1.* 1990. **87**(2): p. 523-7.
291. Smith, A.J., et al., *Requirements for incorporation of Pr160gag-pol from human immunodeficiency virus type 1 into virus-like particles.* 1993. **67**(4): p. 2266-75.
292. Borsetti, A., A. Ohagen, and H.G. Gottlinger, *The C-terminal half of the human immunodeficiency virus type 1 Gag precursor is sufficient for efficient particle assembly.* 1998. **72**(11): p. 9313-7.

293. Park, J. and C.D. Morrow, *The nonmyristylated Pr160gag-pol polyprotein of human immunodeficiency virus type 1 interacts with Pr55gag and is incorporated into viruslike particles.* 1992. **66**(11): p. 6304-13.
294. Lever, A., et al., *Identification of a sequence required for efficient packaging of human immunodeficiency virus type 1 RNA into virions.* 1989. **63**(9): p. 4085-7.
295. Khorchid, A., et al., *Sequences within Pr160gag-pol affecting the selective packaging of primer tRNA(Lys3) into HIV-1.* 2000. **299**(1): p. 17-26.
296. Mak, J., et al., *Role of Pr160gag-pol in mediating the selective incorporation of tRNA(Lys) into human immunodeficiency virus type 1 particles.* 1994. **68**(4): p. 2065-72.
297. Javanbakht, H., et al., *Correlation between tRNALys3 aminoacylation and its incorporation into HIV-1.* 2002. **277**(20): p. 17389-96.
298. Kondo, E., et al., *The p6gag domain of human immunodeficiency virus type 1 is sufficient for the incorporation of Vpr into heterologous viral particles.* 1995. **69**(5): p. 2759-64.
299. Khan, M.A., et al., *Human immunodeficiency virus type 1 Vif protein is packaged into the nucleoprotein complex through an interaction with viral genomic RNA.* 2001. **75**(16): p. 7252-65.
300. Huvent, I., et al., *Interaction and co-encapsidation of human immunodeficiency virus type 1 Gag and Vif recombinant proteins.* 1998. **79 (Pt 5)**: p. 1069-81.
301. Welker, R., et al., *Virion incorporation of human immunodeficiency virus type 1 Nef is mediated by a bipartite membrane-targeting signal: analysis of its role in enhancement of viral infectivity.* 1998. **72**(11): p. 8833-40.
302. Welker, R., et al., *Human immunodeficiency virus type 1 Nef protein is incorporated into virus particles and specifically cleaved by the viral proteinase.* 1996. **219**(1): p. 228-36.
303. Einfeld, D., *Maturation and assembly of retroviral glycoproteins.* 1996. **214**: p. 133-76.
304. Lopez-Verges, S., et al., *Tail-interacting protein TIP47 is a connector between Gag and Env and is required for Env incorporation into HIV-1 virions.* 2006. **103**(40): p. 14947-52.
305. Gottlinger, H.G., et al., *Effect of mutations affecting the p6 gag protein on human immunodeficiency virus particle release.* 1991. **88**(8): p. 3195-9.
306. von Schwedler, U.K., et al., *The protein network of HIV budding.* 2003. **114**(6): p. 701-13.
307. Vogt, V.M., *Proteolytic processing and particle maturation.* 1996. **214**: p. 95-131.
308. Kohl, N.E., et al., *Active human immunodeficiency virus protease is required for viral infectivity.* 1988. **85**(13): p. 4686-90.
309. Hansen, J., et al., *Identification and characterization of HIV-specific RNase H by monoclonal antibody.* 1988. **7**(1): p. 239-43.
310. Gotte, M., X. Li, and M.A. Wainberg, *HIV-1 reverse transcription: a brief overview focused on structure-function relationships among molecules involved in initiation of the reaction.* 1999. **365**(2): p. 199-210.

311. Goff, S.P., *Retroviral reverse transcriptase: synthesis, structure, and function.* 1990. **3**(8): p. 817-31.
312. Ratner, L., et al., *Complete nucleotide sequence of the AIDS virus, HTLV-III.* 1985. **313**(6000): p. 277-84.
313. Jacks, T., et al., *Characterization of ribosomal frameshifting in HIV-1 gag-pol expression.* 1988. **331**(6153): p. 280-3.
314. di Marzo Veronese, F., et al., *Characterization of highly immunogenic p66/p51 as the reverse transcriptase of HTLV-III/LAV.* 1986. **231**(4743): p. 1289-91.
315. Farmerie, W.G., et al., *Expression and processing of the AIDS virus reverse transcriptase in Escherichia coli.* 1987. **236**(4799): p. 305-8.
316. Muller, B., et al., *Co-expression of the subunits of the heterodimer of HIV-1 reverse transcriptase in Escherichia coli.* 1989. **264**(24): p. 13975-8.
317. Le Grice, S.F., et al., *Subunit-selective mutagenesis indicates minimal polymerase activity in heterodimer-associated p51 HIV-1 reverse transcriptase.* 1991. **10**(12): p. 3905-11.
318. Starnes, M.C., et al., *Enzyme activity gel analysis of human immunodeficiency virus reverse transcriptase.* 1988. **263**(11): p. 5132-4.
319. Kohlstaedt, L.A., et al., *Crystal structure at 3.5 A resolution of HIV-1 reverse transcriptase complexed with an inhibitor.* 1992. **256**(5065): p. 1783-90.
320. Jacobo-Molina, A., et al., *Crystal structure of human immunodeficiency virus type 1 reverse transcriptase complexed with double-stranded DNA at 3.0 A resolution shows bent DNA.* 1993. **90**(13): p. 6320-4.
321. Sarafianos, S.G., et al., *Touching the heart of HIV-1 drug resistance: the fingers close down on the dNTP at the polymerase active site.* 1999. **6**(5): p. R137-46.
322. Huang, H., et al., *Structure of a covalently trapped catalytic complex of HIV-1 reverse transcriptase: implications for drug resistance.* 1998. **282**(5394): p. 1669-75.
323. Patel, P.H., et al., *Insights into DNA polymerization mechanisms from structure and function analysis of HIV-1 reverse transcriptase.* 1995. **34**(16): p. 5351-63.
324. Copeland, R.A., *Enzymes: A Practical Introduction to Structure, Mechanism, and Data Analysis*. 2 ed. 2000: Wiley-IEEE.
325. Larder, B.A., et al., *Site-specific mutagenesis of AIDS virus reverse transcriptase.* Nature, 1987. **327**(6124): p. 716-7.
326. Erickson, J.W. and S.K. Burt, *Structural mechanisms of HIV drug resistance.* Annu Rev Pharmacol Toxicol, 1996. **36**: p. 545-71.
327. Smerdon, S.J., et al., *Structure of the binding site for nonnucleoside inhibitors of the reverse transcriptase of human immunodeficiency virus type 1.* Proc Natl Acad Sci U S A, 1994. **91**(9): p. 3911-5.
328. Sarafianos, S.G., et al., *Structure and function of HIV-1 reverse transcriptase: molecular mechanisms of polymerization and inhibition.* J Mol Biol, 2009. **385**(3): p. 693-713.
329. Hsiou, Y., et al., *Structure of unliganded HIV-1 reverse transcriptase at 2.7 A resolution: implications of conformational changes for*

polymerization and inhibition mechanisms. Structure, 1996. **4**(7): p. 853-60.
330. Sarafianos, S.G., et al., *Structures of HIV-1 reverse transcriptase with pre- and post-translocation AZTMP-terminated DNA.* EMBO J, 2002. **21**(23): p. 6614-24.
331. Das, K., et al., *Crystal structures of clinically relevant Lys103Asn/Tyr181Cys double mutant HIV-1 reverse transcriptase in complexes with ATP and non-nucleoside inhibitor HBY 097.* J Mol Biol, 2007. **365**(1): p. 77-89.
332. Condra, J.H., et al., *Identification of the human immunodeficiency virus reverse transcriptase residues that contribute to the activity of diverse nonnucleoside inhibitors.* Antimicrob Agents Chemother, 1992. **36**(7): p. 1441-6.
333. Food and Drug Administration, U.S., *Drugs Used in the Treatment of HIV Infection.* http://www.fda.gov/oashi/aids/virals.html, 2008.
334. Eisenberg, E.J., G.X. He, and W.A. Lee, *Metabolism of GS-7340, a novel phenyl monophosphoramidate intracellular prodrug of PMPA, in blood.* Nucleosides Nucleotides Nucleic Acids, 2001. **20**(4-7): p. 1091-8.
335. Tong, W., et al., *Nucleotide-induced stable complex formation by HIV-1 reverse transcriptase.* Biochemistry, 1997. **36**(19): p. 5749-57.
336. Johnson, A.A., et al., *Toxicity of antiviral nucleoside analogs and the human mitochondrial DNA polymerase.* J Biol Chem, 2001. **276**(44): p. 40847-57.
337. Feng, J.Y., et al., *Relationship between antiviral activity and host toxicity: comparison of the incorporation efficiencies of 2',3'-dideoxy-5-fluoro-3'-thiacytidine-triphosphate analogs by human immunodeficiency virus type 1 reverse transcriptase and human mitochondrial DNA polymerase.* Antimicrob Agents Chemother, 2004. **48**(4): p. 1300-6.
338. Spence, R.A., et al., *Mechanism of inhibition of HIV-1 reverse transcriptase by nonnucleoside inhibitors.* Science, 1995. **267**(5200): p. 988-93.
339. Moyle, G., *The emerging roles of non-nucleoside reverse transcriptase inhibitors in antiretroviral therapy.* Drugs, 2001. **61**(1): p. 19-26.
340. Larder, B.A. and S.D. Kemp, *Multiple mutations in HIV-1 reverse transcriptase confer high-level resistance to zidovudine (AZT).* Science, 1989. **246**(4934): p. 1155-8.
341. Mayers, D., *Rational approaches to resistance: nucleoside analogues.* AIDS, 1996. **10 Suppl 1**: p. S9-13.
342. Saag, M.S., et al., *Extensive variation of human immunodeficiency virus type-1 in vivo.* Nature, 1988. **334**(6181): p. 440-4.
343. Meyerhans, A., et al., *Temporal fluctuations in HIV quasispecies in vivo are not reflected by sequential HIV isolations.* Cell, 1989. **58**(5): p. 901-10.
344. Briones, C., E. Domingo, and C. Molina-Paris, *Memory in retroviral quasispecies: experimental evidence and theoretical model for human immunodeficiency virus.* J Mol Biol, 2003. **331**(1): p. 213-29.

345. Gotte, M., *Inhibition of HIV-1 reverse transcription: basic principles of drug action and resistance.* Expert Rev Anti Infect Ther, 2004. **2**(5): p. 707-16.
346. Meyer, P.R., et al., *A mechanism of AZT resistance: an increase in nucleotide-dependent primer unblocking by mutant HIV-1 reverse transcriptase.* Mol Cell, 1999. **4**(1): p. 35-43.
347. Meyer, P.R., et al., *Unblocking of chain-terminated primer by HIV-1 reverse transcriptase through a nucleotide-dependent mechanism.* Proc Natl Acad Sci U S A, 1998. **95**(23): p. 13471-6.
348. Boucher, C.A., et al., *High-level resistance to (-) enantiomeric 2'-deoxy-3'-thiacytidine in vitro is due to one amino acid substitution in the catalytic site of human immunodeficiency virus type 1 reverse transcriptase.* Antimicrob Agents Chemother, 1993. **37**(10): p. 2231-4.
349. Schinazi, R.F., et al., *Characterization of human immunodeficiency viruses resistant to oxathiolane-cytosine nucleosides.* Antimicrob Agents Chemother, 1993. **37**(4): p. 875-81.
350. Sarafianos, S.G., et al., *Lamivudine (3TC) resistance in HIV-1 reverse transcriptase involves steric hindrance with beta-branched amino acids.* Proc Natl Acad Sci U S A, 1999. **96**(18): p. 10027-32.
351. Selmi, B., et al., *Mechanism-based suppression of dideoxynucleotide resistance by K65R human immunodeficiency virus reverse transcriptase using an alpha-boranophosphate nucleoside analogue.* J Biol Chem, 2001. **276**(51): p. 48466-72.
352. Deval, J., et al., *Mechanistic basis for reduced viral and enzymatic fitness of HIV-1 reverse transcriptase containing both K65R and M184V mutations.* J Biol Chem, 2004. **279**(1): p. 509-16.
353. Deval, J., et al., *A loss of viral replicative capacity correlates with altered DNA polymerization kinetics by the human immunodeficiency virus reverse transcriptase bearing the K65R and L74V dideoxynucleoside resistance substitutions.* J Biol Chem, 2004. **279**(24): p. 25489-96.
354. Sarafianos, S.G., et al., *Taking aim at a moving target: designing drugs to inhibit drug-resistant HIV-1 reverse transcriptases.* Curr Opin Struct Biol, 2004. **14**(6): p. 716-30.
355. St Clair, M.H., et al., *Resistance to ddI and sensitivity to AZT induced by a mutation in HIV-1 reverse transcriptase.* Science, 1991. **253**(5027): p. 1557-9.
356. Parikh, U.M., et al., *Antagonism between the HIV-1 reverse-transcriptase mutation K65R and thymidine-analogue mutations at the genomic level.* J Infect Dis, 2006. **194**(5): p. 651-60.
357. Gotte, M., et al., *The M184V mutation in the reverse transcriptase of human immunodeficiency virus type 1 impairs rescue of chain-terminated DNA synthesis.* J Virol, 2000. **74**(8): p. 3579-85.
358. Larder, B.A., S.D. Kemp, and P.R. Harrigan, *Potential mechanism for sustained antiretroviral efficacy of AZT-3TC combination therapy.* Science, 1995. **269**(5224): p. 696-9.
359. Marchand, B. and M. Gotte, *Site-specific footprinting reveals differences in the translocation status of HIV-1 reverse transcriptase. Implications for*

polymerase translocation and drug resistance. J Biol Chem, 2003. **278**(37): p. 35362-72.
360. White, K.L., et al., *Molecular mechanisms of tenofovir resistance conferred by human immunodeficiency virus type 1 reverse transcriptase containing a diserine insertion after residue 69 and multiple thymidine analog-associated mutations.* Antimicrob Agents Chemother, 2004. **48**(3): p. 992-1003.
361. Prado, J.G., et al., *Relative replication fitness of multi-nucleoside analogue-resistant HIV-1 strains bearing a dipeptide insertion in the fingers subdomain of the reverse transcriptase and mutations at codons 67 and 215.* Virology, 2004. **326**(1): p. 103-12.
362. Menendez-Arias, L., T. Matamoros, and C.E. Cases-Gonzalez, *Insertions and deletions in HIV-1 reverse transcriptase: consequences for drug resistance and viral fitness.* Curr Pharm Des, 2006. **12**(15): p. 1811-25.
363. Ehteshami, M., et al., *Connection domain mutations N348I and A360V in HIV-1 reverse transcriptase enhance resistance to 3'-azido-3'-deoxythymidine through both RNase H-dependent and -independent mechanisms.* J Biol Chem, 2008. **283**(32): p. 22222-32.
364. Das, K., et al., *Crystallography and the design of anti-AIDS drugs: conformational flexibility and positional adaptability are important in the design of non-nucleoside HIV-1 reverse transcriptase inhibitors.* Prog Biophys Mol Biol, 2005. **88**(2): p. 209-31.
365. Hirsch, M.S., et al., *Antiretroviral drug resistance testing in adult HIV-1 infection: 2008 recommendations of an International AIDS Society-USA panel.* Clin Infect Dis, 2008. **47**(2): p. 266-85.
366. El Safadi, Y., V. Vivet-Boudou, and R. Marquet, *HIV-1 reverse transcriptase inhibitors.* Appl Microbiol Biotechnol, 2007. **75**(4): p. 723-37.
367. Larder, B.A., *3'-Azido-3'-deoxythymidine resistance suppressed by a mutation conferring human immunodeficiency virus type 1 resistance to nonnucleoside reverse transcriptase inhibitors.* Antimicrob Agents Chemother, 1992. **36**(12): p. 2664-9.
368. Dueweke, T.J., et al., *A mutation in reverse transcriptase of bis(heteroaryl)piperazine-resistant human immunodeficiency virus type 1 that confers increased sensitivity to other nonnucleoside inhibitors.* Proc Natl Acad Sci U S A, 1993. **90**(10): p. 4713-7.
369. Balzarini, J., *Current status of the non-nucleoside reverse transcriptase inhibitors of human immunodeficiency virus type 1.* Curr Top Med Chem, 2004. **4**(9): p. 921-44.
370. Chow, Y.K., et al., *Use of evolutionary limitations of HIV-1 multidrug resistance to optimize therapy.* Nature, 1993. **361**(6413): p. 650-4.
371. Siegal, F.P., et al., *Severe acquired immunodeficiency in male homosexuals, manifested by chronic perianal ulcerative herpes simplex lesions.* N Engl J Med, 1981. **305**(24): p. 1439-44.
372. *1993 revised classification system for HIV infection and expanded surveillance case definition for AIDS among adolescents and adults.* MMWR Recomm Rep, 1992. **41**(RR-17): p. 1-19.

373. Wald, A. and K. Link, *Risk of human immunodeficiency virus infection in herpes simplex virus type 2-seropositive persons: a meta-analysis.* J Infect Dis, 2002. **185**(1): p. 45-52.
374. Forbi, J.C., et al., *The role of triple infection with hepatitis B virus, hepatitis C virus, and human immunodeficiency virus (HIV) type-1 on CD4+ lymphocyte levels in the highly HIV infected population of North-Central Nigeria.* Mem Inst Oswaldo Cruz, 2007. **102**(4): p. 535-7.
375. Konopnicki, D., et al., *Hepatitis B and HIV: prevalence, AIDS progression, response to highly active antiretroviral therapy and increased mortality in the EuroSIDA cohort.* AIDS, 2005. **19**(6): p. 593-601.
376. Cicin-Sain, L., et al., *Frequent coinfection of cells explains functional in vivo complementation between cytomegalovirus variants in the multiply infected host.* J Virol, 2005. **79**(15): p. 9492-502.
377. Javier, R.T., F. Sedarati, and J.G. Stevens, *Two avirulent herpes simplex viruses generate lethal recombinants in vivo.* Science, 1986. **234**(4777): p. 746-8.
378. Drew, W.L., et al., *Multiple infections by cytomegalovirus in patients with acquired immunodeficiency syndrome: documentation by Southern blot hybridization.* J Infect Dis, 1984. **150**(6): p. 952-3.
379. Dang, Q., et al., *Nonrandom HIV-1 infection and double infection via direct and cell-mediated pathways.* Proceedings of the National Academy of Sciences of the United States of America, 2004. **101**(2): p. 632-637.
380. Kucera, L.S., et al., *Human immunodeficiency virus type 1 (HIV-1) and herpes simplex virus type 2 (HSV-2) can coinfect and simultaneously replicate in the same human CD4+ cell: effect of coinfection on infectious HSV-2 and HIV-1 replication.* AIDS Res Hum Retroviruses, 1990. **6**(5): p. 641-7.
381. Salahuddin, S.Z., et al., *The simultaneous presence and expression of human hepatitis C virus (HCV), human herpesvirus-6 (HHV-6), and human immunodeficiency virus-1 (HIV-1) in a single human T-cell.* Virol J, 2007. **4**: p. 106.
382. Albrecht, M.A., et al., *The herpes simplex virus immediate-early protein, ICP4, is required to potentiate replication of human immunodeficiency virus in CD4+ lymphocytes.* J Virol, 1989. **63**(5): p. 1861-8.
383. Mosca, J.D., et al., *Activation of human immunodeficiency virus by herpesvirus infection: identification of a region within the long terminal repeat that responds to a trans-acting factor encoded by herpes simplex virus 1.* Proc Natl Acad Sci U S A, 1987. **84**(21): p. 7408-12.
384. Lusso, P., et al., *Induction of CD4 and susceptibility to HIV-1 infection in human CD8+ T lymphocytes by human herpesvirus 6.* Nature, 1991. **349**(6309): p. 533-5.
385. McCarthy, M., et al., *Cytomegalovirus and human herpesvirus-6 trans-activate the HIV-1 long terminal repeat via multiple response regions in human fetal astrocytes.* J Neurovirol, 1998. **4**(5): p. 495-511.

386. Regezi, J.A., et al., *Herpes simplex and cytomegalovirus coinfected oral ulcers in HIV-positive patients.* Oral Surg Oral Med Oral Pathol Oral Radiol Endod, 1996. **81**(1): p. 55-62.
387. Lusso, P. and R.C. Gallo, *Human herpesvirus 6 in AIDS.* Immunol Today, 1995. **16**(2): p. 67-71.
388. Jacobson, M.A. and J. Mills, *Serious cytomegalovirus disease in the acquired immunodeficiency syndrome (AIDS). Clinical findings, diagnosis, and treatment.* Ann Intern Med, 1988. **108**(4): p. 585-94.
389. Posavad, C.M., et al., *Severe genital herpes infections in HIV-infected individuals with impaired herpes simplex virus-specific CD8+ cytotoxic T lymphocyte responses.* Proc Natl Acad Sci U S A, 1997. **94**(19): p. 10289-94.
390. Koelle, D.M., et al., *Clearance of HSV-2 from recurrent genital lesions correlates with infiltration of HSV-specific cytotoxic T lymphocytes.* J Clin Invest, 1998. **101**(7): p. 1500-8.
391. Schacker, T., et al., *Changes in plasma human immunodeficiency virus type 1 RNA associated with herpes simplex virus reactivation and suppression.* J Infect Dis, 2002. **186**(12): p. 1718-25.
392. Thio, C.L., et al., *HIV-1, hepatitis B virus, and risk of liver-related mortality in the Multicenter Cohort Study (MACS).* Lancet, 2002. **360**(9349): p. 1921-6.
393. Sulkowski, M.S., et al., *Hepatitis C virus infection as an opportunistic disease in persons infected with human immunodeficiency virus.* Clin Infect Dis, 2000. **30 Suppl 1**: p. S77-84.
394. Zuckerman, R.A., et al., *Herpes simplex virus (HSV) suppression with valacyclovir reduces rectal and blood plasma HIV-1 levels in HIV-1/HSV-2-seropositive men: a randomized, double-blind, placebo-controlled crossover trial.* J Infect Dis, 2007. **196**(10): p. 1500-8.
395. Dunne, E.F., et al., *Suppressive acyclovir therapy reduces HIV cervicovaginal shedding in HIV- and HSV-2-infected women, Chiang Rai, Thailand.* J Acquir Immune Defic Syndr, 2008. **49**(1): p. 77-83.
396. Springer, K.L. and A. Weinberg, *Cytomegalovirus infection in the era of HAART: fewer reactivations and more immunity.* J Antimicrob Chemother, 2004. **54**(3): p. 582-6.
397. De Clercq, E., *Antiviral drugs in current clinical use.* J Clin Virol, 2004. **30**(2): p. 115-33.
398. Chou, S.W., *Cytomegalovirus drug resistance and clinical implications.* Transpl Infect Dis, 2001. **3 Suppl 2**: p. 20-4.
399. Drew, W.L., C.V. Paya, and V. Emery, *Cytomegalovirus (CMV) resistance to antivirals.* Am J Transplant, 2001. **1**(4): p. 307-12.
400. Erice, A., *Resistance of human cytomegalovirus to antiviral drugs.* Clin Microbiol Rev, 1999. **12**(2): p. 286-97.
401. Morfin, F. and D. Thouvenot, *Herpes simplex virus resistance to antiviral drugs.* J Clin Virol, 2003. **26**(1): p. 29-37.
402. Cihlar, T., M.D. Fuller, and J.M. Cherrington, *Characterization of drug resistance-associated mutations in the human cytomegalovirus DNA*

polymerase gene by using recombinant mutant viruses generated from overlapping DNA fragments. J Virol, 1998. **72**(7): p. 5927-36.
403. Huang, L., et al., *The enzymological basis for resistance of herpesvirus DNA polymerase mutants to acyclovir: relationship to the structure of alpha-like DNA polymerases.* Proc Natl Acad Sci U S A, 1999. **96**(2): p. 447-52.
404. Chou, S., et al., *Viral DNA polymerase mutations associated with drug resistance in human cytomegalovirus.* J Infect Dis, 2003. **188**(1): p. 32-9.
405. Weinberg, A., et al., *Mutations conferring foscarnet resistance in a cohort of patients with acquired immunodeficiency syndrome and cytomegalovirus retinitis.* J Infect Dis, 2003. **187**(5): p. 777-84.
406. Smith, I.L., et al., *High-level resistance of cytomegalovirus to ganciclovir is associated with alterations in both the UL97 and DNA polymerase genes.* J Infect Dis, 1997. **176**(1): p. 69-77.
407. Cihlar, T., M.D. Fuller, and J.M. Cherrington, *Expression of the catalytic subunit (UL54) and the accessory protein (UL44) of human cytomegalovirus DNA polymerase in a coupled in vitro transcription/translation system.* Protein Expr Purif, 1997. **11**(2): p. 209-18.
408. Boosalis, M.S., J. Petruska, and M.F. Goodman, *DNA polymerase insertion fidelity. Gel assay for site-specific kinetics.* J Biol Chem, 1987. **262**(30): p. 14689-96.
409. Freisinger, E., et al., *Lesion (in)tolerance reveals insights into DNA replication fidelity.* EMBO J, 2004. **23**(7): p. 1494-505.
410. Hogg, M., S.S. Wallace, and S. Doublie, *Crystallographic snapshots of a replicative DNA polymerase encountering an abasic site.* EMBO J, 2004. **23**(7): p. 1483-93.
411. Yang, G., et al., *Correlation of the kinetics of finger domain mutants in RB69 DNA polymerase with its structure.* Biochemistry, 2002. **41**(8): p. 2526-34.
412. Bestman-Smith, J. and G. Boivin, *Drug resistance patterns of recombinant herpes simplex virus DNA polymerase mutants generated with a set of overlapping cosmids and plasmids.* J Virol, 2003. **77**(14): p. 7820-9.
413. Loregian, A., et al., *Specific residues in the connector loop of the human cytomegalovirus DNA polymerase accessory protein UL44 are crucial for interaction with the UL54 catalytic subunit.* J Virol, 2004. **78**(17): p. 9084-92.
414. Yin, Y.W. and T.A. Steitz, *The structural mechanism of translocation and helicase activity in T7 RNA polymerase.* Cell, 2004. **116**(3): p. 393-404.
415. Thomsen, D.R., et al., *Amino acid changes within conserved region III of the herpes simplex virus and human cytomegalovirus DNA polymerases confer resistance to 4-oxo-dihydroquinolines, a novel class of herpesvirus antiviral agents.* J Virol, 2003. **77**(3): p. 1868-76.
416. Reardon, J.E. and W.H. Miller, *Human immunodeficiency virus reverse transcriptase. Substrate and inhibitor kinetics with thymidine 5'-triphosphate and 3'-azido-3'-deoxythymidine 5'-triphosphate.* J Biol Chem, 1990. **265**(33): p. 20302-7.

417. Sluis-Cremer, N., et al., *Mutational analysis of Lys65 of HIV-1 reverse transcriptase.* Biochem J, 2000. **348 Pt 1**: p. 77-82.
418. Meyer, P.R., et al., *Relationship between 3'-azido-3'-deoxythymidine resistance and primer unblocking activity in foscarnet-resistant mutants of human immunodeficiency virus type 1 reverse transcriptase.* J Virol, 2003. **77**(11): p. 6127-37.
419. Hsiou, Y., et al., *The Lys103Asn mutation of HIV-1 RT: a novel mechanism of drug resistance.* J Mol Biol, 2001. **309**(2): p. 437-45.
420. Hall, J.D. and S. Woodward, *Aphidicolin resistance in herpes simplex virus type 1 appears to alter substrate specificity in the DNA polymerase.* J Virol, 1989. **63**(6): p. 2874-6.
421. Reha-Krantz, L.J., R.L. Nonay, and S. Stocki, *Bacteriophage T4 DNA polymerase mutations that confer sensitivity to the PPi analog phosphonoacetic acid.* J Virol, 1993. **67**(1): p. 60-6.
422. Tsurumi, T., K. Maeno, and Y. Nishiyama, *A single-base change within the DNA polymerase locus of herpes simplex virus type 2 can confer resistance to aphidicolin.* J Virol, 1987. **61**(2): p. 388-94.
423. Franklin, M.C., J. Wang, and T.A. Steitz, *14_Structure of the replicating complex of a pol alpha family DNA polymerase.* Cell, 2001. **105**(5): p. 657-67.
424. Ljungman, P., *Beta-herpesvirus challenges in the transplant recipient.* J Infect Dis, 2002. **186 Suppl 1**: p. S99-S109.
425. Hassan, J. and J. Connell, *Translational mini-review series on infectious disease: congenital cytomegalovirus infection: 50 years on.* Clin Exp Immunol, 2007. **149**(2): p. 205-10.
426. Boppana, S.B., et al., *Symptomatic congenital cytomegalovirus infection: neonatal morbidity and mortality.* Pediatr Infect Dis J, 1992. **11**(2): p. 93-9.
427. Griffiths, P.D. and S. Walter, *Cytomegalovirus.* Curr Opin Infect Dis, 2005. **18**(3): p. 241-5.
428. Deayton, J.R., et al., *Importance of cytomegalovirus viraemia in risk of disease progression and death in HIV-infected patients receiving highly active antiretroviral therapy.* Lancet, 2004. **363**(9427): p. 2116-21.
429. Andrei, G., E. De Clercq, and R. Snoeck, *Novel inhibitors of human CMV.* Curr Opin Investig Drugs, 2008. **9**(2): p. 132-45.
430. De Clercq, E., *New inhibitors of human cytomegalovirus (HCMV) on the horizon.* J Antimicrob Chemother, 2003. **51**(5): p. 1079-83.
431. Deval, J., *Antimicrobial strategies: inhibition of viral polymerases by 3'-hydroxyl nucleosides.* Drugs, 2009. **69**(2): p. 151-66.
432. Reardon, J.E., *Herpes simplex virus type 1 and human DNA polymerase interactions with 2'-deoxyguanosine 5'-triphosphate analogues. Kinetics of incorporation into DNA and induction of inhibition.* J Biol Chem, 1989. **264**(32): p. 19039-44.
433. Talarico, C.L., et al., *Acyclovir is phosphorylated by the human cytomegalovirus UL97 protein.* Antimicrob Agents Chemother, 1999. **43**(8): p. 1941-6.

434. Zimmermann, A., et al., *Phosphorylation of aciclovir, ganciclovir, penciclovir and S2242 by the cytomegalovirus UL97 protein: a quantitative analysis using recombinant vaccinia viruses.* Antiviral Res, 1997. **36**(1): p. 35-42.
435. Eriksson, B.F. and R.F. Schinazi, *Combinations of 3'-azido-3'-deoxythymidine (zidovudine) and phosphonoformate (foscarnet) against human immunodeficiency virus type 1 and cytomegalovirus replication in vitro.* Antimicrob Agents Chemother, 1989. **33**(5): p. 663-9.
436. Boyer, P.L., et al., *Selective excision of AZTMP by drug-resistant human immunodeficiency virus reverse transcriptase.* J Virol, 2001. **75**(10): p. 4832-42.
437. Gotte, M., *Effects of nucleotides and nucleotide analogue inhibitors of HIV-1 reverse transcriptase in a ratchet model of polymerase translocation.* Curr Pharm Des, 2006. **12**(15): p. 1867-77.
438. Ducancelle, A., et al., *Phenotypic characterisation of cytomegalovirus DNA polymerase: a method to study cytomegalovirus isolates resistant to foscarnet.* J Virol Methods, 2005. **125**(2): p. 145-51.
439. Picard-Jean, F., I. Bougie, and M. Bisaillon, *Characterization of the DNA- and dNTP-binding activities of the human cytomegalovirus DNA polymerase catalytic subunit UL54.* Biochem J, 2007. **407**(3): p. 331-41.
440. Loregian, A., et al., *Inhibition of human cytomegalovirus DNA polymerase by C-terminal peptides from the UL54 subunit.* J Virol, 2003. **77**(15): p. 8336-44.
441. Loregian, A., et al., *Residues of human cytomegalovirus DNA polymerase catalytic subunit UL54 that are necessary and sufficient for interaction with the accessory protein UL44.* J Virol, 2004. **78**(1): p. 158-67.
442. Tchesnokov, E.P., et al., *Role of helix P of the human cytomegalovirus DNA polymerase in resistance and hypersusceptibility to the antiviral drug foscarnet.* J Virol, 2006. **80**(3): p. 1440-50.
443. Chaudhuri, M., L. Song, and D.S. Parris, *The herpes simplex virus type 1 DNA polymerase processivity factor increases fidelity without altering pre-steady-state rate constants for polymerization or excision.* J Biol Chem, 2003. **278**(11): p. 8996-9004.
444. Yang, G., et al., *Steady-state kinetic characterization of RB69 DNA polymerase mutants that affect dNTP incorporation.* Biochemistry, 1999. **38**(25): p. 8094-101.
445. Baldanti, F., N. Lurain, and G. Gerna, *Clinical and biologic aspects of human cytomegalovirus resistance to antiviral drugs.* Hum Immunol, 2004. **65**(5): p. 403-9.
446. Le Grice, S.F., C.E. Cameron, and S.J. Benkovic, *Purification and characterization of human immunodeficiency virus type 1 reverse transcriptase.* Methods Enzymol, 1995. **262**: p. 130-44.
447. Burgess, K. and D. Cook, *Syntheses of nucleoside triphosphates.* Chem Rev, 2000. **100**(6): p. 2047-60.
448. Copeland, R.A., *Evaluation of Enzyme Inhibitors in Drug Discovery : A Primer for Medicinal Chemists and Pharmacologists*. 2005, John Wiley & Sons Inc.: Hoboken. p. 295.

449. Copeland, R.A. and John Wiley & Sons Inc., *Enzymes (Second Edition)*. 2000, Wiley-VCH. p. xxx, 416.
450. http://www.ncbi.nlm.nih.gov/Structure/CN3D/cn3d.shtml, *Cn3D, a visualization tool for biomolecular structures, sequences, and sequence alignments.*
451. Gouet, P., X. Robert, and E. Courcelle, *ESPript/ENDscript: extracting and rendering sequence and 3D information from atomic structures of proteins.* Nucl. Acids Res., 2003. **31**(13): p. 3320-3323.
452. Gouet, P., et al., *ESPript: analysis of multiple sequence alignments in PostScript.* Bioinformatics, 1999. **15**(4): p. 305-8.
453. Baldanti, F., et al., *Four dually resistant human cytomegalovirus strains from AIDS patients: single mutations in UL97 and UL54 open reading frames are responsible for ganciclovir- and foscarnet-specific resistance, respectively.* Scand J Infect Dis Suppl, 1995. **99**: p. 103-4.
454. Kati, W.M., et al., *Mechanism and fidelity of HIV reverse transcriptase.* J Biol Chem, 1992. **267**(36): p. 25988-97.
455. Kuchta, R.D., et al., *Kinetic mechanism of DNA polymerase I (Klenow).* Biochemistry, 1987. **26**(25): p. 8410-7.
456. Patel, S.S., I. Wong, and K.A. Johnson, *Pre-steady-state kinetic analysis of processive DNA replication including complete characterization of an exonuclease-deficient mutant.* Biochemistry, 1991. **30**(2): p. 511-25.
457. Deval, J., et al., *Mechanistic insights into the suppression of drug resistance by human immunodeficiency virus type 1 reverse transcriptase using alpha-boranophosphate nucleoside analogs.* J Biol Chem, 2005. **280**(5): p. 3838-46.
458. Diallo, K., M. Gotte, and M.A. Wainberg, *Molecular impact of the M184V mutation in human immunodeficiency virus type 1 reverse transcriptase.* Antimicrob Agents Chemother, 2003. **47**(11): p. 3377-83.
459. Gotte, M. and M.A. Wainberg, *Biochemical mechanisms involved in overcoming HIV resistance to nucleoside inhibitors of reverse transcriptase.* Drug Resist Updat, 2000. **3**(1): p. 30-38.
460. Lacey, S.F. and B.A. Larder, *Novel mutation (V75T) in human immunodeficiency virus type 1 reverse transcriptase confers resistance to 2',3'-didehydro-2',3'-dideoxythymidine in cell culture.* Antimicrob Agents Chemother, 1994. **38**(6): p. 1428-32.
461. Goldschmidt, V. and R. Marquet, *Primer unblocking by HIV-1 reverse transcriptase and resistance to nucleoside RT inhibitors (NRTIs).* Int J Biochem Cell Biol, 2004. **36**(9): p. 1687-705.
462. Menendez-Arias, L., *Mechanisms of resistance to nucleoside analogue inhibitors of HIV-1 reverse transcriptase.* Virus Res, 2008. **134**(1-2): p. 124-46.
463. Sluis-Cremer, N., D. Arion, and M.A. Parniak, *Molecular mechanisms of HIV-1 resistance to nucleoside reverse transcriptase inhibitors (NRTIs).* Cell Mol Life Sci, 2000. **57**(10): p. 1408-22.
464. Basavapathruni, A. and K.S. Anderson, *Reverse transcription of the HIV-1 pandemic.* FASEB J, 2007. **21**(14): p. 3795-808.

465. McGuigan, C., et al., *Successful kinase bypass with new acyclovir phosphoramidate prodrugs.* Bioorg Med Chem Lett, 2008. **18**(15): p. 4364-7.
466. Snoeck, J., et al., *Optimization of a genotypic assay applicable to all human immunodeficiency virus type 1 protease and reverse transcriptase subtypes.* J Virol Methods, 2005. **128**(1-2): p. 47-53.
467. Marchand, B. and M. Gotte, *Impact of the translocational equilibrium of HIV-1 reverse transcriptase on the efficiency of mismatch extensions and the excision of mispaired nucleotides.* Int J Biochem Cell Biol, 2004. **36**(9): p. 1823-35.
468. Marchand, B., et al., *Effects of the translocation status of human immunodeficiency virus type 1 reverse transcriptase on the efficiency of excision of tenofovir.* Antimicrob Agents Chemother, 2007. **51**(8): p. 2911-9.
469. Conant, M.A., et al., *Valaciclovir versus aciclovir for herpes simplex virus infection in HIV-infected individuals: two randomized trials.* Int J STD AIDS, 2002. **13**(1): p. 12-21.
470. Watson-Jones, D., et al., *Effect of herpes simplex suppression on incidence of HIV among women in Tanzania.* N Engl J Med, 2008. **358**(15): p. 1560-71.
471. Celum, C., et al., *Effect of aciclovir on HIV-1 acquisition in herpes simplex virus 2 seropositive women and men who have sex with men: a randomised, double-blind, placebo-controlled trial.* Lancet, 2008. **371**(9630): p. 2109-19.
472. Huang, H., et al., *Structure of a covalently trapped catalytic complex of HIV-1 reverse transcriptase: implications for drug resistance.* Science, 1998. **282**(5394): p. 1669-75.
473. Shirasaka, T., et al., *Emergence of human immunodeficiency virus type 1 variants with resistance to multiple dideoxynucleosides in patients receiving therapy with dideoxynucleosides.* Proc Natl Acad Sci U S A, 1995. **92**(6): p. 2398-402.
474. Ueno, T., T. Shirasaka, and H. Mitsuya, *Enzymatic characterization of human immunodeficiency virus type 1 reverse transcriptase resistant to multiple 2',3'-dideoxynucleoside 5'-triphosphates.* J Biol Chem, 1995. **270**(40): p. 23605-11.
475. Selmi, B., et al., *The valine-to-threonine 75 substitution in human immunodeficiency virus type 1 reverse transcriptase and its relation with stavudine resistance.* J Biol Chem, 2001. **276**(17): p. 13965-74.
476. Deval, J., et al., *The molecular mechanism of multidrug resistance by the Q151M human immunodeficiency virus type 1 reverse transcriptase and its suppression using alpha-boranophosphate nucleotide analogues.* J Biol Chem, 2002. **277**(44): p. 42097-104.
477. Sluis-Cremer, N., et al., *Molecular mechanism by which the K70E mutation in human immunodeficiency virus type 1 reverse transcriptase confers resistance to nucleoside reverse transcriptase inhibitors.* Antimicrob Agents Chemother, 2007. **51**(1): p. 48-53.

478. Sarafianos, S.G., et al., *Glutamine 151 participates in the substrate dNTP binding function of HIV-1 reverse transcriptase.* Biochemistry, 1995. **34**(21): p. 7207-16.
479. Sarafianos, S.G., et al., *Site-directed mutagenesis of arginine 72 of HIV-1 reverse transcriptase. Catalytic role and inhibitor sensitivity.* J Biol Chem, 1995. **270**(34): p. 19729-35.
480. Matamoros, T., B. Kim, and L. Menendez-Arias, *Mechanistic insights into the role of Val75 of HIV-1 reverse transcriptase in misinsertion and mispair extension fidelity of DNA synthesis.* J Mol Biol, 2008. **375**(5): p. 1234-48.
481. Miller, M.D., et al., *Antiviral activity of tenofovir (PMPA) against nucleoside-resistant clinical HIV samples.* Nucleosides Nucleotides Nucleic Acids, 2001. **20**(4-7): p. 1025-8.
482. Meyer, P.R., et al., *Effects of primer-template sequence on ATP-dependent removal of chain-terminating nucleotide analogues by HIV-1 reverse transcriptase.* J Biol Chem, 2004. **279**(44): p. 45389-98.
483. Sluis-Cremer, N., et al., *The 3'-azido group is not the primary determinant of 3'-azido-3'-deoxythymidine (AZT) responsible for the excision phenotype of AZT-resistant HIV-1.* J Biol Chem, 2005. **280**(32): p. 29047-52.
484. Dharmasena, S., et al., *3'-Azido-3'-deoxythymidine-(5')-tetraphospho-(5')-adenosine, the product of ATP-mediated excision of chain-terminating AZTMP, is a potent chain-terminating substrate for HIV-1 reverse transcriptase.* Biochemistry, 2007. **46**(3): p. 828-36.
485. Lacey, S.F., et al., *Biochemical studies on the reverse transcriptase and RNase H activities from human immunodeficiency virus strains resistant to 3'-azido-3'-deoxythymidine.* J Biol Chem, 1992. **267**(22): p. 15789-94.
486. Krebs, R., et al., *Single-step kinetics of HIV-1 reverse transcriptase mutants responsible for virus resistance to nucleoside inhibitors zidovudine and 3-TC.* Biochemistry, 1997. **36**(33): p. 10292-300.
487. Ray, A.S., et al., *Probing the molecular mechanisms of AZT drug resistance mediated by HIV-1 reverse transcriptase using a transient kinetic analysis.* Biochemistry, 2003. **42**(29): p. 8831-41.
488. Tuske, S., et al., *Structures of HIV-1 RT-DNA complexes before and after incorporation of the anti-AIDS drug tenofovir.* Nat Struct Mol Biol, 2004. **11**(5): p. 469-74.
489. Telesnitsky, A. and S.P. Goff, *Reverse Transcriptase and the Generation of Retroviral DNA*, in *Retroviruses*, J.M. Coffin, S.H. Hughes, and H.E. Varmus, Editors. 1997, Cold Spring Harbor Laboratory Press: Cold Spring Harbor, NY, USA. p. 121-160.
490. Seeger, C. and W.S. Mason, *Hepatitis B Virus Biology.* Microbiol. Mol. Biol. Rev., 2000. **64**(1): p. 51-68.
491. Nassal, M., *Hepatitis B viruses: reverse transcription a different way.* Virus Res, 2008. **134**(1-2): p. 235-49.
492. Schinazi, R.F., et al., *Selective inhibition of human immunodeficiency viruses by racemates and enantiomers of cis-5-fluoro-1-[2-*

(hydroxymethyl)-1,3-oxathiolan-5-yl]cytosine. Antimicrob Agents Chemother, 1992. **36**(11): p. 2423-31.
493. Ling, R., et al., *Selection of mutations in the hepatitis B virus polymerase during therapy of transplant recipients with lamivudine.* Hepatology, 1996. **24**(3): p. 711-3.
494. Wainberg, M.A., et al., *Development of HIV-1 resistance to (-)2'-deoxy-3'-thiacytidine in patients with AIDS or advanced AIDS-related complex.* AIDS, 1995. **9**(4): p. 351-7.
495. Gutfreund, K.S., et al., *Genotypic succession of mutations of the hepatitis B virus polymerase associated with lamivudine resistance.* J Hepatol, 2000. **33**(3): p. 469-75.
496. Benhamou, Y., et al., *Long-term incidence of hepatitis B virus resistance to lamivudine in human immunodeficiency virus-infected patients.* Hepatology, 1999. **30**(5): p. 1302-6.
497. Thibault, V., et al., *Hepatitis B virus (HBV) mutations associated with resistance to lamivudine in patients coinfected with HBV and human immunodeficiency virus.* J Clin Microbiol, 1999. **37**(9): p. 3013-6.
498. Fontaine, H., V. Thiers, and S. Pol, *Hepatitis B virus genotypic resistance to lamivudine.* Ann Intern Med, 1999. **131**(9): p. 716-7.
499. Villet, S., et al., *Selection of a Multiple Drug-Resistant Hepatitis B Virus Strain in a Liver-Transplanted Patient.* Gastroenterology, 2006. **131**(4): p. 1253-1261.
500. Nunez, M., et al., *Activity of tenofovir on hepatitis B virus replication in HIV-co-infected patients failing or partially responding to lamivudine.* AIDS, 2002. **16**(17): p. 2352-4.
501. van Bommel, F., et al., *Tenofovir treatment in patients with lamivudine-resistant hepatitis B mutants strongly affects viral replication.* Hepatology, 2002. **36**(2): p. 507-8.
502. Benhamou, Y., R. Tubiana, and V. Thibault, *Tenofovir disoproxil fumarate in patients with HIV and lamivudine-resistant hepatitis B virus.* N Engl J Med, 2003. **348**(2): p. 177-8.
503. Manolakopoulos, S., et al., *Long-term therapy with adefovir dipivoxil in hepatitis B e antigen-negative patients developing resistance to lamivudine.* Aliment Pharmacol Ther, 2008. **27**(3): p. 266-73.
504. Yuan, H.J. and W.M. Lee, *Molecular mechanisms of resistance to antiviral therapy in patients with chronic hepatitis B.* Curr Mol Med, 2007. **7**(2): p. 185-97.
505. Sherman, M., et al., *Entecavir for treatment of lamivudine-refractory, HBeAg-positive chronic hepatitis B.* Gastroenterology, 2006. **130**(7): p. 2039-49.
506. Lai, C.L., et al., *Entecavir versus lamivudine for patients with HBeAg-negative chronic hepatitis B.* N Engl J Med, 2006. **354**(10): p. 1011-20.
507. Tenney, D.J., et al., *Clinical emergence of entecavir-resistant hepatitis B virus requires additional substitutions in virus already resistant to Lamivudine.* Antimicrob Agents Chemother, 2004. **48**(9): p. 3498-507.
508. Sulkowski, M.S., *Management of hepatic complications in HIV-infected persons.* J Infect Dis, 2008. **197 Suppl 3**: p. S279-93.

509. Soriano, V., et al., *A low antiretroviral activity of the antihepatitis B drug entecavir may be enough to select for M184V in HIV-1.* AIDS, 2008. **22**(7): p. 911-2.
510. Sasadeusz, J., et al., *The anti-HIV activity of entecavir: a multicentre evaluation of lamivudine-experienced and lamivudine-naive patients.* AIDS, 2008. **22**(8): p. 947-55.
511. Lin, P.F., et al., *Entecavir exhibits inhibitory activity against human immunodeficiency virus under conditions of reduced viral challenge.* Antimicrob Agents Chemother, 2008. **52**(5): p. 1759-67.
512. Sasadeusz, J., *The anti-HIV antiviral activity of entecavir: the loss of a trusted friend?* J Hepatol, 2007. **47**(6): p. 872-4.
513. Hirsch, M.S., *Entecavir surprise.* N Engl J Med, 2007. **356**(25): p. 2641-3.
514. Marquez, V.E., et al., *Experimental and structural evidence that herpes 1 kinase and cellular DNA polymerase(s) discriminate on the basis of sugar pucker.* J Am Chem Soc, 2004. **126**(2): p. 543-9.
515. Gotte, M., et al., *HIV-1 reverse transcriptase-associated RNase H cleaves RNA/RNA in arrested complexes: implications for the mechanism by which RNase H discriminates between RNA/RNA and RNA/DNA.* EMBO J, 1995. **14**(4): p. 833-41.
516. Carroll, S.S., et al., *Inhibition of hepatitis C virus RNA replication by 2'-modified nucleoside analogs.* J Biol Chem, 2003. **278**(14): p. 11979-84.
517. Deval, J., et al., *Pyrophosphorolytic excision of nonobligate chain terminators by hepatitis C virus NS5B polymerase.* Antimicrob Agents Chemother, 2007. **51**(8): p. 2920-8.
518. Ding, J., et al., *Structure and functional implications of the polymerase active site region in a complex of HIV-1 RT with a double-stranded DNA template-primer and an antibody Fab fragment at 2.8 A resolution.* J Mol Biol, 1998. **284**(4): p. 1095-111.
519. Sarafianos, S.G., et al., *Crystal structure of HIV-1 reverse transcriptase in complex with a polypurine tract RNA:DNA.* EMBO J, 2001. **20**(6): p. 1449-61.
520. Bebenek, K., et al., *A minor groove binding track in reverse transcriptase.* Nat Struct Biol, 1997. **4**(3): p. 194-7.
521. Isel, C., et al., *The emergence of different resistance mechanisms toward nucleoside inhibitors is explained by the properties of the wild type HIV-1 reverse transcriptase.* J Biol Chem, 2001. **276**(52): p. 48725-32.
522. Colonno, R.J., et al., *Week 48 Resistance Surveillance of HIV/HBV Co-Infected Patients Treated with Entecavir in Study AI463038*, in *13th Conference on Retroviruses and Opportunistic Infections*. 2006: Denver, CO, USA.

APPENDIX 1; RESEARCH COMPLIANCE CERTIFICATE

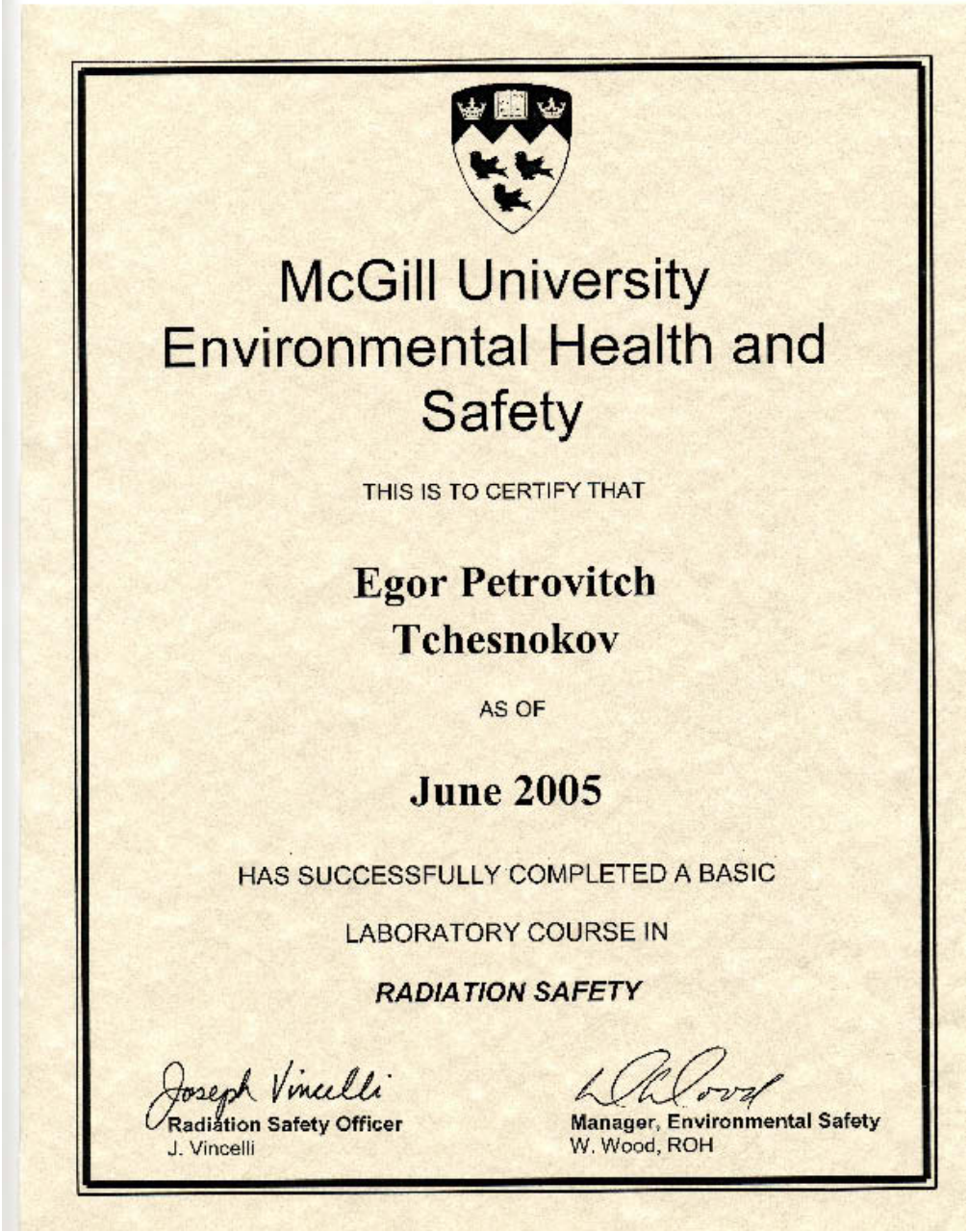

McGill University
Environmental Health and Safety

THIS IS TO CERTIFY THAT

Egor Petrovitch Tchesnokov

AS OF

June 2005

HAS SUCCESSFULLY COMPLETED A BASIC

LABORATORY COURSE IN

RADIATION SAFETY

Joseph Vincelli
Radiation Safety Officer
J. Vincelli

Manager, Environmental Safety
W. Wood, ROH